COMMONWEALTH OF AUSTRALIA

DEPARTMENT OF NATIONAL DEVELOPMENT

BUREAU OF MINERAL RESOURCES, GEOLOGY AND GEOPHYSICS

BULLETIN 87

The Alcoota Fauna, Central Australia

An Integrated Palaeontological and Geological Study

BY

MICHAEL O. WOODBURNE

Museum of Paleontology, University of California,
Berkeley, California

Issued under the Authority of the Hon. David Fairbairn
Minister for National Development
1967

COMMONWEALTH OF AUSTRALIA

DEPARTMENT OF NATIONAL DEVELOPMENT
MINISTER: THE HON. DAVID FAIRBAIRN, D.F.C., M.P.
SECRETARY: R. W. BOSWELL, O.B.E.

BUREAU OF MINERAL RESOURCES, GEOLOGY AND GEOPHYSICS
DIRECTOR: J. M. RAYNER, O.B.E.

THIS BULLETIN WAS PREPARED IN THE GEOLOGICAL BRANCH
ASSISTANT DIRECTOR: N. H. FISHER

Manuscript received: 25 January 1966

Issued: 15 May 1967

Published by the Bureau of Mineral Resources, Geology and Geophysics
Canberra, A.C.T.

Printed by Barker & Co. Pty. Ltd., Melbourne

FOREWORD

Vertebrate remains from Australia were first studied over a century ago by Sir Richard Owen; and thereafter systematic work was carried on only sporadically, until in 1953 Professor R. A. Stirton of the University of California at Berkeley came to South Australia and started an intensive field and laboratory study of the vertebrate faunas of that State. He and his co-workers have continued the study, extending it into the Northern Territory and New Guinea as a consequence of finds by geologists of the Bureau of Mineral Resources, of which the Alcoota fauna is perhaps the richest so far.

Stirton and his co-workers R. H. Tedford and M. O. Woodburne, and M. D. Plane of the Bureau have introduced a new rigour into the study of vertebrate palaeontology in Australia, with which the Bureau is happy to be associated. Geologically, these fossils are of great importance because they provide a clue — sometimes the only clue — to the Cainozoic history of Australia.

Three volumes have been published by the Bureau giving an account of this work *(Bulletins 85, 86 and 87)*. This volume describes the rich concentration of Middle Tertiary fossil vertebrates found near Alcoota homestead, in the Northern Territory.

J. M. RAYNER,

Director

CONTENTS

ILLUSTRATIONS

SUMMARY

A rich concentration of fossil vertebrates has been found in middle Tertiary sediments near Alcoota station in the Northern Territory, Australia.

The sediments, which are about 70 feet thick, comprise a basal drab lacustrine siltstone overlain by red fluviatile siltstone, sandstone, and conglomerate, capped by chalcedonic limestone. They are generally flatlying and are designated the Waite Formation. The Waite Formation rests unconformably on lateritized Archaean gneiss and quartzite. The geological evidence clearly indicates that the laterite antedates the Waite Formation and is, therefore, no later than Miocene in age.

The vertebrate assemblage recovered from the drab lacustrine siltstones at the base of the Waite Formation is designated the Alcoota fauna. It includes a crocodile seemingly related to *C. porosus* of New Guinea and a number of large emu-like birds. A new wallaby-sized macropodid is apparently related to *Dorcopsis* and *Dorcopsulus,* which are also currently found in New Guinea. A new genus of large macropodid may represent an early sthenurine, but it also shows some affinity to the Pliocene and Pleistocene genus *Protemnodon.* The presence of the protemnodont lineage during Alcoota time is firmly established by four isolated upper first incisors, but these teeth probably do not belong to the new genus.

The bulk of the animal remains belong to the extinct family Diprotodontidae. One of these is a new species of *Palorchestes.* The others have been described previously as three new genera and species. Cranial material of these three genera, not available earlier, is described.

The geological and palaeontological evidence indicates that the middle Tertiary climate around Alcoota was at least subtropical. The seasonal precipitation was undoubtedly much more effective than at present. In the dry season, animals were apparently drawn in large numbers to the shores of a lake which had developed in a depression in the old lateritized terrain. Each year some of the animals perished around the shore, and their remains were entombed nearby.

In stage of evolution, the members of the Alcoota fauna are younger than those from the Kutjamarpu fauna (middle Miocene) of South Australia and older than those of the Beaumaris (early Pliocene) fauna from the Sandringham Sands of Victoria. The age of the Alcoota fauna, in these terms, is late Miocene or possibly early Pliocene.

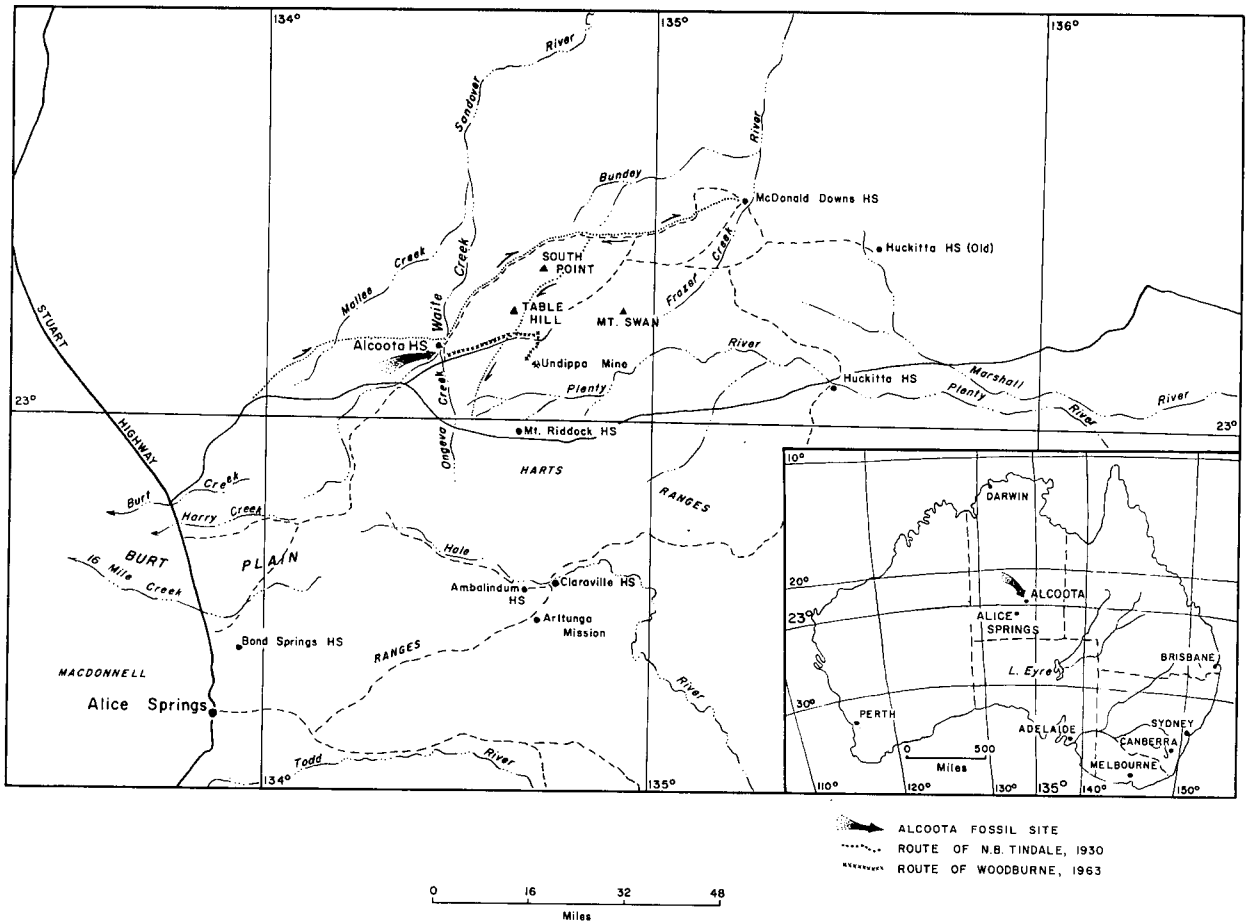

Fig. 1. Index map of the Macdonnell-Harts Ranges, Northern Territory, Australia.

INTRODUCTION

A rich concentration of vertebrate fossils has recently been found in middle Tertiary deposits near Alcoota homestead, in the Northern Territory of Australia (Newsome & Rochow, 1964; Woodburne, 1967). The assemblage of animals represented by the fossils has been named the Alcoota fauna and the enclosing deposits the Waite Formation. The Alcoota fauna is the first Tertiary mammalian assemblage to be recorded from this part of Australia, and furnishes, in comparison with the succession of faunas described from strata in the Tirari Desert east of Lake Eye (Stirton, Tedford & Miller, 1961), a better understanding of the historical background of the modern Australian fauna.

In 1930, N. B. Tindale visited McDonald Downs homestead (Fig. 1) and described (1931, p. 38) flatlying beds consisting of red ferruginous grit overlain by 10 feet of kaolin, 20 feet of limestone, and finally 6 feet of chalcedony. According to Tindale the Tertiary beds between McDonald Downs and Alcoota have 'given rise to a partly dissected plateau, traces of which can be seen in the form of table-topped hills up to one hundred feet in height.' Tindale followed the track which passes north-east from Alcoota, north of Table Hill and South Point, to McDonald Downs (Fig. 1). This track apparently also extended nearly due west from Alcoota and was thus about 4 miles north of the Tertiary sediments which contain the Alcoota fauna.

During his 1931 traverse (Fig. 3) of the MacDonnell and Harts Ranges, C. T. Madigan (1932) found a number of similar low flat-topped erosional remnants in the floodplains of the Hale, Plenty, and Todd Rivers. These erosional remnants contained primarily nonmarine sedimentary rocks of Tertiary age, typically with a chalcedony ('duri-crust') cap, and were grouped (*ibid.*, p. 97, 100) as 'the Arltungan formations'. Near Arltunga Mission ('Paddy's Hole Plain') Tertiary limestones were found to be composed almost completely of *Planorbis* shells, to which a Pliocene or Pleistocene age was attributed. The temporal and geographical separation of these sediments from those of the 'Eyrian Series' of then presumed early Tertiary age (Woolnough & David, 1926; see also Woodard, 1955) was the chief reason for grouping the 'Arltungan formations' as a distinct unit (Madigan, 1932, p. 100). They were said to consist of horizontal alluvial or freshwater sand, clay, gravel, and limestone up to 100 feet thick. One flat-topped hill, 2 miles south-east of Plenty Wells (Huckitta HS of Fig. 1) was described (*ibid.*, p. 99) as being 90 feet high, 50 feet of which were composed of 'grey sandy clay, overlain by 15 feet of red ferruginous sandstone, and capped by 25 feet of white chalcedony, the thickest of such cappings observed'.

The first reference to chalcedony-capped Tertiary deposits at Alcoota is found in a brief statement made by Whitehouse (1940, p. 33) during a discussion of similar features in western Queensland.

The fossil site was apparently well known to local pastoralists and aborigines, and a local collector, Mr R. Gorey, finally brought the Alcoota fossils to the attention of the Resident Geologist at Alice Springs. The subsequent history of the development of the quarries has been outlined in Newsome & Rochow (1964) and Woodburne (1966).

Air-photographs supplied by the Bureau of Mineral Resources (scale 1:50,000) served as a base for the map in Figure 2. It was found that the tops of the higher mesas, hills 2, 4, 5, 6, and 7 of Figure 4, were on about the same level, and this was arbitrarily chosen as the datum relative to which the remaining sections would be positioned. The heights of the two peripheral sections, i.e., New Well and the Undippa Site, are not definitely controlled relative to the others. For purposes of illustration and discussion it was assumed that the chalcedonic limestone which formed the caprock of the sections at New Well and the Undippa Site is at the same stratigraphic and topographic level as that in the other sections.

ACKNOWLEDGEMENTS

The author is indebted to many persons for invaluable help in various phases of the project. Special appreciation is extended to the late Dr R. A. Stirton, Director of the Museum of Paleontology, University of California, and to Dr N. H. Fisher, Chief Geologist of the Bureau of Mineral Resources, Canberra, A.C.T., for their interest in and support of the work. T. Quinlan, D. R. Woolley, and others of the Resident Geologist's staff in Alice Springs, Northern Territory, gave freely of their time and facilities. Paul F. Lawson, of the South Australian Museum, gave invaluable help in the early phase of the project. Our stay in Alcoota was made memorable by the hospitality of Mr. and Mrs. Ivor Paine of Alcoota homestead. Thanks are also given to Mr. P. L. Puckridge, C.B.E., owner of Alcoota station, for granting permission to remove the fossil material.

A large part of the credit for the acquisition of the material upon which this report is based is due to J. E. Mawby and J. E. Ferguson Stewart, who worked in the quarry for nearly three months and whose painstaking efforts resulted in the securing of many fine specimens.

A. E. Newsome and K. A. Rochow, who originally notified Dr Stirton of the site, spent over a week in the field in 1962 with Drs Stirton and Tedford and the author, helped make the initial collection, and placed at our disposal all their previously acquired knowledge of the area.

Dr R. H. Tedford, Department of Geology, University of California, Riverside, and Mr A. R. Lloyd, Bureau of Mineral Resources, made reconnaissance studies

BLOCK DIAGRAM AND GEOLOGIC MAP, ALCOOTA AREA, NORTHERN TERRITORY, AUSTRALIA

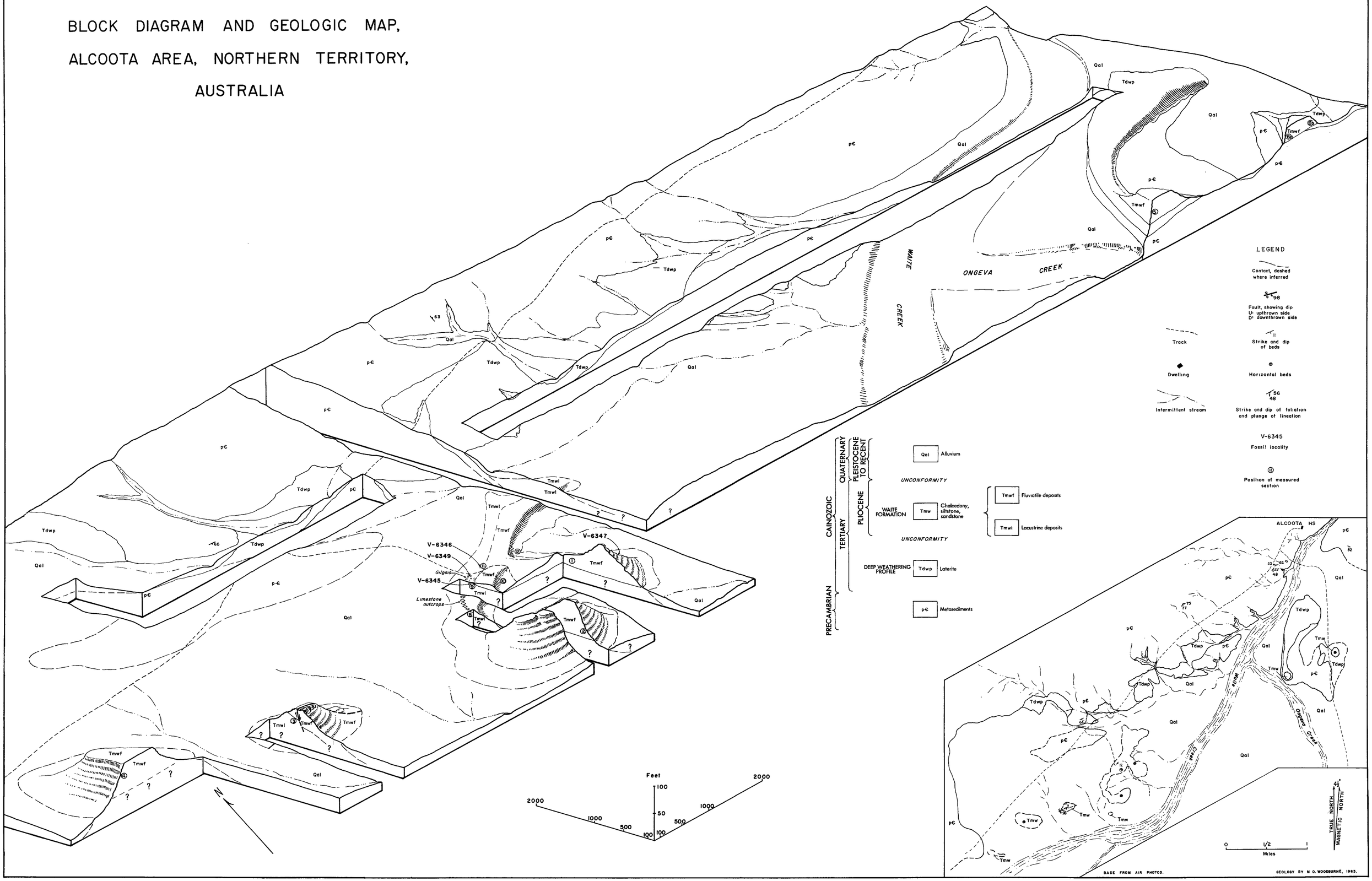

Fig. 2.

of portions of the Northern Territory and Queensland during the 1963 field season. From discussions with them, the author gained a large share of his concept of the geographical setting of the areas containing Madigan's 'Arltungan formations'.

Appreciation is also extended to Mr J. T. Woods, Director of the Queensland Museum, Brisbane, Mr A. Bartholomai of the same institution, Mr H. M. Van Deusen, American Museum of Natural History, New York, and Dr G. L. Jepsen, Princeton University, for the loan of and permission to examine specimens under their care.

The line drawings were prepared by Mrs Augusta F. Lucas and Mrs Jaime P. Lufkin, staff artists of the Museum of Paleontology. Photographs and maps were contributed by the author.

Particular thanks are extended to the National Science Foundation for grant G15957, which made the project possible.

The climate, geomorphology, soil types, vegetation, etc. of the area surrounding Alcoota have been thoroughly described by Perry et al. (1962).

In keeping with the policy of the University of California Museum of Paleontology in all its projects in Australia, and as agreed with the Bureau of Mineral Resources, all type specimens and a representative sample of the fauna will be lodged with the Bureau.

The following abbreviations will be used in the designation of the specimens in this Bulletin: UCMP, University of California Museum of Paleontology; UCMVZ, University of California Museum of Vertebrate Zoology; AMNH, American Museum of Natural History; AM, Australian Museum, Sydney; CPC, Commonwealth Palaeontological Collection, Bureau of Mineral Resources, Canberra, ACT.

Unless otherwise specified, all measurements in the text and in the tables are in millimetres.

GEOLOGY

The Alcoota fossil deposits are found in flatlying erosional remnants which rise above the plain at the junction of Waite and Ongeva Creeks, tributaries of the Sandover River (Fig. 2). To the west, hills of Archaean metamorphics, about 100 feet high, form the western boundary of a flat plain that stretches for 20 to 30 miles to the east and south-east. The plain is covered by a veneer of Quaternary alluvium, with occasional low rises of Archaean rocks.

As shown in Figure 3, the Tertiary sediments of the MacDonnell/Harts Ranges lie mainly on the Arunta Block, which contains the oldest rocks in the Northern Territory. At Alcoota, the Archaean rocks are quartz-biotite-garnet-feldspar gneiss,

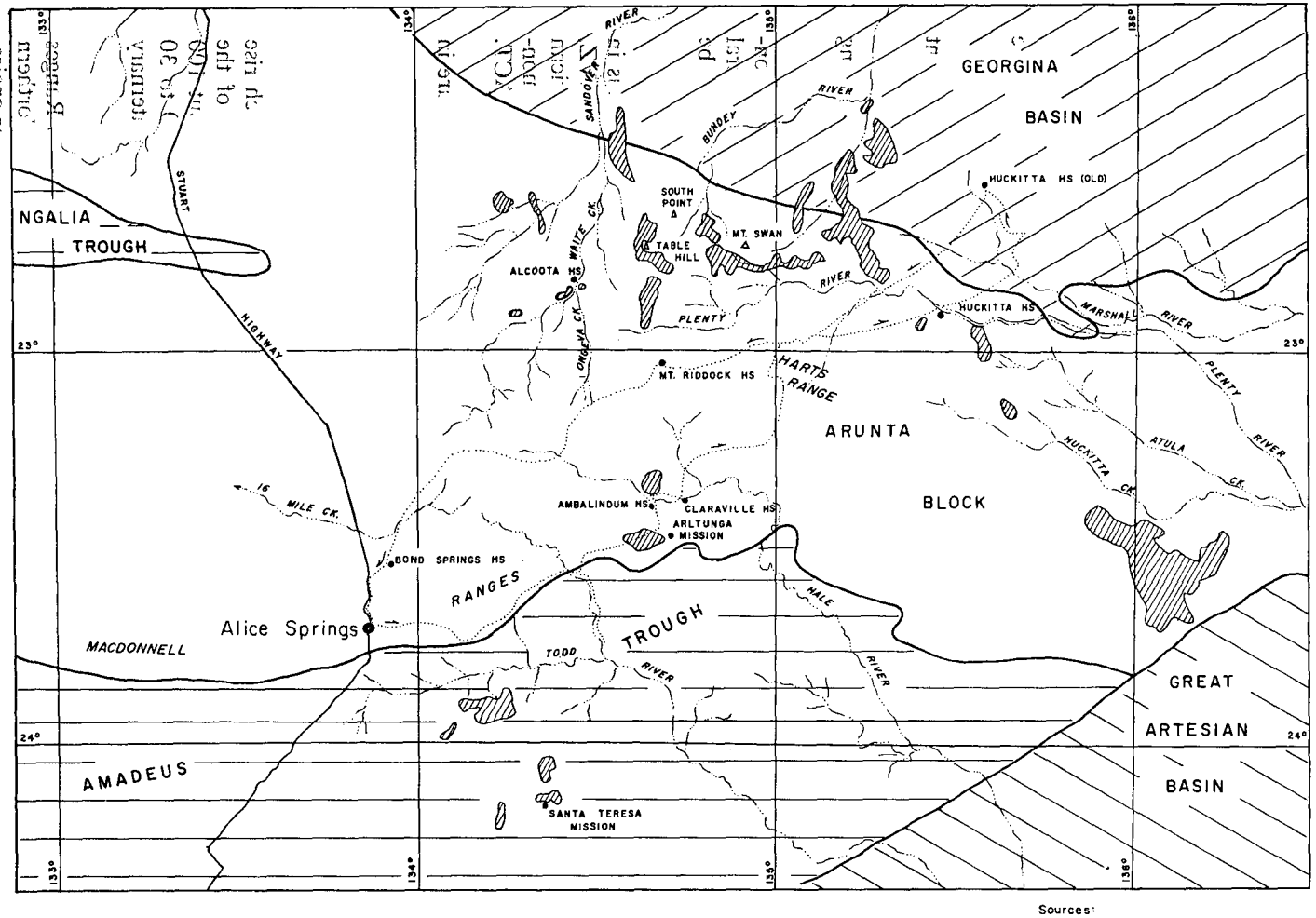

Sources:

STRUCTURAL ELEMENTS: QUINLAN, 1962

TERTIARY DEPOSITS: QUINLAN, 1962; JOKLIK, 1955

TERTIARY DEPOSITS

ROUTE OF C.T. MADIGAN, 1931

Fig. 3. Map of structural elements east of Alice Springs, showing distribution of Tertiary deposits.

interbedded with quartzite; this is probably the Irindina Gneiss of Joklik (1955, pp. 68-74). The post-Archaean rocks that apparently once covered the area have been removed by erosion at some time between Ordovician and Tertiary.

Around Alcoota, Archaean rocks are covered with remnants of a lateritic terrain (Fig. 2), on which flatlying Tertiary sediments rest uncomformably. The first Tertiary sediments were lacustrine, the later ones fluviatile. They accumulated to a thickness of at least 70 feet in a broad depression in the surface of the deep weathering profile (Figs 4 and 5). The subsequent erosion of the sediments, and the presence of small faults (see Fig. 2), indicate renewed crustal movements during the Quaternary. The animal remains are found in the lacustrine Tertiary rocks.

The Tertiary Rocks

Laterite

In measured section 5 (see Appendix), at the south-west end of the first erosional remnant east of Ongeva Creek (Hill 5, Fig. 2), nearly 40 feet of deeply weathered material is exposed in which the only clue to the original texture is the changes in the pastel colours of the soft amorphous powdery rock. This rock, which may be the equivalent of the earthy zone of Owen (1954, p. 179), is overlain by about 5 feet of ferruginous, structureless, fine-grained materal containing scattered black partings and subrounded to subangular particles of coarse sand size. The unit exhibits small-scale columnar weathering and may be equivalent to the massive zone of a laterite profile. The next unit in section 5 is an arenaceous late Tertiary siltstone which rests unconformably on the laterite: if a more complete laterite profile once existed at this site it has since been eroded away.

A pisolitic zone may be preserved in the next erosional remnant to the east (Hill 6). The hill has a basal core of gneiss with steep south, east, and west surfaces. The north surface is covered by a mantle of laterite, which is 30 feet thick at the northern end of the hill, and wedges out to the south. The zone may not be a mature pisolitic zone in the sense of Owen (1954, p. 180): instead of having a concentric structure about a nucleus, the 'pisolites' or pellets are composed of a dense fine-grained rock with scattered black partings and angular to subrounded quartz particles. The pellets resemble the ironstone nodules that occur in the ferruginous zone of laterite profiles in Queensland (Whitehouse, 1940, p. 9).

Another lateritic sequence was studied 4 miles south of the road to Mount Swan homestead, in the east face of a long flat-topped hill south of Table Hill (Fig. 3; Pl. 1). It is represented in section 13 (Appendix) and Figure 4. The top of the laterite, a ferruginous 'pisolitic' rock containing ironstone pebbles, grades down into a massive laterite which overlies weathered metasediments, possibly representing a mottled or pallid zone. In this area the surface of the laterite rises to the south-east, forming the southern edge of the basin in which the Tertiary sediments were laid down (Pl. 1). The laterite surface rises to the east, and, a quarter of a mile south of the site of section 3, the Tertiary sediments between

units 3 and 6 of that section have been pinched out. The edge of the basin could not have been much farther to the south-east.

Other areas of laterite south of Alcoota are shown in Figure 2; all the outcrops visited were found to be underlain by Archaean metamorphics, and it appears that a widespread terrain of Archaean rocks was lateritized. A subsequent period of erosion stripped the lateritic mantle from most of the area; it is preserved only in protected pockets and in the lowlands. The debris stripped from the hills was deposited in the depressions in the form of lacustrine or fluviatile sediment. One of the depressions was what is here called the *Waite Basin* (Fig. 5), and the sediments it contains are the *Waite Formation.* The Waite Basin is not a modern landform; the term describes only the Tertiary basin in which the Waite Formation was laid down.

Age of the Laterite. The angular unconformity between the laterite and the Tertiary sediments shows that the laterite is considerably the older; but the lapse of time represented by it cannot be deduced. The fossil vertebrates in the Waite Formation are probably late Miocene or early Pliocene (p. 169). The laterite is probably no younger than Miocene; but no more precise age can be assigned to it. The following statement by Owen (1954, p. 191) summarizes the position at Alcoota as elsewhere: 'At the present stage of investigation it is profitless to attempt correlation of mature laterites throughout Australia, and, indeed, it is improbable that all developed simultaneously . . . [Broadly speaking] . . . the evidence indicates that lateritization became general in Australia early in the Tertiary Period, and recurred from place to place as conditions permitted perhaps into the Pliocene Epoch.'

Tertiary Sediments

Sediments considered to be of Tertiary age have been found both north and south of the Harts Range (Fig. 3). These 'horizontally bedded . . . alluvial and freshwater sands, clays, gravels, and limestones' (Madigan, 1932, p. 100) may reach 100 feet in thickness, and characteristically occur as flat-topped erosional remnants. Madigan noted that the deposits were very similar, and grouped all occurrences under the name 'Arltungan formations' (Madigan, p. 100). They occur in three major areas: the Todd River Plain, the Hale River Plain around Arltunga Mission, and the Plenty River Plain. Each area is 30 to 50 miles from the others and is physiographically isolated by mountain ranges. Madigan (p. 99) noted that the arrangement of the deposits 'conforms with the present drainage system, but indicates a higher base-level of erosion'. Nevertheless, it is most unlikely that the three groups constitute a single lithogenetic unit.

The various 'Arltungan' sites have been examined in detail by R. H. Tedford and A. R. Lloyd. Both Madigan (1932) and Lloyd (1966) noted differences in detail between the deposits, and the main facts and conclusions can be summarized as follows: (1) Small areas of rocks considered to be of Tertiary age crop out over a considerable area both north and south of the Harts Range. (2) The rock types are broadly similar throughout. (3) The similarity is due to similar modes of

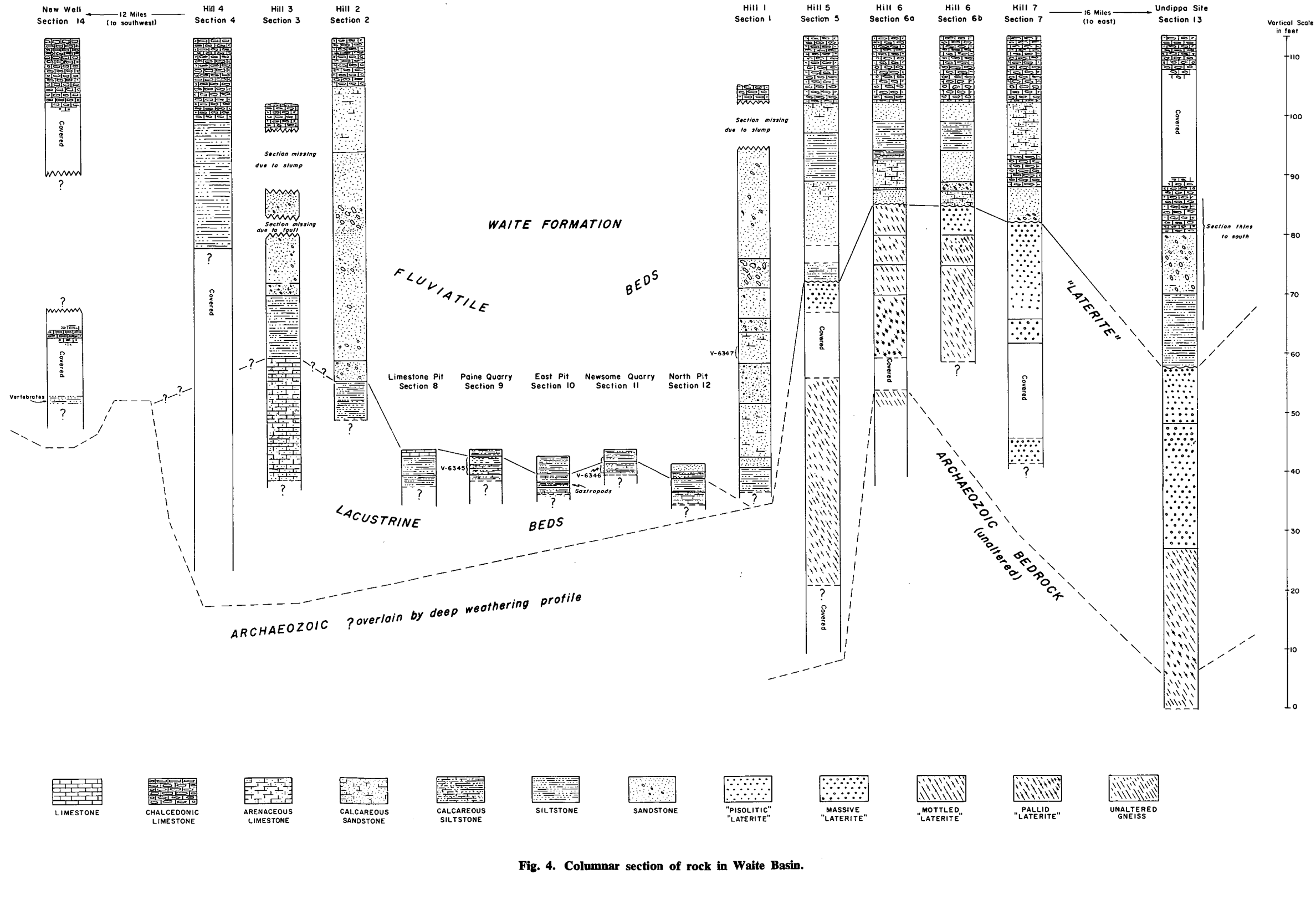

Fig. 4. Columnar section of rock in Waite Basin.

depositional environments. (4) The chalcedonic limestone caprock was developed under similarly ubiquitous conditions. (This caprock probably resulted from silicification of sediments in which the content of calcium carbonate was enriched by soil-forming processes.) (5) The various flatlying deposits are remnants of more extensive fillings of the valleys in which they are found. (6) The history of deposition differed in detail in each of the main areas of accumulation. (7) In the Tertiary the three areas were separated from each other essentially as they are today. (8) Therefore, the 'Arltungan formations' are not a single lithogenetic unit, and the name should not be applied to beds outside the type area.

The Tertiary sediments at Alcoota are found near the eastern edge of a terrain of Archaean gneiss which slopes eastward toward Waite Creek (Fig. 2). Remnants of laterite on the metamorphics have been preserved in sheltered low places in this terrain. The Tertiary sediments can be seen to overlie the laterite unconformably at two localities: in the three hills (Hills 5, 6, and 7, Fig. 2) just east of Ongeva Creek, and at the Undippa Site, 16 miles east of Alcoota (Pl. 1). The three hills represent an irregular Archaean ridge capped by a thinner Tertiary section than is found in neighbouring outcrops to the west (Fig. 4). About 12 miles east of Alcoota on the road to Mount Swan homestead, the flat-topped mesas are capped by chalcedonic limestone (site 1), but the underlying sediments are obscured by rubble. A better exposed section at site 2 includes about 70 feet of sediments similar to those at Alcoota, in which there are two chalcedonic limestone layers about 30 feet apart.

At site 3, unweathered quartzite and feldspathic gneiss with vertical foliation trending east-west are exposed on a flat plain. To the east, weathered gneiss is found in a small hill, the top of which is about 70 feet above the valley floor. Remnant textures persist about half way up the hill and grade into a ferruginous vuggy fine-grained structureless silicified rock which seems to represent the laterite profile. Archaean gneiss continues to crop out to the south-west (sites 4 and 5), but it is more weathered than at site 3. At sites 4 and 5 the laterite contains ironstone pellets, presumably from a higher part of the profile. The remnant foliation in the gneiss at site 4 trends 080° and dips 70°SE.

At site 6 the lateritized Archaean terrain rises to the south-east (Pl. 1) and is exposed in the east face of a long mesa. The lateritized surface is overlain unconformably by flatlying Tertiary sediments similar to those found at Alcoota and at site 2 (Pl. 1, section 13). As the laterite surface rises, the Tertiary section becomes thinner, and the Undippa area must have been close to the southern edge of a Tertiary basin which formed in a depression in the old lateritized terrain. Laterite also caps parent rock east of the Tertiary-capped mesa; so the eastern edge of the basin must also have been nearby.

In summary, a Tertiary basin was formed in a depression or broad valley in the old lateritized surface between the Undippa area and Alcoota. It may have been bounded on the south and west by the Archaean hills which are still present (Fig. 5). The eastern edge of the basin is indicated by the presence of laterite-covered Archaean rocks east of the Tertiary exposures.

The area of the Waite Basin is now drained by Waite and Ongeva Creeks, tributaries of the Sandover River system, which locally flows north. Madigan (1932) suggested that the main drainage features in the MacDonnell-Harts Ranges have existed for a long time and that the Tertiary sediments are old fillings of the valleys in which they are now found. This seems to be true of the sediments in the Waite Basin. They are at an altitude of about 2100 feet, whereas Tertiary sediments at Mount Swan and Red Tank (site of Madigan's 'Arltungan formations' at Plenty Wells) are at 1500 to 1600 feet. It seems likely that, in contrast to the sediments in the Waite Basin, they were laid down in an east-flowing system, now represented by the Plenty River, which has eroded headward into the southern periphery of the Undippa-Alcoota area, from which it was formerly excluded.

Waite Formation (Fig. 5)

The Waite Formation is defined as a sequence of freshwater sediments overlying laterite unconformably and overlain, if at all, only by Quaternary alluvium. The Waite Formation occupies the Waite Basin. It consists of a lower sequence of green siltstone of lacustrine origin, which is fossiliferous, and a thicker upper sequence of red fluviatile siltstone, sandstone, and conglomeratic sandstone capped by chalcedonic limestone. The type locality is the south face of the north-eastern end of a hill 4 miles south of Alcoota (Fig. 5, Hill 2), and the type section is detailed in the Appendix (section 2). The formation is 70 to 100 feet thick, and its age is late Miocene or early Pliocene.

The lower lacustrine sequence consists chiefly of light green evenly bedded siltstone and some limestone, and contains gastropods and vertebrate remains. In the deeper part of the Basin, west of Waite Creek, a thin transitional zone separates the lacustrine and fluviatile sequences; it is marked by a change in colour, and a gradual increase in diversity of mineral content and particle size. The fluviatile sediments account for about two-thirds of the total thickness of the formation. They are poorly bedded and lenticular. The massive red coarse sandstone and conglomerate weather to a conspicuous and characteristic terraced configuration. Only scattered weatherworn vertebrate fossils have been found in the fluviatile beds.

The sediments west of Waite Creek best display the features of the formation. For convenience in discussion the hills in which they occur have been numbered consecutively from north-east to south-west. Hill 1, which contains the principal fossil site in the upper sequence (Locality V6347, Fig. 2), is a small conspicuous pointed red erosional remnant at the northern edge of the plain. Hill 2 contains the type section (Pl. 2, Fig. 2), which is the most complete single exposure of the sequence. The fault in Hill 3 gives evidence of small-scale earth movements; Hill 3 also contains the southernmost exposure of the basal drab lacustrine component. Hill 4 contains the southernmost known exposure of the fluviatile sequence; the lacustrine sequence is possibly obscured by rubble. West of Hill 1 there is a long low rise trending north-east (Fig. 2), along whose western face are the green claystone and siltstone beds that bear the bulk of the vertebrate fossils. The sites of the measured sections detailed in the Appendix are shown in Figure 2.

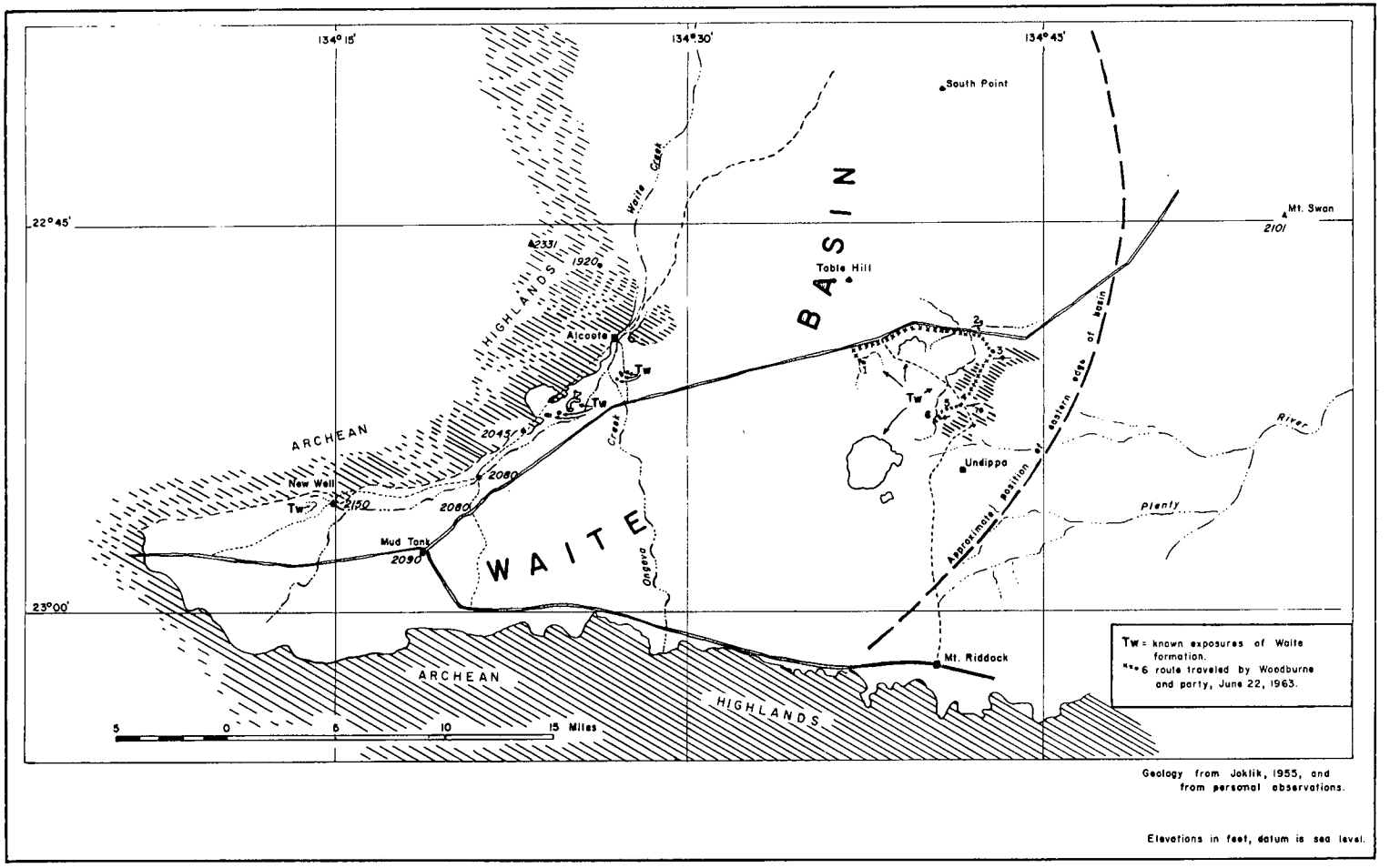

Fig. 5. Site of Waite Tertiary Basin.

The hills east of Waite Creek (Fig. 2) likewise form a natural descriptive unit and have been numbered consecutively from west to east. The Tertiary section is thinner here than to the west; the Waite Formation rests unconformably on an irregular surface of lateritized Archaean metamorphics.

Lacustrine sequence. The green or drab limy sediments at the base of the sections in Hills 2 and 3 and in exposures in the deeper part of the basin west of Hill 1 (Figs 2 and 4) differ sharply from the generally coarser red sediments in the higher parts of most of the measured sections, as follows:

Lacustrine deposits	*Fluviatile deposits*
1. Generally fine-grained; claystone, siltstone; more homogeneous; large clasts rare, mostly smooth and rounded.	1. Generally coarser-grained; sandstone, conglomerate, conglomeratic sandstone, and siltstone. Large clasts common and characteristically angular to subrounded.
2. Colour green or drab.	2. Colour basically red, except where secondarily obscured by calcium carbonate cement.
3. Bedding distinct, small-scale, regular and even.	3. Bedding indistinct, massive, lenticular.
4. Primary calcium carbonate as flaggy limestone, often bearing reed-like plant remains.	4. Calcium carbonate chiefly as cementing medium; general upward increase in lime content in most sections. Chalcedonic limestone caprock and other concentrations of $CaCO_3$ seem to represent secondary accumulations due to soil-forming activities.
5. Generally few minerals in coarse (sand-size) fraction.	5. Wide mineral range in coarser fraction (up to cobble size).
6. Scattered centre of residual red siltstone surrounded by green siltstone of same lithology suggests reduction of formerly red deposits.	6. No evidence that colour of deposits has changed since deposition except at zone of transition with the lacustrine beds in the deeper parts of the basin.
7. Lacustrine gastropods and vertebrate fossils present.	7. No gastropods, some vertebrate fossils.

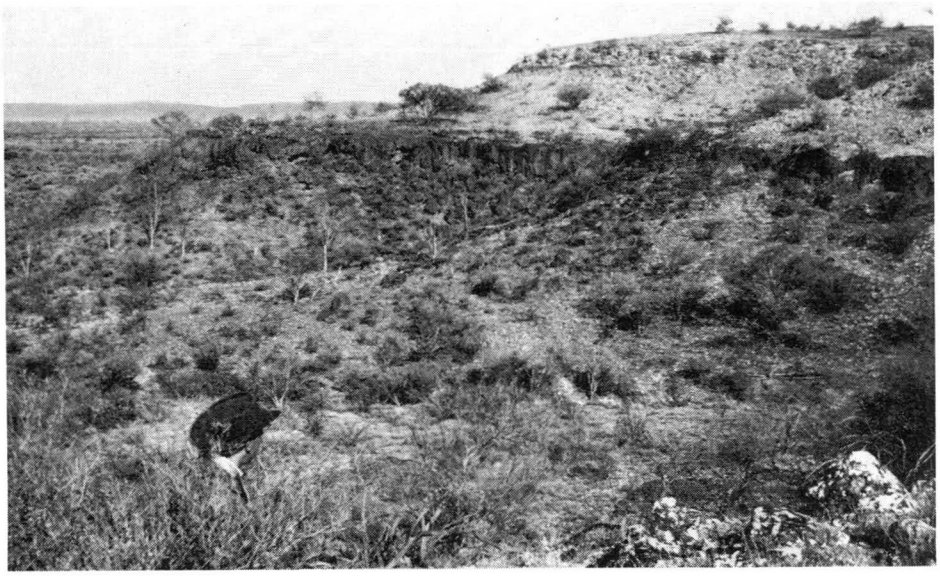

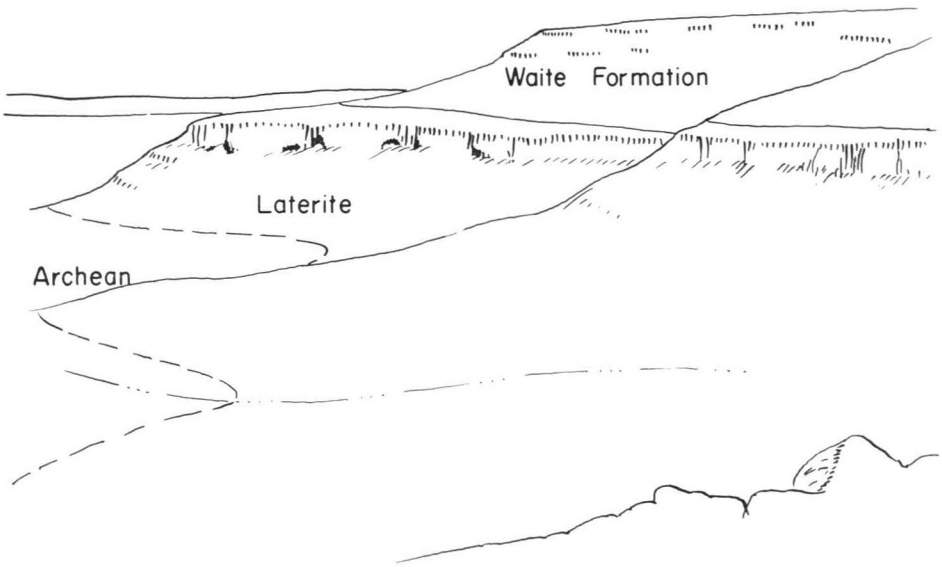

Plate 1. Photograph and sketch of north-west dipping laterite-covered Archaean terrain which is unconformably overlain by horizontal deposits of Waite Formation. Site 6, Undippa area. Photo taken toward south-west.

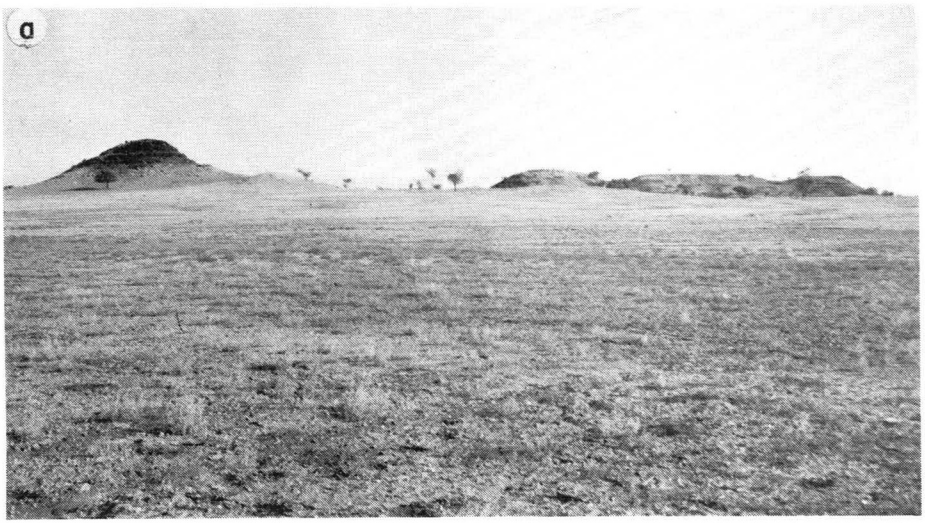

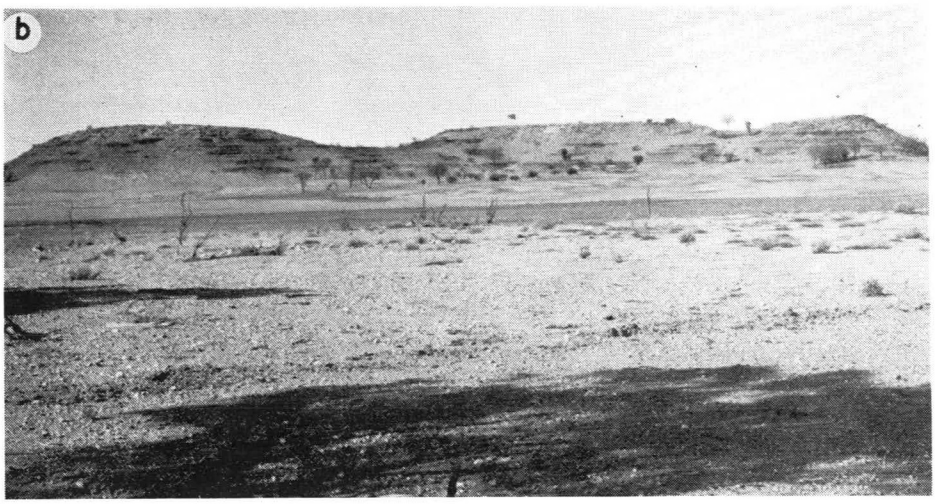

Plate 2. (a) **Hills 1 and 2 as seen from north-west edge of plain east of Waite Creek. Upper, red fluviatile portion of Waite Formation is exposed in these hills.**

(b) **North-west face of Hill 2, which contains the type section of the Waite Formation.**

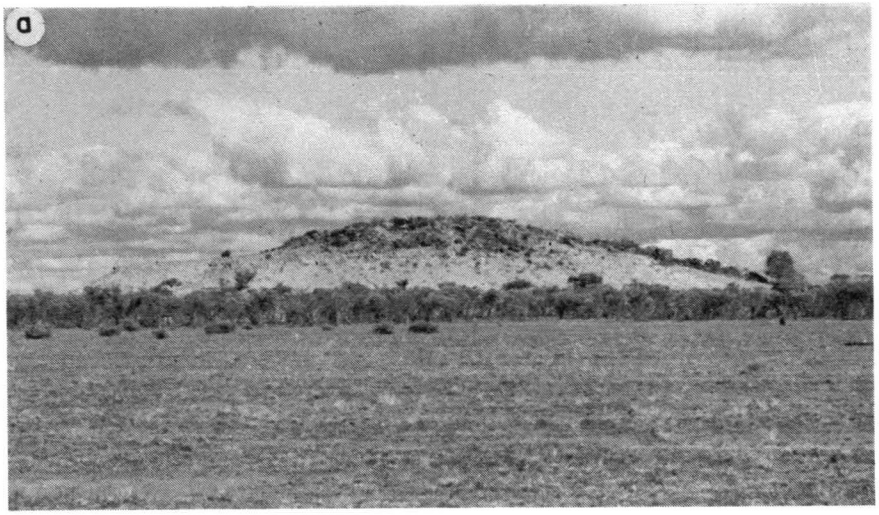

Plate 3. (a) North face of Hill 3. Light coloured beds in lower half belong to green lacustrine portion of Waite Formation, upper dark beds to red fluviatile portion. Upturned edges of caprock slump blocks can be seen along western (right) crest of hill.

(b) View of upturned caprock slump blocks which lie along southern face of Hill 3. These blocks lie on the downthrown side of the small fault which nearly bisects this hill from east to west. Trace of fault is just off photo to right (north).

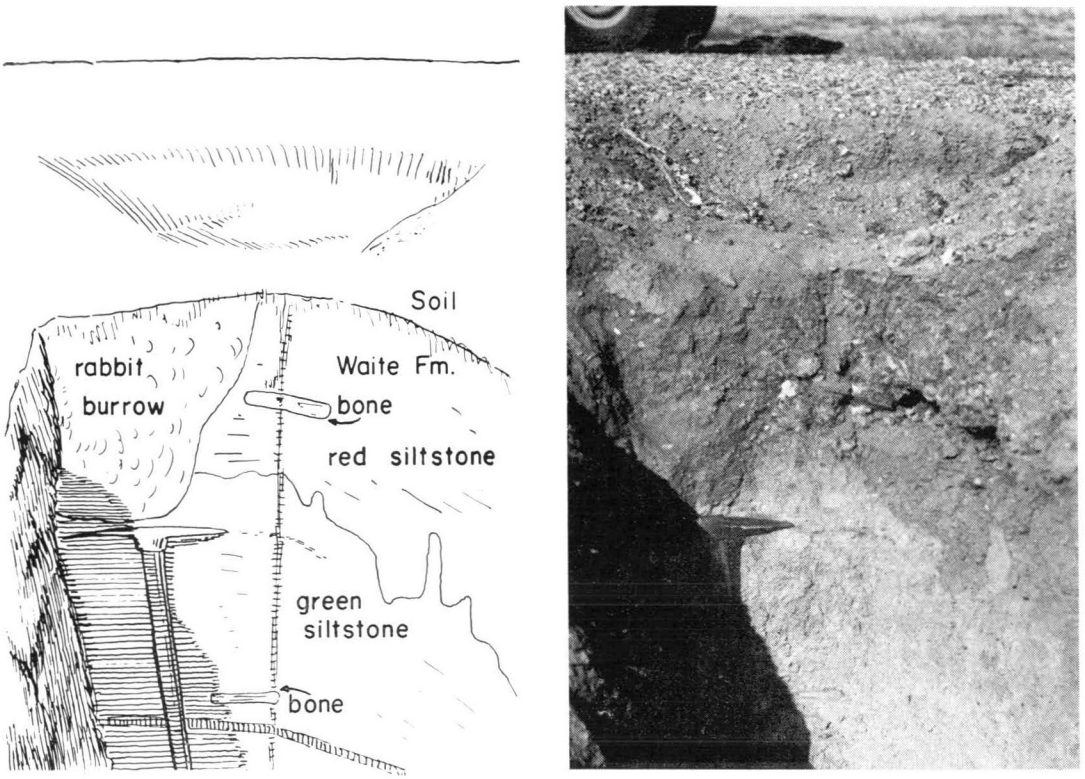

Plate 4. Photograph and sketch of pit at Newsome Quarry (V6346). Note that bone occurs in both the upper, red, transitional, siltstones and the underlying, green, lacustrine, part of the Waite Formation. The red-green interface is irregular; the bedding of the deposits is horizontal.

Plate 5 (a) West face of Paine Quarry (V6345). Transition between green lacustrine and red fluviatile deposits of the Waite Formation occurs just below the ledge upon which the newspapers are lying. Hill 1 lies in the background.

(b) Closer view of west face of Paine Quarry. Base of fossil-bearing unit is marked by top of lower whisk broom. Note dip of regular, even bedding.

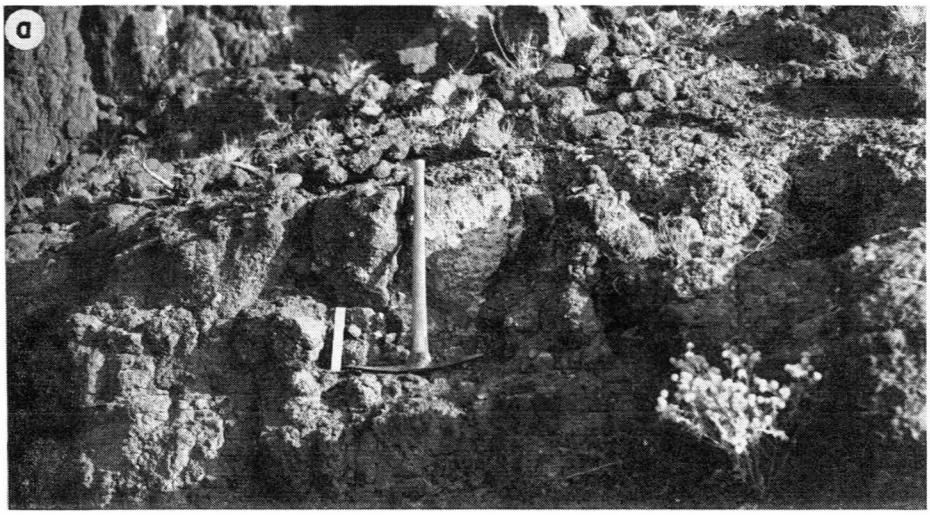

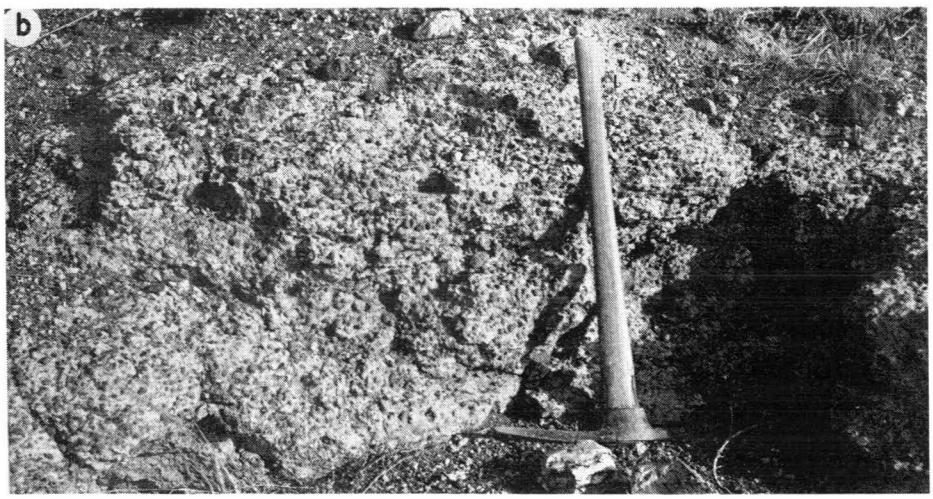

Plate 6. (a) Fluviatile deposits of Waite Formation as seen in the north-west face of Hill 1 (unit 7 of section 5). Angular to rounded bedrock clasts occur on either side of pick. Pick is 18 inches long. Note massive, poorly bedded character of deposit.

(b) Fluviatile deposits of Waite Formation, west face of Hill 1 (unit 4, section 6). Pebble conglomerate; pebbles apparently reworked from ironstone nodules of ferruginous zone of laterite profile.

The lower sequence was laid down in a lake or a series of large ponds in a poorly drained lowland. The fine grainsize of these deposits may reflect their derivation from fine-grained materials found in the upper parts of the laterite profile. If so, the sediments must have been charged with ferric oxide, and their present green colour is due, at least in part, to its reduction in a lacustrine environment. Indeed, scattered patches of red siltstone, completely surrounded by green siltstone, are found throughout the sequence.

Tabular blocks of limestone up to 6 inches thick occur in the lacustrine beds at Hill 3 (section 3) and the Limestone Pit (section 8). Reed-like plant remains have been found in limestone flags which crop out between the Limestone Pit and Paine Quarry (Fig. 2). The limestone unit of section 8 is at the same topographic level as the outcrop of the fossil-bearing unit at the west end of Paine Quarry. Because the beds at Paine Quarry dip to the south-east, and because the pit of Section 8 is east of the line of strike of the beds at Paine Quarry, the limestone at section 8 may be stratigraphically above the fossil-bearing beds at Paine Quarry. On the surface just west and north of Paine Quarry (Fig. 2) there are numerous subcircular shallow silt-filled gilgais. The depressions (shelves) are separated by slightly raised areas (puffs) formed of concentrated fragments of fossil bone and caprock. These structures are generally similar to the *stony gilgai* of Hallsworth, Robertson, & Gibbons (1955, p. 7), and indicate that there have been relatively recent differential movements of soil particles due to swelling and contraction in response to alternating wet and dry conditions. Since gilgais may extend down as far as 6 feet (*ibid.*, p. 4-9), the limestone that crops out a short distance to the south may be absent here.

At Paine Quarry the sequence contains clasts up to 3 inches across. By far the commonest are smooth rounded white quartz pebbles; there are also minor amounts of rose quartz, subangular metamorphic fragments, some unreduced ferruginous siltstone, and a few rounded clasts of silicified mudstone. All the clasts may be derived from local sources, though the white quartz and mudstone obviously represent a different phase of erosional history from the metamorphic fragments. Perhaps, whatever their source, the clasts were brought into the lake during periods of increased runoff (see also p. 164).

Except for a few well-worn skeletal remains of giant ground-birds at locality V6347 (Hill 1), and the silicified, much abraded bone fragments found at the New Well site (Fig. 4), almost all vertebrate fossils from the Waite Formation were collected at the quarries west of the north-east-trending rise (Fig. 2). From south to north, these quarries are: Paine Quarry (V6345), Rochow localities 1 and 2 (V6349), and Newsome Quarry (V6346). The fossils are found in the green lacustrine beds and, less abundantly, in the overlying red siltstone, which is considered transitional between the two sequences.

Transition. In the deeper parts of the Waite Basin, the lacustrine and fluviatile sequences are separated by a zone of transition, marked by increasing redness, increasing variety of minerals in the sand fraction, and the introduction of montmorillonite into the clay fraction. The zone can be seen in sections 9, 10,

11, and 12 (see Appendix), which were measured in the long low rise west of Hill 1 (Fig. 2). The addition of montmorillonite was demonstrated by X-ray diffractometer determination on units 6 and 7 of section 9 (Paine Quarry). Quartz, calcite, and kaolinite were present in both units, but montmorillonite only in unit 7.

Fluviatile sequence. Around the edges of the basin the sharp contact between the lacustrine and fluviatile sequences may represent a depositional unconformity. Away from the margins, as at Newsome Quarry, the red beds thicken sharply to the east, and at Paine Quarry this thickening is conformable with a 12° eastward dip of the lacustrine beds. Although faintly indicated, the bedding planes of the red transitional deposits at Paine Quarry also seem to dip eastward. Elsewhere, above the transition zone, the red beds seem to be flatlying, and it is probable that the dips observed at Paine Quarry reflect the initial configuration of the basin rather than post- or syn-depositional subsidence. The topographically lowest exposure of the fluviatile beds is at the base of Hill 1, which can be seen (Fig. 4) to be in the deepest part of the Waite Basin.

Fluviatile sediments make up the bulk of the Waite Formation. They are usually found in massive outcrops (Pls 2, 6) with a characteristic steep-sided surface. This probably reflects some sort of subtle lithological control, because well defined horizontal bedding planes are not apparent. Although the steps resemble those produced on the weathered surface of laterites, their upper surfaces are tilted when, as at Hill 3, other strata are demonstrably tilted.

A medium to coarse sand predominates, but there are also frequent conglomeratic units with cobbles up to 6 inches across. The difference in the detailed lithology between the two sides of Hill 6 (Fig. 4) and the irregular conglomeratic units shown in Plate 6a illustrate the lenticular fluviatile nature of the beds. Grainsize and mineral content are very variable, the beds are lenticular, and the fossils abraded; all these characters show that the beds were laid down under a higher energy regimen than that of the underlying green siltstone. They were derived from a laterite: this is demonstrated by the similar red colour, the presence of small blue-black particles in the sediments, and the occurrence of reworked ironstone pellets (units 4 and 6, section 1; Pl. 6b), which are similar to those found in the laterite at the north end of Hill 6. On the other hand, the large number of angular subrounded bedrock clasts indicates that the old lateritic terrain of the source area had been eroded down to bedrock in places. The freshness of the bedrock clasts and other coarse particles in the conglomerate suggests that the Waite Basin was not far removed from the source area, which was probably the Archaean highlands to the south.

Caprock. The hills containing the Waite Formation are all capped by a chalcedonic limestone caprock. Although patchy in places, the replacement of lime by silica is almost complete in the main body of the caprock. The caprock forms massive blocks 5 to 10 feet thick and its surface, which is irregularly pitted, is a dull pearly grey, slightly reddened by limonitic stain. These features, and the decrease of siliceous replacement toward the base of the unit, are similar to those found in the caprocks of the Kalahari Desert (Frankel & Kent, 1938).

The tops of many of the hills near the Alcoota fossil deposits are on about the same level as the caprock overlying the Waite Formation, but instead of Tertiary sediments, these other hills are composed of lateritized and unweathered bedrock. A caprock similar to that covering the Waite Formation was found only on the hills in which the bedrock is covered by laterite.

Since many of the hills around the fossil deposits are at the same level, the area must have remained stable for a long enough time to be reduced to a near-peneplain, and caprock developed by soil-forming processes wherever the substrate was suitably porous. The limestone was apparently replaced by silica at some indeterminable later time.

Limestone caprocks have been developed in diverse terrains in various parts of the world and are often known as caliches. Although the detailed steps in the origin of this rock type have been subject to some dispute, there seems to be a consensus that it represents a Cca-horizon of an old pedocal soil profile, developed in a semiarid to subhumid climate (Brown, 1949, p. 14; Hibbard & Taylor, 1960, p. 24). Such a climate would not affect the red fluviatile sediments of the Waite Formation.

It is also compatible with the siliceous replacement of the limestone of the caprock to form a silcrete. Frankel & Kent (1938, p. 31) postulate that the similar replacement of the caliche in the Kalahari Desert took place on a peneplain surface during torrid seasons of an alternating wet and dry climate.

The second layer of calcium carbonate concentration is less well defined than caprock. It occurs about 30 feet below the top of the sections in the hills east of Ongeva Creek (sections to the right of Hill 1 in Fig. 4). There the rock varies laterally from a dense limestone to a calcareous sandstone, and its vertical position varies from section to section. If the limestone represents a former Cca-horizon, it was developed under the influence of a somewhat rolling topography.

The hills west of Ongeva Creek (left of Hill 1 in Fig. 4) show a thick, massive sequence of conglomeratic sandstone and siltstone, with little secondary enrichment of calcium carbonate other than the final caprock.

History of the Waite Basin

The depositional and climatic history of the Waite Basin may be summarized as follows. In the final phase of laterite formation, the site of the basin was a broad shallow depression bounded by laterite-covered Precambrian gneiss on the west, south and east. The outlet was probably to the north, and the basin itself may have contained a broad stream valley which was part of the north-flowing pre-Sandover River system. Possibly because of uplift in the Archaean highlands, fine-grained red detritus began to be supplied to the basin by streams flowing over the lateritized terrain. The initial site of deposition, at

least in the type area of the Waite Formation, was a lake in which the red colour of the sediment was reduced to green, and even regular bedding was imparted to the deposits. The initial sediments may have been laid down in a climate somewhat similar to that under which the laterite was developed. In view of the chemical precipitates found in various parts of the Waite Formation, however, the beginning of deposition in the basin may indicate that the climate in the area was changing from more tropical to more temperate.*

As erosion cut deeper into the laterite in the source area, the deposits in the Waite Basin began to show greater mineralogical and textural diversity. The basin may have sagged slightly at about this time, and certainly became better drained owing to a gradual lowering of the watertable. This change may have been aided by the gradual onset of a more temperate climate, with seasonal aridity reflected in the freshwater limestone found stratigraphically above the fossil deposits south of Paine Quarry. Such a climate, in conjunction with the better drainage, would preserve the red colour of the incoming sediments. The three major zones of limestone were all probably laid down during periods of seasonal aridity, in conjunction with the periodic slowing down or cessation of deposition. The general even spacing of the limestones in the stratigraphical column also suggests that the bulk of the Waite Formation was deposited in a warm climate characterized by periodic aridity, and that chemical precipitation took place only when the supply of detritus lessened. Deposition of clastic material was probably also spasmodic; and the conglomeratic lenses may have been laid down during periodic floods.

The fluviatile beds may originally have been much thicker than the 60 or 70 feet now preserved, but at some point a well-defined period of erosion produced a relatively flat surface across the basin and on to the surrounding Archaean rocks. On or just below this surface abundant calcium carbonate was precipitated, possibly as part of a pedocal soil profile formed under semiarid to subhumid conditions. After the accumulation of lime and before the final dissection of the area into its present topography, the limestone was largely replaced by silica. The silica was derived from the surrounding area, possibly from previously silicified parts of the laterite profile, and a continuation or slight intensification of the climatic conditions would probably be conducive to silicification.

A small near-vertical fault disrupts the beds of the Waite Formation in Hill 3, and divides the hill longitudinally into a northern upthrown side and a southern

---

* As reported in a letter dated 8 August 1966, from K. H. Edworthy to J. N. Casey of the Bureau of Mineral Resources, up to 345 feet of variably coloured clays were encountered in a stratigraphic test hole (ALCOOTA (BMR) SCOUT No. 1) drilled adjacent to the vertebrate locality V-6345. The deposits have been tentatively dated as Tertiary, and their subsurface presence indicates that the Waite Basin had a considerably longer history than is determinable from the surficial beds discussed herein. It seems likely from the description of these subsurface deposits that the Waite Basin underwent a number of periods of both lacustrine and fluviatile deposition prior to the time when the Alcoota fossils were deposited. Although the actual date of the subsurface deposits is not now determinable, they are probably, at least in part, considerably older than late Miocene and the theoretical upper limit for the age of the laterite in this area should be lowered somewhat. I am indebted to M. D. Plane of the Bureau of Mineral Resources for bringing the above letter to my attention.

downthrown side. Beds on both sides of the fault dip to the south-east, but the dip could be measured accurately only on the upthrown side. On the east end of the hill, the beds strike 210° and dip 15° SE; on the west end, the strike is 236° and the dip 11° SE. At the east end of the hill the apparent vertical displacement of the fault is 5 feet; to the west it dies out in a monoclinal fold in arenaceous limestone.

As a result of the faulting the caprock has been eroded off the upthrown side and slumped on the downthrown side. The slumped block is a massive elongate fractured tabular slab more than 5 feet thick; it is now tilted to the south-east, and its upturned northern edge forms a ridge along the whole crest of the hill (Pl. 3a, b). Thus the full thickness of the Waite Formation at Hill 3, and the extent of the hiatus between the caprock and the beds on which it now rests uncomfortably, are unknown.

Geological History

The geological history of the Alcoota area may be tabulated as follows:

1. *Precambrian to Close of Palaeozoic*: Deposition, folding and intrusion of rocks of Arunta Block, followed by deposition in Proterozoic and Lower Palaeozoic. Major orogeny about end of Ordovician; Archaean exposed by erosion of younger rocks in core of anticlinorium.

2. *Mesozoic and Early Tertiary*: Regional uplift at end of Cretaceous, and probably local uplift in early Tertiary.

3. *Early to Middle Tertiary*: Development of deep weathering profile (laterite) on uplifted terrain after period of stillstand and peneplanation. The laterite formed a broad low dome, sloping in all directions away from the central core, north-east of Alice Springs. Possible silicification of part of the profile, then or later.

4. *Middle Tertiary*: Erosion, probably due to renewed uplift. This resulted in the stripping of most of the laterite and redeposition of the derived sediments in local basins formed in depressions (e.g., the Waite Basin) in the laterite surface. The depressions may have been controlled by pre-existing lines of weakness, because the various late Tertiary sediments and the underlying laterite remnants both seem to occur as old fillings of present-day river valleys.

5. *Late Tertiary*: (a) Relatively quiet period during which the area was peneplaned or nearly so. During this time a pedocal soil may have developed over large areas and a caliche formed from it. (b) At the same time, or later, patchy silicification of the surface and near-surface limestone occurred.

6. *Quaternary*: Dissection and erosion by renewed stream activity due to uplift or increased precipitation or both. Tertiary valleys breached by headward erosion of streams. The present drainage pattern may have been initiated at this time, though the major drainage lines seem to be controlled by long-extent lines of weakness in the bedrock. Small-scale faulting in the Waite Basin may have occurred at this time.

PALAEONTOLOGY

Class REPTILIA

Order CROCODILIA

Family CROCODYLIDAE

CROCODYLUS Laurenti, 1788

CROCODYLUS sp.

(Pl. 7)

Dermal scutes of a probable new species of crocodile are quite common in the deposits at Paine Quarry. The posterior portion of the cranium of a young individual, a right premaxillary, and a left dentary fragment were also recovered.

The cranial fragment, UCMP 70939, consists of the skull table, part of the pterygoids, the suspensorium, and the basicranium. The pterygoids have been crushed into the area of the braincase so that, except for the condyle, the basicranium is largely obscured. The lateral temporal fenestrae have also been constricted by the quadrate, having been pushed somewhat dorsally. The most characteristic features may be seen in the skull table, the dorsal surface of which is thoroughly pitted in the usual crocodilian fashion (Pl. 7). Other than this, it seems that the dorsal surface of the table was flat. The greatest width, measured across the squamosals, is 85.0. The length of the table, from the posterolateral tip of the squamosal to the point opposite which the fronto-postorbital suture meets the orbit, is 62.0. The transverse width across the quadrates is 129.2.

The frontal widens posteriorly to the fronto-postorbital suture. The anterolateral corner of the table is broadly rounded. The lateral edges of the table diverge posteriorly and have a shallow concavity just posterior to the postorbito-squamosal suture. The posterior edge of the table extends inward and slightly anteriorly from each side to meet a central, posteriorly convex, portion 27.4 wide. The supraorbital fenestrae are each about 20.8 long and 15.0 wide and about 15.5 apart. The anterolateral corner of each fenestra is acuminate, but both the lateral and medial borders are gradually rounded. The fronto-parietal suture, which is slightly chevron-shaped, convex posteriorly, barely touches the anterolateral corner of each fenestra. The fronto-parietal suture is 34.9 long.

The postorbitals, subtriangular because of the rounded anterolateral corner, are 28.0 long and 18.5 wide. The squamosals, thickly 'L'-shaped because of the supratemporal fenestrae, are about 36.5 long and 30.0 wide. The parietal is 46.0 long and 34.9 wide anteriorly and 22.4 wide posteriorly. The triangular supraoccipital is 15.0 long and 14.3 wide.

This specimen is small, and apparently belongs to a young individual. Because of the shape and size of the various parts of the crocodile skull may vary con-

siderably with respect to the ontogenetic age it is difficult to place a great deal of weight on features of the skull table in isolated individual specimens such as this one. However, the following comparisons may prove to be instructive. The only species which, on geographic grounds at least, warrant comparison with the Alcoota species are *Crocodylus johnsoni,* the endemic Australian freshwater form, *C. porosus,* a generally marine and brackish water form in the Malaysian area, which also inhabits fresh water in New Guinea, and *C. novo-guineae,* a predominantly freshwater crocodile from New Guinea, the Sulu Archipelago, and the Philippines (data from Wermuth, 1953). Unfortunately, no actual specimens were available for comparison.

The skull table of the Alcoota species is generally like that of *C. porosus,* except that the frontal is not excavated dorsally between the orbits, the frontal does not wedge sharply into the parietal, and the parietal does not extend conspicuously anterior to the supratemporal fenestrae. The shape of the fenestrae in *C. porosus* is shown to be angulate in Wermuth (*ibid.,* Fig. 53), but the fenestrae are more nearly circular in a series of specimens illustrated by Kälin (1933, Pl. 16). The acuminate anterolateral corner of the fenestrae in the Alcoota form is similar to the condition in *C. porosus,* and both of these species differ in this respect from *C. novo-guineae* and *C. johnsoni.* In *C. novo-guineae* the frontals are not excavated as in *C. porosus,* but otherwise the skull tables of the two New Guinea species are similar. Except for having a broad, relatively smooth fronto-parietal suture, the skull table of *C. johnsoni* is much like that of *C. novo-guineae.* Of these three species, the cranial table of the Alcoota form is probably closest to that of *C. porosus.* The fossil seems to differ from all three recent species in the relatively small size of its supratemporal fenestrae, the fact that the parietal does not extend anteriorly beyond the fenestrae, and the relatively large size of the supraoccipital.

The premaxillary, UCMP 70940, is about 41.0 wide and 51.7 long along the midline. Its anterior outline is rather broad. Only one tooth, the third, is in place, but alveoli are present for four more. Thus, of the five premaxillary teeth, 1 and 2 are small and set close together; 3 and 4 are two to three times as large as the first two, while the fifth is small, about the same size as 1 and 2. The teeth are evenly spaced in the premaxilla. The pits which receive the dentary teeth lie internal to the premaxillary teeth. The premaxillo-maxillary suture is broadly W-shaped, if both halves are taken together.

This premaxillary is decidedly unlike the elongate bone in *C. johnsoni,* in which the teeth are all about the same size and are spaced rather far apart. The premaxillo-maxillary suture is more W-shaped in the Alcoota species than in either *C. porosus* or *C. novo-guineae.* In the size relations of its premaxillary teeth, the Alcoota fossil is most like *C. porosus.*

In the dentary fragment, UCMP 70941, the symphysis is 51.8 long and extends back to a level opposite the anterior edge of the fifth tooth. The total fragment is 106.3 long and 27.5 wide across the level of the fifth tooth. The first mandibular tooth is in place, eight other teeth are represented by alveoli. The first three

teeth are relatively small, about the same size, and each is spaced about 5.0 from its neighbour. The fourth tooth is more than twice the diameter of the first three and is accommodated by a slight bulge in the lateral outline of the mandible. The next three teeth, smaller than the first three, are closely approximated to each other, and form a unit which is separated by a space of about 5.0 from the fourth tooth and by a space of 11.5 from the eighth. The eighth tooth is about the same size as 5, 6 and 7. It lies closely adjacent from the ninth, which is slightly larger, about the size of teeth 1, 2, and 3.

The elongate mandible of *C. johnsoni*, with the symphysis extending back to the sixth or seventh tooth, is clearly unlike that of the fossil. On the other hand, except for having an enlarged first tooth, the mandible of *C. porosus* is quite like that of the Alcoota form. This New Guinea species differs, apart from the large first tooth, in having a more pronounced lateral bulge at the tooth 4. The mandible of *C. novo-guineae* was not figured by Schmidt (1928), but apparently the symphysis extends back to a point between the fifth and sixth teeth (*ibid.*, Pl. 181).

It seems, therefore, that the Alcoota crocodile may be more closely related to the forms currently living in New Guinea than to the endemic *C. johnsoni*. In this analysis, characters from the apparently adult premaxillary and dentary are given more weight than those seen in the seemingly juvenile skull table. The fossil material probably represents a new species, but because comparative series of *C. porosus, C. novo-guineae* or *C. johnsoni* are lacking, it is deemed unwise to propose a formal species name at this time.

Class AVES

It was intended that the avian material be described by the late Dr Alden H. Miller of the Museum of Vertebrate Zoology. Shortly before his untimely death Dr Miller informed me that the bulk of the material comprises foot elements of large flightless birds. A small species of *Genrornis* as well as a larger, moa-sized form is present. Other elements pertain to an eagle or hawk-like species.

Class MAMMALIA

Infraclass METATHERIA Huxley, 1880

Order MARSUPIALIA Illiger, 1811

Superfamily DASYUROIDEA Simpson, 1930

Family THYLACINIDAE Bonaparte, 1838

Genus THYLACINUS Temminck, 1824

THYLACINUS POTENS[1], sp. nov.

(Fig. 6-9, Tab. I-III)

Holotype: CPC 6746, a palatal fragment with RM^2-M^4 and LP^2-M^2, preserved. Other teeth are represented by roots and alveoli.

[1]*potens* — powerful. In allusion to the massive character of this large thylacinid.

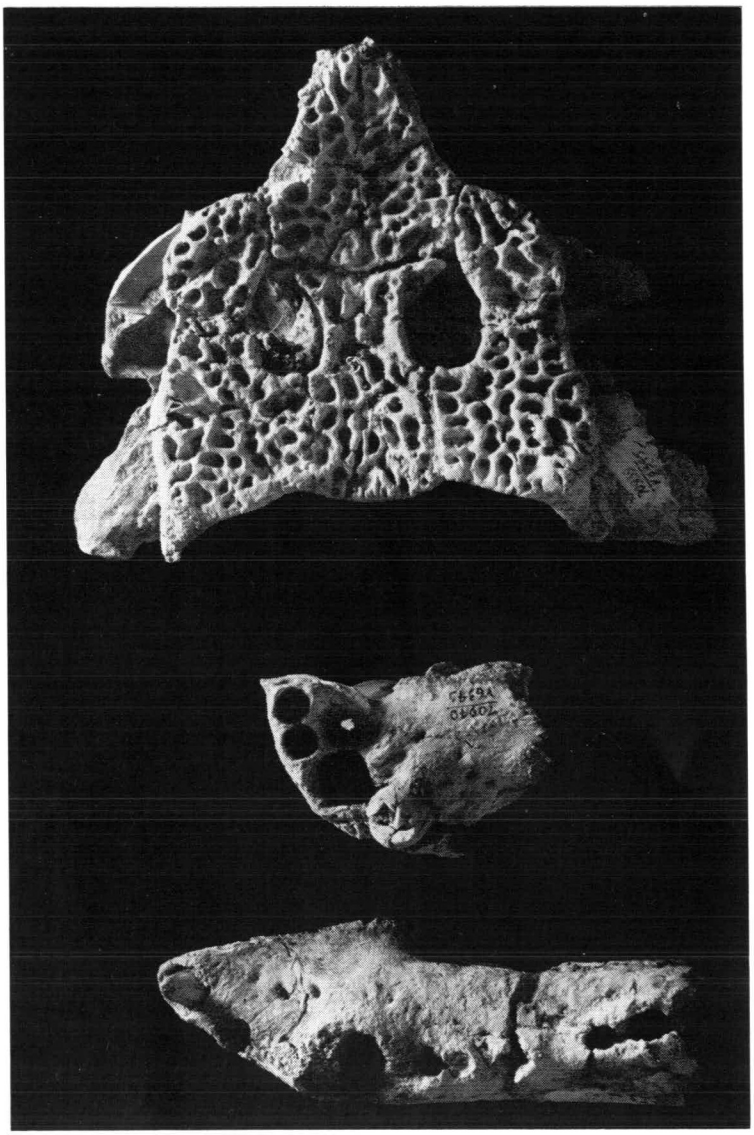

Plate 7. *Crocodylus* **sp.** *Upper:* **Dorsal view of skull table, UCMP 70939. Two thirds natural size.**

Middle: **Palatal view of right premaxillary, UCMP 70940. Two thirds natural size.**

Lower: **Occlusal view of left dentary fragment, UCMP 70941. Two thirds natural size.**

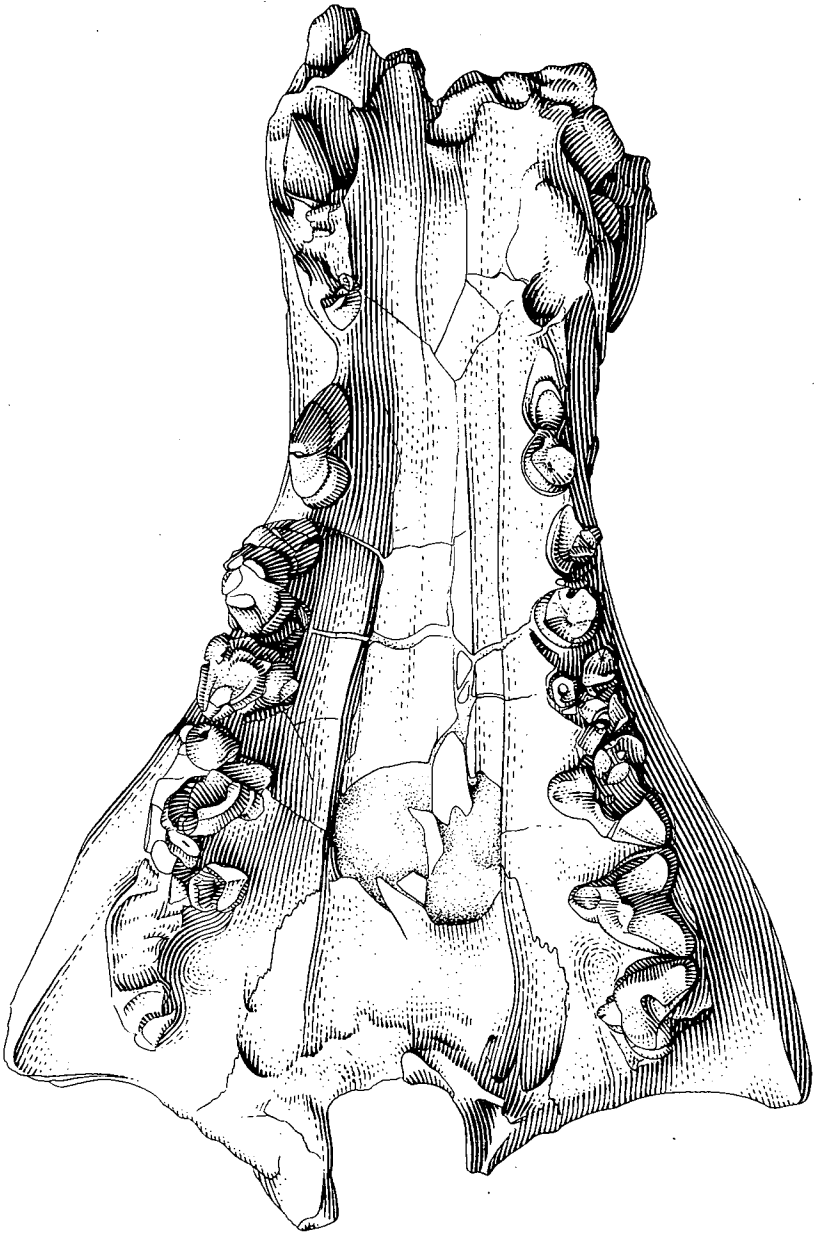

Fig. 6. *Thylacinus potens,* **sp. nov., palatal view of holotype, CPC 6746. Two-thirds natural size.**

Paratypes: UCMP 66971, nearly complete left M^3; UCMP 71012, left M^4 parastyle; UCMP 66199, left lower canine; UCMP 66026, left mandible fragment with M_2-M_4; UCMP 71011, left mandible fragment with P_3-M_1; UCMP 66649, left calcaneum; UCMP 69677, left astragalus; UCMP 69657, partial left Mtt. IV; UCMP 69658, right Mtt. IV; UCMP 69659, partial right Mtt. III.

Specific Diagnosis: Large thylacinid, more massive than *T. cynocephalus* or *T. rostralis;* P^2 and P^3 longer than M^1; premolars slant strongly posteriorly; large (4.0) diastem between canine and P^1; P^2 close to P^3 as in *T. rostralis,* not situated nearly equally between first and third premolars as in *T. cynocephalus;* M^1 nearly equidimensional, transverse width across protocone and parastyle slightly (0.8) greater than length of tooth, not 3.0-4.0 smaller; M^2 and M^3 of nearly same size; except for length of M^1 and length and transverse diameter from protocone to metastyle of M^3, all upper teeth larger by at least 1.0 than corresponding teeth of *T. cynocephalus* and *T. rostralis;* distinct stylar cusp present anterior to metastyle and posterior to labial cleft on M^2 as well as M^3; strong labial cleft in stylar area of M^1-M^2; transverse width from protocone to parastyle of M^3 slightly (0.1 to 0.7) greater than length, rather than about 3.0 smaller; metastylar wing of M^3 relatively small; infraorbital foramen opens above rear of M^1 rather than above rear of M^2 or anterior end of M^3. Palatal fenestrae small relative to size of palate; palate arched slightly longitudinally, with low transverse ridge separating incisive foramina from rest of palate; transverse palatine ridge strongly developed. Mandible massive; talonid of M_3 considerably narrower than trigonid (rather than being about same size as or slightly larger than trigonid as in *T. cynocephalus* and *T. rostralis*); hypoconid of M_4 a high pointed cuspid; teeth small relative to massive jaw.

Type Locality: Paine Quarry, V6345, Waite Formation, 4 miles south-west of Alcoota station, 2.1 miles south-west of junction of Waite and Ongeva Creeks, Northern Territory, Australia.

Age: Alcoota fauna; late Miocene or possibly early Pliocene.

Description of Holotype: The holotype is illustrated in Figure 6. Very little of the lateral snout region of CPC 6746 is preserved. The lateral surface of the maxilla anterior to the zygomatic arch is smoothly convex. There is no suggestion of a constriction of the snout between P^2 and the zygomatic arch, as seen in *Thylacinus cynocephalus.* The infraorbital foramen opens on to the lateral surface of the maxillary slightly anterodorsal to the maxillary base of the zygoma, and about 22.5 above the alveolar border of the posterior root of M^1. In the adult specimens (specimens in which all teeth are emplaced and wear is discernible on at least M^1) of the modern species which have been studied, and in a specimen from the Menindee fauna of New South Wales (UCMP 53038), which will be described in a forthcoming publication by Dr R. H. Tedford, the infraorbital foramen is 7.5 to 17.1 above the alveolar border above the rear of M^2 or anterior end of M^3. The portion of the snout preserved suggests that it would be somewhat triangular in anterior view. The widths of the palate,

measured between the medial surfaces of the posterior roots of the premolars and between the protocone roots of the molars, are 19.0, 21.8, 29.3, 31.4, 36.5, 45.9, 58.9 respectively. The anterior base of the zygoma is quite low, lying just above M^2 and M^3. The large size of the palatal fragment with respect to comparable parts of *Thylacinus cynocephalus* is shown by many features. Thus, the distance from the middle of the posterior root of P^1 to the middle of the protocone of M^4 is 91.3 in the Alcoota fossil, whereas the comparable measurement ranges from 64.2-75.9 in ten adult specimens of the modern species.

The central part of the palate seems to have been somewhat crushed dorsally. The original cross-sectional configuration of the palate may have been a broad U, the central portion being relatively flat, then sloping down to the medial edges of the alveoli of the teeth. The presence of a raised midsagittal ridge is faintly suggested for that part of the palate between the incisive foramina and the palatine fenestrae. The midsagittal ridge is paralleled by a second ridge on each side of the palate, which begins about 6.0 medial to the anterior root of P^3 and extends posteriorly to the region of the small foramina anterior to the transverse palatine ridge. These ridges form the lateral border of the palatine grooves which extend forward from the palatine fenestrae. The ridges and grooves are more robustly developed in the Alcoota species than in later forms. Three small foramina lie on each side of the midline at the anterolateral corners of the palatine vacuities. The most anterior of these is located at the end of the ridge bounding the palatine grooves, about 11.2 lateral to the midline, and seems to extend anteriorly into the palatine bone. The second foramen is located 6.4 posterolateral to the first and seems to be directed posterodorsally. These two foramina are located within a small ovoid depression in the palatine. The lateral rim of this depression separates the first two foramina from a third which is located 6.2 lateral to the second. The second is the largest of the three, and projects dorsolaterally in a pocket which is roofed by a sharp anterolaterally directed lip of bone about 7.4 long. Specimens of *T. cynocephalus* have only one foramen in this region. It projects posteriorly in a nearly horizontal plane into the rather weak postorbital bar, and seems to be analogous in position to the most anteromedial of the foramina in *T. potens*.

The transverse palatine ridge is only partly preserved. It apparently extended at least 3.2 below the general level of the palate, and formed a posteriorly concave bony bar about 3.5 thick which extends across the rear of the palate. This structure is almost absent in *T. cynocephalus*. The inside transverse width of the choanal aperture, the anterior end of which lies 6.5 posterior to M^4, is 17.8.

A pair of palatine fenestrae are found on either side of the midline opposite M^2 and M^3. They are somewhat distorted by fracturing, but the anterior end of the left fenestra lies 43.2 anterior to the choanal aperture, opposite the parastyle of M^2 and 56.8 posterior to the alveolus of P^1. Details are rather poorly preserved in this region, and the dimensions of the fenestrae can only be estimated. The length of that on the right seems to be 16.0, while the width at the anterior end of the left fenestra is 5.0. These fenestrae in the Alcoota fossil are much smaller than found in *T. cynocephalus*. Nine adult specimens of the

modern species at hand have foramina measuring 19.8-28.5 long by 8.6-10.5 wide. In the Alcoota specimens, shallow palatal grooves lead anteriorly from the fenestrae and die out medial to the alveoli of P^1. They do not reach the incisive foramina. The lateral boundary of the grooves is formed by the lateral sagittal ridges mentioned above. The ends of the incisive foramina seem to extend posteriorly to a line passing between the anterior halves of the canine alveoli. A short depression extends posteriorly from these to a line passing between the posterior ends of the canine alveoli. In *T. cynocephalus,* the posterior ends of the incisive foramina terminate between the canine and P^1, and are not associated with a posteriorly extending depression as in *T. potens.* In longitudinal section, the surface of the palate of *T. potens* is arched dorsally in the area between the transverse palatine bar and the anterior end of M^1. Anterior to this the palate is essentially flat except for a broad transverse ridge at the diastema between the canine and P^1. It effectively separates the palatal surface from the depression leading into the incisive foramina. This feature is not present in *T. cynocephalus.*

The tooth rows diverge posteriorly from P^2-M^4. P^1 is situated slightly medial to the canine. This contrasts with the condition in the Tasmanian Wolf, in which the first two and sometimes the third premolars are on a line which extends posteriorly or posteromedially from the canine. In the modern species, the dentition begins to diverge markedly at M^1 rather than at P^2. The medial edges of the canine alveoli are 21.4 apart, while those of P^1 are 19.0 at the posterior root. Corresponding transverse measurements between the medial edges of the posterior roots of the remaining premolars are: P^2, 21.8; P^3, approximately 29.3. The transverse distances between the alveoli of the roots supporting the molar protocones are: M^1, 31.4; M^2, 36.5; M^3, 45.9; M^4, about 58.9. Similar measurements between the molars in *T. cynocephalus* are from 10 percent to 20 percent smaller, while those taken between the premolars are about the same in both species. This indicates that the width of the palate at the last molar is greater relative to the width between the premolars in *T. potens* than in *T. cynocephalus.* The length of the diastema between the canine and P^1 is about 4.0; that between P^1 and P^2 is 6.6; that between P^2 and P^3 is only 1.5. The situation in *T. cynocephalus* is often the reverse of that in the Alcoota form. In *T. potens* the diastemata generally increase in length posteriorly and P^2 is more nearly equally spaced between P^1 and P^3. Although not clearly determinable because of the disruptive effects of calcite which encrusted the bone, P^1 seems to have been two-rooted, as are P^2 and P^3. All the molars are three-rooted, the internal and posterior roots of M^4 being set quite close together. The massiveness of the premolars increases progressively posteriorly. P^3 is conspicuously larger than M^1; while M^1 is smaller than M^2. M^2 is essentially the same size as M^3. M^3 is larger than M^4. The lengths of the premolar alveoli are: P^1, 14.5; P^2, 16.4; P^3, 19.0.

There is a deep pit in the palate between the protocone alveoli of M^4 and M^3. A similar, but shallower, pit occurs between the protocone alveoli of M^3 and M^2, but not between M^2 and M^1. A similar situation occurs in the Tasmanian Wolf, except that an additional pit occurs between M^1 and M^2.

Dentition: The incisor-bearing portion of the snout is missing. The canine and P^1 are only represented by poorly preserved alveoli. P^2 on the right side is nearly complete. Its single cusp is inclined markedly posteriorly and is situated over the central portion of the tooth. Its anterior surface slopes on to that of the anterior root; its posterior surface is nearly vertical, and extends to a shelf which projects abruptly posteriorly over the posterior root. The main transverse axis of the tooth slants posteroventrally to a greater degree than in *T. cynocephalus*. The length, measured at the base of the enamel, is 5.5. All measurements are approximate because of the cracks which penetrate the tooth.

P^3 is best preserved on the right side, but even this is highly fractured. The configuration of P^3 seems to have been like P^2, but P^3 is considerably larger and more massive. The approximate length of the tooth at the base of the enamel is 16.0; the approximate width is about 8.8. As in P^2, the main axis of P^3 seems to slant strongly posteroventrally.

The right M^1 is equally fractured in addition to being well worn. Enough of the pattern remains to indicate that the paracone and metacone were both present and distinct. The metacone is larger than the paracone. The metastyle is longer and larger than the parastyle. The labial surface of the stylar area is relatively flat, as is the posterolingual surface of the tooth between the metastyle and protocone. The presence or absence of the small stylar cusp found anterior to the tip of the metastyle in M^1 of *Thylacinus cynocephalus* cannot be determined in this specimen. The anterior border of the tooth was apparently emarginated between the parastyle and protocone. The protocone is mostly broken, but its main axis slants anterolingually in occlusal view. The transverse diameter of the tooth across the protocone and parastyle is about 12.8; that across the protocone and metastyle is 13.5. The length of the tooth across the stylar cusps is about 12.0.

M^2 is larger than M^1. The transverse diameter across the protocone and parastyle is about 13.9; that across the protocone and metastyle is 17.5. The length is about 15.7. The labial surface of M^2 between the parastyle and metastyle is more sharply emarginated than in M^1 and more so than in the modern species of *Thylacinus*. The posterolingual surface between the metastyle and protocone is slightly convex with a small emargination just labial to the posterior base of the protocone. The anterior surface of the tooth is distinctly emarginated between the parastyle and protocone. The basal outline of the protocone is broadly U-shaped: it is not constricted at its point of attachment to the body of the tooth as in some specimens of *T. cynocephalus*. The occlusal axis of the protocone, taken as the line passing through the transverse valley between the paracone and metacone and through the apex of the protocone, is directed less anteriorly than in M^1 and more so than in M^3. The protocone bears antero- and posterolabially directed crests. Each extends to the base of the longitudinal depression separating the protocone from the labial cusps and connects to one of a pair of ridges which extend lingually from the apices of the paracone and metacone, respectively. The greatest longitudinal dimension of the protocone is 6.4. The transverse distance from the bottom of the pit between

the protocone and the base of the labial cusps and the lingual base of the protocone is about 4.7. The tooth is broken to the extent that the paracone and much of the parastyle are missing. Enough of the metastyle is preserved to show the concave profile of the ridge which passes anterolingually between the posterior tip of the metastyle and the apex of the metacone. A second, similarly concave ridge passes along the labial edge of the ectoloph, and ends in the posterior half of a small cusp which corresponds to the stylar cusp found posterior to the labial cleft in M^2 of *T. cynocephalus*.

M^3 is of similar size, but is less massively constructed than M^2. This is in sharp contrast to *T. cynocephalus,* in which M^3 is conspicuously larger than M^2. The transverse diameter across the protocone and parastyle is 15.9. That across the protocone and metastyle is 19.0. The length across the stylar cusps is 15.2. The greatest longitudinal dimension of the protocone is 6.1. The lingual base of the protocone is 3.9 lingual to the base of the pit between the protocone and the labial cusps. A small anterior cingulum is found between the tip of the parastyle and the emargination between the parastyle and protocone. This emargination is less pronounced than in M^2. There is no posterior cingulum, but in comparison with M^2, the emargination between the metastyle and protocone seems more pronounced in M^3, possibly because of the relatively smaller mass of its protocone as compared to the rest of the tooth. As in M^2, the labial emargination of the tooth is more strongly developed than in *T. cynocephalus.* The basal outline of the protocone seems to be more V-shaped in M^3. The occlusal axis of the cusp, as defined for M^2, passes more lingually and less anteriorly in M^3. The stylar 'wings' are of more nearly equal size in M^3 than in M^2. The metacone is higher than the paracone. The anteroposterior distance between the crests of the ridges which traverse the lingual faces of the paracone and metacone is less than in M^2 (4.0 for M^2, 3.3 in M^3). A pair of concave ridges, one connecting the parastyle to the anterior edge of the paracone and the other connecting the parastyle to the labial face of the paracone, delineate an ovoid wear surface similar to that developed between the metastyle and metacone. A small stylar cusp is situated midway between the metacone and metastyle. There is no comparable cusp in this tooth in the modern species.

M^4 is an obliquely oriented tooth in which the metacone has been lost and the metastylar wing has been reduced. Only the protocone, paracone, parastyle, and reduced metastyle remain. The tooth is rather poorly preserved in that a large piece of the ectoloph has been broken away posterolabial to the paracone and the enamel covering has been eroded off the protocone. The parastyle forms a sharp cusp at the anterolabial corner of the tooth. It connects to the tip of the paracone by a posterolingually directed crest. The crest from the parastyle is directed toward the protocone, and the paracone is situated somewhat anterolingual to it. The anterolingual wall of the tooth between the parastyle and base of the paracone is devoid of a basal cingulum in the holotype but not in UCMP 71012. The anterolingual surface slants toward the apex of the paracone. The lingual wall of the paracone passes anteroposteriorly at nearly a right angle to the anterior wall. The body of the crown above the posterolabial root is, in this stage of wear, about 4.2 above the base of the enamel and is nearly at

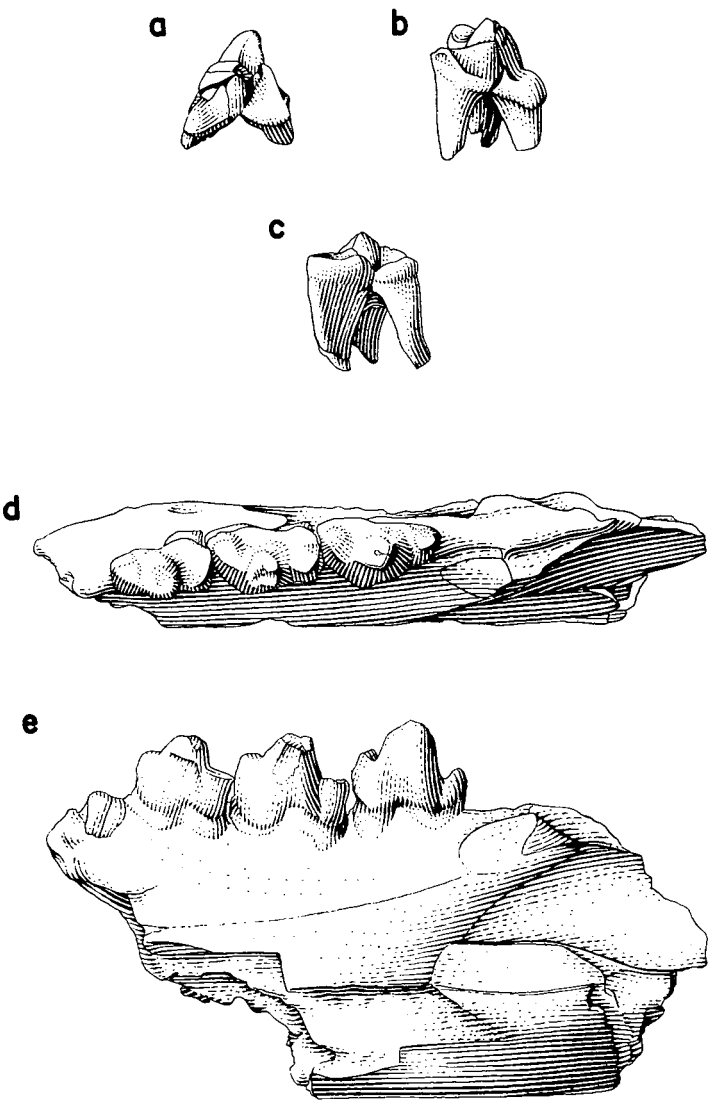

Fig. 7. *Thylacinus potens,* **sp. nov., a, occlusal view; b, anterior view; c, labial view of LM^3 UCMP 66971. d, occlusal view; e, lateral view of left mandible fragment, UCMP 66026. Two-thirds natural size.**

the same level as the tip of the paracone. Although poorly preserved, this portion of the tooth is rather cusp-like in occlusal view.

The portion of the stylar area of the tooth which remains suggests that the labial surface was rather straight, although obliquely oriented, and that the posterolabial surface of the tooth sloped anterolingually toward the crest between the paracone and parastyle.

The protocone is present, although it is considerably reduced relative to the rest of the tooth. In occlusal view the axis of the protocone is directed slightly posterolingually, but less so than in *T. cynocephalus*. Enough remains of the protocone to indicate that it formed a distinct cusp, but the material is insufficient to determine whether a pair of transverse ridges extended from the apex to the paracone and metacone, as in M^2 and M^3.

The approximate distance from the parastyle to the protocone is 15.8; the distance from the metastyle to parastyle is 12.2. The distance across the protocone and metastyle is 9.9. The transverse distance from the lingual base of the paracone to that of the protocone is about 2.9. The anteroposterior length of the protocone, as measured at its junction with the base of the paracone, is about 3.9.

Paratypes (Fig. 7): The isolated M^3, UCMP 66971, is complete except for the apices of the paracone and metacone and a small piece of the metastylar wing. The tooth is identified as M^3 because the parastylar wing makes nearly a straight angle with the anterior wall of the protocone, the metastylar wing is relatively slender transversely and the protocone is smaller relative to the rest of the tooth than in M^2. The specimen is in about the same stage of wear as the left M^3 of the type and differs from it mainly in having a protocone with a smaller anteroposterior diameter (5.9 to 6.1) and a larger transverse diameter (4.2 to 3.9), as measured from the lingual base of the cusp to the bottom of the pit lingual to the paracone. See Table 1 for measurements.

Both the isolated tooth and M^3 of the type have a suggestion of a small stylar cusp posterolabial to the metacone and posterior to the labial cleft between the parastylar and metastylar wings. This cusp is not present in M^3 of *T. cynocephalus*.

Table 1 shows the results of a series of measurements which were made on a number of specimens of *Thylacinus cynocephalus*. Corresponding measurements for *T. potens* are included for comparison. As indicated by Ride (1964, p. 106) *T. cynocephalus* shows strong sexual dimorphism with respect to size. Since the sex was determined for only five of the sixteen specimens of *T. cynocephalus* available for this study, it was necessary to treat the sample as a single entity. This accounts for the rather high coefficient of variation (V) calculated for some of the dimensions in Tables 1 and 2.

Some of the data in Tables 1 and 2 are presented graphically in Figures 8 and 9. From Table 1 and Figure 8 it is clear that *T. potens* differs from *T. cynocephalus* in actual size in most tooth dimensions as well as in the relative proportion of parts of a tooth to each other, and also to comparable parts of other teeth. Thus, the premolars of *T. potens* are not only actually larger than those of *T. cynocephalus,* but are also relatively much larger as compared to the size of the molars. M_1 of *T. potens* is actually larger in all three parameters measured than in *T. cynocephalus*. More conspicuously, however, the transverse diameter of the tooth measured between the protocone and parastyle is about the same as its other parameters in *T. potens,* while in *T. cynocephalus,* the

transverse diameter is much less than in the other dimensions of the tooth. M^2 of *T. potens,* on the other hand, is actually larger than, but of about the same proportions as, the same tooth in *T. cynocephalus.* In the length from the parastyle to the metastyle and from the protocone to metastyle of M^3, *T. potens* is similar to *T. cynocephalus.* The two species differ conspicuously, however, in that the protocone-parastyle length is about the same as that from the parastyle to the metastyle in the Alcoota fossil, but in the Tasmanian Wolf, the protocone-parastyle length is very short. Like M^2, M^4 of the Alcoota fossil is larger than, but of similar proportion to, that of the later species.

UCMP 66206 is a left mandible fragment in which M^2-M^4 and the anterior portion of the masseteric fossa are preserved. The inner surface of the mandible is somewhat crushed and is largely eroded away. The specimen was found at the base of unit 7 in Paine Quarry in the red siltstone immediately above the green lacustrine beds and is somewhat leached. This has resulted in the loss of much of the original enamel surface; the major features, however, are still clear.

TABLE 1

Comparison of upper tooth dimensions in *Thylacinus potens* sp. nov., with a series of *Thylacinus cynocephalus* (Harris).

Comparison of lower molar and jaw dimensions of *Thylacinus potens,* n. sp., with a series of *Thylacinus cynocephalus* (Harris).

		Thylacinus cynocephalus					*Thylacinus potens*	
Character		$\overline{X}$	OR	N	S	V	CPC 6746	UCMP 66971
P^1	L	6.2 ±.105	5.5–7.0	16	.420 ±.074	2.848 ±.403		
	W	3.3 ±.065	2.9–3.7	16	2.88 ±.050	8.545 ±1.510		
P^2	L	8.3 ±.125	7.4–9.3	16	.500 ±.088	6.024 ±1.065	12.4	
	W	3.8 ±.061	3.4–4.2	16	.224 ±.039	5.844 ±1.040	5.5	
P^3	L	10.6 ±.145	9.8–11.7	15	.582 ±.106	5.494 ±1.003	16.0	
	W	5.0 ±.081	4.5–5.7	16	.326 ±.058	6.514 ±1.51	8.8	

TABLE 1 (Continued)

Character		*Thylacinus cynocephalus* $\overline{X}$	OR	N	S	V	*Thylacinus potens* CPC 6746	UCMP 66971
M^1	L	10.9 ±.113	10.3–11.8	15	.436 ±.079	3.998 ± .730	12.0	
	W_1	7.8 ±.115	7.2–9.1	15	.447 ±.082	5.733 ±1.047	12.8	
	W_2	11.5 ±.113	10.8–12.4	15	.439 ±.080	3.820 ±0.697	13.5	
M^2	L	13.2 ±.159	12.1–14.6	16	.639 ±.113	4.841 ±0.856	15.7	
	W_1	10.0 ±.109	9.3–10.5	16	.436 ±.077	4.358 ±0.770	13.9	
	W_2	15.0 ±.147	13.8–16.2	16	.668 ±.118	4.457 ±0.788	17.5	
M^3	L	15.1 ±.173	13.7–16.0	15	.669 ±.128	4.636 ±0.846	15.2	14.6
	W_1	12.0 ±.172	10.6–13.2	15	.668 ±.122	5.565 ±1.016	15.9	14.7
	W_2	17.8 ±.248	15.9–19.1	15	.949 ±.173	5.331 ±0.973	19.0	17.5
M_4	L	9.7 ±.249	8.3–10.7	10	.787 ±.176	8.113 ±1.814	12.2	
	W_1	12.6 ±.372	10.5–13.9	10	1.177 ±.263	9.341 ±2.089	15.8	
	W_2	7.8 ±.310	6.2–8.8	10	.980 ±.219	12.568 ±2.810	9.9	

Right tooth is measured except where left is only tooth represented, or happens to be at the highest or lowest extreme of the observed range for the series.

$\overline{X}$ = mean; OR = observed range; N = number measured; S = standard deviation; V = coefficient of variation; L = length; W = transverse width; W_1 = width, protocone to parastyle; W_2 = width, protocone to metastyle.

TABLE 2

Comparison of lower molar and jaw dimensions of *Thylacinus potens*, n. sp., with a series of *Thylacinus cynocephalus* (Harris).

		Thylacinus cynocephalus					*Thylacinus potens*
Character		$\bar{X}$	OR	N	S	V	UCMP 66206
M_2	L_1	12.0 ±.127	11.3–13.0	15	.493 ±.090	4.104 ±0.749	13.0
	W_1	5.7 ±.072	5.2–6.1	15	.279 ±.051	4.895 ±.0894	6.8
	W_2	6.2 ±.102	5.5–6.8	15	.394 ±.072	6.350 ±1.159	6.8
	L_2	3.6 ±.081	3.1–4.5	15	.313 ±.057	8.700 ±1.589	4.0
M_3	L_1	14.0 ±.143	12.9–15.3	15	.554 ±.101	3.957 ±0.723	14.5
	W_1	6.9 ±.105	6.2–7.6	15	.395 ±.072	5.725 ±1.045	8.3
	W_2	6.8 ±.165	5.4–7.7	15	.627 ±.114	9.218 ±1.686	6.2
	L_2	4.1 ±.089	3.6–4.8	15	.348 ±.063	8.488 ±1.531	3.4
M_4	L_1	16.0 ±.229	14.4–17.3	13	.826 ±.162	5.162 ±1.012	15.4
	W_1	7.8 ±.138	6.8–8.4	14	.515 ±.097	6.602 ±1.248	8.8
	W_2	4.3 ±.171	3.3–5.3	12	.592 ±.121	13.767 ±2.811	5.1
	L_2	2.9 ±.114	2.3–3.7	13	.410 ±.080	14.138 ±2.773	3.5
M_4*		28.6 ±.958	23.0–33.3	10	3.028 ±.677	10.608 ±2.374	37.0

Right teeth were measured except where left was the only tooth represented or happened to be at the highest or lowest extreme of the observed range for the series.

$\bar{X}$ = mean; OR = observed range; N = number measured; S = standard deviation; V = coefficient of variation; L_1 = anteroposterior length; W_1 = width across trigonid; W_2 = width across talonid; L_2 = length of talonid.

* Depth of jaw just behind M_4.

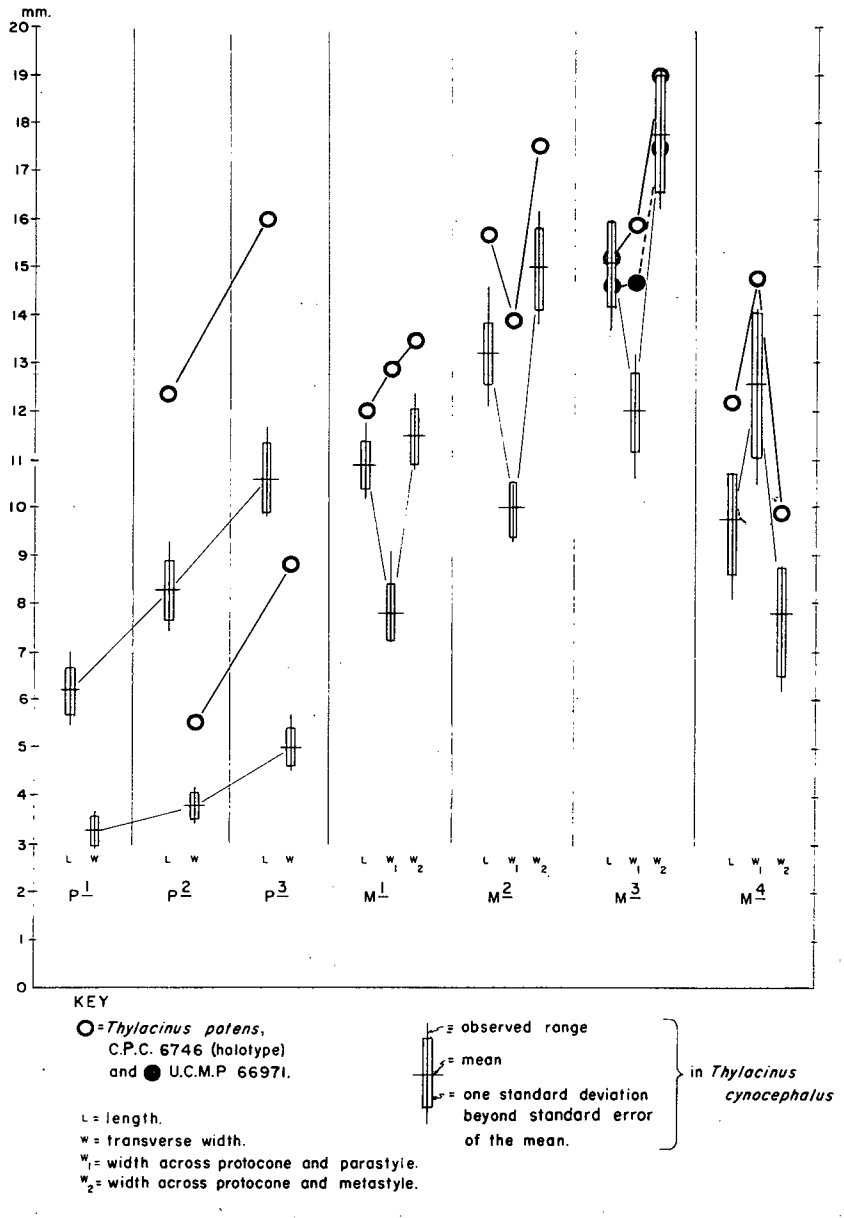

Fig. 8. Upper tooth dimensions in *Thylacinus potens* sp. nov., and a series of *Thylacinus cynocephalus*.

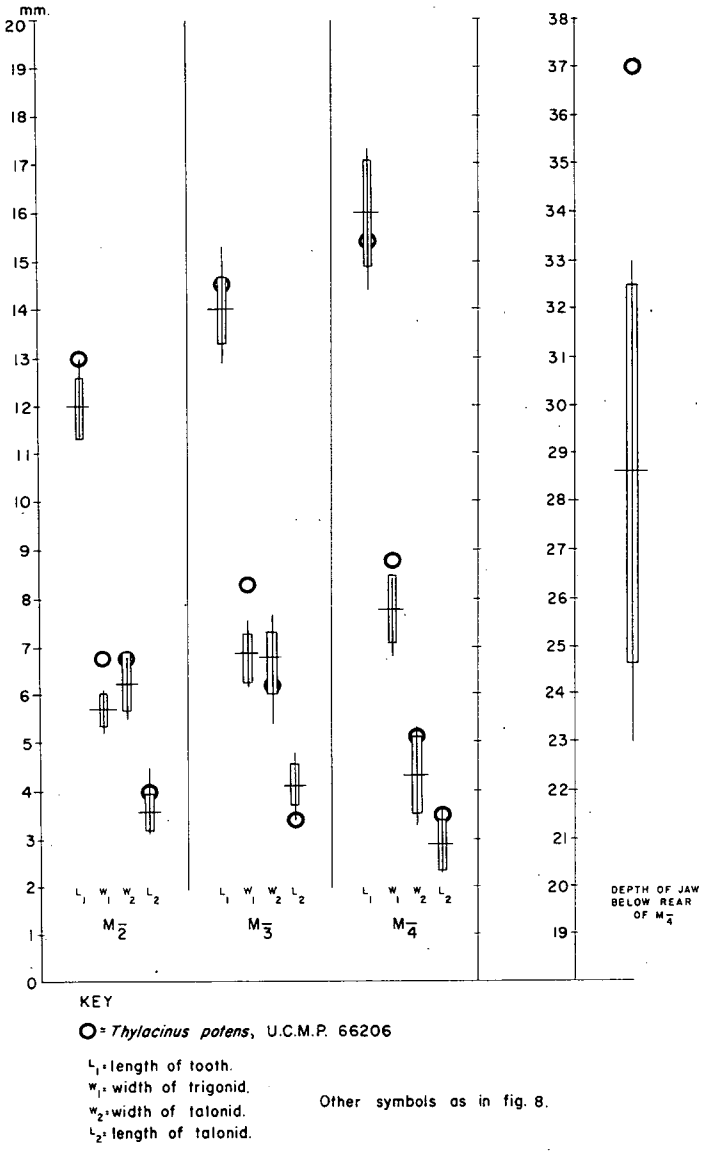

Fig. 9. Lower molar and jaw dimensions in *Thylacinus potens* sp. nov., and a series of *Thylacinus cynocephalus*.

The anterior tip of the masseteric fossa is about 19.0 below the alveolar border of the posterior root of M_4 as compared to 12.7-15.1 in seven adult specimens of the modern species. The ventral border of the fossa is parallel to the ventral edge of the jaw, which is oriented horizontally for the purposes of this discussion. The dorsal border of the fossa rises posterodorsally at an angle of about 40° with respect to the ventral border. The dorsal rim of the masseteric fossa continues anteriorly as a slightly raised ridge which descends progressively anteriorly. In UCMP 66206, the ridge lies 15.0 below the alveolar border of the anterior root of M^2. The surface of the mandible dorsal to the ridge and ventral to the alveoli is smooth and gently concave as seen in anterior view. The depth of the mandible measured just posterior to the talonid of M_4 is 37.0 as compared to 28.0-33.3 for seven adult specimens of *T. cynocephalus*. This measurement may be too small because the mandible may have been slightly crushed dorsoventrally. The lateral surface of the mandible below the masseteric fossa slopes sharply ventromedially at an angle of about 55°. This, as well as the transverse thickness of the jaw below the rear of M_4 (16.0), may be exaggerated somewhat by the suggested slight dorsoventral crushing, but it is nevertheless clear that this specimen is more robust than any Recent specimen examined as well as the small thylacinid from Lake Menindee (UCMP 53038). However, the angle at which the surface of the jaw slopes medially below the fossa is similar to that seen in *T. cynocephalus*.

The three teeth preserved in this specimen are set close together; the paraconid of M_3-M_4 projects lingual to the entoconid of the preceding tooth. The axes of the roots and of the cuspids in all of the teeth slant posterodorsally at an angle of about 10° from a vertical line, and the wear surface developed across the tops of the cuspids is essentially perpendicular to this. The posterior slant of the teeth is greater than in the Menindee thylacinid but is equalled in some Recent specimens. M_2 is about 13.0 long and 6.8 wide across both the trigonid and talonid; the basal outline of the tooth is thus essentially rectangular. Owing to the posterior slant of the tooth the paraconid is higher than the talonid. The worn tip of the paraconid is 5.2 above the basal enamel; the talonid is 4.9 above it on the labial side, and about 3.0 above on the lingual side. The longitudinal length of the talonid is 4.0. In this stage of wear the occlusal surface of the paraconid is flat. The cusp is situated anterolingual to the protoconid and is connected to the anterior side of that cusp by a posterolabial ridge. The anterolabial shearing surface of the tooth slants outward and downward to the base of the crown. The protoconid is the largest cusp of the tooth. It is essentially circular in occlusal view and is situated about midway along the tooth. The occlusal surface of the paraconid projects anterolingually from the anterior surface of the protoconid and the occlusal surface of the talonid projects posteriorly but is offset slightly lingually from the posterior surface of the protoconid. In this stage of wear the talonid is a nearly featureless flat surface which is developed across almost the total width of the tooth. The labial surface of the talonid slants ventrolaterally toward the base, but the remaining sides are essentially vertical. The hypoconulid forms a small spur at the posterolingual corner of the talonid which is slightly impressed into the anterolabial base of the paraconid of M_3.

M_3 is not as heavily worn as M_2 and its morphology is closer to that of M_4. M_3 is 14.5 long. Its trigonid is 8.3 wide and its talonid 6.2; the tooth is thus not rectan-

gular in occlusal outline. It is more expanded at the base of the protoconid than in *T. cynocephalus*. The trigonid tapers anterolingually from the protoconid to the paraconid. The protoconid-paraconid shearing surface is steeper than in M_2 and does not slant anterolabially toward the base as steeply as in M_2. There is only a faint suggestion of a cingulum at the base of this surface. The paraconid connects to the protoconid by means of the shearing ridge along the anterolabial surface of the tooth but is otherwise separated from the protoconid by a posterolingually directed valley which deepens toward the lingual base of the trigonid. In this stage of wear (less worn than M_2) the protoconid has a bluntly triangular outline, the apex of which points posterolingually. In lateral view, the protoconid occupies a relatively greater portion of the crown than in M_2, the talonid in particular being comparatively smaller than that in the second molar. The talonid of M_2 is also transversely reduced relative to those in *T. cynocephalus*. The hypoconid bears an anterolingual crest which attaches to the mid-longitudinal base of the protoconid. A nearly crescentic wear surface, concave anterolingually, is developed on the talonid of M_3 and is continuous from the lingual ridge of the hypoconid through the hypoconid and entoconid. The entoconid occurs as the lingual tip of the occlusal crescent, while the hypoconulid forms a slight posterior spur labial to the entoconid. A steep shallow valley or indentation occurs on the labial half of the talonid anterior to the hypoconid and posterior to the posterolabial base of the paraconid. The worn tip of the paraconid lies about 5.1, that of the hypoconid 5.6 and that of the entoconid 2.4 above the base of the enamel. The anteroposterior length of the talonid is 3.4.

M_4 is the largest of the lower molars preserved in this specimen. It is 15.4 long, the trigonid is 8.8 wide, and the talonid is 5.1 wide and 3.5 long. The proportion of the total crown occupied by the talonid is smaller in M_4 than in M_2 or M_3. The tooth tapers anterolingually from the body of the protoconid to the paraconid, and even more conspicuously posteriorly to the tip of the talonid. The steep anterolabial paraconid-protoconid shearing surface is as in M_3, and except for being larger and more massive, the configuration of the trigonid of M_4 is much like that of the preceding tooth. The talonid is reduced to a single cuspid, probably the hypoconid. It connects by a small longitudinal ridge to the posterior surface of the protoconid. On either side of this ridge, a shallow valley descends to the base of the tooth and separates the talonid from the trigonid. The paraconid rises 6.8 above the base of the enamel. The hypoconid, nearly unworn in the tooth, is 3.0 above the base of the crown. It is more clearly separated from the trigonid than in modern specimens of *Thylacinus,* and projects higher from the base of the crown.

From Table 2 and Figure 7 it can be seen that *T. potens* has a longer M_2 and a greater trigonid width of M_2-M_4 than in *T. cynocephalus*. Also, in *T. potens* the trigonid of M_2 is as wide as the talonid rather than being usually narrower, and the trigonid of M_3 is much wider than the talonid instead of being about the same size. The lower molars of *T. potens* are similar in size to, but different in some proportions from, those of *T. cynocephalus*. As the upper molars are small relative to the size of the snout fragment, so the lower molars are small relative to the large, massive lower jaw fragment. The other mandible fragment, UCMP 71011, is poorly preserved and contributes little to the morphology of *T. potens*. The left

lower canine, UCMP 66194, is larger than in *T. cynocephalus* and *T. rostralis*. The anteroposterior length at the base of the enamel is 9.3. The width is 6.8.

UCMP 66649 is a left calcaneum which is considerably more massive than and nearly twice as long as the calcaneum of the small thylacinid from Lake Menindee, but is nearly the same size as that of a Recent male specimen, AMNH 35744. In dorsal view the shaft of the calcaneum narrows to a transverse width of 8.8, 16.6 anterior to the tuber calcanii then widens slightly to the rear of the astragalar facette. The astragalar facette is situated asymmetrically on the shaft and projects conspicuously medially. The medial portion of the facette is a dorsally concave flange, with a sharp posterior and lateral edge, which slopes smoothly anteriorly and slightly laterally to the medial side of the cuboid facette. In contrast to this, the medial astragalar facette of *T. cynocephalus* is a sharp medial projection which is separated by a strong indentation from the medial border of the cuboid facette. The dorsal surface of this portion of the facette slants somewhat ventromedially and is separated from the more lateral portion by a longitudinal ridge, which is also concave dorsally. The lateral portion of the facette consists of a posterior condyloid swelling anterior to which is a longitudinally elongate dorsally concave pit. In *T. cynocephalus* the lateral condyloid portion is separated from the medial projection by a shallow valley. This valley is nearly absent in *T. potens*. Also, the pit anteromedial to the condyloid process in *T. cynocephalus* is not as elongate as in *T. potens*. Lateral and 6.6 ventral to the posterior knob of the astragalar facette is a longitudinal flange which projects slightly laterally over the surface of the shaft and bears three small ovoid pits. The most posterior of the pits is almost directly below the lateral edge of the posterior knob of the astragalar facette. A small portion of the bone is missing anterior to the foremost of the three pits, but the lateral flange bearing them seems to blend anteromedially with the broadly rounded dorsolateral border of the shaft just posterior to the lateral edge of the cuboid facette. A similar series of pits is found in *T. cynocephalus*. In dorsal view, the outline of the cuboid facette is concave anteromedially, the anterolateral edge being the most anterior point of the calcaneum. Both the cuboid facette and the astragalar facette are wider relative to the length of the shaft in *T. cynocephalus* than in *T. potens*. At the posterior end of the shaft, a small valley separates a higher lateral from a lower medial boss. These bosses, absent in the modern form, are found at the lateral and medial corners of the dorsal extremity of the tuber calcanei, and are the only conspicuous features on this part of the shaft.

In posterior view the tuber has an asymmetrical heart-shaped outline, the lateral half of the 'heart' being higher than the medial. The tuber is relatively narrower than in *T. cynocephalus*. The posterior surface is gently convex and, except for a slight ventrally directed extension of the valley between the two dorsal lobes, is devoid of distinctive characters.

In anterior view the long axis of the ovate, anteriorly concave cuboid facette is directed transversely and slightly dorsomedially. Except for the astragalar facette, the cuboid facette is the broadest feature on the shaft. There is no facette for articulation with the navicular. Just medial to its mid-transverse point the cuboid facette is joined by the prominent ventral longitudinal ridge. The cuboid facette in

T. potens is more regularly ovoid than in *T. cynocephalus,* in which the lateral portion is distinctly higher than the medial portion.

The ventral longitudinal ridge extends the complete length of the shaft and is slightly wider at the posterior tubercle. The outline of the medial portion of the astragalar facette, as seen in ventral view, is concave anteromedially, this portion of the facette having its greatest lateral extent at its posterior border. The lateral outline of the lateral flange, as seen in this view, is broadly convex laterally.

TABLE 3

Comparative Measurements of Calcanea of *Thylacinus potens* and *T. cynocephalus*

	Thylacinus potens	*Thylacinus cynocephalus*		
		Recent AMNH 35744		*Fossil form,* Lake Menindee, N.S.W.
Greatest AP length	50.9	43.7	44.2	31.2
Greatest width across astragalar facette	21.1	19.3	19.5	13.0
AP length of astragalar facette to anterolateral edge of cuboid facette	24.8	20.0	20.6	15.5
Greatest width, cuboid facette	16.5	16.8	17.0	11.4
Greatest height, cuboid facette	11.2	9.0	9.0	8.2
Greatest height, tuber calcanei	18.0	15.5	15.0	10.9
Width, tuber calcanei	12.2	12.7	12.3	8.3
Vertical height through posterior swelling of astragalar surface	19.4	16.4	16.7	

The major feature visible in medial view is that portion of the astragalar facette which is supported by a posteroventrally convex sustentaculum. Ventral to the sustentaculum a slight groove extends toward the tuber calcanei, parallel to the ventral edge of the shaft, which is slightly convex ventrally. The dorsal flange of the astragalar facette overhangs a small pit just medial to the posterior knob of the facette. This pit is not developed in *T. cynocephalus.* A small groove extends posterodorsally and slightly laterally from the pit onto the dorsal surface of the shaft posterior to the astragalar facette.

The three small pits described above are visible in lateral view. They are supported by the lateral flange, which is composed of an anterior and a posterior limb. The anterior limb supports the second and third pits and descends slightly an-

teriorly. The posterior limb bears the first pit and descends slightly posteriorly. In the modern form the posterior part of the flange is flat and lies about 1.5 below the anterior part, which is also flat. A small nutrient foramen is found 4.5 below the posterior edge of the foremost pit on the anterior limb of the fibular flange. The dorsal surface of the shaft is only slightly concave posterior to the astragalar facette. The ventral surface of the shaft below the astragalar facette is convex; posterior to this it is convex. Unfortunately, comparative Recent material was not available for the astragalus and metatarsals at the time of this study. The general size of these elements is compatible with their association with the calcaneum of *T. potens*. In comparison with elements belonging to a small fossil thylacinid from the Lake Menindee fauna, the heavier, more massive construction of the Alcoota material is evident. In comparison with photographs taken of the left pes of AMNH 42259, a Recent *T. cynocephalus,* the metatarsal elements of the Alcoota species are only slightly longer, but are more massive. The greatest length of the astragalus is 20.9, and the greatest width 21.8. The length of UCMP 69658, the complete right Mtt. IV, is 66.2. The width and height of its proximal facette are 9.2 and 12.5. The greatest depth of the shaft is 10.4, measured 11.0 anterior to the distal surface. The thickness of the shaft at this point is 6.8. The width of the distal tip of UCMP 69658 is 10.8, the height is 9.4.

Discussion: The Alcoota specimens have been assigned to the genus *Thylacinus* because its features correspond, in general, to those of the modern species: the elongate rostrum; the complete, uncrowded and unreduced premolar dentition; the absence of a metaconid in the lower molars; the strongly developed talonid, particularly on M_4; the main shearing crest of lower molars passing from protoconid and hypoconid; the relatively low angle at which the coronoid process ascends from the horizontal ramus; the relatively slender upper molars with their transversely elongate protocones; the strong posterior slant of the upper premolars. It should be clear from the previous description that the Alcoota fossils are deserving of a separate specific designation. In fact, if more material were available it would probably have been possible to differentiate this form at the generic level. Ride (1964) has clearly shown that the range of variation seen in the modern *Thylacinus cynocephalus* is such as to include various Pleistocene and Recent specimens, i.e., *T. spelaeus* Owen, 1845, and *T. breviceps* Krefft, 1868. Ride (*ibid.,* p. 105) has also pointed out that *T. major* Owen, 1877, may have been applied to a posterior dentition of *Sarcophilus* set in a ramus of *Thylacinus*. Ride (p. 106, 107) also indicated that a small variant of the modern species may have existed during the Pleistocene in Western Australia. The Pleistocene form from Lake Menindee, New South Wales, UCMP 53038, may represent another population of this smaller variant.

The features of the dentition of *T. rostralis* DeVis, 1894 (Pleistocene of Queensland) have been determined from casts of the type. It seems that *T. rostralis* resembles *T. potens* in P^2 being close to P^3, but differs in having molar dimensions and proportions like those of *T. cynocephalus* and being otherwise rather like the Recent species. Many of the dimensions of *T. potens* could represent an allometric increase over those of *T. cynocephalus,* but other features show that the Alcoota fossil has many peculiarities which are different either in proportion or in kind from the Pleistocene and modern forms.

The small palatal fenestrae, the presence of a stylar cusp anterior to the metastyle of M^3, the more symmetrical arrangement of the parts of the upper molars and the strong cleft in the labial outline of the upper molars, could be interpreted as primitive features relative to a remote dasyuroid ancestry. On the other hand, those features mentioned above as showing that the fossil is a thylacinid indicate that this lineage was still, in the late Miocene or early Pliocene, nearly as distinct from any known dasyurid as are the Pleistocene and Recent members of the genus. If *Thylacinus,* or the Thylacinidae, diverged from the Dasyuridae, as seems probable, the time of divergence was surely no later than middle Tertiary and was probably much earlier.

?Superfamily PERAMELOIDEA Osborn, 1910

?Family PERAMELIDAE Waterhouse, 1838

A very large bandicoot may be represented by UCMP 65621, a partial right jaw with M_3 and M_4. Only the upper half of the jaw is present on the labial side. The anterior portion of the masseteric fossa is preserved, but the dorsal border which leads into the coronoid process is missing. Only enough of the lingual surface is preserved to show that this part of the jaw is completely smooth, there being no suggestion of a postalveolar process.

Unfortunately, the dental pattern of the teeth is almost worn away. The anterolingual corner of M_3 is missing. Except for a small enamel lake on the lingual part of the talonid, the enamel is confined to the periphery of the crown and extends down the same distance on the lingual and labial sides. The tooth bears only a very slight labial constriction at the transverse valley. There is some indication that the lingual constriction may have been stronger, but this is suggested mainly by the configuration of the roots and may not have been reflected in the crown. The dentine of the trigonid occlusal surface has a broadly lophate configuration in which a transverse crest separates an anteriorly sloping surface from one which slopes posteriorly. The enamel at the labial end of the trigonid is slightly convex anterior to the transverse crest and is taken to represent the base of the protoconid. Posterior to this, the enamel projects posterolabially, then lingually, forming a small crescent whose posterolingual extremity lies 1.8 labial to the small enamel lake. This crescent is considered to represent the labial outline of a small, cingulum-like structure similar to that found at the anterior base of the hypoconid in M_3 of *Thylacomys*. Posterior to the crescent, the enamel wall curves posteriorly and lingually around the base of the hypoconid to the base of the entoconid. The anterior part of the base of the entoconid is missing. The prominent, but small, enamel lake appears to lie just anterolabial to the entoconid. A third lower molar whose construction is such that it would, upon being worn down, produce a similar lake cannot be found in any of the fossil or Recent marsupials at hand. The original length of the tooth is not determinable because of the appression facettes developed at the anterior and posterior ends. It is now 11.8 long, was at least 9.2 wide across the trigonid, and is 8.6 wide across the talonid.

M_4 is much smaller than M_3, being only 9.1 long, 6.9 wide across the trigonid, and about 5.8 wide across the talonid. The posterior taper of M_4 is similar to, but

not as strong as, that in *Thylacomys*. Again, the enamel is restricted to the periphery of the crown and is developed equally on the labial and lingual sides. The enamel passes across the anterior edge of the tooth to the labial side and forms a sharp crescent at the end of the anterior cingulum. Posterior to this, a larger crescent indicates the position of the protoconid. The enamel then continues in a straight line posterolingually to the rear of the tooth and swings lingually around the narrow talonid. The anterior base of the talonid and posterior base of the trigonid is outlined by a major lingual re-entrant which forms a pit between the two moieties of the tooth. The enamel border then continues along the lingual base of the metaconid to the anterior cingulum.

Subject to the difficulties of reconstructing the occlusal pattern which will develop from an unworn tooth, the features of the Alcoota specimen are in many ways generally compatible with those seen in specimens of *Thylacomys lagotis*. The following combination of characters found in this specimen can be duplicated only in adult specimens of the Peramelidae as presently known: posteriorly tapering M_4; M_4 about one-third the size of M_3; teeth with relatively broad talonid; trigonid and talonid apparently of transverse lophodont or sublophodont construction; presence of deep pit on lingual half of M_4 between the trigonid and talonid; smooth lingual surface of the jaw which lacks any suggestion of a postalveolar process; ascending ramus joins the horizontal ramus so closely behind the tooth row that there is no oblique medial coronoid furrow. Of the modern and fossil bandicoots available for comparison, the Alcoota specimen seems moderately close to, but considerably larger than, *Thylacomys*.

In *Thylacomys,* the roots of the lower molars are characteristically nearly fused and the enamel extends much farther down the labial than the lingual side of the tooth. In the fossil, the roots are distinct. They are transversely oriented, but with flat anterior and posterior surfaces, and diverge from each other. They taper from base to tip. As mentioned above, the enamel on the labial side of the tooth extends down as far as that on the lingual side in the fossil specimen.

The basal outline of the teeth of the fossil is still elongate and essentially rectangular, whereas in this late stage of wear M_3, at least, of *Thylacomys* is subovate or square. While the features of the crown of the fossil tooth somewhat resemble those of *Thylacomys,* the roots of the teeth in the fossil are more like those of other, less specialized, bandicoots. The large size of the Alcoota fossil, as well as the other peculiarities which can be seen in this very fragmentary specimen, suggest that a new genus and species is represented. However, in view of the scanty remains and the late stage of wear of the teeth, it does not seem reasonable to propose a new name at this time.

Superfamily PHALANGEROIDEA Weber, 1928

? Family VOMBATIDAE Iredale & Troughton, 1934

An incomplete right upper first incisor, UCMP 70518, may be a representative of the Vombatidae. The fragment is 30.0 long from tip to base. It is 7.2 wide at the tip. Its anteroposterior length at the tip is 4.6.

The medial surface of the tooth is slightly excavated along the length of the tooth. The lateral surface is slightly convex in cross-section. The enamel is chiefly limited to the outer, anterior, surface. It extends only 2.5 on to the medial surface and about 4.0 on to the lateral surface. The occlusal outline of the tooth narrows posteriorly, and is therefore subtriangular. That the specimen is in an early stage of wear is suggested by the fact that the enamel of the medial surface wraps around the posterior side as it approaches to within 4.2 of the occlusal surface.

A pair of grooves 1.4 apart extend proximally along the anterior surface. The grooves are nearly parallel for 8.0, but thereafter they diverge sharply and fade out about 18.0 from the tip. The curvature of the enamel surface in lateral view falls on an arch, the radius of which is about 25.0. Although the fragment is broken proximally, the enamel is continuous along the outer surface. The base of the crown is not present. There is no evidence either for or against the possibility that the base of the enamel would have been close to the proximal tip of the specimen as preserved. The length of the enamel, measured along the curvature of the outer surface, is about 33.5.

Although upper incisors with an extensive enamel-covered outer surface are known in members of the Diprotodontidae (*Diprotodon, Euryzygoma* [syn. *Diarcodon*]), the size and general configuration of this specimen suggest affinity with the Vombatidae. None of the fossil or recent wombat material in the collections at Berkeley includes an upper incisor in such an early stage of wear. The distal cross-section of the Alcoota fossil is more regularly triangular than that usually seen in incisors of adult wombats. At the base of the specimen, however, the cross-section is skewed, with the enamel surface curving strongly posterolaterally. The medial surface is still flat. The posterolateral surface, broken in this specimen, would be short and posteromedially oriented. Although this fossil incisor is not particularly close to any known vombatid, it is even less like comparable teeth found in other phalangeroid families.

Family MACROPODIDAE Owen, 1838

Two new genera have been recognized among the macropodid material recovered from the quarries at Alcoota. The cranial and postcranial osteology of the smaller of the two species is the most completely documented of all the forms in the Alcoota fauna. This small macropodid is referred to the subfamily Potoroinae.

The larger macropodid is not referred to a particular subfamily, as it shows affinities to both the Macropodinae and Sthenurinae. Specimens of this larger macropodid are relatively rare.

A third macropodid, possibly a protemnodont, is represented by only four upper first incisors. This form has not been formally named. Additional post-cranial elements in the collection may be referable to these three taxa, or may represent new forms: because postcranial are not associated with cranial elements in the quarries, the question is at present indeterminable.

It became evident during the course of this study that it was necessary to re-evaluate the position of *Dorcopsis* Schlegel & Müller, 1842, and *Dorcopsulus* Matschie, 1916, with respect to the classical macropodid subfamilies. It has been useful to follow the practice proposed by Woods (1960) in retaining the genera *Hypsiprymnodon* Ramsay, 1876, and *Propleopus* Longman, 1924, in the Potoroinae along with *Hypsiprymnodon, Potorous, Caloprymnus, Aepyprymnus,* and *Bettongia.* This is the procedure utilized by Simpson (1945), and for purposes of a general consideration, at least, seems to be warranted by the many similarities in the postcranial osteology of *Hypsiprymnodon* and classical potoroines and the agreement in various characters of their teeth, crania, mandibles, and soft anatomy (see Woods, 1960, for summary).

TABLE 4

Genera and species of macropodids examined, with an indication of the material by which each taxon was represented.

	Cranium	Mandible	Adult	Juvenile	Postcranial skeleton
Potoroinae —					
Hypsiprymnodon moschatus	X	X	X	X	—
Potorous tridactylus	X	X	X	X	X
Aepyprymnus rufescens	X	X	X	—	—
Bettongia penicillata	X	X	X	—	—
Bettongia cuniculus	X	X	X	—	X
Dorcopsulus macleayi	X	X	X	—	—
Dorcopsulus vanheuri	X	X	X	X	X
Dorcopsis hageni	X	X	X	X	—
Dorcopsis strata	X	X	X	X	—
Dorcopsis muelleri	X	X	X	X	—
Macropodinae —					
Dendrolagus dorianus	X	X	X	X	—
Dendrolagus goodfellowi	X	X	X	X	X
Dendrolagus ursinus	X	X	X	X	—
Dendrolagus inustus	X	—	X	—	X
Dendrolagus lumholtzi	X	X	X	X	—
Setonix brachyurus	X	X	X	X	X
Lagostrophus fasciatus	X	X	X	X	X
Peradorcas concinna	X	X	X	X	—
Lagorchestes conspicillatus	X	X	X	X	X
Thylogale thetis	X	X	X	X	X
Thylogale brachyurus	X	X	X	X	—
Thylogale billardieri	X	X	X	X	—
Wallabia bicolor	X	X	X	X	—
Wallabia rufogrisea	X	X	X	X	X
Wallabia eugenii	X	X	X	X	—
Petrogale penicillata	X	X	—	X	—
Petrogale xanthopus	—	—	X	—	X
Onychogale unguifera	X	X	X	X	X
Megaleia rufa	X	X	X	X	—
Macropus major	X	X	X	—	X

Abbie (1937) stressed the importance of forward penetration into the mandible of the enlarged common inferior dental and masseteric canals as a character by which members of the Potoroinae could readily be distinguished from the Macropodinae.

The presence of a large common canal in the small macropodid in the Alcoota fauna, which also shows strong affinities with *Dorcopsis* and *Dorcopsulus,* drew attention to the possibility that these New Guinea genera might also share this character. Inspection of specimens of *Dorcopsis hageni* and *Dorcopsulus vanheuri* has shown that, although the mandible of these species is not as swollen antero-ventrally to the masseteric fossa and below the tooth row as are mandibles of more typical potoroines, the mandibular foramen extends downward into a large common masseteric and inferior dental canal which continues anteriorly at least to the rear of M_2. Although other workers in Australia had considered *Dorcopsis* as a macropodine (i.e., Wood Jones, 1924), neither *Dorcopsis* nor *Dorcopsulus* is mentioned by Abbie (1937); specimens may not have been available to him at the time of his study.

Subfamily POTOROINAE Trouessart, 1898

The content of the Potoroinae is essentially that of Simpson (1945, p. 47), with the addition of *Dorcopsis, Dorcopsulus,* and the new genus which will be described below. Characters by which potoroines may be distinguished from macropodines include: relatively large number of ridgelets on P^2; P^2 lacking a posterointernal cusp; P^3 simple, with no lingual cuspidate cingulum; P^3, about as long as combined length of M^1-M^2; molars low-crowned, links poorly developed, labial exit of transverse valley not obstructed by merging of crests which lead into the valley from tips of paracone and metacone; low angle of orientation of auditory meatus; small masseteric tuberosity; mandible generally with conspicuous bulge in ventral border; large common masseteric and inferior dental canal extending forward in body of ramus to at least below M_2; calcaneum with strong sustentaculum; anteromedial crest extending from inner edge of condyloid facette of calcaneum to anteromedial corner of calcaneum, rugose plantar surface of calcaneum separated from ventral lip of cuboid facette by a relatively wide, smoothly concave space; astragalus with rather symmetrical strongly arched ventral medial surface between head and posterior tubercle.

This diagnosis of the subfamily is not meant to be exhaustive, because the characters used were determined largely by those represented in the fossil material at hand.

A new genus of potoroine has been found in the Alcoota fauna which is a member of the lineage which produced *Dorcopsis* and *Dorcopsulus.*

Genus DORCOPSOIDES[1] nov.

Genotypic species: *Dorcopsoides fossilis* sp. nov.

Generic diagnosis: A potoroine macropodid larger than *Hypsiprymnodon,*

[1]dorkopsoides — *Dorcopsis*-like.

Potorous, Aepyprymnus, Bettongia, Dorcopsis or *Dorcopsulus;* but smaller than *Propleopus*; P^2 simple, sectorial, moderately massive; posterolabial corner of tooth with strongly oblique orientation; lingual base with three convex salients; dP^3 with strong posterolingual orientation of protoloph, parastyle elongate, mesostyle forms distinct cusp on labial shearing crest; midlink poorly developed; combined length of P^2 and dP^3 about equal to that of M^1 and M^2; P^3 not conspicuously higher-crowned than molars; molars low-crowned; rear of maxillary base of zygomatic arch lies above M^3; uppermost surface of maxillary shelf nearly horizontal, does not descend posteriorly toward rear of M^4, broadly convex transversely; attachment area of *M. masseter* on zygomatic arch separated into two surfaces by low posteroventrally directed crest; mastoid process large, expanded distally into rhomboid cross-section; mandibular ramus deep, 5 to 6 times height of hypoconid of M_3; common masseteric and inferior dental canal extends forward in body of ramus at least to a point under M_2; cuboid with extremely large medial ventral tuberosity. The genus also exhibits the characters listed above in the diagnosis of the subfamily. *Dorcopsoides* is further distinguished from other potoroines in possessing several features more commonly found among typical macropodines, i.e., lower incisors relatively short and deep; M^4 not greatly reduced; leading edge of ascending ramus nearly vertical; calcaneum with lateral indentation in flange below excavation in lateral surface of condyloid facette.

DORCOPSOIDES FOSSILIS[1] sp. nov.

(Figs 10-13, Tab. 5-15)

Holotype: CPC 6750, palatal fragment with RP^3-M^4, LP^3, partial LM^1, complete LM^3-M^4, most of right zygomatic arch, right mastoid and auditory region, partial basicranium, occipital condyles.

Paratypes: UCMP 69453, RP^2, dP^3, M^1; UCMP 66998, RP^2, P^3, P^3-M^2; UCMP 69539, LP^2, dP^3, P^3-M^2; UCMP 69537, RdP^3, M^1, M^3-M^4; UCMP 69545, maxillary fragments with RM^2-M^4, LP^3-M^3; UCMP 69540, LP^3; UCMP 65873, LP^3; UCMP 65874, LP^3-M^1; UCMP 65983, LM^1; UCMP 65895, RM^3; UCMP 69544, LM^4; UCMP 69538, right upper molar fragment; UCMP 69542, left upper molar fragment; UCMP 69606, RI_1; UCMP 66614, RI_1; UCMP 69608, LI_1; UCMP 69607, LI_1; UCMP 69611, right jaw with P_2, dP_3, P_3-M_3; UCMP 65961, right jaw fragment with P_2, dP_3-M_2; UCMP 65912, right jaw with P_3-M_4; UCMP 67067, RP_3; UCMP 69609, left jaw fragment with I_1, P_3-M_1; UCMP 65913, right jaw fragment with M_1-M_4; UCMP 65980, left jaw fragment with M_1-M_4; UCMP 69612, left jaw fragment with M_1-M_4; UCMP 65979, left jaw fragment with I_1, M_1-M_3; UCMP 69605, right jaw fragment with M_2-M_4; UCMP 65881, LM_2; UCMP 65865, right jaw fragment with M_3; UCMP 69546, right jaw fragment with partial M_3-M_4; UCMP 69610, left jaw fragment with M_3-M_4; UCMP 66201, molar and jaw fragments; UCMP 66198, UCMP 69613-69622, twelve right calcanea; UCMP 66638, UCMP 67040, UCMP 69623-69629, nine left calcanea; UCMP 66632, UCMP 69630, UCMP 69632, six

[1] *fossilis* — with reference to the fossil rather than present-day occurrence of the species.

right astragali; UCMP 65884, UCMP 66976, UCMP 69633-69637, nine left astragali; UCMP 69639-69641, three right cuboids; UCMP 69638, UCMP 69642-69644, four left cuboids; UCMP 66645, a carpal; UCMP 67082, left navicular; UCMP 66648, left metatarsal sesamoid; UCMP 69645, carpal; UCMP 65888, UCMP 65975, UCMP 69646-69656, UCMP 66639, sixteen right fourth metatarsals, UCMP 69661-69667, UCMP 66616, eight left fourth metatarsals; UCMP 66615, UCMP 69668-69670, four right fifth metatarsals; UCMP 67048, UCMP 67027, UCMP 66629, UCMP 67070, UCMP 69671-69676, ten left fifth metatarsals; UCMP 65911, UCMP 66196, UCMP 69680-69686, twelve right proximal fourth phalanges; UCMP 69687-69688, UCMP 66613, UCMP 66635, UCMP 67097, five left proximal fourth phalanges; UCMP 67058, UCMP 67086, UCMP 69689, three right distal fourth phalanges; UCMP 69690-69691, two left distal fourth phalanges; UCMP 66637, UCMP 67084, UCMP 69692, three right proximal fifth phalanges; UCMP 69693-69695, UCMP 69713-69714, five left proximal fifth phalanges; UCMP 69696, one right distal fifth phalanx; UCMP 69697, one left distal fifth phalanx.

Specific diagnosis: That of genus until other species are described.

Type locality: Paine Quarry, V6345, Waite Formation, 4 miles south-west of Alcoota station and 2.1 miles south-west of junction of Waite and Ongeva Creeks, Northern Territory, Australia.

Age: Alcoota fauna; late Miocene or possibly early Pliocene.

Description of holotype: In most cases it was not possible to measure a series of specimens for any of the species with which the fossil was compared. As a standard, skulls belonging to large male individuals were sought for comparison, but these were not always available. Size comparisons between fossil and Recent specimens will be valid, therefore, in a general way, and are intended as a rough guide. The features unique to *Dorcopsoides fossilis* are distinctive enough to demonstrate its separation from other forms without having to rely on detailed differences in actual size.

When the palatal portion of CPC 6750 is placed in a reasonable position relative to the occipital fragment (Fig. 10) it is apparent that the skull of *Dorcopsoides fossilis* is larger than that of any known species of *Dorcopsis* or *Dorcopsulus*. It is somewhat larger than that of *Dendrolagus dorianus* (AMNH 153630) and smaller than *D. ursinus* (AMNH 151823).

The transversely arched palatal surface seen in the holotype may have resulted from postmortem transverse crushing of the specimen. It does not seem likely, however, that this feature is totally artificial. The palate is broken just anterior to a small nutrient foramen 10.5 anteromedial to the left premolar. The incisors, canines, and incisive foramina are not preserved in CPC 6750. Posteriorly, the palate is only partly preserved, but medial to the anterior half of the left last molar, a rounded surface forms an anteriorly concave U-shaped opening which must correspond with the posterior edge of the left palatal fenestra. Neither the

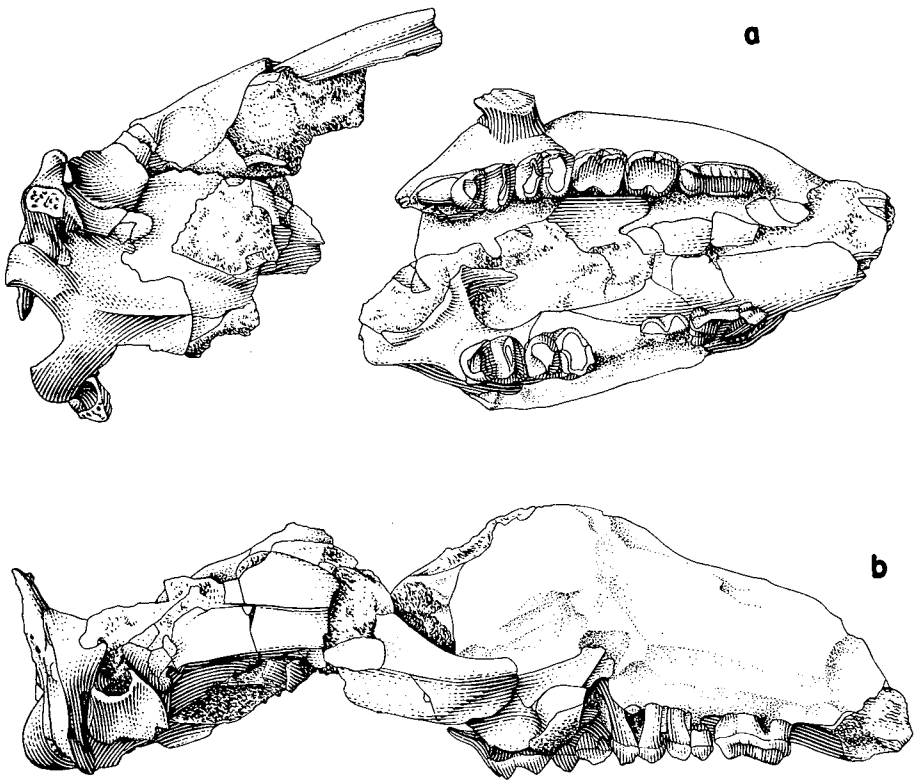

Fig. 10. *Dorcopsoides fossilis* **gen. nov., sp. nov.** a, **Palatal view of holotype, CPC 6750. Natural size.** b, **Lateral view of right side of above. Natural size.**

anterior end of this fenestra nor any part of that on the right side is preserved. The preserved portion is 5.6 wide and extends forward to, at least, the level of the rear of M^3. Posterior to the fenestra, the anterior edge of the choanal fossa leads anteromedially toward the midline, at which point it is absent. A diagonal groove in the palatal surface lies between the choanal aperture and the rear of the palatal fenestra. Three foramina are aligned along the anterolateral edge of this groove, generally similar to the condition in *Dendrolagus* and in contrast to the numerous perforations found posterior to the large palatal fenestrae in *Dorcopsis* and *Dorcopsulus*. In these genera a second, smaller palatal fenestra may occupy most of the space medial to M^4 and posterior to the main fenestra. A palatine fenestra is present in *Dorcopsoides fossilis,* but not in *Dendrolagus*.

The maxillopalatine suture can be seen to lead posteriorly from the lateral edge of the palatine fenestra for a distance of 8.6 in CPC 6750, but elsewhere its route is obscure.

As is common in macropodids, each tooth row in CPC 6750 is slightly bowed outward and M^4 is conspicuously set inward relative to M^3. Unfortunately, the

teeth of the holotype are in a late stage of wear; the occlusal pattern of M^1 and M^2 is almost absent and nearly obliterated in M^3. The basic features of P^3, M^3-M^4 are still determinable, however. P^3 is an elongate tooth with a blunt posterior end and broadly pointed anterior tip. P^3 is about 2.0 shorter than the total length from M^1 to M^3 (see Table 5). P^4 is constricted to a width of 3.4 about 3.6 anterior to its posterior end. The posterior end is 0.3 narrower than the main body of the tooth. A single crest extends from the posterolabial corner to the anterior tip of the tooth. The crest forms an apex over the anterior root and a second apex at the posterior cusp and dips down in between. The anterior apex of the tooth is developed into a blade-like cusp. Four small ridgelets occur on the labial side of the shearing crest between the anterior cusp and the posterior cusp. This brings the total number of ridgelets to 6, the number of intervening grooves to 5. The ridgelets decrease in magnitude posteriorly, the fifth being very small and occurring mainly as a minute swelling of the shearing crest. A small labial and lingual cingulum lead posteriorly from the base of the large anterior ridgelet, and fade out at the point of greatest transverse constriction of the tooth. Even in this late stage of wear, it can be seen that P^3 is higher-crowned than the molars. The disparity in crown height is not as great as in *Dorcopsis* and *Dorcopsulus,* however, and resembles more closely the condition found in *Dendrolagus* and other macropodines.

The molars are low-crowned, but their advanced stage of wear hinders judgement as to their original height. M^1 and M^2 have an almost square occlusal outline due to the development of appression facettes on their anterior and posterior sides. Enough enamel remains on the labial side of the first two molars to show the conspicuous flat triangular facettes which are present, even in this stage of wear, on the posterior side of the paracone and anterior side of the metacone. In M^1 and M^2 the base of the labial edge of the facette on the paracone is expanded into a small mesostyle; the lingual crest intersects the transverse valley 1.3 and 1.8 medial to the labial crests in M^1 and M^2, respectively. M^1 tapers slightly anteriorly, the protoloph being 0.2 narrower than the metaloph. The metaloph, however, is progressively narrower in M^2 to M^4. In M^4, it can be seen that the anterior cingulum extends across the total width of the tooth. The protoloph and metaloph are posteriorly concave. The two lophs are connected by a midlink which is developed chiefly from the anterior surface of the metaloph. A small lingual cingulum is present in M^3 and M^4. The short posterior cingulum of M^4 is continuous at each end with a crest which connects to the tip of the metacone and hypocone, respectively. A short anterior crest connects the tip of the paracone to the anterior cingulum. In M^3 the weak facette on the posterior face of the paracone is delineated by a pair of crests, which diverge toward the bottom of the transverse valley. The labial of the two crests intersects the transverse valley at the edge of the tooth. The lingual crest is directed medially and meets the valley about 0.8 medial to the labial crest. A corresponding facette on the anterior side of the metacone is but weakly expressed. In M^4 these facettes are absent. A single crest from the paracone diminishes posteriorly and terminates at the transverse valley. In all the molars, the transverse valley is freely open; the crests on the labial sides of the protoloph and metaloph do not tend to unite in a strong, obstructing, ridge. The molar row on the right side is

curved, concave ventrally in lateral view. This is probably not indicative of the condition in the living animal: the molar series of the left side, and in other specimens, is straight in lateral view. The curvature on the right side seems to be caused by the portion of the maxillary holding M^3 and M^4 having been bent downward during preservation.

The right zygomatic arch is nearly complete. The maxillary base of the arch lies just above the roots of M^3 and its anteroposterior dimension is about the same as the length of that tooth. The maxillary shelf is posterior to the base of the zygoma and leads anteriorly into its anterior base. In ventral view, this shelf is directed posteromedially from the base of the arch. In lateral view the shelf seems to be directed posteroventrally, but this part of the maxilla, which also bears M^3 and M^4, has been bent downward during preservation. Only the dorsal part of the masseteric tuberosity is preserved. It was probably located above the posterior root of M^2 and anterior root of M^3. In posterior view, the lateral surface of the maxilla covering the molar roots curves smoothly into the medial surface of the dorsal part of the tuberosity. The medial surface of this portion of the tuberosity is about 5.3 from the lateral surface and above the posterior root of M^3. The remaining portion of the zygomatic arch is attached to the basicranial and occipital part of the specimen. The jugal part of the arch is preserved posterior to the masseteric tuberosity and below the postorbital process of the jugal. The portion of the jugal which extends posterior to the postorbital process is missing. The dorsal surface of the jugal is concave upward. Below this, the dorsal masseteric crest is similarly concave but to a lesser degree. The portion of the jugal occupied by the origin of *M. masseter* slopes ventromedially. A smaller, blunter crest which descends posteroventrally below the dorsal masseteric crest divides the ventrolateral surface of the jugal into two parts. The surface below the second crest is anteroventrolaterally concave, while that between the second and dorsal crests is flatter and faces more laterally. In general, the curvature of the dorsal and ventral borders of the jugal, and that of the dorsal masseteric crest, resembles the condition in *Dendrolagus goodfellowi* rather than *Dorcopsis* or *Dorcopsulus*. The jugal in CPC 6750 differs from all of these genera in being more massive and having a second ventral masseteric crest.

The dorsal part of the zygomatic process of the squamosal is partly preserved. The lateral and ventral parts of the squamosal arch are preserved, in a fractured state, anterior to the auditory region. The flat ovate surface of the glenoid has a greatest length of 9.1; its greatest width is 9.0. It is about the same size as and otherwise similar to that found in *Dendrolagus goodfellowi*. The small oblique postglenoid process, 6.8 long, is partly preserved and lies just anterior to the lateral rim of the tympanic bone. The tympanic is large (10.2 wide, 9.2 long). Its ventral surface forms a dome-like arch with all its edges sloping outward and downward from the centre. There may have been some postmortem alteration of orientation of the tympanic. It is now inclined dorsolaterally at an angle of about 30° with respect to a horizontal plane passing across the ventral surface of the condyles. This is a considerably flatter orientation than is found in either *Dendrolagus, Dorcopsis* or *Dorcopsulus*. The outer edge of the tympanic, at the ventral border of the external auditory meatus, is relatively straight in

ventral view, not so sharply indented as in *Dendrolagus*. The anterior border of the tympanic overlaps the posterior surface of the postglenoid process for about 4.4 transversely. The circular auditory meatus is not closed dorsally. It is joined by an anterior and posterior ridge to the front and rear flanges of the ventrally concave tympanic bone. The posteromedial corner of the tympanic is joined to the alisphenoid by a straight anteromedially directed suture 5.0 long. The suture then turns abruptly more anteriorly for a distance of 5.0, at which point a rugose flange forms the anteromedial corner of the tympanic. This flange is 5.0 wide anterolaterally and joins the transverse crest which forms the anterior edge of the ventral surface of the tympanic. Dorsal to the flange and transverse crest, and medial to the postglenoid process of the squamosal, the tympanic bears an anterolaterally oriented rib which extends dorsally along the anterior surface of the bone. The rib forms the medial wall of a broadly V-shaped sulcus which rises along the anterior surface of the tympanic deep to the orifice of the external auditory meatus and posteromedial to the postglenoid process. The ventral opening of this sulcus, bounded anteriorly by the postglenoid process, and posteriorly by the tympanic, may correspond to the postglenoid foramen.

The posterior part of the zygomatic arch seems to have been crushed medially, for there is only a small space available for the zygomatic sulcus between the outer surface of the cranium and medial surface of the arch. The alisphenoid bulla is crushed in CPC 6750. The postglenoid process is broken near its middle part, but seems to have been obliquely oriented as in *Dendrolagus goodfellowi*. The ventral surface of the basicranium medial and anterior to the tympanic is composed of a mixture of crushed bone and matrix. Thus the positions of the Eustachian canal, entocarotid foramen, foramen ovale, and transverse canal cannot be determined.

The basioccipital is strongly keeled. A well developed sulcus was apparently present on each side of the keel. The basisphenoid is largely missing. The laterally concave basal part of the right pterygoid, which forms the medial wall of the pterygoid fossa, can still be seen. Posterior to the basioccipital, the occipital condyles are preserved. In ventral view, the outline of the foramen magnum given by the condyles in *Dorcopsis* and *Dorcopsulus* is a relatively deep V, whereas in *Dendrolagus* the outline is generally shallower and more U-shaped. The condition in CPC 6750 is more like that of *Dorcopsis*. The condyles are broad as in *Dorcopsis* with a slightly convex ventral articular surface. The anterior edge at the medial base of the condyles is not ventrally excavated for a large condyloid foramen as in *Dendrolagus*. The foramen can be seen in ventral view, however, and is thus somewhat more anterior, relative to the edge of the condyle, than in either *Dendrolagus, Dorcopsis,* or *Dorcopsulus*. About 1.0 anterolingual to the condyloid foramen is the accessory condyloid foramen. It lies well in front of the anterior edge of the condyle, and in this respect resembles the condition in *Dendrolagus;* the proximity of the accessory to the condyloid foramen is, on the other hand, similar to the condition in *Dorcopsis*. On the interior surface of the condyle, the accessory condyloid is situated anterior and ventral to the condyloid foramen, rather than only anterior to it as in *Dendrolagus*. A transversely elongate (3.0) and anteriorly concave posterior lacerate foramen lies anteromedial to the base of the paroccipital process and 3.0 anterolateral to

the accessory condyloid foramen. The posterior lacerate foramen tends to be more obliquely oriented and ovate in *Dendrolagus*. The condition in CPC 6750 is like that in *Dorcopsis,* where the foramen is more transversely oriented, elongate, and anteriorly concave. The posterointernal edge of the condyle is a straight nearly vertical lip in CPC 6750 and resembles that of *Dorcopsis*. Near the dorsal extremity of the condyle, its anterior edge bears a sharp excavation, the condyloid sulcus, which causes the dorsal tip to be rather sharply pointed and directed anteriorly and slightly dorsally in lateral view. A similar excavation occurs in the anterior edge of the condyle in *Dorcopsis, Dorcopsulus,* and *Dendrolagus,* but the tip is directed almost vertically in *Dendrolagus*. The condition in *Dorcopsis* and *Dorcopsulus* is about intermediate between that of *Dendrolagus* and CPC 6750. In posterior view the tip of the condyle of CPC 6750 is pointed and directed dorsolaterally. In *Dendrolagus* the tip is rather blunt, in *Dorcopsis* and *Dorcopsulus* it is sharper. About 1.5 dorsal and slightly medial to the tip of the condyle in the fossil specimen, is a small foramen. A foramen is present in a generally similar position in the above three modern genera. In CPC 6750 this small foramen is situated near the top of the condyloid sulcus which separates the condyle from the convex occipital surface of the basal portion of the paroccipital process. This part of the paroccipital process is composed of a broad dorsomedially directed ridge which becomes narrower and sharper and curves more vertically just above the dorsal tip of the condyle. The distal portion of the paroccipital process is broken off, revealing a cancellous internal structure. A flange-like mastoid process is situated anterolateral to the paroccipital process and bears a blunt, swollen tip which projects 7.0 below the ventral border of the external auditory meatus, down to about the level of the ventral edge of the condyles. The terminus of the mastoid process is directed ventrolaterally in posterior view and curves slightly anteriorly in lateral view. In posterior view, the lateral edge of the mastoid process forms a sharp crest, inclined slightly dorsomedially in its ventral part, but which turns abruptly more medially at the level of the dorsal tip of the condyles. The exoccipital-mastoid suture generally parallels the lateral edge of the process up to the level of the tip of the condyles. Dorsal to this, the suture extends nearly vertically and joins the lambdoidal crest about 9.5 above the tip of the condyle. The mastoid-squamosal suture essentially follows this crest so that the anterior surface of the mastoid process is composed of the squamosal. The mastoid foramen is located in a deep groove, about 3.8 below the dorsomedial tip of the mastoid. This groove lies just behind and is parallel to the lambdoidal crest. It is deepest in its dorsal part and becomes constricted by a triangular boss 9.0 ventrolateral to the dorsomedial tip of the mastoid and 7.3 dorsolateral to the dorsal tip of the condyle. Ventral to the triangular boss, the groove becomes shallower and considerably wider and fades out above the distal end of the mastoid process. In ventral view the distal tip of the mastoid assumes a nearly rhomboid shape. The lateral edge continues dorsally as the lateral mastoid crest. The medial edge would have been continuous with the anterior base of the paroccipital process if it had not been broken off. The posterior crest continues dorsally as a low ridge which leads to the lateral edge of the paroccipital process near the exoccipital-mastoid suture. The anterior crest of the mastoid tip fades out quickly in the anteriorly concave surface of the mastoid process.

In *Dorcopsis* and *Dorcopsulus,* the mastoid process is neither as large nor as expanded ventrally as in CPC 6750. The condition seen in the fossil is most closely approached by *Dendrolagus.* Except in degree, the other features of the occiput in *Dorcopsis hageni* most closely resemble those of *Dorcopsoides.* The fossil, however, is considerably more massive and rugose.

In lateral view the surface of the glenoid is on a level which nearly bisects the external auditory meatus, but it may have been shifted downward during fossilization. Because of postmortem crushing the nature of the postzygomatic and subsquamosal foramina may not be determined. A partly preserved circular opening in the roof of the tympanic cavity may represent the supratympanic foramen. Between the tympanic and the anterior squamosal lamina of the mastoid process is a deep cleft which may represent the stylomastoid fissure; an opening within this fissure may be the stylomastoid foramen.

Inside the cranial cavity, the nearly flat, dorsolaterally oriented, rhomboid surface of the right petrosal is visible. Its posterodorsal corner is just internal to the dorsal tip of the mastoid. From this point the petrosal descends in two consecutive anteriorly concave arcs to the dorsal corner of the internal opening of the posterior lacerate foramen. A small internal opening of the fenestra rotunda lies just dorsal to the posterior lacerate foramen. The dorsal corner of the posterior lacerate foramen is 9.0 ventromedial to the posterodorsal edge of the petrosal. The posterior border of the foramen is composed of a pair of concavities in the anterior surface of the basioccipital. The anterior border of the posterior lacerate foramen is formed by the sharp posteroventral corner of the petrosal, which divides the foramen into a bilobate orifice. The anterior lobe continues anteromedially as a groove in the ventral edge of the petrosal which parallels its contact with the basioccipital. This groove terminates in matrix 7.3 anterior to the posteroventral corner of the petrosal. A blunt chevron-shaped orifice opens out of the bone just anterior to the groove, but it is obscured anteriorly by matrix and bits of crushed bone. The anterior edge of the blunt chevron is formed by an acuminate spur which leads antero-medioventrally from the subarcuate fossa and is located on the anteromedial corner of the petrosal. The tip of this spur is 10.5 anterior to the posteroventral corner, 15.3 anteromedial and ventral to the posterodorsal corner and 10.4 medial to the anterolateral corner of the petrosal. The conspicuously free tip of the spur in *Dendrolagus dorianus* differs from the condition in *Dorcopsoides,* where it is directed ventrally as well as anteromedially and seems to contact the alisphenoid.

The anterior edge of the petrosal, which would contact the squamosal, forms, as exposed here, a smooth, slightly concave, strap-like surface. The lateral surface is formed of two parts. The anterior part is 3.8 long, slightly concave, and directed posterolaterally. It would have been just medial to the inner surface of the squamosal, which forms the medial wall of the epitympanic sinus or postzygomatic foramen. The posterior (4.4 long) part of the lateral surface of the petrosal is covered by the squamosal just anterior to its contact with the mastoid. The outer edge of the 4.8 wide subarcuate fossa lies 1.6 medial to the anterior part of the lateral edge of the petrosal. The fossa extends posterolaterally into the body of the squamosal just anterior to the mastoid. The posteromedial edge of this fossa is bounded by a small knob whose apex is 6.7 anterodorsal

to the posteroventral corner of the petrosal. A shallow, circular depression 3.2 wide lies posteroventral to the knob. Anterior to this depression is the 2.7 wide fundus of the floccular fossa, which penetrates laterally and divides into anterior and posterior channels. The anterior channel divides into dorsal and ventral diverticula. The posterior channel is larger and descends slightly anterolaterally. In *Dorcopsis hageni* the dorsal diverticulum of the anterior channel is confluent with the lateral opening of the Fallopian aqueduct and is designated as the median opening of that duct. There is a small depression ending in an anteriorly opening slit just posterior to the knob below the subarcuate fossa. This may represent the apertura externa aqueducti vestibuli, which is found in a similar position in specimens of *Dendrolagus goodfellowi*. In *Dorcopsis* and *Dorcopsulus* this feature tends to occur more anteriorly relative to the subarcuate fossa than in *Dorcopsoides*.

Paratypes: The portion of the maxilla posterior to the anterior base of the zygomatic arch and dorsal to M^3 and M^4 is preserved in three specimens other than the holotype; UCMP 69539, UCMP 69545, and UCMP 65895. At the anterior end of the shelf a nearly circular maxillary foramen about 2.4 in diameter leads forward into the anteroventral floor of the orbit. The foramen lies above the metaloph of M^2 in mature specimens and on a transverse line 6.5 anterior to the posterior edge of the maxillary base of the zygomatic arch. The surface of the maxilla is inclined slightly upward immediately anterolateral to the foramen; a shallow groove issues from the foramen and leads slightly posteromedially above the tooth row. Between this groove and the zygomatic arch the dorsal surface of the maxillary shelf is a broad ridge which is convex upward in outline. It curves posteromedially from a point above and slightly lateral to the ectoloph of M^2 to a point over the entoconid of M^4. As indicated in recent specimens of *Dendrolagus* and *Dorcopsis,* the shelf continues posteromedially to the pterygoidal wing of the alisphenoid, but this area is not represented in the fossil material at hand. A sharply defined groove 0.3 wide lies on the uppermost surface of the shelf in one of the specimens (UCMP 69545). It issues from a small foramen 4.5 posterolateral to the maxillary foramen. Other small foramina occur on the lower medial surface of the maxillary shelf; these are mainly posterior to the maxillary foramen and medial to the groove. Lateral to the uppermost surface of the shelf the anterior base of the zygomatic arch is about 4.5 thick (vertically). The lateral edge of the maxillary shelf is rounded and curves smoothly on to the nearly vertical surface of the maxilla lateral to the roots of the posterior molars. In dorsal view, the lateral edge of the shelf intersects the median wall of the zygomatic arch at a moderately narrow angle, similar to the condition in *Dendrolagus goodfellowi* and *Dorcopsulus vanheuri,* but is much narrower than in *Dendrolagus dorianus* or *Dorcopsis hageni.* The vertical thickness of the base of the zygoma is most like that of *Dendrolagus dorianus,* as is the position of the maxillary foramen with respect to M^2 and to the anterior end of the orbital fossa. In contrast, the lateral edge of the maxillary shelf in *D. dorianus* is somewhat concave laterally as seen in dorsal view, whereas that of the fossil is convex. In this feature, *D. goodfellowi* and *Dorcopsulus vanheuri* are most like the fossil. The Alcoota genus differs from all Recent specimens at hand in the broad convexity of the uppermost surface of the shelf.

In *Dorcopsis* and *Dorcopsulus* this part of the maxillary shelf is nearly flat and is continuous with the upper surface of the base of the zygoma. In *Dendrolagus* and *Dorcopsoides,* the dorsal surface of the base of the zygoma is distinctly lower than that of the maxillary shelf.

Second premolar (Fig. 11e, f). There are three specimens of P^2 in the sample (Table 5). P^2 is an elongate, irregularly ovate premolariform tooth with one anterior and two posterior roots. The longitudinal shearing blade is not quite centred over the long axis of the tooth, but is slightly labial to the midline. The tooth is thickest at the posterior third, and tapers slightly in front of and behind this point. The lingual border is composed of three small salients. The anterior and posterior of these are of about the same length (1.5), but the middle one is nearly twice as long as the others. The shearing blade is composed of 4 or 5 vertical ridgelets separated by 3 or 4 grooves. The largest of the ridgelets are at the anterior and posterior ends of the tooth. Those in between diminish in

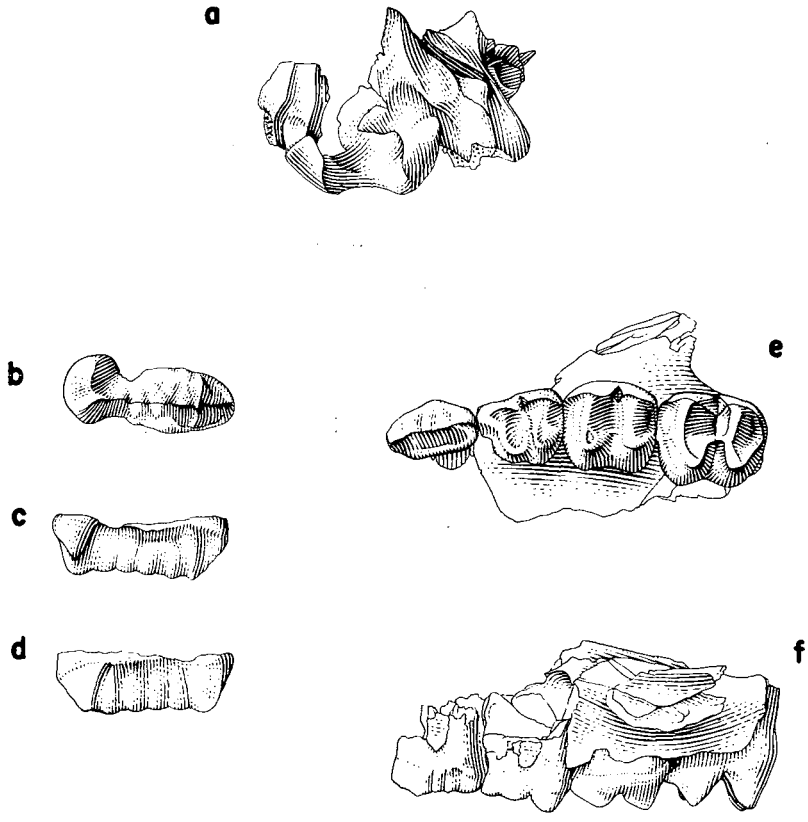

Fig. 11. *Dorcopsoides fossilis* **gen. nov., sp. nov.** a, **occiput of holotype. CPC 6750. Natural size.** b, **occlusal view;** c, **lingual view;** d, **labial view of** LP^3**, taken from its crypt above** P^2 **and** dP^3 **of UCMP 69539. Part of the lingual border of this incompletely formed tooth is missing, as are its roots.** e, **occlusal view and,** f, **labial view of left maxillary fragment with** P^2–M^2**. Twice natural size.**

TABLE 5

Upper Cheektooth Measurements in *Dorcopsoides fossilis*

		Length, P^2	Width, P^2	Length, dP^3	Width^1, dP^3	Width^2, dP^3	Length, P^3	Width^1, P^3	Width^2, P^3
CPC 6750 . .	R	----	----	----	----	----	11.3	4.4	4.2
	L	----	----	----	----	----	----	----	----
UCMP 69545 . .	L	----	----	----	----	----	----	----	----
	R	----	----	----	----	----	10.7	4.3	4.2
UCMP 65874 . .		----	----	----	----	----	11.7	4.7	4.7
UCMP 65983 . .		----	----	----	----	----	----	----	----
UCMP 65895 . .		----	----	----	----	----	----	----	----
UCMP 65944 . .		----	----	----	----	----	----	----	----
UCMP 65873 . .		----	----	----	----	----	10.7	4.8	4.6
UCMP 69540 . .		----	----	----	----	----	----	----	3.7
UCMP 69543 . .		6.1	3.4	6.0	3.9	5.0	----	----	----
UCMP 69539 . .		6.6	3.4	5.9	3.9	4.8	10.6	3.9	4.3
UCMP 69537 . .		----	----	6.4	4.7	5.4	----	----	----
UCMP 66998 . .		6.4	3.7	6.5	----	5.4	10.6	3.9	4.4
Range		6.1–6.6	3.4–3.7	5.9–6.5	3.9–4.7	4.8–5.4	10.6–11.3	3.9–4.8	3.7–4.7

Width^1 = width across anterior moiety of dP^3 and P^3.
Width^2 = width across posterior moiety of dP^3 and P^3.
* = tooth too worn to give accurate measurement.
f = tooth fractured, measurement too large.

		Length M^1	Width, M^1	Length, M^2	Width, M^2	Length, M^3	Width, M^3	Length, M^4	Width, M^4
CPC 6750 . .	R	6.8	6.2	7.1	6.8	7.8	7.4	8.4	6.8
	L	----	----	----	----	8.4f	7.4	8.2	6.7
UCMP 69545 . .	R	----	----	7.2	6.1	7.6	6.1	7.6	5.7
	L	6.8	6.1	7.1	6.4	7.5	6.2	----	----
UCMP 65874 . .		7.3	6.5	----	----	----	----	----	----
UCMP 65983 . .		7.0	6.1	----	----	----	----	----	----
UCMP 65895 . .		----	----	----	----	8.7	6.9	----	----
UCMP 65944 . .		----	----	----	----	----	----	7.9	6.8
UCMP 65873 . .		----	----	----	----	----	----	----	----
UCMP 69540 . .		----	----	----	----	----	----	----	----
UCMP 69543 . .		6.8	6.0	----	----	----	----	----	----
UCMP 69539 . .		6.6	5.8	7.4	6.2	----	----	----	----
UCMP 69537 . .		7.9	----	----	----	8.2	7.0	8.2	6.5
UCMP 66998 . .		6.6	5.8	7.6	6.1	----	----	----	----
Range		6.6–7.9	5.8–6.5	7.1–7.6	6.1–6.8	7.5–8.7	6.1–7.4	7.6–8.4	5.7–6.8

	Length, P^2-dP^3	Length, M^1-M^2	Length, M^1-M^3	Length, M^1-M^4	Height, anterior cusp of P^3	Height, posterior cusp of P^3	Height, metacone of M^2	Height, metacone of M^3
CPC 6750 . . R	----	13.8	21.5	30.0	*	*	*	*
L	----	----	----	----	----	----	----	----
UCMP 69545 . . R	----	----	----	----	----	----	----	----
L	----	13.9	21.4	29.0	3.7	3.5	2.8	2.8
UCMP 65874 . .	----	----	----	----	----	----	----	----
UCMP 65983 . .	----	----	----	----	----	----	----	----
UCMP 65895 . .	----	----	----	----	----	----	----	----
UCMP 65944 . .	----	----	----	----	----	----	----	----
UCMP 65873 . .	----	----	----	----	----	----	----	----
UCMP 69540 . .	----	----	----	----	----	----	----	----
UCMP 69543 . .	----	----	----	----	----	----	----	----
UCMP 69539 . .	12.5	13.6	----	----	*	*	3.3	----
UCMP 69537 . .	----	----	----	----	----	----	----	----
UCMP 66998 . .	12.6	13.9	----	----	*	*	3.8	----
Range	12.5–12.6	13.6–13.9	21.4–21.5	29.0–30.0	3.7	3.5	2.8–3.8	2.8

magnitude posteriorly. The ridgelet just in front of the posterior one is so small as to be readily lost as wear progresses. This accounts for the variability in the ridgelet-valley count. The anterior ridgelet is located in the anterior third of the tooth. Anterior to its apex, the shearing crest descends toward the anterior tip. Posterior to the first ridgelet, the height of the shearing crest remains about the same. In unworn teeth, at least, the posterior ridgelet is as high above the base of the crown as the anterior ridgelet. The tooth sustains the greatest amount of wear on the lingual surface of the shearing blade. Consequently, the ridgelets and valleys are most clearly seen on the labial side. There is only a slight tendency for a lingual shelf to develop at the base of the tooth as wear progresses. In the unworn condition, no cingula are present.

The second upper premolar of *Dorcopsoides fossilis* resembles those of other potoroines, including *Dorcopsis* and *Dorcopsulus,* in its simple, slender construction and in lacking any suggestion of a posterointernal cusp. Among the potoroines, the relatively massive construction of the tooth in *D. fossilis* is most closely approached in *Dorcopsis hageni.* While the lingual base of P^2 in *Dorcopsulus vanheuri* seems to be relatively smooth, that of *D. hageni* is irregular, as is that of *Dorcopsoides.* P^2 of the Alcoota genus differs from that of *Dorcopsis* in being widest posteriorly and tapering slightly anteriorly. *Dorcopsoides fossilis* seems to be unique in the sharply oblique posterolabial corner of P^2.

Deciduous third premolar (Fig. 11e, f). Four dP^3's are available for study. This is a three-rooted submolariform tooth which tapers anteriorly and which bears a strong parastylar shearing cusp. In addition to its anterior connexion to the parastyle, the paracone is connected by a short posterior crest to a mesostyle. The mesostyle is prominently developed. The nearly straight labial margin of the tooth is oriented strongly anterolingually except for a slight constriction at the transverse valley. Although the lingual border of the tooth is oriented obliquely, it is composed of an anterior and a posterior salient which represent the lingual bases of the protoloph and metaloph, respectively. The lingual ends of the lophs are separated by an emargination at the opening of the transverse valley. The protoloph, which is shorter than the metaloph, is oriented perpendicular to the obliquely oriented labial border of the tooth. Thus, the protoloph is directed posterolingually, and converges toward the lingual end of the metaloph. Even in unworn specimens, the metacone is the highest of the principal cusps. The hypocone, although lower than the paracone, is higher than the protocone. The parastyle and mesostyle, about equal in height, are both lower than the paracone. As it passes across the ectoloph, the transverse valley becomes constricted owing to the shearing crests on the posterior side of the mesostyle and anterior side of the metacone. The posterior crest from the metacone continues lingually as a short posterior cingulum which attaches to the midposterior side of the hypocone. In a similar manner a slight anterior cingulum extends from the base of the parastylar ridge to the anterolingual side of the protocone. Labial and lingual cingula are absent.

The general morphology of the deciduous upper premolar of *Dorcopsoides* is found in a number of the smaller kangaroos, including *Potorous, Dorcopsis,* and *Dorcopsulus* among the potoroines and *Dendrolagus, Lagostrophus,* and *Peradorcas* among the macropodines. In general, however, the simple construction, elongate parastylar shearing cusp, posterolingual orientation of the protoloph, prominent mesostyle, and absence of a strong midlink in dP^3 of *Dorcopsoides* is most like that of *Dorcopsulus vanheuri.* The main differences are that it is about twice the size of and has a more strongly developed anterior taper of its basal outline than dP^3 of *D. vanheuri.*

Third premolar (Fig. 11d). There are five P^3's in the sample other than those of the holotype. This elongate sectorial tooth is supported by a single anterior and a large posterior root. Like P^2, it has an elongate serrate crest which nearly bisects the tooth into right and left halves. The crest is straight for its anterior two-thirds, then swings posterolabially to the main posterior cusp. The posterior cusp is connected by a short, low transverse crest to a smaller posterolingual cusp. The tooth is constricted just anterior to the transverse posterior lobe, which is composed of the main posterior cusp and the smaller cusp posterolingual to it. Anterior to the constriction, the labial and lingual borders are convex outward; the two sides taper gradually toward the rather blunt anterior tip. Posterior to the constriction, the tooth is expanded into the posterior lobe described above. As can be seen in Table 5, the tooth has about the same maximum width in front of the constriction as behind it. In unworn teeth, the six vertical ridgelets separated by five valleys can be clearly seen. The foremost and hindmost ridgelets are

the largest; the intervening ones decrease progressively in magnitude posteriorly. As in P^2, the ridgelet just anterior to the main posterior cusp is so small that it tends to be lost in advanced stages of wear. The first ridgelet and the posterior cusp tend to be of about the the same height. In lateral view the shearing crest diminishes in height posteriorly to the valley between the fourth and fifth ridgelet, then rises again to the apex of the posterior cusp. The shearing crest slopes sharply behind the last cusp to the base. The slope of the crest between the apex of the first ridgelet and the anterior base of the tooth is gradual. The labial and lingual sides of the shearing crest are steep. The base of the tooth flares out abruptly, but it is doubtful if the basal swellings should be considered as cingula. The anterior ridgelet is strong on both the labial and lingual sides of the tooth. The lingual ridgelet, in particular, is much stronger than the others on that side of the crest, and persists even into advanced stages of wear when most other features of the lingual side of the tooth have been obliterated.

The upper third premolar of *Dorcopsoides fossilis* most clearly resembles that of *Dorcopsis* and *Dorcopsulus* of the potoroines. In the vertical orientation of the ridgelets and valleys of the shearing blade, the slight labial as well as the lingual constriction of the basal outline, closest resemblance to the fossil is shown by *Dorcopsis atrata* and species of *Dorcopsulus*. P^3 of *Dorcopsoides* differs from all species of *Dorcopsis* and *Dorcopsulus* in being relatively low-crowned, in the posterolabial curvature of the posterior end of the shearing blade and in the absence of a strong crest along the posterior side of the main rear cusp; and from that of the macropodines in the rather symmetrical position of the crest at the shearing blade which nearly bisects the tooth into right and left halves, and the absence of a lingual cingulum.

First molar (Fig. 11e, f; Table 5). The sample includes eight M^1's. They are subquadrate, bilophodont, mesostyle-bearing teeth which have two anterior roots and one posterior root. The tooth tapers slightly anteriorly; the protoloph is 0.2-0.4 narrower than the metaloph. A strong parastylar ridge continues the posterolabial shear from P^3. The mesostyle is near the labial extremity of the transverse valley at the posterolabial base of the paracone. This style develops from the ridge which descends posterolabially from the apex of the paracone and forms the labial border of the triangular facette found on its posterior surface. The medial border of the facette is formed by a posteromedial ridge which intersects the transverse valley 1.0-1.3 medial to the mesostyle. A corresponding facette is developed on the anterior surface of the metacone, but no cusp develops on its labial border. The anterior and posterior pair of ridges meet in the transverse valley to form a low obstruction. The protoloph and metaloph are parallel and, in the unworn state, are concave posteriorly. The metacone is higher than the paracone, which is higher than the hypocone. The protocone is the lowest of the primary cusps. A sharp midlink connects the protoloph to the metaloph near the median longitudinal axis of the tooth. The link is directed anterolingually. The anterior cingulum extends from the parastyle to the anterolingual or mid-anterior base of the protocone. A small lingual cingulum is present. The posterior cingulum occurs as part of an anterodorsally concave ridge which connects the hypocone to the metacone. There is no labial cingulum.

Second molar (Fig. 11, f; Table 5). Five M^2's have been recovered. M^2 is essentially like M^1, but differs in being slightly larger and more elongate, having a less obliquely oriented anterolabial base, a protoloph as wide as or slightly wider than the metaloph, and a smaller mesostyle posterior to the paracone. Also, the midlink may be slightly stronger and less anterolingually oriented than in M^1. The metacone of M^2 is slightly (1.0) higher-crowned than that of M^1.

Third molar (Table 5). Six M^3's are present. M^3 is basically similar to M^2; it differs in being longer, the metaloph being markedly narrower than the protoloph, in lacking the facettes on the posterior surface of the paracone and the anterior surface of the metacone, in lacking a mesostyle, and in having a more broadly open transverse valley. The height of the metacone is about the same as that of M^2.

Fourth molar (Table 5). There are five M^4's in this sample. M^4 is nearly as long as M^3, but the metaloph is considerably (0.8-1.3) narrower than the protoloph, there are no facettes on the labial cusps, the mesostyle is absent, the midlink is small and the transverse valley is broadly open.

In labial view the protoloph of all four molars is broader, less acuminate, and less trenchant than the metaloph. UCMP 69545 supports the observation made on the holotype that the tooth row is slightly bowed outward and that M^4 is definitely inset relative to M^3. The hypsodonty of the teeth increases but slightly from M^1 to M^3, then decreases slightly to M^4. The general size of the teeth also increases slightly to M^3, then decreases to M^4.

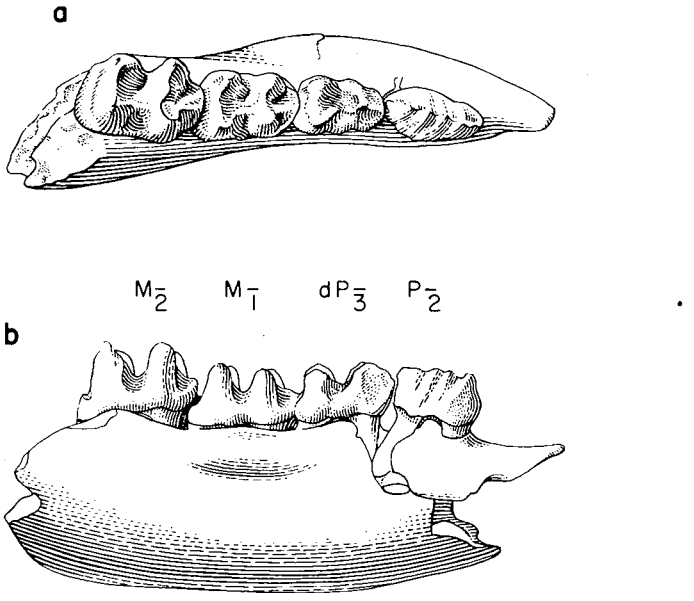

Fig. 12. *Dorcopsoides fossilis* **gen. nov., sp. nov.** a, **occlusal view;** b, **labial view of right juvenile mandible fragment with P_2, dP_3, M_1 and M_2, UCMP 65961. Twice natural size.**

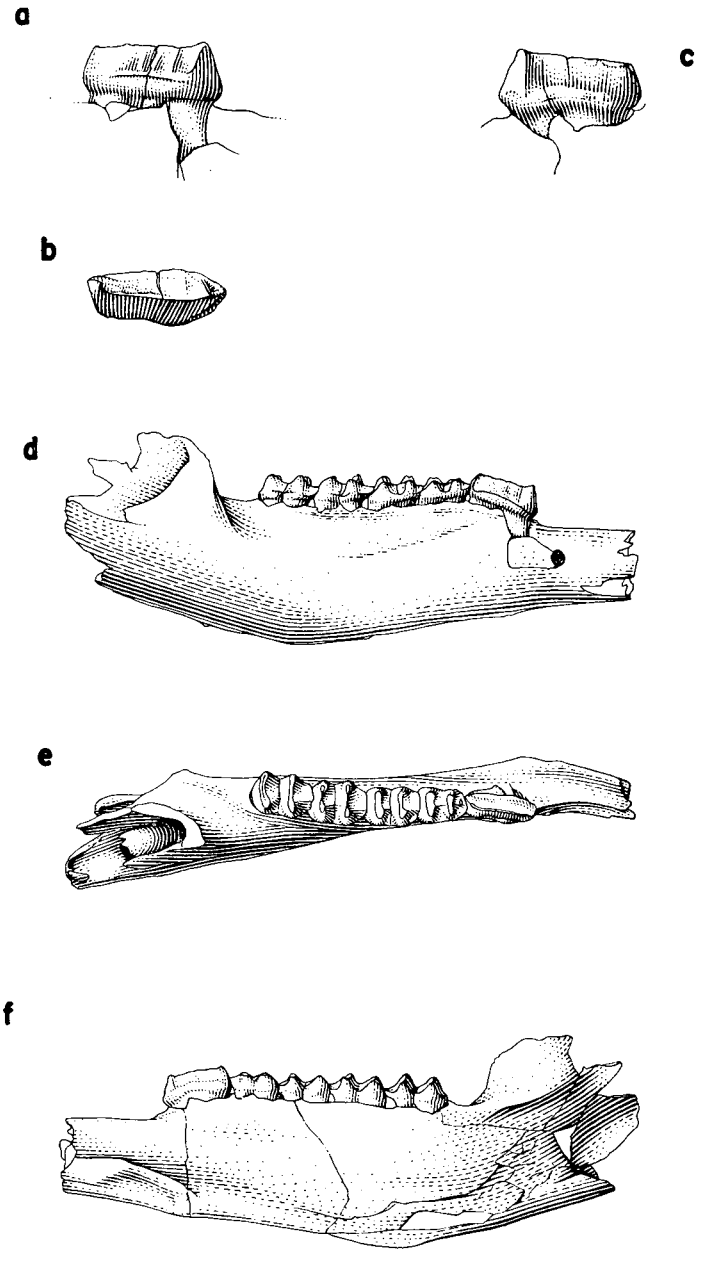

Fig. 13. *Dorcopsoides fossilis* **gen. nov., sp. nov.** a, **labial;** b, **occlusal, and** c, **lingual view of** RP_3, **UCMP 65912. Twice natural size.** d, **labial;** e, **occlusal, and** f, **lingual view of right adult mandible fragment, UCMP 65912. Natural size.**

The upper molars of *Dorcopsoides fossilis* show closest resemblance to those of *Dorcopsis* and *Dorcopsulus* in being low-crowned teeth in which the transverse valley is broadly open in labial view and the axes of the lophs are inclined anteriorly. This condition is approached in species of *Dendrolagus,* but the valley is narrower and more sharply V-shaped. Further resemblance of *Dorcopsoides* to *Dorcopsis* and *Dorcopsulus* is shown by the presence of the mesostyle at the base of the crest which lies along the posterior side of the paracone in M^1 and M^2, the presence of a triangular, transversely flat facette on the rear of the paracone and anterior surface of the metacone, and the molar gradient in which the teeth increase slightly in size posteriorly to M^3, then decrease to M^4. Facettes on the paracone and metacone of M^1 and M^2 are also found in *Dendrolagus goodfellowi, D. dorianus,* and to a smaller degree in *Petrogale penicillata, Thylogale thetis, Wallabia rufogrisea,* and *Potorous tridactylus,* but mesostyles are not developed in these forms. Mesostyles do occur in M^1 and M^2 of *Bettongia penicillata,* but facettes are not formed.

Mandible (Fig. 13d, e, f; Table 6). The mandible of *Dorcopsoides fossilis* is represented by five specimens. Of those pertaining to adult individuals, UCMP 65912 is nearly complete. The incisor, angle, and ascending ramus are missing. The mandible of *Dorcopsoides fossilis* is deepest (15.3-18.5) below the hypolophid of M_3. The ventral border slopes smoothly upward anterior and posterior to this point. A slight ventral concavity occurs below M_1, and is expressed as a ventrally projecting point below the anterior root of P_3. The anterior border is slightly concave and slants anterodorsally toward the lower edge of the incisor alveolus. The anterior edge of the coronoid process ascends nearly vertically and is posterior to M_4. The alveolar border is nearly straight from M_1 to M_4. Anterior to M_1 the labial alveolar border of P_3 descends gradually to the dorsal edge of the diastemal crest. The configuration of the lingual alveolar border is substantially the same as the labial, except that it continues posteriorly as the postalveolar shelf. The terminology applied to the mandible and lower dentition follows that in Stirton (1966a). The postalveolar process, at the end of the postalveolar shelf, lies from 4.8 to 9.7 behind M_4. The lateral edge of the shelf slopes upward into the medial edge of the coronoid process. The anterior edge of the coronoid process is posterior to M_4 in mature specimens. Thus the anterolaterally oriented medial coronoid furrow likewise remains totally behind M_4.

The mid-lateral surface of the mandible is convex anterior to the masseteric fossa, but becomes flat below M_2-P_3. The mental foramen is located 5.2 below the diastemal crest and 3.5 anterior to the anterior root of P_3. The ventral edge of the masseteric fossa extends downward to a point about 3.0 below the alveolar row. On the medial surface, 4.9-6.2 below and behind the postalveolar process is the vertically elongate, ovate, mandibular foramen. The foramen is 6.3-8.2 high and about 3.4 wide. The large masseteric canal is confluent with the inferior dental canal. Their common canal extends forward under the tooth row to at least M_2. As Abbie (1939, p. 266-9) points out, this condition is characteristic of the potoroines and hypsiprymnodontines rather than the macropodines. However, the common canal in *Dorcopsoides* is relatively not as large as in *Potorous, Aepyprymnus, Bettongia,* and *Hypsiprymnodon.* Also, the posterior opening of

the mandibular canal in *Dorcopsoides* is dorsally elongate, not subcircular, and the ventral border of the mandible below the mandibular foramen is narrow instead of being transversely expanded as in the potoroine and hypsiprymnodontine genera listed above. The masseteric foramen, which connects the masseteric fossa with the inferior dental canal, is farther forward in *Dorcopsoides* than in those genera, and cannot be seen in lateral view. In this feature, as well as the general size and shape of the mandibular foramen, masseteric canal, common inferior dental and masseteric canal, degree of angularity of the ventral edge of the mandible, and relatively small difference in size between the mandibular foramen and posterior opening of the masseteric canal, *Dorcopsoides* is most like *Dorcopsis hageni*. *Dorcopsoides, Dorcopsis,* and *Dorcopsulus* seem to be nearly intermediate between the potoroine and hypsiprymnodontine (*sensu* Abbie) kangaroos on one hand and the macropodines on the other. In this regard, it seems possible that Abbie did not see specimens of *Dorcopsis* and *Dorcopsulus,* for he does not mention them in his 1939 review.

The medial surface of the mandible is flat, and slants slightly ventromedially relative to the vertical symphyseal surface. No digastric process can be found, nor is there any evidence of a genial pit. The dorsal surface of the symphyseal portion anterior to P_3 is sharp and, although lower, is nearly parallel to the trend of the alveolar border. The ventral border of the jaw is rather sharp, and curves laterally and posteriorly from the rear of the symphysis. At the anterior end of the pterygoid fossa, the jaw has become only slightly wider than at the rear of M_3 (8.1-8.7).

Lower incisor (Table 6). There are six incisors or incisor fragments in the sample. I_1 is an elongate lanceolate laterally compressed tooth. The root is almost straight and nearly circular in cross-section, and extends backward in the ramus to a point below P_3. The dorsal and ventral edges of the blade are both convex, upward and downward respectively, so that the vertical height of the tooth just anterior to the root (5.4-6.4) is about 1.0 greater than that of the root itself. The labial surface is smoothly convex in unworn specimens and curves anteromedially toward the tip. Above and below the anteriorly tapering enamel-covered crown the dorsal and ventral blades of the tooth are thin.

The lower incisor of the Alcoota genus resembles that of *Dorcopsis* and *Dorcopsulus,* among the potoroines, in being relatively short and deep instead of long and slender. I_1 of *Dorcopsoides* does not differ in its essential morphology from those of typical macropodines.

Second lower premolar (Fig. 12, Table 6). Two P_2's are available for study. Both are elongate, anteriorly tapering premolariform teeth with one anterior and one posterior root. A nearly straight longitudinal shearing crest composed of four ridgelets and three grooves nearly bisects the tooth into right and left halves. Anterior to the first, large, ridgelet the crest slopes downward and anteromedially to the anterior tip. Posterior to the tip the labial and lingual sides diverge toward the point of greatest transverse width, at the posterior third of the tooth. The labial surface is smoothly convex. The lingual surface bears a shallow

TABLE 6

Measurements on lower teeth and jaws of *Dorcopsoides fossilis*

	Depth, enamel just anterior to shaft, I_1	Length, unworn tip to shaft/cap margin, I_1	Width, transverse to medial shaft/cap margin, I_1	Length, P_2	Width, P_2	Length, dP_3	Posterior width, dP_3	Length, P_3	Width, P_3
UCMP 69606	5.4	----	2.8						
UCMP 66614	5.7	8.8	3.1						
UCMP 69608	6.2	12.4	3.3						
UCMP 69607	6.4	----	3.1						
UCMP 69611	5.7	----	2.9	5.4	2.9	5.6	4.1	8.7	2.7*
UCMP 65961				6.0	3.2	5.6	4.1		
UCMP 65912								9.8	3.8
UCMP 67067								9.3	3.8
UCMP 69609	5.8							----	----
UCMP 65913									
UCMP 65980									
UCMP 69612									
UCMP 65979									
UCMP 69605									
UCMP 65881									
UCMP 65865									
UCMP 69546									
UCMP 69610									
Range	5.4–6.4	8.8–12.4	2.8–3.3	5.4–6.0	2.9–3.2	5.6	4.1	8.7–9.8	3.8

---- = element present but unsuitable for measurement.
* = immature, not fully formed; too small.
+ = crushed, undistorted measurement would have been larger.
Width[1] = width of anterior moiety.
Width[2] = width of posterior moiety.

	Length, M_1	Width[1], M_1	Width[2], M_1	Length, M_2	Width[1], M_2	Width[2], M_2	Length, M_3	Width[1], M_3	Width[2], M_3
UCMP 69606									
UCMP 66614									
UCMP 69608									
UCMP 69607									
UCMP 69611	----	4.2	4.8	7.4	5.1	5.3			
UCMP 65961	7.2	4.2	4.7	7.8	5.1	5.3			
UCMP 65912	6.5	4.3	4.8	7.1	5.3	5.2	8.0	5.8	5.6
UCMP 67067									
UCMP 69609	----								
UCMP 65913	----		----	----	----	----	8.4	6.3	6.2
UCMP 65980	6.2	4.3	4.9	6.8	5.3	5.1	8.0	6.0	5.5
UCMP 69612	6.3	4.3	4.8	7.0	5.2	5.3	8.0	5.8	5.3
UCMP 65979	----	----	5.0	8.1	5.3	5.2	8.3	5.3	----
UCMP 69605				7.4	5.5	5.2	8.0	5.9	5.5
UCMP 65881				7.5	5.0	5.2	8.0	5.6	5.5
UCMP 65865							----		5.8
UCMP 69546							7.8	6.0	5.7
UCMP 69610									
Range	6.2–7.2	4.2–4.3	4.7–5.0	6.8–8.0	5.0–5.3	5.1–5.3	7.8–8.4	5.3–6.3	5.5–6.2

TABLE 6 (Continued)
Measurements on lower teeth and jaws of *Dorcopsoides fossilis*

	Length, M_4	Width[1], M_4	Width[2], M_4	Length, P_2-dP_3	Length, M_1-M_2	Length, M_1-M_3	Length, M_1-M_4	Length, postalveolar process to rear M_4
UCMP 69606								
UCMP 66614								
UCMP 69608								
UCMP 69607								
UCMP 69611				11.1	----			
UCMP 65961				11.0	14.8			
UCMP 65912	8.1	5.7	5.3		13.0	20.2	27.8	8.9
UCMP 67067								
UCMP 69609								
UCMP 65913	8.8	5.9	5.6		----			4.8
UCMP 65980	7.9	5.8	5.3		13.1	21.2	28.9	9.7
UCMP 69612	8.3	5.8	5.3		12.8	20.8	28.7	
UCMP 65979								
UCMP 69605	8.3	5.9	5.2					6.9
UCMP 65881								
UCMP 65865								
UCMP 69546	8.2	5.5	5.1					
UCMP 69610								6.3
Range	7.9–8.8	5.5–5.9	5.1–5.6	11.0–11.1	12.8–14.8	20.2–21.2	27.8–28.9	4.8–9.7

	Length, postalveolar process to front P_3	Depth, bottom of mental foramen to dorsal edge, jaw	Distance, anterior base P_3 to rear mental foramen.	Depth, jaw below rear M_3	Height, hypoconid M_3	Height, mandibular canal	Width, mandibular canal	Width, jaw at rear M_3
UCMP 69606								
UCMP 66614								
UCMP 69608								
UCMP 69607								
UCMP 69611								
UCMP 65961								
UCMP 65912	46.4	5.2	3.6	18.5	2.5	8.2	1.8+	8.5
UCMP 67067								
UCMP 69609								
UCMP 65913								
UCMU 65980				18.5	2.8			
UCMP 69612								
UCMP 65979								
UCMP 69605				15.3	3.3			8.2
UCMP 65881								
UCMP 65865				15.7	3.7			8.7
UCMP 69546				18.0	----			8.6
UCMP 69610				17.0		6.3	3.4	8.1
Range	46.4	5.5	3.6	15.3–18.5	2.5–3.7	6.3–8.2	3.4	8.1–8.7

emargination just behind the base of the anterior ridgelet, but posteriorly the surface becomes convex and continues around to the end of the tooth. The large anterior ridgelet bears strong labial and lingual crests which slant slightly anterodorsally, but the other crests become smaller posteriorly. The posterior ridgelet is represented by only a large cusp on the shearing crest and has no labial or lingual crest. The posterior end of the tooth forms a sharp point which terminates slightly lingual to the anterior end of dP_3. There are no anterior, posterior, labial, or lingual cingula. In lateral view the top of the shearing crest is a nearly straight line, the anterior and posterior cusps are at about the same height over the base of the tooth.

The second lower premolar of *Dorcopsoides* is like that of *Dorcopsis* and *Dorcopsulus* in general morphology. Although the ridgelets and grooves are more weakly developed in the Alcoota genus than in any other potoroine examined, it has four ridgelets which slant anterodorsally, like that of *Dorcopsis* and *Dorcopsulus*. *Potorous tridactylus* on one hand and *Dendrolagus dorianus* on the other, have only three ridgelets in P_2 and the ridgelets are oriented vertically. In other macropodines, such as *Peradorcus concinna*, there are as many ridgelets as in *Dorcopsoides*, but they are oriented vertically.

Deciduous lower premolar (Fig. 12, Table 6). There are also only two dP_3's in the sample. This is an anteriorly tapering submolariform tooth with one anterior and one posterior root. The anterior half of the lingual surface is nearly flat and directed anterolabially. The base of the labial surface displays three convex salients. Both labial and lingual surfaces taper markedly from the metaloph to the anterior apex of the tooth. A posterolingually directed shearing crest begins at a small cusp at the anterior end of the tooth (paraconid), continues across and down the posterolingual side of the fused protoconid and metaconid to the transverse valley. The entoconid bears a slight anterior and posterior crest and is connected by a short transverse lophid to the hypoconid, which is situated above the hindmost of the three convex salients. The fused protoconid and metaconid also bears a short posterolabial crest. The crest turns abruptly posteriorly before descending into the transverse valley and continues posterolabially up the anterior face of the hypoconid. The middle of the convex salients lies just anterior to the labial opening of the transverse valley. The labial surface of the shearing crest, above the anterior salient, is steep, smooth, and slightly concave. There are no cingula, but in UCMP 65961 a short low transverse crest extends lingually from the anterior tip of the tooth. The metaconid is the highest cuspid; the entoconid is higher than the hypoconid.

The deciduous lower third premolar of such macropodines as *Peradorcas concinna* is a molariform small version of M_1. The protolophid, although narrower than the hypolophid, is fully developed and contains a low protoconid at its labial extremity. The protoconid is connected by a sharp forelink to a small cuspid at the anterior tip of the tooth, which may be termed the paraconid. The paraconid, unlike that in M_1, is also connected by a smaller ridge to the metaconid.

In the potoroine *Potorous tridactylus,* the protolophid is present but less well developed. The protoconid connects by a short crest to the anterior apex of the tooth, which though not developed as a distinct cuspid, sends off a short posterolingual crest to the metaconid. The protoconid is also connected posteriorly across the labial end of the transverse valley to the hypoconid.

In *Dendrolagus dorianus* the morphology of dP_3 is close to but not identical with that of *Dorcopsoides fossilis.* The protoconid is still connected to the anterior apex of the tooth and also to the hypoconid by a posterior longitudinal crest. The protoconid has shifted lingually in position and is only slightly separated from the metaconid.

In *Dorcopsis, Dorcopsulus,* and *Dorcopsoides* the protoconid and metaconid are fused into a single acuminate cuspid which is connected anteriorly to the apex of the tooth and posteriorly to the hypoconid. In detail, the anterior tapering of the basal outline and the presence of three conspicuous labial basal salients, so markedly developed in dP_3 of *Dorcopsoides fossilis,* is most closely resembled by the somewhat less extreme condition found in *Dorcopsulus vanheuri.*

Third premolar (Fig. 13, Table 6). Four P_3's have been found, one having been obtained from its crypt below dP_3 in UCMP 69611. P_3 is an elongate premolariform serrate tooth with one anterior and one posterior root. In mature, fully formed specimens the labial and lingual basal borders diverge posteriorly from the rather blunt anterior apex so that the tooth is widest near its anterior third. The labial and lingual sides then converge to the slight constriction in the posterior third and continue to the moderately broad posterior end. The longitudinal shearing crest bisects the tooth into right and left halves. It is essentially straight in the anterior two-thirds, but curves posterolingually at the posterior end of the tooth. The crest is composed of a large anterior ridgelet and a posterior cusp with four intervening ridgelets which decrease in size posteriorly. The grooves which separate the ridgelets also decrease in width and depth posteriorly. The anterior ridgelet is strongly developed on the labial and lingual sides of the tooth. A crest slopes down from its apex to the anterior end of the tooth. The other ridgelets are best developed on the labial side of the tooth. There are no ridgelets associated with the posterior cusp. There are no anterior, posterior, labial or lingual cingula, although the anterior half of the lingual base is slightly expanded. The dorsal edge of the shearing crest is relatively horizontal in lateral view, but when the tooth is in position in the mandible, it is directed anterolaterally relative to the molars, and the crest slopes slightly downward anteriorly.

The lower premolar of *Dorcopsoides fossilis* is of the same general construction as those teeth in *Dorcopsis* and *Dorcopsulus* and resembles P_3 of the potoroines generally in the relatively high number of delicately formed ridgelets. P_3 of *Dorcopsoides* differs from that of *Dorcopsis* and *Dorcopsulus* in its relatively low crown height and oblique orientation in the mandible.

First lower molar (Figs 12 and 13; Table 6). Six M_1's have been recovered. This is a subrectangular, elongate molariform tooth with a small forelink and midlink, but no hindlink. As can be seen from Table 6, the tooth tapers anteriorly

so that the protolophid is 0.5-0.6 narrower than the hypolophid. Both lophids are oriented transversely relative to the longitudinal axis of the tooth and both are slightly concave anteriorly. On the lingual side is a slight inflexion at the transverse valley and on the labial side a small convex cingulum is present. Both the lingual cuspids, the protoconid and hypoconid, have slight longitudinal crests on their anterior and posterior surfaces. The labial cuspids, the metaconid and entoconid, are more conical. The forelink descends anterolingually from the apex of the protoconid, then turns abruptly more anteriorly to end near the midpoint of the anterior cingulum. The midlink descends in a similar manner from the apex of the hypoconid and connects to a small spur from the protolophid near the middle of the transverse valley. Anterior and posterior cingula are well developed, the anterior being broader anteroposteriorly but narrower transversely than the posterior cingulum. The anterior cingulum extends labially beyond its junction with the forelink and is from 3.0 to 3.5 wide, or about three-fourths the width of the protolophid. There is no lingual cingulum. The hypolophid is higher than the protolophid.

Other lower molars. Eight M_2's, eight M_3's and seven M_4's are available for study. These teeth are essentially like M_1; each molar is longer than the one in front of it. M_4 and M_2 are slightly narrower than M_3. There is also a slight progressive posterior increase in height of crown, but this does not approach the magnitude typical of the Macropodinae. The posterior cingulum extends more distinctly around to the labial end of the hypolophid in M_3 and M_4. The point at which the forelink intersects the anterior cingulum moves more labially toward the rear of the dental series, but the midlink continues to terminate near the middle of the transverse valley. In M_4 the width of the hypolophid relative to the protolophid is considerably less than in M_3.

The lower molars of *Dorcopsoides, Dorcopsis,* and *Dorcopsulus* are more lophodont and higher-crowned than those of typical potoroines. In this sense these genera are more like macropodines, and this suggests that they are advanced over the general potoroine condition. In the vertical orientation of the axes of the molar lophids in *Dorcopsoides,* the resemblance is to *Dorcopsulus* and *Dorcopsis* and typical potoroines rather than to *Dendrolagus* and other macropodines. The molar gradient of *Dorcopsoides,* with a slight posterior size increase to M_3, then a decrease in width to M_4, also points to a potoroine rather than macropodine affinity.

Calcaneum. Twenty-two calcanea (Table 7) have been found which, on the basis of their size, seem to belong to *Dorcopsoides,* although they are not associated with any unequivocal remnant parts of the genus. They are typical macropodid calcanea with a moderately wide cuboid facette (14.1-15.5 in 9 mature specimens), whose anterior surface interlocks with the cuboid. In Table 7 the specimens have been separated into two groups. The first comprises those in which the epiphysis at the posterior tip has not yet fused with the shaft. The epiphyseal cap is uniformly lost, and the specimens are considered to be juvenile. The specimens of the second group are mostly larger, and the length

of the tuber calcanei, with its completely ankylosed epiphyseal cap, is considerably greater relative to the size of the area occupied by the astragalar facettes than in the juvenile forms.

With the specimen lying on its plantar surface with the dorsal surface uppermost, the anteriorly projecting lateral portion of the cuboid facette protrudes 3.2-4.0 (in 10 mature specimens) beyond the anterior edge of the medial portion. The anterior edge of the lateral portion of the facette is about 1.0 narrower than the medial portion. The calcaneum articulates with the astragalus on four facettes. The first is triangular. It lies on the dorsal surface of the anterolateral tip of the calcaneum and projects posteromedially. Posteromedial to the lateral crest, which serves as an attachment area for the lateral ligament, the second astragalar facette forms a broad dorsally convex condyle. The condyle tapers toward the centre of the calcaneum. Posteromedial to this a dorsally convex flange above the rear of the sustentaculum forms a third astragalar facette. The flange is separated from a fourth astragalar facette, which lies anterior to it, by a diagonal ridge. The ridge leads posterolaterally from the fourth facette to the medial end of the condyloid facette. A small triangular concavity is developed on the fourth facette between the diagonal ridge and the anterodorsal edge of the adjacent cuboid facette. A small knob about 4.0 posterolateral to the posterior flange (third astragalar facette) lies on the dorsal crest of the shaft behind the medial edge of the astragalar condyle. The dorsal crest of the shaft leads posteriorly to a broad low knob on the tuber calcanei. In posterior view, the cross-section of the tuber calcanei is subtriangular, with the dorsal apex shifted somewhat lateral to the midline.

In lateral view, the condyloid astragalar facette is supported by a ventrally concave flange which slopes slightly anteroventrally. This flange forms the attachment for the lateral ligament. The lateral surface of the condyle is excavated by a nearly square pocket. The lateral extremity of the flange is located about 7.5 above the flat ventral border of the shaft. The posterior surface of the tuber calcanei can be seen to slant posteroventrally in lateral view.

In medial view, the dorsally concave surface of the flange-like astragalar facette (facette 3) is supported by a sustentaculum 9.5 thick, whose ventral surface extends posteriorly from the ventromedial edge of the cuboid facette, then curves posterodorsally and ends on the medial surface of the shaft just behind the sustentaculum. The dorsal surface of the shaft is slightly concave. The medial surface of the sustentaculum is slightly excavated. The posterior surface of the sustentaculum bears a shallow ventromedially oriented groove.

In plantar view the broad, nearly flat plantar surface tapers gradually anteriorly, and comes to a point, at the lateral edge of the tuber calcanei, 6.0-7.5 posterior to the edge of the midventral portion of the cuboid facette. The shaft is only slightly excavated laterally. The sulcus tarsi between the ventrolateral edge of the sustentaculum and the medial surface of the shaft is narrow and shallow. The anterior edge of the plantar surface is separated from the midventral portion of the cuboid facette by a shallow, smooth, slightly concave area.

TABLE 7

Measurements of Calcanea of *Dorcopsoides fossilis*

Specimen	Age	Greatest length	Length, astragalar facette	Greatest width	Width, cuboid facette	Height, cuboid facette	Depth, tuber calcanei behind astragalar condyle	Width, tip of tuber calcanei
UCMP 66198	J	27.8	13.9	18.0	12.5	10.2	10.0	----
UCMP 69613	J	----	----	17.6	----	----	----	----
UCMP 69614	J	32.8	16.2	20.5	14.6	----	11.7	----
UCMP 69615	J	27.9	13.9	----	12.1	----	10.4	----
UCMP 69616	J	28.1	14.3	----	----	----	9.8	----
UCMP 69617	J	28.3	14.4	18.1	12.8	10.5	----	----
UCMP 69618	M	41.0	16.8	----	----	----	14.6	13.6
UCMP 69619	M	41.6	16.7	21.5	14.9	----	13.7	----
UCMP 69620	J	38.0	16.4	22.4	14.6	12.7	13.1	----
UCMP 69621	M	42.2	16.4	22.7	15.8	----	----	14.1
UCMP 69622	?	----	15.6	----	----	----	----	----
UCMP 67008	M	41.8	15.8	----	----	----	----	13.0
UCMP 66638	M	35.7	13.9	18.9	14.3	----	13.0	13.0
UCMP 67040	M	40.6	15.7	20.5	15.1	11.8	13.6	13.3
UCMP 69623	M	40.4	16.1	21.0	15.5	----	13.9	----
UCMP 69624	M	39.5	15.1	20.3	14.1	11.7	13.7	13.0
UCMP 69625	M	43.6+	16.9	23.1	15.5	----	14.4	----
UCMP 69626	M	43.4	16.2	22.3	14.7	12.8	14.9	13.8
UCMP 69627	J	39.0	15.8	22.5	15.7	12.7	14.0	----
UCMP 69628	M	38.2	15.3	20.8	14.4	11.5	13.3	13.0
UCMP 69629	J	31.1	15.5	----	13.9	----	11.7	----
Range		27.8–43.6	13.9–16.9	17.6–23.1	12.1–15.8	10.2–12.8	9.8–14.9	13.0–14.1
Range juvenile	J	27.8–39.0	13.9–16.4	17.6–22.5	12.1–15.7	10.2–12.7	9.8–14.0	
Range, adult	M	35.7–43.6	13.9–16.9	18.9–23.1	14.1–15.8	11.5–12.8	13.0–14.8	13.0–14.1

J = juvenile; epiphyseal cap of tuber calcanei not fused to shaft.

M = mature; epiphyseal cap of tuber calcanei ankylosed to shaft.

In anterior view, the cuboid facette can be divided into three segments. A transversely elongate, subrectangular medial portion lies well behind the other two surfaces. A vertically elongate portion occupies the dorsal two-thirds of the lateral side of the facette and is smoothly confluent with a small, transversely dognate midventral portion. The medial portion lies in the dorsal half of the facette and is separated from the ventral portion by a deep transverse sulcus about 7.0 wide, which terminates about 2.5 lateral to the medial edge of the calcaneum. The medial edge of the cuboid facette slopes smoothly, ventrolaterally around to its ventral edge.

Although the size of the calcaneum of *Dorcopsoides fossilis* is nearly that of *Wallabia rufogrisea,* its proportions and characteristics are most close to those found in *Dorcopsulus vanheuri.* It resembles *Bettongia* and *Potorous* in the strong development of the sustentaculum, the anteromedial crest extending from the inner edge of the astragalar condyle toward the fourth astragalar facette, the relatively wide dorsal surface of the tuber calcanei, and the separation of the rugose portion of the plantar surface from the cuboid facette by a relatively wide, smooth space. Additional characters in common with *Dorcopsulus* but absent in potoroines are: indentation of the lateral flange just below the pit in the lateral side of the condyloid facette; marked medial tapering of the condyloid facette, slight excavation of the lateral surface of the tuber calcanei just above the lip-like lateral edge of the plantar surface; relatively flat plantar surface; wide, relatively short transverse diameter of ventral cuboid facette; marked projection of ventral cuboid facette anterior to the adjacent edge of the sustentaculum.

The short, dorsoventrally flattened calcaneum of *Dendrolagus* shows little resemblance to that of *Dorcopsoides.* The calcaneum of *Setonix* is rather like that of *Dorcopsoides* in the large size of the sustentaculum and the lateral indentation in the flange below the pit in the side of the condyloid facette, but differs conspicuously in the large pit bounded by a strong lateral crest in the anterolateral corner of the first astragalar facette, the poor development of the lateral flange, and the forward extension of the rugose plantar surface of the tuber calcanei toward the cuboid facette. Except for differing in certain details, the calcanea of *Lagorchestes hirsutus* and *Lagostrophus fasciatus* are like that of *Setonix.*

The calcanea of *Thylogale thetis, Petrogale xanthopus, Wallabia rufogrisea, Macropus erubescens,* and *Megaleia rufa* resemble one another and differ from *Dorcopsoides* in having a dorsolaterally rather than transversely oriented ventral cuboid facette, a broad flat ventral rugose surface of the tuber calcanei which extends anteriorly to reach the ventral cuboid facette, and a condyloid facette which neither tapers medially nor continues as an oblique crest to the anteromedial corner of the astragalus. Except in *Thylogale,* the lateral surface of the tuber calcanei above the edge of the rugose plantar surface is rather deeply excavated.

Astragalus. Fifteen astragali have been recovered. In Table 8 the specimens have been treated as a single unit, as there are no obvious means of separating

them into two age classes. Except for the anteriorly projecting navicular process, or head, the outline of the astragalus is trapezoidal with the anterior and posterior surfaces essentially parallel, while the lateral and medial surfaces converge posteriorly. The lateral edge of the trochlea, at the dorsal border of the lateral malleolus, is slightly convex laterally and parallels the medial rim of the trochlea. The deepest portion of the trochlear sulcus occurs about 3.5 lateral to the medial rim. The parallel anterior and posterior borders of the trochlea are oriented obliquely with respect to the lateral and medial border. The surface of the lateral malleolus is nearly flat. A broad but relatively shallow pit separates the medial edge of the trochlea from the medial tubercle. A low, narrow oblique ridge is directed across the surface of the medial malleolus to the posteroventromedial corner of the trochlea. Below this ridge, the oblique surface of the medial malleolus is flat, slanted dorsolaterally. The medial tubercle is separated from the head of the astragalus by a shallowly concave surface which slopes ventromedially. The navicular facette of the head is, in dorsal view, slightly anteriorly convex.

In anterior or distal view, the navicular facette of the head slants ventromedially and tapers as it curves posteroventrally. Lateral to the head, the sigmoid anterior calcaneal articular surface faces anteroventrally. This surface is nearly flat and can be divided into a lateral and medial portion. The lateral portion faces anteromedially as well as anteroventrally. The medial portion, which occurs at the medial base of the head and lies farther under the anterior edge of the astragalus than the lateral portion, faces anterolaterally as well as anteroventrally. Just below the anterior lip of the trochlea is a small triangular boss. In ventral view, the ventrally concave, medially tapering concave middle calcaneal facette lies between two ventrally projecting processes. These processes are part of the anteroventral and posteroventral edges, respectively, of the lateral malleolus. Opposite the lateral malleolus, on the medial side of the astragalus, the head and posterior process bound a ventrally concave arch which is about as deep as, but larger than, the middle calcaneal facette. Lateral to this medial arch, which is about 5.0 wide, a deep posterolaterally directed pocket represents the astragalar sulcus. The sulcus is located posterior and medial to the middle calcaneal facette as well as anterior and lateral to the posterior process. The posterior process lies at the posteromedial corner of the astragalus and bears the posterior calcaneal facette. This facette is convex medially, but becomes flatter as it tapers laterally to fade out near the midline of the astragalus.

The astragalus of *Dorcopsoides* is slightly larger than available specimens of *Wallabia rufogrisea.* In *Potorous tridactylus, Bettongia cuniculus, Dorcopsulus vanheuri,* and *Dorcopsoides,* the arc formed by ventral concavity between the head of the astragalus and the posterior tubercle is relatively deep, and semicircular, while in the macropodines studied (Table 4) the ventral concavity is broad and shallow because the posterior tubercle projects much more posteriorly then ventrally. In *Dorcopsoides* and *Bettongia* the anterior border of the trochlea is relatively straight, in *Potorous* and *Dorcopsulus* it is excavated. In most other features, the calcaneum of *Dorcopsulus,* although much larger, is considerably like that of *Dorcopsulus vanheuri.*

Cuboid (Table 9). Seven cuboids have been found. The dorsal surface of the cuboid roughly resembles a square, from the posterolateral corner of which an

TABLE 8

Measurements of astragali of *Dorcopsoides fossilis*

	Side	Length, navicular facette to posterior process	Length, anterior to posterior rim of middle calcaneal sulcus	Transverse width, anterior rim of middle calcaneal sulcus to medial tubercle	Transverse width, posterior rim of middle calcaneal sulcus to posterior process
UCMP 66632a	R	19.6	9.5	21.7	16.8
UCMP 66632b	R	----	10.9	----	----
UCMP 66632c	R	----	----	----	----
UCMP 66632d	R	----	----	----	16.7
UCMP 69630	R	17.0	7.8	----	14.8
UCMP 69632	R	----	7.2	----	15.3
UCMP 65884a	L	18.6	9.1	22.1	16.7
UCMP 65884c	L	----	7.8	----	14.6
UCMP 65884d	L	----	----	20.6	----
UCMP 66976	L	----	8.8	----	----
UCMP 69633	L	19.6	----	----	----
UCMP 69634	L	18.4	8.4	21.0	15.3
UCMP 69635	L	----	----	----	----
UCMP 69636	L	19.7	9.0	23.3	17.8
UCMP 69637	L	17.6	7.4	20.4	16.1
Range		17.0–19.7	7.2–10.9	20.4–23.3	14.6–17.8

L-shaped portion has been removed. The dorsal edge of the distal facette for Mtt. IV is slightly sinuous, being convex in its medial and concave in its lateral half. The dorsal surface slopes smoothly on to the lateral surface. The L-shaped notch in the proximolateral corner corresponds to the anteriorly projecting portion of the calcaneum. The medial half of the proximal surface is somewhat wider than the lateral half. The medial surface of the cuboid is concave. Just below the dorsal edge of the medial surface a nearly rectangular medial pit 3.5 long is separated to a variable degree from the ventral medial sulcus. This sulcus leads posteroventrally on to the plantar surface just anterior to the medial edge of the plantar calcaneal facette. On the medial surface of the cuboid

dorsal to the medial plantar sulcus is the triangular, flat navicular facette. The entocuneiform facette is located at the anterior portion of the medial surface of the cuboid anterior to the medial plantar sulcus and the medial pit. It widens as it extends ventrally to end on the medial surface of the plantar tuberosity, and slants slightly anteromedially. Just dorsal to the base of the medial plantar tuberosity, the facette is constricted by a salient in the ventral plantar sulcus.

In ventral view the medial plantar tuberosity is about 2.5 proximal to the distal surface of the cuboid. Its lateral surface slopes into a deep, slightly anteromedially oriented furrow which separates the medial from the large lateral plantar tuberosity. This tuberosity, about 8.4 long and 7.0 wide, occupies the proximal two-thirds of the lateral half of the plantar surface. The tuberosity is subovate, with a sharply pointed anteromedial corner. The convex surface of the tuberosity rolls up on to the lateral face of the cuboid, and terminates just below the edge of the lateral dorsal calcaneal facette. A well developed furrow separates the lateral plantar tuberosity from the ventrally projecting lip of the Mtt. V facette. The furrow continues posterodorsally on to the lateral face of the cuboid and fades out just above the lateral exposure of the lateral plantar tuberosity. The dorsal half of the lateral surface of the cuboid is relatively flat. It curves smoothly across the dorsolateral edge of the bone to become the dorsal surface.

TABLE 9

Measurements of cuboids of *Dorcopsoides fossilis*

		Greatest proximo-distal length of dorsal surface	Lesser proximo-distal length of dorsal surface	Transverse width at anterior edge of dorsal surface	Vertical height through medial ventral tuberosity	Vertical height through lateral ventral tuberosity
UCMP 69639	R	11.0	8.3	14.5	14.1	13.6
UCMP 69640	R	11.9	8.0	14.6	13.5	13.3
UCMP 69641	R	12.5	8.9	13.9	----	----
UCMP 69638	L	13.7	9.7	16.6	15.3	16.0
UCMP 69642	L	12.8	8.5	----	----	----
UCMP 69643	L	11.5	8.0	14.2	13.8	14.2
UCMP 69644	L	11.0	7.7	14.4	14.4	----
Range		11.0–13.7	7.7–9.7	13.9–16.6	13.5–15.3	13.3–16.0

In distal view the transversely elongate, slightly concave facette for Mtt. IV occupies most of this face of the cuboid. A small spur of the facette at the ventromedial corner extends slightly posteriorly on to the plantar surface. The lateral portion of the Mtt. IV facette is interrupted by a slight dorsolaterally directed crest which is the upper and medial boundary of the triangular concave facette for Mtt. V. A small rectangular transversely elongate pit lies along the midventral border of Mtt. IV facette, and separates the medial apex of the Mtt. V facette from the ventrolateral spur mentioned above.

The proximal surface of the cuboid is separated into two portions. The concave transversely elongate lateral dorsal calcaneal facette occupies most of this half of the bone. The medial dorsal calcaneal facette is vertically elongate and slopes smoothly posteroventrally and medially on to the plantar calcaneal facette. This is limited to the medial half of the plantar portion of the cuboid and is separated, at its dorsolateral corner, by a small depression from the border of the lateral dorsal facette.

The cuboid of *Dorcopsoides fossilis* has the largest medial plantar tuberosity, relative to the size of the other elements of the bone, of any of the macropodids studied. The closest resemblance to *Dorcopsoides* in this and other features was found in the cuboid of *Setonix brachyurus*.

Navicular. Only one navicular, UCMP 67082, has been recovered which is the correct size to articulate with the astragali. This element is from the left side and is about the size of that found in *Wallabia rufogrisea*. The vertical height of the bone in *Dorcopsoides* is 11.9. The anteroposterior length measured at the dorsal end of the proximal and distal facettes is 6.8. The transverse width across the distodorsal corner is 4.7.

The medial surface of the bone is flat and smooth except for a slight flange developed at the medial border of the astragalar facette and the swelling of the plantar tuberosity located at the posteroventral corner of the bone. The anteroventral corner of the bone is broken on the medial side so that the entocuneiform facette is absent. The profile of the astragalar facette is only slightly concave in medial view and slants posteriorly to only a small extent. In proximal view, the dorsally elongate astragalar facette is nearly vertically oriented. The labial outline is medially convex in its dorsal two-thirds, then bows out for the proximoventral tuberosity. The ventral half of the lateral border of the facette is laterally convex. A low salient projects laterally above this, whereafter the lateral edge of the facette continues to its narrow dorsal edge.

In lateral view, a flat triangular cuboid facette occupies the distodorsal corner of the bone. Below this, a laterally projecting flange buttresses the plantar portion of the ectocuneiform facette located on the distal surface of the navicular. Elsewhere, the lateral surface of this element is smooth.

In anterior view the ectocuneiform facette faces slightly anteromedially in its dorsal half, but then curves ventrolaterally lateral to the base of the broken entocuneiform facette, and faces anteroventrolaterally.

In plantar view, the surface of the posteroventral tuberosity is flat, subovate and slightly elongate anteroposteriorly. In dorsal view the sides of the narrow dorsal surface are mutually concave. The distal end is wider than the proximal. The navicular of *Dorcopsoides* does not have the strong proximal extension of the plantar tuberosity of *Potorous tridactylus* and *Bettongia cuniculus*. Of the specimens studied, the naviculars of *Dorcopsoides* and *Dorcopsulus* alone have the nearly straight profile of the astragalar facette and slightly projecting plantar tuberosity. Other features such as the lateral salient just above the midlateral edge of the astragalar facette and the posteroventrolateral elongation of the ectocuneiform facette are also found in *Thylogale thetis*.

Metatarsal IV (Table 10). Twenty-four fourth metatarsals are of the correct size and construction to articulate with other foot elements referred to *D. fossilis*. In about one-third of these tarsal elements the shaft is slender and the plantar surface is poorly keeled, the plantar cuboid tuberosity is somewhat small. Elements of this character may pertain to either female or immature individuals. They do not differ fundamentally from the remaining metatarsals in this sample and are treated as belonging to the same species.

In dorsal view, the sides of the slender shaft are nearly parallel. Distally, the shaft expands to the base of the head, then narrows somewhat at the sides of the articular surface. Proximally, the lateral side of the shaft extends obliquely to the lateral apex of the base. The medial surface of the base is slightly excavated for the ectocuneiform. The dorsal surfaces of the distal half of the shaft and of the head are nearly flat. Proximally, the dorsal surface is broadly rounded.

In proximal view, the slightly convex cuboid facette occupies most of this end of the bone. This facette forms a transversely elongate triangle, the dorsal edge of which is broadly arched. The medial edge is only slightly excavated for the ectocuneiform so that the plantar tuberosity is almost directly beneath the medial edge of the shaft. The lateral side is excavated below to receive the closely applied Mtt. V. The ventral apex of the cuboid facette extends on to the posterodorsal surface of the plantar tuberosity. The apex of this smooth surface is either narrowly rounded or broadly pointed.

The flat anteroventral surface of the plantar tuberosity is obliquely oriented and receives the proximal facette of the sesamoid, which lies between the ento-cuneiform and the ventral base of Mtt. V. The lateral, ventral, and medial surfaces of the posteroventrally projecting plantar tuberosity are slightly concave. An elongate ventral crest extends anterolaterally from the base of the plantar tuberosity and blends into the ventral surface of the shaft about 15.0 behind the lateral edge of the head. Near its midlength, the medial surface of this crest is slightly longitudinally excavated; proximal to this, it is slightly swollen. The lateral surface of the shaft dorsal to the crest is smooth and flat and faces ventrolaterally. At the proximal end of this surface, the elongate bilobate articulation facette for Mtt. V extends from just beneath the tip of the laterally expanded base to just above the lateral border of the plantar sesamoid facette.

TABLE 10

Measurements on Metatarsal IV of *Dorcopsoides fossilis*

	Side	Greatest length	Transverse width, proximal end	Vertical height, proximal end	Transverse width, distal end	Vertical height, distal end	Greatest vertical height, shaft	Smallest vertical height, shaft
UCMP 65888a . . .	R	79.1	15.0	13.9	14.6	9.8	11.9	7.5
UCMP 65888b . . .	R	----	----	----	16.5	10.7	----	8.4
UCMP 65888c . . .	R	----	13.1	12.5	----	----	----	----
UCMP 65975 . . .	R	----	----	13.6	----	10.4	----	----
UCMP 66639 . . .	R	----	12.3	10.9	----	----	----	----
UCMP 69646 . . .	R	80.2	15.0	13.9	15.0	10.4	12.1	7.8
UCMP 69647 . . .	R	74.7	----	12.7	----	9.4	10.8	7.6
UCMP 69648 . . .	R	----	14.1	12.8	----	----	10.7	----
UCMP 69649 . . .	R	----	14.5	14.0	----	----	11.5	----
UCMP 69650 . . .	R	----	13.8	12.6	----	----	11.5	----
UCMP 69651 . . .	R	----	----	12.3	----	----	9.8	----
UCMP 69652 . . .	R	----	----	12.7	----	----	----	----
UCMP 69653 . . .	R	----	----	----	----	9.6	----	----
UCMP 69654 . . .	R	----	----	14.1	----	----	----	----
UCMP 69655 . . .	R	----	----	12.4	----	----	10.8	----
UCMP 69656 . . .	R	----	----	----	----	10.7	----	----
UCMP 66616 . . .	L	----	----	----	----	----	----	----
UCMP 69662 . . .	L	84.7	----	13.6	----	11.7	12.3	8.8
UCMP 69663 . . .	L	76.1	14.9	----	14.7	10.0	11.3	8.2
UCMP 69664 . . .	L	----	14.4	12.3	----	----	9.5	6.4
UCMP 69665a . . .	L	----	15.0	14.5	----	----	11.4	----
UCMP 69665b . . .	L	----	----	----	15.6	10.3	----	----
UCMP 69666 . . .	L	----	----	----	----	----	10.4	----
UCMP 69667 . . .	L	80.3	15.1	14.0	15.0	10.0	12.2	8.2
Range		74.7–84.7	12.3–15.1	10.9–14.5	14.6–16.5	9.4–11.7	9.5–12.3	6.4–8.8

The lateral profile of the head is smoothly rounded but slightly downturned relative to the long axis of the shaft. The distal condyles are not conspicuously different from those in other small macropodids.

Metatarsal IV of *Dorcopsoides* is slightly smaller than that of *Wallabia rufogrisea.* Metartarsal IV of *Lagorchestes hirsutus, Thylogale thetis, Petrogale xanthopus, Wallabia rufogrisea, Macropus erubescens* and *Megaleia rufa* differ from that of *Dorcopsoides* in having the plantar tuberosity more centrally positioned under the shaft, having a well defined excavation on the medial surface of the bone, the dorsal edge of the proximal surface being strongly concave instead of broadly convex. Except in *Petrogale xanthopus, Thylogale thetis,* and *Wallabia rufogrisea,* the shaft is long and slender and does not thicken abruptly proximal to the head. In *Setonix brachyurus,* the plantar tuberosity is slightly more lateral in position than in *Dorcopsoides,* but these two forms resemble each other in the small extent to which the medial surface of the basal portion is excavated, the proximally convex cuboid articulation surface, the transversely expanded shaft proximal to the head, the bilobate outline of the articulation facette for Mtt. V, the sharp lateral apex of the cuboid facette, and the moderately acuminate plantar apex of that facette. The major feature in which Mtt. IV of *Dorcopsoides* differs from that of *Setonix* and at the same time resembles that of *Dorcopsulus* is its general proportions. Mtt. IV of *Setonix* is relatively much more massive. In other details, such as the bilobate Mtt. V facette, the acuminate ventral apex of the cuboid facette, and the slight degree of excavation of the medial surface of the base, *Dorcopsoides* is distinctly different from *Dorcopsulus.* The presence of a broadly bilobate Mtt. V facette in Mtt. IV of *Petrogale xanthopus* suggests that a facette of this type has been occasionally developed in macropodine kangaroos, but perhaps not in the known potoroine genera.

Metatarsal V (Table 11). Fifteen fifth metatarsals of *Dorcopsoides* have been recovered. This element is slightly shorter than but relatively not as slender as that of *Wallabia rufogrisea.* Two specimens are noticeably more slender than the others and may represent either immature or small female individuals. The proximal base bears the obliquely oriented facettes for the cuboid and Mtt. IV. Anterior to this the shaft narrows to about its midlength before expanding to the head, which contains the articulation surface for the proximal phalanx.

A moderately sharp crest extends anteromedially from the lateral base of the cuboid facette, then curves and fades out along the dorsal edge of the bone, which becomes progressively flatter distally. The dorsal swelling common to the central and medial condyles occupies most of the dorsum of the head. The lateral condyle is prominently set off from this by a broad sulcus.

The lateral surface of the proximal two-thirds of the shaft is flat and faces dorsolaterally. At the proximal end a small dorsally concave groove separates the basal lateral buttress of the cuboid facette from the slightly swollen and proximally rounded tuberosity. The dorsal border of the shaft is arched, the plantar border is concave, particularly in the distal one-third. The medial surface of the shaft is broadly rounded. The shallow knob at the base of the head

lies slightly dorsal to the rear of the medial pit. Peripheral to the pit, the medial condyle becomes differentiated ventrally from the rest of the head and fades out into the shaft posteriorly. The central condyle is the largest, and is situated closer to the medial than lateral side. The smaller lateral condyle bears an indistinct pit in its lateral surface. Toward the proximal end, there are a pair of small crests anterior to the ventral ovoid portion of the Mtt. IV facette. Between these two crests, a shallow sulcus leads anteriorly from the base of the facette. The facette is supported on a medially projecting base. Except for a short posteroventrally directed crest the ventral Mtt. IV facette is totally isolated from the medial edge of the cuboid facette which is supported by a cup-shaped

TABLE 11

Measurements on Metatarsal V of *Dorcopsoides fossilis*

	Side	Greatest length	Oblique length, proximal tuberosity to medial end Mtt. IV facette	Greatest vertical height of shaft	Least vertical height of shaft	Oblique width, medial end Mtt. IV facette to proximo-lateral corner, cuboid facette	Transverse width, head	Vertical height, head through central condyle
UCMP 66615	R	----	----	11.0	7.1	----	----	----
UCMP 69668	R	67.8	12.8	11.1	6.5	11.0	10.3	9.0
UCMP 69669	R	----	----	10.4	----	----	----	----
UCMP 69670	R	68.0	13.7	10.8	6.3	10.3	10.4	9.0
UCMP 69671	R	----	----	7.5	----	----	----	----
UCMP 66629	L	----	----	----	6.2	----	----	9.7
UCMP 67027	L	68.2	13.5	10.5	6.3	10.8	----	----
UCMP 67048	L	----	----	11.7	----	12.8	----	----
UCMP 67070	L	----	----	----	6.3	----	10.6	9.4
UCMP 69661	L	71.7	15.7	11.3	6.9	12.9	11.9	10.7
UCMP 69672	L	----	----	----	6.2	----	9.7	9.8
UCMP 69673	L	----	----	----	----	----	8.4	7.8
UCMP 69674	L	----	----	----	5.9	----	9.8	9.6
UCMP 69675	L	----	13.1	10.7	----	11.7	----	----
UCMP 69676	L	----	12.9	10.8	----	11.0	----	----
Range		67.8–71.7	12.8–15.7	11.7–7.5–	7.1–5.9–	12.9–10.3–	11.9–8.4–	10.7–7.8–

TABLE 12

Measurements on Proximal Phalanx IV in *Dorcopsoides fossilis*

	Side	Length	Proximal width	Proximal height	Distal width	Distal height
UCMP 65911	R	30.7	13.9	10.8	11.3	7.4
UCMP 66196a	R	----	----	----	11.6	7.2
UCMP 66196b	R	30.5	13.1	9.9	----	6.8
UCMP 66196c	R	28.9	13.2	9.0	10.5	6.6
UCMP 66196d	R	29.0	12.5	8.8	10.3	5.9
UCMP 69680	R	32.4	14.4	9.9	10.9	6.8
UCMP 69681	R	28.8	12.8	9.1	9.8	5.8
UCMP 69682	R	29.1	13.3	9.7	10.7	6.3
UCMP 69683	R	29.8	13.9	9.9	10.9	6.7
UCMP 69684	R	30.5	13.6	9.8	10.5	6.6
UCMP 69685	R	27.8	13.2	9.4	10.2	6.4
UCMP 69686	R	30.3	12.8	9.7	10.5	6.6
UCMP 69687	L	----	----	----	10.1	6.2
UCMP 66613	L	32.2	13.8	10.2	10.7	6.6
UCMP 66635	L	29.6	12.7	9.1	10.4	5.9
UCMP 67097	L	31.6	14.5	10.5	11.7	6.9
Range		27.8–32.4	12.5–14.5	8.8–10.8	9.8–11.7	5.8–7.4

process. Dorsally, the ovoid ventral Mtt. IV facette is connected by a short narrow isthmus to the more elongate dorsal portion of the facette. The cuboid facette, which lies proximal to the Mtt. IV facette and occupies all of the proximal surface, is obliquely triangular and proximally concave. The ventromedial apex ends in the cup-shaped process. A dorsolateral corner protrudes beyond the general border of the shaft. Proximal to and below this the facette extends on to the dorsal surface of the plantar tuberosity. Ventrally a deep anteromedially elongate sulcus separates the tuberosity from the ventromedial process, and quickly fades out beneath the base of the Mtt. IV facette. The surface of the ventromedial process supports the lateral portion of the plantar sesamoid.

TABLE 13

Measurements on Distal Phalanx IV in *Dorcopsoides fossilis*

	Side	Length	Proximal width	Proximal height	Distal width	Distal height
UCMP 67058	R	17.7	10.7	8.7	9.0	5.9
UCMP 67086	R	16.3	9.3	7.9	8.7	5.2
UCMP 69689	R	18.2	11.4	8.9	9.8	6.1
UCMP 69690	L	17.1	10.4	8.3	9.3	5.7
UCMP 69691	L	18.8	11.4	8.7	9.7	5.8
Range		16.3–18.8	9.8–11.4	7.9–8.9	8.7–9.8	5.2–6.1

TABLE 14

Measurements on Proximal Phalanx V of *Dorcopsoides fossilis*

	Side	Length	Proximal width	Proximal height	Distal width	Distal height
UCMP 66637	R	20.6	----	9.7	8.2	6.5
UCMP 67084	R	18.2	8.7	7.6	6.9	5.8
UCMP 69692	R	20.0	11.9	9.8	8.6	6.9
UCMP 69693	L	20.0	9.9	8.4	7.2	6.2
UCMP 69694	L	19.4	10.3	8.8	7.7	6.4
UCMP 69695	L	21.3	11.3	9.5	8.4	7.1
UCMP 69713	L	18.6	9.7	8.5	7.2	5.9
UCMP 69714	L	----	----	----	6.2	5.3
Range		18.2–21.3	8.7–11.9	7.6–9.8	6.2–8.6	5.3–7.1

The fifth metatarsal of *Dorcopsoides* is most like that of *Setonix brachyurus*. The transversely elongate cuboid facette with its medial apex ending in a somewhat cup-shaped process is found in *Dorcopsulus vanheuri* and *Setonix brachyurus*. Mtt. V of *Dorcopsoides* differs from that of *Dorcopsulus* and resembles *Setonix* in the proximal elongation of the large plantar tuberosity, the separation of Mtt. IV facette into two parts, and the strong separation of the medial Mtt. IV facette from the cuboid facette. *Dorcopsoides* differs from *Setonix* in the more lateral position of the dorsolateral corner of the cuboid facette, the more medial position of the medial Mtt. IV facette, the greater development of the ventromedial process, and the relatively more slender proportions of the shaft, as well as in absolute size. The ventromedial process is most elaborately developed in members of the Potoroinae. The nearly complete loss of this feature in macropodines other than *Setonix* may indicate that *Setonix* represents a remnant of a primitive lineage within the subfamily.

Proximal phalanx IV (Table 12). Fifteen proximal phalanges of the fourth digit have been identified as probably belonging to *Dorcopsoides fossilis*. These are slightly smaller than similar elements in *Wallabia rufogrisea*. The proximal profile is lower than in *Setonix brachyurus* or *Dorcopsulus vanheuri*, is not symmetrical, and tapers laterally as in various macropodines.

Distal phalanx IV (Table 13). Five distal phalanges of the fourth digit have been recovered. These elements, smaller than in *Wallabia rufogrisea*, have a moderately high proximal profile as in *Bettongia cuniculus, Potorous tridactylus, Thylogale thetis*, and *Setonix brachyurus*, rather than the low profile found in forms such as *Macropus erubescens, Megaleia rufa*, and *Petrogale penicillata*. This phalanx is shorter relative to the proximal phalanx than in *Bettongia* and *Potorous*.

Proximal phalanx V (Table 14). There are eight proximal metatarsals of the fifth digit in the sample. These are the short, laterally excavated elements with the high triangular proximal profile usually found in this digit in the Macropodidae. This element in *Dorcopsoides fossilis* is relatively not as slender as in *Potorous tridactylus*, but has proportions similar to that of *Setonix brachyurus*.

Distal phalanx V (Table 15). There are only two of these bones in the collection. They are larger and have a narrower dorsal border than, but are otherwise like, the homologous element in *Setonix brachyurus*. The fifth distal phalanges of *Potorous tridactylus* and *Lagostrophus fasciatus* are relatively longer and more slender than in *Dorcopsoides*. The element in *Petrogale xanthopus* has about the same proportions as in *Dorcopsoides* but lacks the greater posterior projection of the medial lobe of the proximal articulation surface common to *Setonix* and *Dorcopsoides*.

Discussion. Dorcopsoides fossilis is a wallaby-sized macropodid which is smaller, in most respects, than an adult specimen (UCMVZ 127651) of *Wallabia rufogrisea frutica* in the collections of the Museum of Vertebrate Zoology, Berkeley. It is more closely related to potoroine than to macropodine forms. In particular,

TABLE 15

Measurements on Distal Phalanx V of *Dorcopsoides fossilis*

	Side	Length	Proximal width	Proximal height	Distal width	Distal height
UCMP 69696	R	12.2	9.4	7.6	8.6	5.6
UCMP 69697	L	10.7	8.2	7.0	7.5	4.6
Range		10.7–12.2	8.2–9.4	7.0–7.6	7.5–8.6	4.6–5.6

the close affinity of *Dorcopsoides fossilis* seems to be with the lineage which produced *Dorcopsis* and *Dorcopsulus*. The ancestry of *Dorcopsoides fossilis* is unknown. The undescribed potoroine from the late Oligocene Ngapakaldi fauna of South Australia (Stirton, Tedford, & Miller, 1961, p. 36) may prove to be a suitable morphological forerunner. It is nevertheless clear from its partial resemblance to certain typical macropodines, as well as the fusion of the protoconid and metaconid of dP_3 and other features which place it squarely in the path of *Dorcopsis* and *Dorcopsulus,* that *Dorcopsoides* represents a rather wide departure from any stem potoroine.

As shown by its shorter juvenile and adult premolar dentition, relatively lower-crowned teeth, weaker crests from the labial cusps in upper molars, a less obstructed transverse valley, and other similarities to classical potoroines, *Dorcopsoides fossilis* is clearly more primitive than *Dorcopsis or Dorcopsulus.* On the other hand, the many specializations in *Dorcopsoides* which indicate close affinity with *Dorcopsis* and *Dorcopsulus* also show that this lineage was already distinct and well separated from those of other macropodids by Miocene time.

An illustration of the complexity of the macropodid phyletic history is shown by the fact that *Dorcopsoides, Dorcopsulus* and *Dorcopsis* share the following characters with typical macropodines: combined length of P^2 and dP^3 about equal to that of M^1 and M^2; M^4 not greatly reduced; lower incisors relatively short and deep; leading edge of ascending ramus nearly vertical; rear of maxillary base of zygomatic arch above M^3, not M^2; nearly horizontal uppermost surface of maxillary shelf does not slope ventrally toward the rear of the molar series; P_3 not so conspicuously higher-crowned than molars; lateral indentation of lateral flange of calcaneum. Because of the lack of an adequate fossil record of

the Macropodidae, the possibility that these three genera have converged with typical macropodines in these features cannot be evaluated. It is, however, evident that the separation of the potoroines from the macropodines is not sharp in all respects, and it seems premature to follow Pearson (1950) in elevating these units to family rank at this time.

A medium-sized macropod of the general *Dorcopsis-Dendrolagus* type has been described from the late Pliocene Awe fauna of New Guinea (Plane, 1967b, p. 14). Unfortunately, this form is known only from two specimens, a right maxillary fragment with M^1-M^4 and an isolated right M^3. Other, postcranial, material has been referred to this species, but the association is not certain. The teeth of the New Guinea animal are slightly larger than those of *Dorcopsoides fossilis* and also differ in the strong posterior tapering of M^4 and M^3. The New Guinea form differs not only from *D. fossilis* but also from specimens of *Dorcopsis hageni, Dorcopsulus vanheuri, Dendrolagus dorianus,* and *D. goodfellowi* in having the maxillary foramen above the metaloph of M^3 rather than being located more anteriorly. Except for small mesostyles, the teeth of the New Guinea form resemble those of species of *Dendrolagus*. Further resemblance to *Dendrolagus* is seen in the palatal surface. Although the palate is preserved only up to 4.5 medial to M^3 and M^4 in the New Guinea fossil, enough is present to show that the maxillopalatine suture passes anteromedially and does not lie close to the medial roots of the molars. In the specimens available for comparison, this suture extends anteriorly or slightly anterolabially quite close to the medial roots of M^3 and M^4 in *Dorcopsis* and *Dorcopsulus,* while it is directed anteromedially in *Dendrolagus* and is not as closely approximated to the medial roots of the last two molars. The postcranial material which has been referred to the New Guinea fossil apparently shows closest similarities to *Dorcopsulus* (Plane, *ibid.,* p. 50). In view of the uncertainty concerning the association of this material, its value in assessing the affinity of the New Guinea form may be questionable. The features of the teeth and surrounding bone suggest that the New Guinea fossil is not related to *Dorcopsoides, Dorcopsis* or *Dorcopsulus,* but rather to *Dendrolagus.*

Subfamiliae Incertae

The next form to be described is a large macropodid which shows, on one hand, a number of characters which are prophetic of Pliocene and Pleistocene protemnodonts and, on the other, characters which are found in late Cainozoic members of the Sthenurinae. Because the late Cainozoic history of the Macropodidae is poorly understood and because temporally and structurally intermediate forms are absent, the animal cannot be assigned to a subfamily. Its characters show, however, that the protemnodont and sthenurine lineages may not have been too far separated from each other in the late Miocene and that they may have shared a common ancestry in the middle Tertiary — of which *Hadronomas* may be a representative.

Genus HADRONOMAS[1], nov.

Genotypic species: Hadronomas puckridgi, sp. nov.

Generic diagnosis: P^3; basic construction similar to that of *Protemnodon,* but shorter, generally narrower, lower-crowned; greater number of cusps (7) on shearing blades; no lingual cingulum, no extensive linear valley between shearing blade and lingual cingulum; no deep pocket developed between transverse crest and posterior cingular crest. M^1: with low shelf-like anterior cingulum; sharp postparaconal, premetaconal and postmetaconal crests; postparaconal and premetaconal facettes developed at labial end of lophs; no forelink; midlink small; hindlink present from apex of hypocone to posterior base of metacone; lingual cingulum present; labial and lingual basal outline of lophs nearly straight; enamel surface not crenulated. *Mandible*: slender; relatively flat labial and lingual surfaces; nearly straight ventral border, depth below M_4 considerably greater than that below P_3; depth of mandible about seven times greater than height of unworn M_4 protoconid. I_1 slender; elongate; nearly straight vertical posterior border of enamel on lateral surface of tooth with posterior salient in ventral third. P_3 elongate, serrate; six cuspids, with labial and lingual vertical ridgelets associated with first five; labial and lingual cingula present; shearing crest concave lingually; tooth does not taper strongly anteriorly. *Lower molars*: low-crowned, with cingulum extending across anterior end of tooth for nearly total width of protolophid; lingual termination of cingulum abrupt, separated from base of metaconid by definite lingual emargination; lophids conspicuously wider near crest than at base of crown; enamel surface not crenulated; M_4 smaller and lower-crowned than M_3; hypolophid of M_4 conspicuously narrower than protolophid.

HADRONOMAS PUCKRIDGI[2] sp. nov.

(Figs 14-17; Tables 16, 17)

Holotype: CPC 6751, right mandible with P_3-M_4 preserved.

Paratype: UCMP 70511-70513, three RP^3; UCMP 70510, UCMP 70563, two LP^3; UCMP 70521, maxillary fragments with RM^1, LM^3 and LM^4; UCMP 70520, maxillary fragment with RM^2-M^3; UCMP 70519, LM^3-M^4; UCMP 65981, LM^3; UCMP 69765, RI_1; UCMP 69775, LI_1; UCMP 66463, right mandible with I_1, P_3-M_4; UCMP 65976, RP_3-M_1; UCMP 70526, partial mandible with LI_1, P_3-M_4; UCMP 70525, LP_3 in mandible fragment; UCMP 70524, LM_2-M_4; UCMP 70523, RM_1; UCMP 70522, RM_3.

---

[1] Hadros = large; nomas = nomad. In reference to the probable wandering habits of this large macropodid.

[2] Named in honour of Mr P. L. Puckridge, owner of Alcoota station.

Specific diagnosis: That of genus until other species are described.

Locality: V6345, Paine Quarry, Waite Formation, 4.0 miles south-west of Alcoota station and 2.1 miles south-west of junction of Waite and Ongeva Creeks, Northern Territory, Australia.

Age: Alcoota fauna; late Miocene or possibly early Pliocene.

Description and discussion of holotype (Fig. 14; Table 17). The holotype, CPC 6751, is a fragmentary mandible containing a complete but slightly worn cheektooth dentition. The bone of the mandible is fractured. M_1 is fractured, M_2 and M_3 are less so. M_4 is in perfect condition. Except for lacking a small portion of its lingual cingulum and being transversely cracked across the middle of the tooth, P_3 is also completely preserved.

In occlusal view, the cheektooth row is straight. The length from P_3 to M_4 is 60.4. Although it is poorly preserved, it can be seen that the mandible was slender but deep. As preserved, the mental foramen is about 2.0 anterior to P_3 and the ventral edge is 5.5 below the diastemal crest. The diastemal crest is moderately sharp.

Lower third premolar (Fig. 14; Table 17). P_3 is an elongate serrated shearing tooth with one anterior and one posterior root. The labial and lingual walls of the shearing blade are relatively steep. The crest of the blade, which is slightly concave lingually and extends from the posterolingual corner to the anterior apex of the tooth, is composed of six cuspids. These have been numbered antero-posteriorly from 1 to 6 for descriptive purposes. Cuspids 1 to 5 are small, but 6 is about 4.3 long. A labial and a lingual ridgelet descend vertically from each cuspid toward the base of the crown. Most of the ridgelets merge into the small labial and lingual cingula. No ridgelets are associated with the last cuspid and the cingula are absent at its base. The lingual cingulum extends around to the anterior apex of the tooth, but the labial cingulum does not persist past the second ridgelet. The shearing crest does not extend down the anterior and posterior ends of the blade as a sharp ridge. In labial view the profile of the shearing crest is essentially straight. As indicated in Table 17, the crown of the tooth is higher at the anterior than the posterior end. In occlusal view, the labial and lingual bases of the crown are somewhat curved in conformity with the curvature of the shearing crest. The lingual outline is, however, straighter than that of the labial side.

The lower third premolar of *Hadronomas puckridgi* is, in some respects, closer to the basic morphology of *Sthenurus* than to that of *Protemnodon*. The number of cuspids on the shearing blade is particularly indicative of this. In forms such as *Protemnodon* and *Prionotemnus*, P_3 tapers strongly anteriorly and lacks any suggestion of a labial cingulum, and the ridgelets associated with the cuspids are poorly developed. In certain species of *Sthenurus*, such as *S. andersoni*, P_3 does not taper strongly anteriorly in spite of the trenchant cingulum which has developed on the posterolabial portion of the tooth. Also, in *Sthenurus* the ridgelets associated with the cuspids are not only numerous but well defined. Therefore, although

it is difficult to make phyletic determinations in the absence of annectant forms, P_3 of *H. puckridgi* is suitably constructed to provide the morphological basis for the derivation of P_3 in *Protemnodon* by suppression of the cingula and reduction in prominence and number of the cuspids and ridgelets, or derivation of the P_3 of *Sthenurus* through emphasis on the development of the labial cingulum.

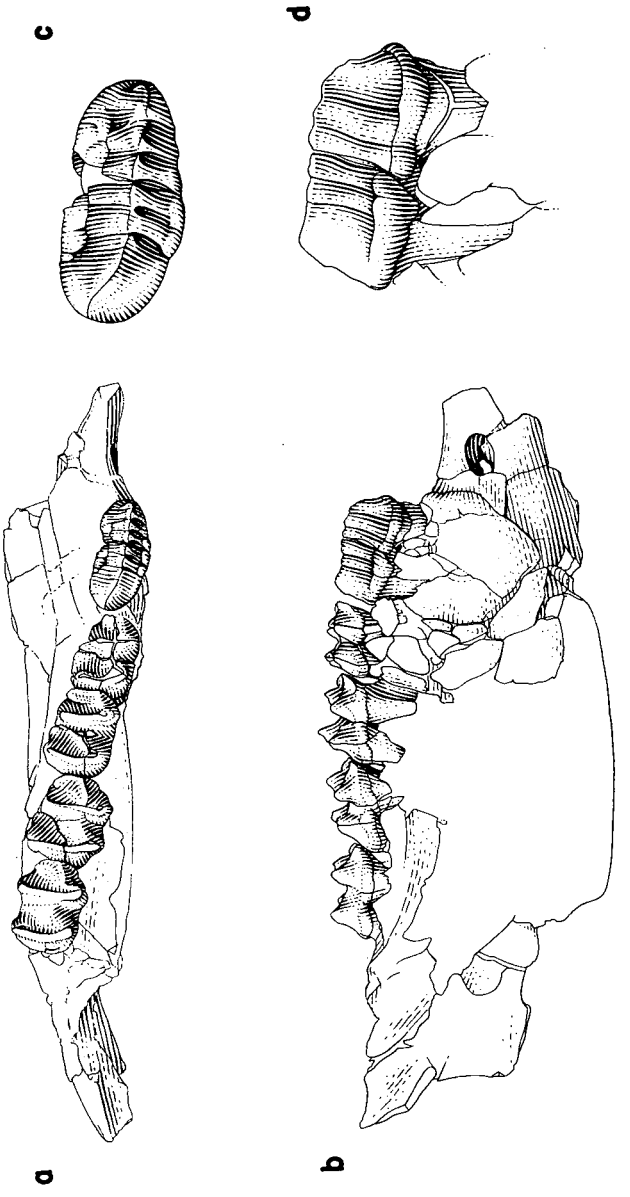

Fig. 14. *Hadronomas puckridgi* **gen. nov., sp. nov.** a, **occlusal and** b, **labial view of holotype. CPC 6751, right mandible fragment with P_3-M_4. Natural size.** c, **occlusal, and** d, **labial view of P_3 of holotype, CPC 6751. Twice natural size.**

Lower molars (Fig. 14; Table 17). The first lower molar is a low-crowned bilophodont tooth in which the forelink and midlink are rather poorly developed. The anterior cingulum is relatively broad and shelf-like. Its lingual end is distinctly separated from the base of the metaconid by a shallow emargination. The labial end of the cingulum blends into the base of the protoconid. The forelink joins the cingulum slightly labial to the midline of the tooth. A lingual cingulum is absent except at the transverse valley. A poorly developed labial cingulum occurs at the base of the protolophid and hypolophid. The crests of the lophids are slightly concave anteriorly and are oriented transversely with respect to the long axis of the tooth. In labial view the profile of the transverse valley is U-shaped. Although a distinct posterior cingulum is not developed, the base of the hypolophid bulges out over the posterior root in lateral view. In occlusal aspect the protolophid is narrower than the hypolophid. The axes of the lophids are nearly vertical in labial view.

The morphology of M_2-M_4 is like that of M_1. In general the width of the hypolophid relative to that of the protolophid decreases posteriorly. The size and crown height of the molars increases to M_3, then decreases to M_4. In contrast to M_1, a labial cingulum is absent in M_2-M_4, and the greatest width of the lophid is actually measured near the apex of the crest, not at the base. In Table 17 the widths of the teeth were taken at the base of the crown.

The greatest width of the protoconid and hypoconid is measured above the base of the crown in *Hadronomas, Sthenurus,* and *Protemnodon.* In *Sthenurus andersoni* and *Hadronomas puckridgi* the discrepancy between the maximum width of the lophid and its basal width is greater than in either Pliocene or Pleistocene species of *Protemnodon.* Further resemblance between *H. puckridgi* and *S. andersoni* and other species of *Sthenurus* is seen in the relatively low midlink and forelink and the rather abrupt lingual termination of the anterior cingulum, which is separated from the base of the metaconid, in occlusal view, by a small but distinct lingual emargination. *H. puckridgi* also resembles species of *Sthenurus* and differs from *Protemnodon* in that M_4 is smaller and lower-crowned than M_3, and the hypolophid of M_4 is conspicuously narrower than the protolophid. Lower molars of *Hadronomas puckridgi* differ from those of both *Sthenurus* and *Protemnodon* in being lower-crowned and in having an anterior cingulum which extends across the tooth for nearly the total length of the protolophid.

Description and Discussion of Paratypes.

Upper Dentition. Premolar (Fig. 15; Table 16): Five upper third premolars are represented by the material at hand, one of which is only a fragment. P^3 is an elongate, relatively broad sectorial serrate tooth supported by a slender anterior root and a massive posterior root. The basal outline of the tooth tapers to the broadly rounded anterior end. The slightly convex labial outline of the tooth is interrupted by two shallow emarginations, which are located approximately 4.0-5.0 posterior to the anterior apex and anterior to the rear of the tooth. The

lingual outline is somewhat smoother than the labial, but may be broken by a pair of similarly placed emarginations, or by a slight bulge in the anterior third (Fig. 15).

The crest of the shearing blade is situated nearly over the midline of the tooth (Fig. 15) and extends in a slightly sinuous fashion from the posterolabial corner to the anterior apex. The crest is divided into seven cusps. For descriptive

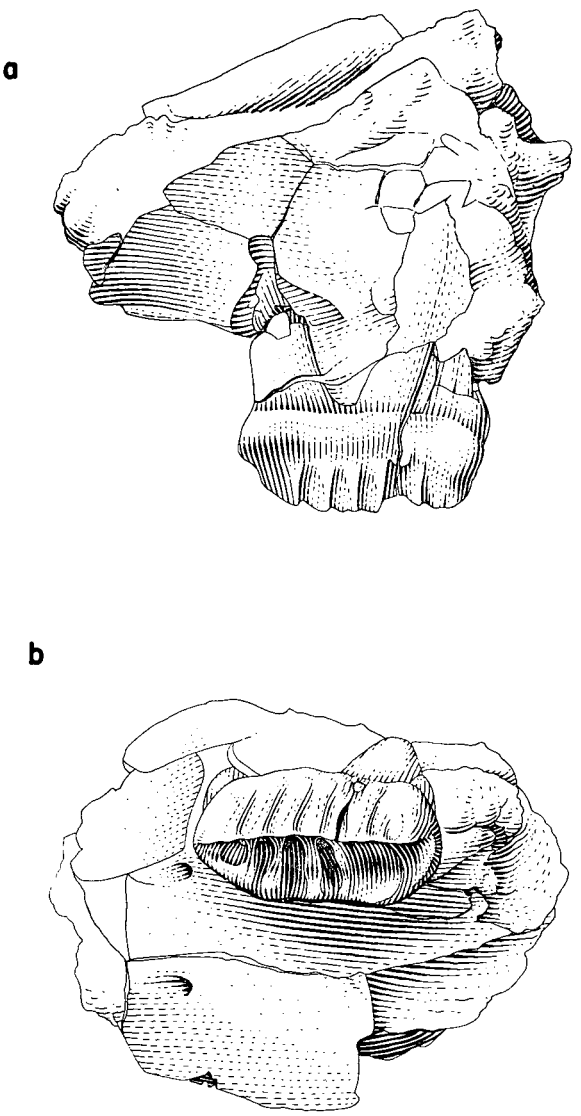

Fig. 15. *Hadronomas puckridgi* **gen. nov., sp. nov.** a, **labial and** b, **occlusal view of LP^3, UCMP 70563. Twice natural size.**

purposes, these have been numbered from 1 to 7 from the anterior end. A vertical ridgelet lies on the labial surface of the shearing blade in association with all but the posterior-most cusp. The ridgelet on the labial side of cusp 1 is not as well developed as the others. On the lingual surface of the shearing blade, ridgelets are associated with all but cusp 6 and those leading to cusps 1 and 5 are weakly developed. The lingual ridgelets for cusps 1 to 5 expand at their bases into the lingual cingulum. Although it is prominently developed, the lingual cingulum is not as massive as in species of *Protemnodon* and has not begun to form a lingual shearing crest as in *Sthenurus*.

A short, low, transverse crest connects the posterolingual corner of the cingulum to the posterior cusp of the shearing blade. In some specimens (Fig. 15), the transverse crest is slightly curved, convex anteriorly. A posterior cingulum is only slightly developed as a short ridge between the posterior base of the shearing blade and the posterolingual corner of the cingulum. A labial cingulum is only faintly suggested. There is no anterior cingulum. In labial view the crest of the shearing blade is essentially straight, and parallels the base of the crown. As shown in Figure 15, a rather well defined basin is bounded by the lingual wall of the shearing blade, the short transverse crest, the lingual cingulum and the fifth ridgelet.

The upper third premolar of *Hadronomas puckridgi* generally resembles that of the species of *Protemnodon*. *Protemnodon* is used here in the sense of Stirton (1963) and Plane (1967), i.e., for large extinct macropodids having large, multiserrate premolars and other distinctive features which set them apart from smaller living species commonly referred to the genus *Wallabia*. Comparison of the dimensions of P^3 in Table 16 with those for *Protemnodon otibandus* (Plane, 1967b, p. 35) and various Pleistocene forms (Stirton, 1963, Table 2) shows that P_3 in *Hadronomas puckridgi* is shorter, generally narrower, and lower-crowned than in the Pliocene and Pleistocene protemnodonts. *H. puckridgi* also differs from *Protemnodon* in lacking a strong, elongate shearing crest between the anterior cusp and the apex of the tooth, in lacking the sectorial lingual cingulum, in lacking a longitudinal basin enclosed between the shearing blade and the lingual cingulum, in lacking the deep pocket between the short posterior transverse crest and the posterior cingular crest and in having a greater number of ridgelets and grooves.

In the greater number of ridgelets and grooves, and in the relatively wide space between the short posterior transverse crest and posterior cingular crest, *Hadronomas* seems to be closer to *P. otibandus* from the Awe fauna than to other protemnodonts. In other features, however, the Pliocene and Pleistocene species of *Protemnodon* are closer to each other than any one of them is to *Hadronomas puckridgi*.

Molars (Fig. 16; Table 16). The only M^1 in the sample is not completely preserved. It is bilophodont, with a poorly developed midlink. The forelink is not preserved, but to judge from the posterior molars it was probably absent in M^1. A sharply developed longitudinal postparaconal crest is continuous across

the transverse valley to the premetaconal crest. A postmetaconal crest joins the arcuate postlink. In posterior view, the hindlink is closest to the base of the crown on the labial side of the tooth. From this point it descends toward the apex of the hypocone. A short lingual cingulum is present only at the transverse valley. There is no labial cingulum, but labial to the sharp postparaconal crest

TABLE 16

Measurements on upper cheekteeth of *Hadronomas puckridgi*

	Side	Tooth	Length	Width[1]	Width[2]	Height of crown[3]	Height of crown[4]	Height, unworn protocone	Height, unworn hypocone	Height, unworn paracone	Height, unworn metacone
UCMP 70512	R	P^3	14.8	6.9	----	6.9	5.0				
UCMP 70513	R	P^3	15.2	6.3	7.8	6.8	5.9				
UCMP 70510	L	P^3	16.7a	7.8	----	----	----				
UCMP 70563	L	P^3	16.4	7.1	8.4	6.9	6.3				
UCMP 70521	L	M^1	10.8a	----	10.4			----	----	----	----
UCMP 70564	L	M^2	11.3	10.7	10.8			----	----	----	----
UCMP 65981	L	M^3	11.9	11.0	10.8			----	----	----	----
UCMP 70564	L	M^3	11.9	10.7	10.4			----	----	----	----
UCMP 70521	L	M^3	12.2a	11.2	10.5			----	----	----	----
UCMP 70519	L	M^3	10.8	10.3	9.5			6.4	5.4	4.6	4.8
UCMP 70564	L	M^4	11.1	9.7	8.2			4.9	4.7	3.8	3.9
UCMP 70521	L	M^4	----	10.6	----			----	----	----	----
UCMP 70519	L	M^4	----	9.8	----			5.3	----	3.7	----

[1] In premolars this dimension is taken across the tooth opposite the first cusp. In molars it represents the width of the protoloph.

[2] In premolars this dimension is taken across the tooth opposite the last cusp. In molars it represents the width of the metaloph.

[3] Taken on the labial side of the tooth opposite the first cusp.

[4] Taken on the labial side of the tooth opposite the last cusp.

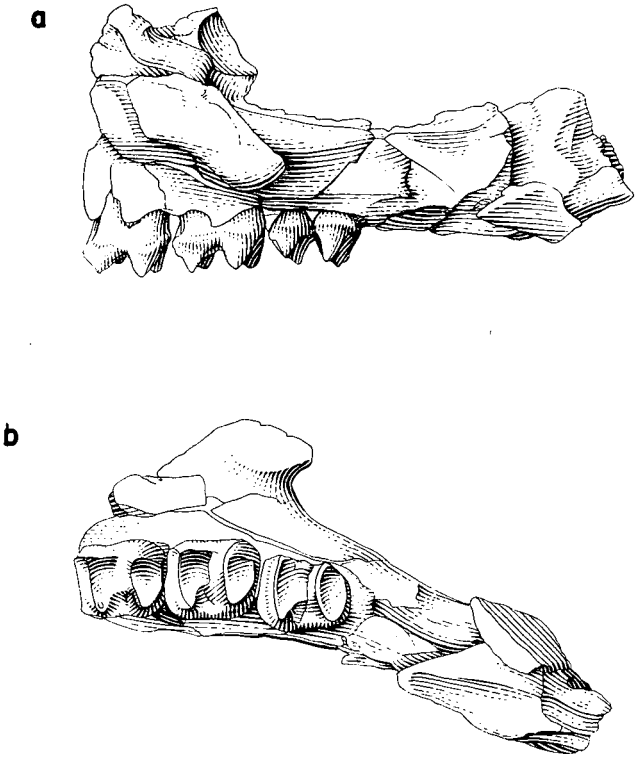

Fig. 16. *Hadronomas puckridgi* **gen. nov., sp. nov.** a, **labial and** b, **occlusal view of left maxilla fragment with M^2-M^4, UCMP 70564. Natural size.**

a less sharply defined ridge leads towards the mouth of the transverse valley from the apex of the paracone, and joins a similar ridge from the apex of the metacone. In this fashion, postparaconal and premetaconal facettes are developed at the labial end of the protoloph and metaloph, rather like those in *Dorcopsoides fossilis,* but on a larger scale. There is no mesostyle in M^1 of *Hadronomas*. The lingual remnant of the anterior cingulum shows it to be 1.5 broad (anteroposteriorly). Its lingual end is sharply set off from the anterior base of the protocone. In posterior view the profile of the labial surface of the metacone is strongly convex owing to its basal expansion. The profile of the lingual surface of the hypocone, also swollen, nevertheless slants strongly labially from base to tip. The lingual surface of the protocone is similarly constructed. Although the protoloph is not completely preserved, it appears to have been about as wide as the metaloph.

The remaining molars are constructed essentially as in M^1. The longitudinal postparaconal, premataconal, and postmetaconal crests are present, but the more labial pair of ridges between the paracone and metacone are less developed. A short preparaconal crest is present between the paracone and anterior cingulum of M^2, so that a similar structure was probably present on M^1 as well. The

labial set of ridges are absent on M^4. In M^2-M^4 the anterior cingulum extends across the tooth for nearly the total length of the protoloph. These posterior molars are larger than M^1 and become progressively more elongate posteriorly. Whereas the labial profile of the transverse valley is V-shaped and the axes of the lophs are vertical in M^1, the transverse valley becomes progressively wider and the axes of the lophs slant progressively more anteroventrally from M^2 to M^4. The protoloph of M^2 is nearly the same width as that of the metaloph, but in M^3 and M^4 the metaloph is progressively reduced.

The upper molars of *Protemnodon otibandus* are of the same general construction as those of *Hadronomas puckridgi* but differ in having a preparaconal crest on M^1-M^4, an incipient forelink, a more sharply defined midlink, less well defined postparaconal and premetaconal facettes, and more tightly closed transverse valleys, in being larger and higher-crowned, and in lacking a lingual cingulum. M^1 of *H. puckridgi* is about the same size as that of *P. otibandus,* but M^2-M^4 are smaller and lower crowned. Also the labial and lingual basal outline of M^2-M^4 in *H. puckridgi* are nearly flat while in *P. otibandus* they are decidedly convex.

The low crown height, poorly developed midlinks, and absence of a forelink of the upper molars of *Hadronomas* are in even stronger contrast to Pleistocene specimens of *Protemnodon. P. otibandus* resembles *H. puckridgi* in the labial and lingual profile of the molars as seen in posterior view: the steep, nearly straight profile of the labial and lingual surfaces of the protoloph and metaloph seen in the Pleistocene protemnodonts is quite different.

The upper molars of *Hadronomas puckridgi* are suitably constructed to be the morphological forerunners of those found in *Sthenurus* as well as those of *Protemnodon*. The increase in height of crown between *Hadronomas* and *Sthenurus* is no greater than that between *Hadronomas* and *P. otibandus*. Furthermore, upper molars of *Sthenurus* have retained the nearly straight labial and lingual basal outline, the flat shelf-like anterior cingulum, the sharp preparaconal, postparaconal, premetaconal, and postmetaconal crests, the hindlink, and the labial and lingual profile of the lophs seen in *Hadronomas*. *Sthenurus,* however, has lost the postparaconal and prematacónal facettes, still retained to a relatively small degree in *Protemnodon otibandus*. The crenulation of the enamel surface of the upper molars in *Sthenurus* is an obvious difference from *Hadronomas*. The upper molars of *H. puckridgi* differ in many details from those of *Protemnodon* and *Sthenurus;* however, the Alcoota form seems generally closer to *P. otibandus* from the middle Pliocene Awe fauna of New Guinea than to other forms. This may simply be because *P. otibandus* is the oldest and most primitive member of its lineage, with the exception of the poorly represented *P. buloloensis*: a middle Pliocene sthenurine, were it to be discovered, would probably be no further removed from *H. puckridgi* in its basic characters than is *P. otibandus*.

Mandible: There are four fragmentary mandibles in the collection, including that of the type. The best preserved is UCMP 66463 (Fig. 17). The bone is fractured, but except for a slight compression of the ventral portion below M_3 and M_4 the specimen is undistorted.

With the occlusal surface of the teeth oriented as nearly horizontally as possible, the ventral border of the mandible is directed posteroventrally. In UCMP 70526, the ventral border of the ramus is slightly concave in lateral view. The greatest depth of the horizontal ramus, as preserved in the specimens at hand, occurs below the rear of M_4. In UCMP 70526 the ramus is 36.4 deep and 12.8 wide at this point. In UCMP 66463, comparable measurements are 36.0 and 13.8.

Just behind the last molar, the anterior edge of the ascending ramus extends dorsally at an angle of about 60°. The anteroventral edge of the masseteric fossa is broadly curved, and extends down to a level slightly below that of the molar alveoli. The labial alveolar border is broadly concave dorsally from behind M_4 to the front of M_1, then turns abruptly anteroventrally below M_3. The diastemal crest (23.5 long in UCMP 70526, 20.2 in UCMP 66463) slants slightly downward in front of P_3, but then becomes dorsally convex above the root of I_1.

In UCMP 70526 the mental foramen is 2.6 wide, its posterior edge is 1.8 anterior to the root of P_3, and its ventral edge is 4.5 below the diastemal crest. Comparable measurements in UCMP 66463 are 2.9, 3.3, and 3.8; those for UCMP 65960 are 3.3, 4.9, and 3.4.

The lateral surface of the mandible is nearly flat; it is only slightly convex anterior to the masseteric fossa. A faintly developed groove extends slightly anterodorsally from a point 10.9 below the alveolar border at the rear of M_2 in UCMP 66463 and continues toward the ventral tip of the posterior root of P_3. This seems to represent the labial groove which is well developed in *Protemnodon* and other macropodines (Stirton, 1963, p. 123). In UCMP 70526 this groove begins 12.8 below the rear of M_2 and extends anterodorsally for about 20.5 to a point just behind the ventral end of the posterior root of P_3.

In medial view, the inner surface of the horizontal ramus is also quite flat. The postalveolar process forms a small overhanging lip at the end of the postalveolar shelf 14.1 posterior to the rear of M_4. The outline of the medial alveolar border is the same as that on the labial side of the ramus. The anterior edge of the mandibular foramen forms a broad posteriorly concave arc, the front edge of which is 22.3 behind the rear of M_4. Except for P_3, the cheekteeth lie dorsal to the foramen, as does the postalveolar process.

The symphysis in UCMP 66463 is 11.5 deep. It extends posteroventrally to a point below the rear of P_3. The diastemal crests project dorsally 7.2 beyond the symphyseal sulcus. In UCMP 70526 the symphysis is 11.0 deep and 36.9 long; the diastemal crest is 7.2 above the symphyseal sulcus. The symphyseal region is nearly straight. It extends slightly anterodorsally, but at a steeper angle than the ventral border of the ramus. The incisor extends anterodorsally in the same direction as the symphysis.

The chief points of resemblance between mandibles of *Hadronomas* and *Protemnodon* are the relatively flat labial and lingual surface, the presence and position

TABLE 17

Measurement on lower cheekteeth of *Hadronomas puckridgi*

	Side	Tooth	Length	Width[1]	Width[2]	Greatest width of premolar	Height at anterior cuspid	Height at posterior cuspid	Height, unworn protoconid	Height, unworn hypoconid	Height, unworn metaconid	Height, unworn entoconid
CPC 6751 . .	R	P_3	14.9	6.1	6.7	7.3	6.6	6.3				
UCMP 66463 . .	R	P_3	14.9	6.1	6.7	8.1	----	6.6				
UCMP 65976 . .	R	P_3	14.1	6.6	6.8	7.8	7.3	6.6				
UCMP 70526 . .	L	P_3	13.7	----	----	----	----	----				
UCMP 70525 . .	L	P_3	13.7	5.9	6.1	7.3	6.1	5.9				
UCMP 65960 . .	L	P_3	13.8	5.6	6.2	7.3	----	----				
UCMP 66463 . .	R	M_1	11.0	8.4a	8.5				----	----	----	----
UCMP 65976 . .	R	M_1	11.1	7.5	8.0				----	----	----	----
UCMP 70526 . .	L	M_1	10.0a	7.2	7.3				----	----	----	----
CPC 6751 . .	R	M_2	11.3a	----	----				----	----	----	----
UCMP 66463 . .	R	M_2	11.3	8.1	8.4				----	----	----	----
UCMP 70526 . .	L	M_2	11.0	7.9	7.5				----	----	----	----
UCMP 70524 . .	L	M_2	11.4	----	8.2				----	----	----	----
CPC 6751 . .	R	M_3	11.9	8.3	7.9				----	----	----	----
UCMP 66463 . .	R	M_3	11.6	8.7	9.0				----	----	----	----
UCMP 70522 . .	R	M_3	12.3	7.9	7.3				6.3	6.0	4.8	----
UCMP 70526 . .	L	M_3	11.6	8.1	7.8				----	----	----	----
UCMP 70524 . .	L	M_3	12.2	8.4	8.7				4.9s	5.2s	4.7s	5.7s
CPC 6751 . .	R	M_4	11.5	8.5	7.3				----	----	----	----
UCMP 66463 . .	R	M_4	11.9	8.3	7.9				4.9	4.7	4.5	4.5
UCMP 70526 . .	L	M_4	11.8	8.4	7.3				4.8	3.7	3.3	3.9
UCMP 70524 . .	L	M_4	11.3	8.4	8.0				5.2	5.3	----	4.1

Width[1] = width, anterior moiety.
Width[2] = width, posterior moiety.
a = approximate.
s = slightly worn.

of the labial groove, the relatively straight ventral border (*P. otibandus*), and the elongate slender symphysis with nearly parallel dorsal and ventral borders.

The great depth of the adult mandible (about 7 times the height of the unworn protoconid of M_4) and the fact that the mandible is considerably deeper below M_4 than below P_3 separate *Hadronomas* from almost all other macropodines, including *Protemnodon*. A notable exception to this is seen in mandibles of *Sthenurus*. In particular, that of the type of *Sthenurus andersoni,* AM F946, is considerably deeper below M_4 than below P_3, and the ventral border is nearly straight. This, and other mandibles of *Sthenurus,* differ from that of *Hadronomas* in having a short deep symphysis, a relatively convex labial surface, and the labial groove extending forward to a point anterior to P_3 just below the diastemal crest.

Lower dentition, Incisor (Fig. 17). There are two well preserved lower incisors in the collection. UCMP 69765, RI_1, is in a late stage of wear. A prominent occlusion surface is developed on the upper edge of the crown. The enamel is limited to the labial surface of the tooth, and its greatest depth, just anterior to the base of the crown, is 10.0. Just posterior to the crown, the root is 9.0 deep and 6.8 wide. In UCMP 69775, the crown is 10.2 deep; the root is 9.1 deep and 6.0 wide. In lateral view the root is straight except for a slight convexity of its ventral border. In dorsal view the medial surface of the root is straight; the lateral surface is slightly bowed outward. In lateral view, the nearly straight posterior edge of the enamel passes vertically toward the ventral edge of the tooth, but has a distinct posterior salient in the ventral third.

In its general slenderness and in the posterior salient of the enamel in the ventral portion of the crown, I_1 of *Hadronomas puckridgi* resembles that of *Protemnodon otibandus*. The posterior edge of the enamel in I_1 of *Prionotemnus, Sthenurus,* and the Pleistocene protemnodonts is chevron-shaped, with the open end of the chevron facing posteriorly.

Lower molars (Figs 14, 17; Table 17): The description of the lower molars of the holotype adequately covers the paratypic material. Slight variations in dimensions can be seen in Table 17.

No postcranial elements which may be critical to the phyletic assignment of the species can be definitely assigned to *H. puckridgi*. On the basis of the available dental material, the Alcoota genus is better suited as an ancestor to *Sthenurus* than to *Protemnodon*. In either case the morphology would have to change considerably. Perhaps there was sufficient time for these changes to take place; but until intermediate forms are discovered the phyletic link must remain tentative, and the apparently complex history of the Tertiary Macropodidae obscure.

Certain large foot elements are probably assignable to *H. puckridgi,* but are not definitely associated with the dental material. So as to keep potentially ambiguous elements away from the genotypic and paratypic material, they are only tentatively assigned to the species.

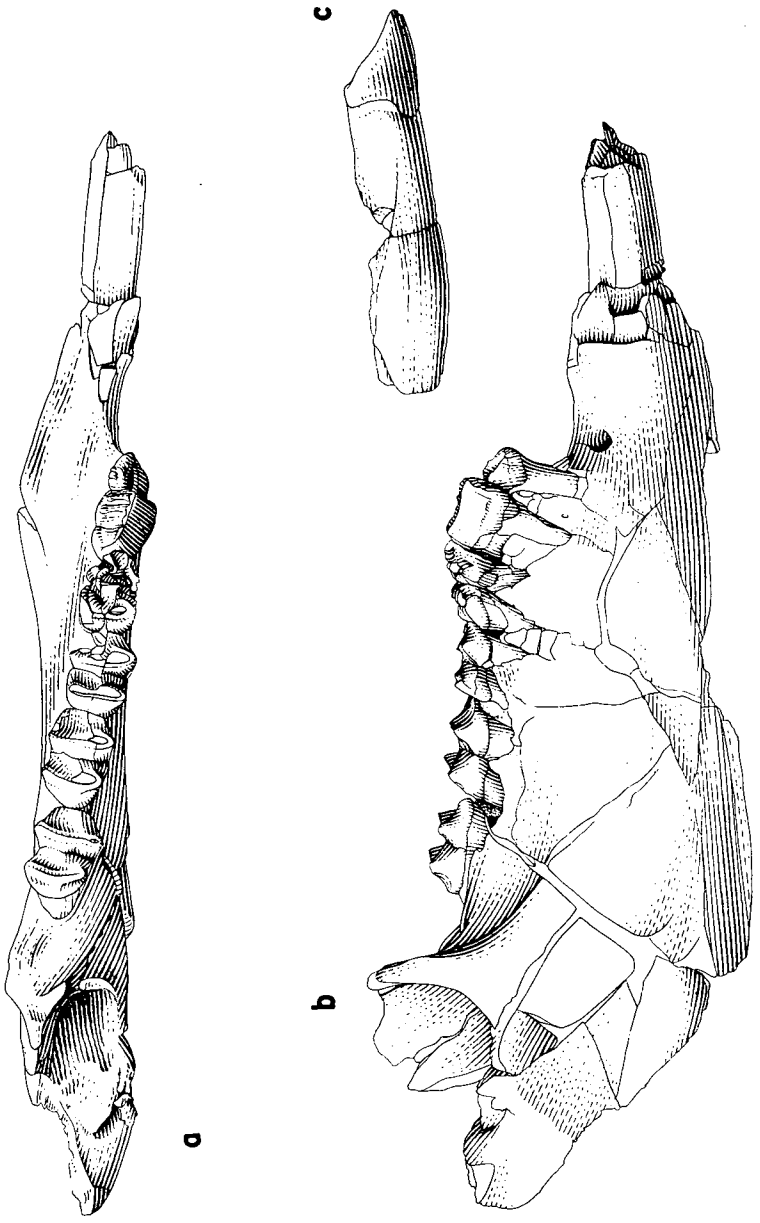

Fig. 17. *Hadronomas puckridgi* **gen. nov., sp. nov.** a, **occlusal and** b, **labial view of right mandible fragment, UCMP 66443.** c, **labial view of right I_1, UCMP69765. All natural size.**

cf. HADRONOMAS PUCKRIDGI

The material consists of UCMP 67062, right astragalus; UCMP 70527, 66530, 70806, 70814, 70805, five left astragali; UCMP 66625, right calcaneum; UCMP 67026, left calcaneum; UCMP 66529, 67034; two right cuboids; UCMP 67001, 66597, 67033, 67061, four left cuboids; UCMP 70530, 70529, two right fourth metatarsals; UCMP 66603, 66600, 66595, 70532, four left fourth metatarsals; UCMP 66524, 66526, 66527, 66528, 67004, 70531, six right fifth metatarsals; UCMP 70858, 65865, two left fifth metatarsals; UCMP 65890, 70535, 70533, 70540, 70539, 67092, 70538, eight proximal right fourth phalanges; UCMP 70536, 70537, two left proximal fourth phalanges; UCMP 70826, right navicular; UCMP 70815, left ectocuneiform.

Postcranial elements of the genus *Procoptodon* Owen, 1873, are used in the ensuing discussion because comparable material definitely assignable to *Sthenurus* was not available. *Procoptodon* is probably more specialized than *Sthenurus;* nevertheless broad comparisons with *Procoptodon* may provide inferences on contrasts between Sthenurine morphology and general macropodine characters.

Astragalus. Five astragali are present in the collection which, from their size and morphology, seem to be probably referable to *Hadronomas.* In dorsal view the trochlea is a nearly regular trapezoid. Anteromedial to the trochlea the prominent distal tuberosity bears the navicular facette. A medial process lies proximal to the distal tuberosity and medial to the trochlea. The process is separated from the medial edge of the trochlea by a broad ovate sulcus.

In ventral view a relatively massive ridge is developed between the proximal tuberosity and the posterior process of the middle calcaneal facette. The ridge forms the proximal boundary to the astragalar sulcus. The calcaneal facette is ventrally concave and broad. It tapers laterally rather abruptly. The subcircular astragalar sulcus is located posterolateral to the middle calcaneal facette.

In distal view, the navicular facette on the distal tuberosity slants medially and tapers slightly toward the plantar surface. The profiles of the lateral and medial malleoli also slant away from the trochlea at a relatively low angle. The surface of the lateral malleolus is slightly concave and its profile in lateral view is a rather tight arch. In medial view the ventral profile of the medial malleolus between the proximal and distal tuberosities is a subangular nearly symmetrical arch. Although not as smooth as in *Dorcopsoides fossilis,* the ventral profile of the malleolus is more symmetrical and is less sharply angulate than in most other macropodines.

These astragali seem to be distinct from those of the other macropodines examined in the following combination of characters: lateral and medial malleolar surfaces slant outward away from trochlea; navicular facette is slender and ventrolaterally oriented; distal edge of lateral malleolus curves posterolaterally from edge of trochlea; trochlea does not taper markedly proximally; surface between

TABLE 18

Measurements on astragali of cf. *Hadronomas puckridgi*

	Side	Length, proximal to distal process	Length anterior to posterior rim of middle calcaneal sulcus	Transverse width, anterior rim of middle calcaneal sulcus to median tubercle	Width posterior rim, middle calcaneal sulcus to proximal process
UCMP 67062	R	40.0	16.0	45.4	35.5
UCMP 70527	L	----	14.8a	41.5a	----
UCMP 66530	L	37.9a	18.3a	40.3a	30.4a

a = approximate.

medial process and distal tuberosity slants anterolaterally as seen from above; transverse ridge at proximal edge of trochlea is relatively broad and massive, as seen in plantar view; anterior surface of lateral malleolus faces anteriorly rather than ventrally and is therefore as visible in distal view as is the navicular facette. The specimens were compared with the astragali of *Protemnodon* and *Procoptodon* and of various macropodine species represented by postcranial material as indicated in Table 4. Although they are not close to any of these forms, the Alcoota astragali most generally resemble that of *Protemnodon*. The astragalus of *Sthenurus* was not available for comparison at this time.

Calcaneum. Two calcanea in the collection could articulate with the astragali. UCMP 66525 is by far the most complete. UCMP 67026 consists of little more than the astragalar facettes. The calcaneum is relatively stout and massive. The greatest length is 92.5. The total length of the area occupied by the astragalar facettes is 36.1. The greatest width is 41.1. The cuboid facette is 33.1 wide and about 28.7 high. The lateral portion of the cuboid facette extends 3.5 anterior to the medial portion.

There are three facettes for articulation with the astragalus. The first is a small rectangular ventromedially oriented surface about 18.2 long which lies at the anterodorsomedial corner of the cuboid facette. The other two facettes are well developed, one on the lateral and the other on the medial side of the calcaneum. The distal edge of the lateral facette lies 12.3 posterior to the lateral cuboid facette, and is developed as a transversely elongate condyle. The upper surface of this condyle is broadly arched and is not sharply separated proximally from the shaft. The steep anterior surface of the condyle forms the rear edge of a shallow but distinct circular pocket. The lateral surface of the condyle

is excavated by a posteroventrally expanding sulcus which lies posterior to the lateral process. Medially the condyle narrows slightly. The medial astragalar facette is largely broken away; but it seems to have been a rather steep flat flange-like surface which faced distally. The medial facette is developed above the sustentaculum, the medial surface of which is pocketed and rugose. The sustentaculum is at least 26.0 deep. Although bone is missing at the base of the sustentaculum, it appears that the sulcus tarsi is only slightly developed. The ventral edge of the sustentaculum does not extend medially as a strong process.

The surface of the shaft below the lateral process is deeply excavated; the lateral process is prominently developed. The rugose plantar surface of the shaft extends distally to connect, at its anteromedial corner, to the plantar edge of the medial cuboid facette. A shallow, dorsolaterally directed sulcus about 5.0-6.5 wide does, however, separate the medial portion of the anterior end of the rugose plantar surface from the rest of the cuboid facette.

In distal view, the cuboid facette consists of a broad dorsal portion and a narrow ventral portion. Both the medial and lateral dorsal facettes are continuous with the ventral portion. The sulcus which commonly extends between the medial dorsal facette and the ventral facette in other macropodids is not well developed. The medial dorsal facette is 18.3 wide, the width of the lateral dorsal facette is only 12.7.

Like the astragali, these calcanea are not similar to any of the macropodine calcanea examined. In particular, the extreme discrepancy in width between the lateral and medial parts of the dorsal cuboid facette, the deep pocket distal to the condyloid astragalar facette, the steep, strongly concave distal surface of this condyle, the poor separation of the rear of the condyloid facette from the adjacent shaft, and the lack of a distinct sulcus between the ventral and medial part of the dorsal cuboid facettes are characters which sharply differentiate the Alcoota calcanea from those of other macropodines.

On the other hand, although calcanea of *Sthenurus* were not available for comparison, the Alcoota calcanea strikingly resemble those of *Procoptodon;* the Alcoota genus is apparently close to the sthenurine lineage in this respect.

Navicular. A right navicular, UCMP 70821, is of the correct size and configuration to articulate with the other foot elements designated as cf. *Hadronomas.* The specimen is 32.5 high, 8.8 wide at its dorsal end and 12.1 wide ventrally.

A slightly rugose crest lies atop the bone. The outer, medial, surface is smooth and slightly convex dorsoventrally. Anteriorly, the ectocuneiform facette curves ventromedially relative to the profile of the outer surface. This facette, 19.0 high, is separated by a narrow crevice from the flat, ovate entocuneiform facette. In lateral view, the facette is smoothly and evenly convex. In lateral view, the entocuneiform facette lies slightly ventral and conspicuously posterior to the lower part of the ectocuneiform facette. The lateral surface, which faces the cuboid,

is somewhat excavated. The cuboid facette, in the dorsal third of this surface, consists of two parts. The distal part is nearly square and slants anteromedially. The proximal part is subrectangular, slants posteromedially, and lies slightly lower than the distal portion. The elongate astragalar facette is posteriorly concave in lateral view. In posterior view the facette is narrowest dorsally, broadest ventrally. At its ventral end the facette expands slightly medially on to the small posteroventral tuberosity.

This navicular differs from that of most other macropodines; it is considerably larger, the ectocuneiform facette does not diverge sharply posteroventrally from the dorsal portion; the entocuneiform facette lies conspicuously posterior to the lower ectocuneiform facette. No particular resemblance is shown to *Procoptodon*. A navicular of *Sthenurus* was not available for comparison.

Ectocuneiform. The left ectocuneiform, UCMP 70815, is 34.4 high. The plantar tuberosity is 16.4 long and 9.3 wide. The length measured between the dorsal edges of the navicular and Mtt. III facettes is 15.2. The dorsal edge of the bone consists of a crest, dorsally convex in lateral view. The lateral surface is vertically excavated. The cuboid and Mtt. IV facettes in the lower part of the upper half of the bone are poorly developed. Ventrally, a broad but shallow pit is developed just above the plantar tuberosity. The pit receives the medial surface of the medial plantar tuberosity of the cuboid.

Posteriorly, the navicular facette is 19.0 high, and 9.6 wide ventrally. The shallow posteriorly concave facette has a slender triangular outline. Anteriorly, a narrow, ovate, moderately concave Mtt. III facette is 13.3 high and 6.2 wide. Medially, the broad entocuneiform sulcus widens anteriorly. The dorsal border of the sulcus is formed by an oblique straight nearly continuous ridge. The anterior portion of this ridge is formed by the mesocuneiform facette, which thus extends well back on to the medial surface of the ectocuneiform. The posterior portion of the ridge is formed by the dorsal edge of the entocuneiform facette.

The navicular differs from those of other macropodines in the sharply triangular outline of the navicular facette, the posterior position of the mesocuneiform facette, the dorsal borders of the mesocuneiform and entocuneiform facettes being aligned in a straight anterodorsally oblique ridge, and in the fact that the anteroposterior length of the bone is no greater ventrally than dorsally.

Cuboid. Six cuboids can articulate with the calcanea. The dorsal edge of the distal Mtt. IV facette is sinuous; concave in the lateral portion and convex in the medial. The dorsal surface slopes smoothly on to the lateral surface.

The navicular facette lies along the proximal corner of the medial surface of the cuboid. The facette is generally vertically elongate and rectangular except for a short triangular anterior expansion at its plantar end. An ovate ectocuneiform facette lies distal to the navicular facette. Below this the medial surface of the cuboid extends ventrolaterally as a broad relatively shallow sulcus to

the base of the lateral plantar tuberosity. A small medial plantar tuberosity lies distomedial to the lateral tuberosity. The medial tuberosity is a small distomedially oriented process which lies just below the medial plantar portion of the calcaneal facette. The lateral tuberosity is also distomedially oriented. It has a subovate outline in plantar view and its plantar surface is broadly rounded. The dorsal border of the lateral process is separated from the lateral surface of the cuboid by a deep sulcus which extends distoventrally from the lateral tip of the calcaneal facette and continues on around to the distal surface of the cuboid to terminate below the lateral edge of the Mtt. IV facette.

On the distal surface the Mtt. IV and Mtt. V facettes form a nearly continuous broad dorsal arch. Below this is a slender tear-drop-shaped plantar continuation of the Mtt. IV facette. A shallow, nearly vertical sulcus separates this ventral portion of the facette from the terminus of the sulcus, described above, which wraps around the lateral surface of the bone.

These cuboids are not particularly like those of any other macropodids examined. The massiveness, the rounded dorsal surface, the relatively high position of the facette for Mtt. V, the smooth confluence between the facette for Mtt. V and that for Mtt. IV, the slender ventral portion of Mtt. IV facette, which is situated near the midline of the bone rather than along its medial surface, and the very reduced medial tuberosity on the plantar surface are the main distinctive features.

TABLE 19

Measurements on cuboids of cf. *Hadronomas puckridgi*

	Side	Greatest proximo-distal length of dorsal surface	Lesser proximo-distal length of dorsal surface	Transverse width at distal edge of dorsal surface	Vertical height through medial ventral tuberosity	Vertical height through lateral ventral tuberosity
UCMP 66529	R	28.6	19.7	36.9	32.1	33.5
UCMP 67034	R	28.1	19.3	36.1	----	----
UCMP 67001	L	24.0	18.0	30.5	----	33.1
UCMP 66597	L	29.8	19.8	35.0	----	31.3
UCMP 67033	L	27.5	18.9	34.7	----	----
UCMP 67061	L	28.3	18.7	35.4	----	32.2
Range		24.0–29.8	18.0–19.8	30.5–36.9	32.1	31.3–33.5

Fourth metatarsals. Of the five fourth metatarsals in the collection, only one (UCMP 70532) is complete, and it is considerably fractured. It does, however, give a good approximation of the total length of this element (157.5). The transverse width at the proximal end is 29.3 in UCMP 70530, 31.4 in UCMP 66600, and 30.6 in UCMP 66603. The vertical height at the proximal end of these three specimens is 28.2, 30.7 and 30.5 respectively; the distal end is not preserved. The transverse width of the distal end of the bone is 32.9 in UCMP 70529, and about 32.4 in UCMP 70532. The vertical height of the distal end is 25.0 and 21.3.

Between the two ends, the shaft is rather slender in dorsal view. It begins to broaden slightly in the distal half. Toward the proximal end the right side is flattened, to accommodate Mtt. V, and the plantar surface is keeled. The cross-section of the bone near the middle of the shaft is thus subtriangular, with a convex dorsal surface and a sharp plantar keel.

In proximal view, the facette for the cuboid is also subtriangular, with a broad, somewhat arched dorsal portion and a slenderer plantar portion located nearly at the midline of the bone. The medial surface is only slightly excavated for the ectocuneiform. The lateral surface is excavated to receive Mtt. V. The plantar portion of the cuboid facette lies atop the plantar tuberosity.

In lateral view, the Mtt. V facette consists of a dorsal and ventral lobe. The dorsal lobe is more elongate vertically while the ventral lobe is more circular. The ventral lobe of Mtt. V facette lies along the lateral surface of the plantar tuberosity and is separated by a short longitudinal ridge from the sesamoid facette.

This facette slants proximoventrally and supports the sesamoid, which lies between the entocuneiform and the base of Mtt. V. The distal surface of the bone is generally similar to other macropodid metatarsals and does not require description.

It is clear from their relatively massive build that these fourth metatarsals resemble those of *Sthenurus* or *Protemnodon* more than those of other macropodids. The fourth metatarsal of *Protemnodon* is, of course, considerably stouter and shorter. Although the shaft is not well preserved, the available material from Alcoota indicates that the lateral profile, although possibly not curved dorsally, is more like that of *Sthenurus* than of *Protemnodon,* as is the configuration of the cuboid facette and the relations of the Mtt. V facette with that for the plantar sesamoid. The Alcoota fourth metatarsals are, however, relatively narrower, deeper and more slender than in either *Protemnodon* or *Sthenurus* and do not resemble closely those of any of the macropodids examined.

Fifth metatarsals. Six fifth metatarsals articulate with the other foot elements. Three of these, UCMP 66526, UCMP 66528, and UCMP 65865, are essentially complete. The fifth metatarsal is moderately short and massive, with a strong curvature of its dorsal edge as seen in lateral view. The lengths of the three complete elements are, in the order given above, 146.5, 132.8, and 143.6. The

greatest depth of the shaft, measured about 30.0 distal to the proximal tip, is 26.0, 23.8, and 25.8. The narrowest point on the shaft, as seen in lateral profile, is measured about 28.0 from the distal tip and is 12.8, 11.2, and 13.2 in the three specimens.

In dorsal view, Mtt. V is slender, 13.5, 12.1, and 12.7 wide at the point through which the proximal height was measured. The dorsal edge is rather sharp proximally but becomes more rounded distally; the plantar border is also relatively narrower proximally, but this keeled edge does not carry as far distally as it does on the dorsal surface. The shaft narrows somewhat at its midlength, but then widens again toward the distal tip. As in other macropodids, the distal articular surface is asymmetrical; its profile in dorsal view slants posterolaterally. The medial surface is relatively flat and straight; the lateral surface is somewhat concave in dorsal view.

The facette for Mtt. IV slants ventromedially. Its dorsal portion is narrower and more elongate than its ventral, more circular portion. In plantar view, the base of the lower portion of the facette does not project strongly from the medial surface of the bone and is separated from the ventral keel by only a narrow, weakly developed sulcus. The cuplike cuboid facette, which faces largely proximally, also extends along the medial surface of the proximal tuberosity which is developed from the lateral side of the shaft.

The large size and relatively short, massive build are the chief features which distinguish these fifth metatarsals from those of other macropodids. The only stouter Mtt. V is that of *Protemnodon*.

Proximal fourth phalanx. Eight proximal fourth phalanges have been recovered which articulate satisfactorily with the fourth metatarsals described above. These phalanges are constructed much like comparable elements in typical macropodines, and are unlike those in *Protemnodon*. The cruciate fossa, on the plantar surface just distal to the proximal articulation, is large and well defined, as are the raised oblique ridges which bound the fossa laterally. These features are not well developed in macropodines. Specimens similar to these Alcoota materials have been noted in collections from Bingara, N.S.W., made by Leslie F. Marcus, but

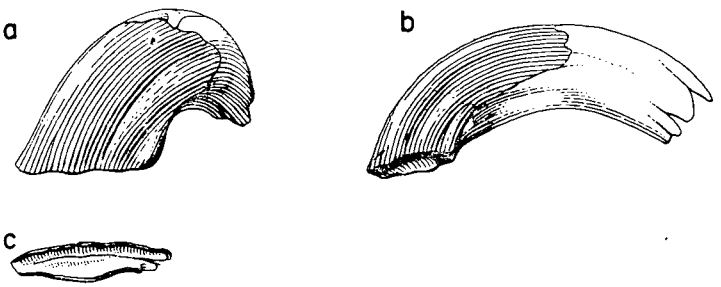

Fig. 18. *Protemnodont,* a, **anterior;** b, **labial and** c, **occlusal view of left I^1, UCMP 70543. The anterior edge in** c **is uppermost. All natural size.**

whether they should be allocated to *Procoptodon* or other large macropodids is not clear. The range in dimension of the Alcoota phalanges is: Length, 50.5-56.7 (average of seven specimens, 53.5); proximal width, 24.9-29.6 (average of nine specimens, 27.2); proximal height, 16.9-21.5 (average of eight specimens, 19.4); distal width, 21.1-26.7 (average of nine specimens, 23.6); distal height, 13.0-15.9 (average of nine specimens, 13.3).

?Protemnodont

Four upper first incisors with wide, curved anterior surfaces have been recovered. In general morphology they seem to resemble comparable teeth of Pleistocene members of the genus *Protemnodon* Owen, 1878. The specimens, UCMP 70541, 70542, 70543, three right first upper incisors, and UCMP 70544, a left upper incisor, are transversely broad distally, but taper progressively toward the base of the root. When oriented in a natural position with the occlusal surface lying on a horizontal plane, the longitudinal axis of the tooth diverges from a vertical mid-sagittal plane at an angle of about 30°. In the same orientation, the outer, enamel-bearing surface of the tooth is strongly curved so that, in lateral view, the highest point on the tooth is near the base of the crown. The tip of the root actually lies below this. The curvature of the outer surface of the tooth falls on an arc, the radius of which is about 25.0.

All the teeth are in a moderately early stage of wear. At the tip of the crown, the enamel is continuous from the anterior surface around to the posterior side of the tooth. The greatest development of enamel occurs anteriorly, but it also extends dorsally on the posterior side for 9.2-13.2 in the specimens at hand. The outline of the cross-section of the tooth is, except for the occlusal surface, triangular, with the base of the triangle corresponding to the broad, somewhat rounded anterior surface of the tooth. The apex of the triangle is posterior and the greatest development of enamel on the posterior side of the crown occurs at this apex. Dorsal to the occlusal surface the enamel folds over on to the anteromedial and posterolateral edges of the tooth for only a short distance.

At the occlusal surface, the cross-sectional outline of the tooth is posterolaterally elongate. The anterior and posterior edges of the occlusal surface are, except for a slight mid-posterior bulge, nearly parallel. In UCMP 70541, there is a small bulge in the mid-anterior surface as well, but in other specimens a groove is formed in this area, which extends up the anterior enamel face almost to the base of the crown. The groove is most strongly developed in UCMP 70542. In all of the available specimens a broad but very shallow sulcus is also present on the anterior surface about 3.5 medial to the posterolateral corner of the tooth. It does not extend as far toward the base of the crown as does the mid-anterior groove. The length of the enamel cap in UCMP 70544, the most complete of the specimens, as measured along the curvature of the anterior surface, is 32.0. The anteroposterior length of the crown has been measured at the posterior base of the enamel cap and at the anterior base of the enamel. The former dimension in the four specimens is: UCMP 70541, 8.5; UCMP 70542,

8.7; UCMP 70543, 8.9; UCMP 70544, 8.7. The second dimension, which can be taken only on 70544, is 9.3. The transverse width of the tooth, measured in the same plane as but perpendicular to the length, is, at the posterior base of the enamel: UCMP 70541, 15.3; UCMP 70542, 15.0; UCMP 70543, 14.9; UCMP 70544, 15.5. Again, the width of the tooth measured at the anterior base of the crown is available only for UCMP 70544: 13.7.

These teeth are most like the upper first incisors of *Protemnodon*. I^1 in the Alcoota form is larger than in many species of *Protemnodon,* but approaches that found in various Pleistocene specimens, such as AM F38785 and AM F17599 (see Stirton, 1960, p. 113-116, Fig. 5-6). In Pleistocene species, the width of I^1 tends to increase toward the base of the crown; but in the Alcoota specimens, like *P. otibandus* of the middle Pliocene Awe fauna and *Prionotemnus palankarinnicus* from the late Pliocene Palankarinna fauna, the crown tapers toward the root. Also, the occlusal outline of I^1 in the Pleistocene protemnodonts is rather rectangular with a wide, flat posterior surface. On the other hand, that of the Alcoota specimens, *P. otibandus,* and *P. palankarinnicus,* is a narrow apex. In the development of grooves on the anterior surface, the Alcoota material resembles some of the Pleistocene species of *Protemnodon* and some specimens of *P. otibandus*.

With the longitudinal axis of the root oriented in a natural position, i.e., slightly divergent posteriorly in dorsal view, the anterior surface of the crown of the Alcoota tooth is oriented nearly normal to the mid-sagittal plane. This suggests that the occlusal outline formed by the right and left halves of the incisor dentition would be broadly U-shaped. This character, along with the presence of a prominent mid-posterior apex of the occlusal outline, indicates that these specimens may represent a form which was close to the lineage which produced *Protemnodon*. The Alcoota incisors are, however, distinct from those of most other members of this lineage by their large size, and are unique in the sharply defined narrow anteromedial and posterolateral edges of the crown. If these four incisor teeth do in fact represent a member of the protemnodont lineage this lineage had achieved at least some of its typical specializations by the late Miocene, and may have been already well isolated from other macropodine lineages.

Macropodid, large

A number of isolated upper incisors may pertain to an early representative of the Sthenurinae. The material consists of UCMP 68978, 70517, two right upper first incisors; UCMP 70516, a left upper first incisor; UCMP 70515, a right upper third incisor; UCMP 70514, a left upper third incisor.

The first incisors have an asymmetrically triangular occlusal outline. In the specimens at hand, the enamel is limited entirely to the anterior surface. The

medial surface is flat. The smooth enamel-covered anterior surface is slightly curved and extends posterolaterally from the anteromedial corner of the crown. The posterolateral surface curves posteromedially from the lateral edge of the enamel to the posteromedial corner of the tooth. The root tapers toward its tip. In lateral view the tooth is moderately curved, the radius of curvature being about 25.0. The length of the tooth, measured in an anterolateral direction through the base of the enamel, is 8.7 in UCMP 66978 and 9.0 in UCMP 70516. The width, measured in the same plane as but perpendicular to the length, is 8.0 in UCMP 66978 and 8.2 in UCMP 70516.

I^3 is a rather slender, posteriorly elongate tooth, the crown of which is considerably longer than the root. The relatively narrow anterior surface of the crown (5.3 wide at the base in UCMP 70515, 4.5 in UCMP 70514), is flat. A conspicuous vertical rib is developed at the anterolateral corner of the tooth in UCMP 70515. Posterior to this the lateral enamel-covered surface is essentially flat and extends back to the acuminate posterior corner. The medial surface is also nearly flat in occlusal view. It extends diagonally to the anteromedial corner of the tooth, and bears a shallow sulcus near the posterior third, which fades out toward the rear of the root. The occlusal diameter of the tooth broadens toward the base. The greatest width of the crown (5.5 in UCMP 70515 and 5.0 in UCMP 70514) is measured across the posterior third. The greatest length, measured in the same plane as but perpendicular to the width, is 11.9 and 9.9 in the two teeth.

In lateral view the anterior edge continues anteroventrally from the root, but the posterior edge of the crown is directed posteroventrally whereas that of the root is nearly vertical. The base of the crown is slightly higher on the lateral than on the medial side of the tooth. Except for curving anteroventrally toward the occlusal surface at the anterior end of the tooth, the contact between the crown and the root is a straight line on both sides of the tooth. The base of the enamel is continuous around the posterior end of the tooth and does not extend down toward the occlusal surface. The root is relatively slender. It tapers gradually toward the tip. The outer surface continues the curvature of the lateral surface of the crown. The anterior and posterior surfaces are essentially flat. The medial surface is somewhat less curved than the lateral surface.

Macropodid, small

A relatively small macropodid, which is about one-fourth larger than *Dorcopsoides fossilis,* but considerably smaller than the other macropodid material in the collection, is represented by various postcranial elements. In general the proximal fourth phalanges are longer and more massive and have a more deeply triangular proximal cross-section than do those of *Dorcopsoides.* On the other hand, a number of proximal fifth phalanges, while also longer and wider than in *Dorcopsoides,* have a lower proximal cross-section.

Family DIPROTODONTIDAE Gill, 1872

Four genera of diprotodontids have been recovered in the Alcoota fauna. One of these is a new species of *Palorchestes* Owen, 1873. The other three, *Pyramios, Kolopsis,* and *Plaisiodon,* were largely described in an earlier publication (Woodburne, 1967). Crania of these three genera were not available earlier and are described here, and revised generic diagnoses are given.

In the cranial descriptions the terminology utilized has followed that in Stirton (1967a). In order to describe the bony elements of that part of the cranium medial to the zygomatic arches, I have found it useful to subdivide the area into a number of fossae. The terminology applied to these fossae is drawn from a standard source, such as Sisson & Grossman (1953 and other editions). For convenience, these areas are listed and defined below.

Temporal fossa: That portion of the cranium bounded medially by the squamosal and parietal bones and laterally by the posterior part of the zygomatic arch. The posterior boundary of the fossa is formed by the lambdoidal crest; the anterior boundary by the infratemporal crest or crests.

Infratemporal crests: A crest or pair of crests which lie anterodorsal to the glenoid fossa and dorsal to the optic-anterior lacerate foramen just posterior to the point at which the marked constriction of the lateral walls of the cranium usually occurs. These crests separate the temporal and infratemporal fossae.

Infratemporal fossa: A broad, shallow and sometimes poorly defined fossa bounded dorsally by the infratemporal crests, posteriorly by the glenoid fossa, ventrally by the pterygoid fossa and anteroventrally by the pterygopalatine fossa. This fossa lies dorsal to the optic-anterior lacerate foramen; its anterior border is poorly defined and is essentially continuous with the pterygopalatine and orbital fossae.

Pterygoid fossa: This small fossa is bounded medially by the pterygoid bone and laterally by the pterygoid flange of the alisphenoid. The fossa is usually open laterally and posteriorly. It is posterior to and separated from the pterygopalatine fossa by the pterygoid flange of the alisphenoid. The pterygoid fossa is poorly separated anterodorsally by a broad low ridge from the infratemporal fossa.

Pterygopalatine fossa: This elongate fossa extends anteriorly from the pterygoid fossa, incorporating the optic-anterior lacerate, sphenopalatine and maxillary foramina. Its ventral border is generally formed by the maxillary ridge and the interior surface of the maxillary base of the zygomatic arch. At its anterior end, the fossa is poorly separated from the orbital fossa which lies dorsal to it; posterodorsally, the pterygopalatine and infratemporal fossae are poorly differentiated.

Orbital fossa: The anterior boundary is formed by the edge of the orbit. The fossa incorporates the lacrimal foramen and extends upward at least to the lacrimal tuberosity. The posterior and ventral borders of this fossa are not well defined.

Subfamily PALORCHESTINAE Tate, 1948

PALORCHESTES Owen, 1873

PALORCHESTES PAINEI[1], sp. nov.

(Figs 19-24, Tables 20-23)

Holotype: CPC 6752, somewhat crushed cranium, nearly complete; lacking rostrum, condyles, left paroccipital and mastoid processes.

Paratypes: UCMP 70553, palatal fragment with LI^3, LP^3-M^3, RP^3-M^4; UCMP 66521, left maxillary fragment with P^3-M^4; UCMP 70550, right maxillary fragment with P^3-M^4; UCMP 70547, anchylosed pair of mandibles, LP_3-M_4 and RM_1-M_4; UCMP 70546, anchylosed pair of mandibles, right and left P_3-M_4; UCMP 67147, right mandible fragment with M_3-M_4; UCMP 70552, right mandible with M_3-M_4; UCMP 66596, left mandible fragment with M_2-M_4; UCMP 70551, left mandible with M_1-M_4; UCMP 70549, left mandible with M_3-M_4; UCMP 70560, RI^2; UCMP 67056, LI^2; UCMP 70559, RI^3; UCMP 70558, 70557, two I^3; UCMP 70556, RI_1; UCMP 70555, LI_1.

Specific Diagnosis: Cranium: rostrum elongate, excavated dorsally, slightly downturned anteriorly; infraorbital foramen large, above M^2; frontal depression absent; cranium deep vertically through frontals; zygomatic arch strongly arched in lateral view; zygomatic arch composed mainly of jugal anteriorly; paroccipital process laterally elongate; condyloid sulcus wide, deep; medial glenoid process present; postglenoid process small; epitympanic fenestra exposed in superficies meatus area; epitympanic sinus large, divided dorsally into anterior and posterior portion. Upper premolar: constructed as in *Palorchestes parvus* but smaller, lower-crowned, relatively wider, lacking cingulum between protocone and anterior end of tooth. Upper molars: constructed basically as in *Palorchestes parvus* but smaller, lower-crowned, midlink double in M^1 and M^2, forelink and hindlink single in M^1. Mandible: robust; digastric process rarely developed; postdigastric sulcus small; ramus deeper below M_3 than below P_3; wide median coronoid furrow; masseteric fossa and posterior masseteric eminence prominent. Lower premolar: constructed basically as in *P. parvus* but considerably smaller, lower-crowned. Lower molars: as in *P. parvus* but smaller, lower-crowned, links less strongly developed, labial cingulum absent; lower dentition small relative to size of mandible.

---

[1] Named in honour of Mr Ivor Paine, manager of Alcoota station.

Type locality: Paine Quarry, V6345, Waite Formation, 4 miles south-west of Alcoota station, 2.1 miles south-west of the junction of Waite and Ongeva Creeks, Northern Territory, Australia.

Age: Alcoota fauna; late Miocene or possibly early Pliocene (cf. p. 000).

Description: Except for its prominent, relatively elongate rostrum, the cranium of *Palorchestes painei* is short, deep and, in dorsal view (Fig. 19), nearly square in outline. The tip of the rostrum, missing in the holotype, CPC 6752, is preserved in UCMP 70553. As restored from these two specimens, the length from the tip of the rostrum to the hindmost projection of the lambdoidal crest is about 304.8. Other measurements are included in Table 20. In UCMP 70553, the tip of the rostrum is somewhat abraded away. The premaxillary spine, located in the midline at the anteroventral end of the narial aperture, is low. It rises only about 36.6 above the diastemal crest just behind I^3. With the occlusal surface of the cheekteeth oriented as nearly horizontally as possible, the 75.9-long lateral profile of the diastemal crest drops anteroventrally from P^3 (Fig. 22a). Thus, the posterior edge of the alveolus of I^3 is 39.0 below the anterior alveolar border of P^3. Although the premaxillaries are somewhat crushed at the edge of the narial aperture in the holotype, the depth of the rostrum just anterior to P^3 was probably not much greater than 42.0. Just posterior to the premaxillary spine, the vertical depth of the rostrum is 33.4 in UCMP 70553. The dorsal edge of the rostrum slopes anteroventrally and the depth of the rostrum actually decreases between these two points. Behind P^3, the rostrum rises at an angle of about 45° to the narial notch.

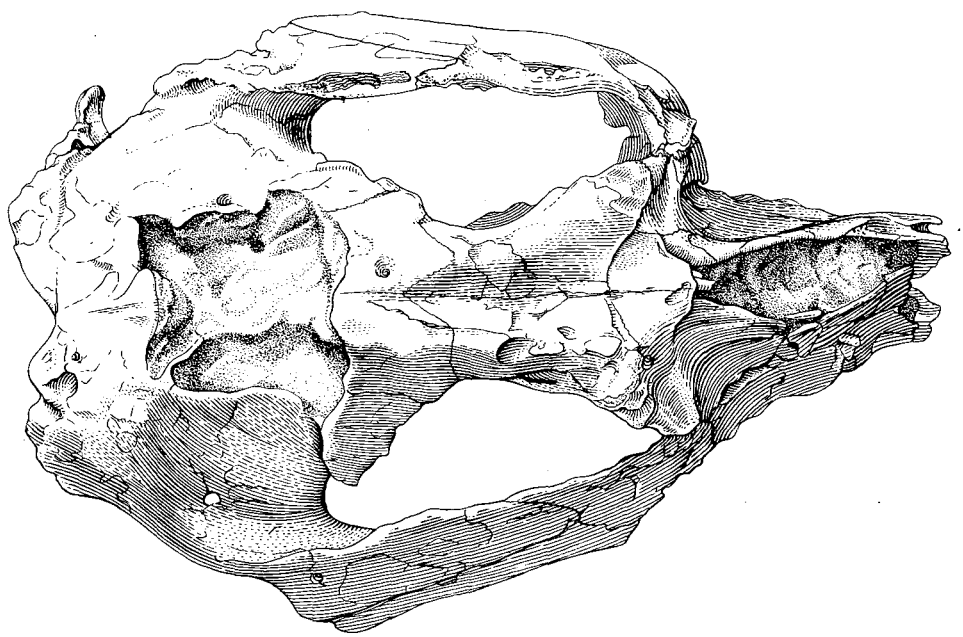

Fig. 19. *Palorchestes painei* **sp. nov. Dorsal view of holotype, CPC 6752. One half natural size.**

As shown by Woods (1958, Fig. 4) the occlusal outline of the incisor dentition is nearly transversely straight in *Palorchestes parvus*. Only LI^1 and RI^3 are preserved in place in the Alcoota material. The alveoli for the other incisors are preserved, however (Fig. 22). The occlusal outline of the Alcoota species is convex anteriorly. This contrasts with the nearly straight occlusal outline in *P. parvus*. As shown in UCMP 70553, the diastemal crests are relatively sharp, but the edge of the crest does not project downward from the adjacent palatal surface to any great extent, except near I^3. The palatal surface is generally flat transversely. A median sulcus begins opposite the anterior end of M^1, and expands to a width of 16.2 and a depth of about 5.6 opposite P^3. From this point forward to the incisive foramina, about 35.0 anterior to P^3, the sulcus deepens to about 8.5 and its sides diverge slightly. The lateral edges of the sulcus blend into the palatal surface anterior to the incisive foramina so that the palate here is uniformly concave behind the incisors. A broad flat surface separates the sulcus from the diastemal crests. In UCMP 70553 the width of the palate just behind I^3 is 45.0, the width opposite the incisive foramina is 42.6, and that just in front of P^3 is 49.0.

Farther back along the palate, the maxillae are nearly flat and are unbroken by palatal fenestrae. The palatal surface between the cheekteeth is nearly flat transversely, and slightly arched longitudinally. The anterior edge of the interpterygoid fossa is not well preserved, but it does not seem to have extended anteriorly much beyond the rear of M^4. A small nutrient foramen lies opposite the anterior end of M^1. A single poorly preserved anterior palatine foramen occurs about 5.0 medial to the posterior alveolar border of M^4. The maxillo-palatine suture extends anteriorly and slightly medially from the anterior palatine foramen to the middle of M^3. The suture then curves abruptly across the palate to the midline. The length of the palatine bone as exposed on the palatal surface is 41.0.

The tooth rows are slightly concave medially and diverge posteriorly. The transverse distance between the protocones of P^3 is 39.0 in UCMP 70553. The width between the protocones of M^4 would be about 48.0 in UCMP 70553 and possibly 50.0 in the holotype.

The sutural relationships of the bones which make up the rostrum are difficult to determine. It seems that the premaxillo-maxillary suture leads anteriorly out of the incisive foramina for about 8.9 before turning posterolaterally to cross the diastemal crest about 30.0 anterior to P^3. The suture continues postero-dorsally just below the dorsal edge of the rostrum and makes a broad wedge with the nasal posterolateral to the narial notch. The naso-maxillary suture continues posterodorsally to join the frontal about 27.0 posterolateral to the narial notch. The fronto-nasal suture then continues diagonally across the dorsal surface of the cranium to the midline. The nasal suture at the midline extends 28.4 from the tip of the nasal spine, as preserved, to the fronto-nasal contact.

In dorsal view (Fig. 19) the frontal crests diverge slightly anteriorly, forming the lateral boundaries of the shallow frontal depression. The fronto-nasal suture

TABLE 20

Cranial measurements of *Palorchestes painei*

(Measurements taken on holotype unless otherwise specified)

Length, ventral edge of foramen magnum to I^1 (reconstructed from holotype and UCMP 70553)	269.0a
Length, rostrum, from anterior edge of orbit to I^1 (reconstructed from holotype and UCMP 70553)	128.0a
Length, rostrum, from anterior edge of orbit to tip of snout above narial aperture	12.5
Length, anterior edge of orbit to ventral edge of foramen magnum	147.5a
Length, anterior edge of orbit to lambdoidal crest	155.5
Length, fronto-parietal suture to lambdoidal crest	92.8
Length, tip of nasal spine to fronto-nasal suture	27.7
Length, diastema, I^3-P^3 (UCMP 70553, right side only)	71.2
Length, tooth row, P^3-M^4. UCMP 70553. Left side	92.6
UCMP 70050. Right side	87.8
UCMP 66521. Left side	88.9
Length, tip of masseteric process to ventral edge of foramen magnum	139.4a
Length, tip of masseteric process to tip of paroccipital process	142.6a
Length, anterior edge of choanal aperture to ventral edge of foramen magnum	97.6a
Width, cranium at anterior edge of orbit	85.2
Width, greatest, across zygomatic arch just anterior to glenoid fossa	118.5
Width, across rostrum at level of infraorbital foramen	52.9a
Width, across tips of masseteric processes	108.0a
Width, occiput across tips of paroccipital processes	141.0a
Width, between medial edge of alveoli of P^3 (UCMP 70553)	39.9
Width, between medial edges of I^3 (UCMP 70553)	33.3a
Width, across lateral surface of maxilla between M^2 and M^3 (UCMP 70553)	76.8a
Width, between medial alveoli of M^4 (UCMP 70553)	40.0a
Width, choanal fossa	36.2a
Depth, narial aperture from dorsal tip to posterior edge of premaxillary crest (reconstructed from holotype and UCMP 70553)	99.0
Height, rostrum above palate at point between M^1 and M^2	105.8
Height, cranium above metacone of M4	123.0
Height, occiput, basioccipital to lambdoidal crest	80.0

a = approximate.

extends about 27.0 anterolaterally across the anterior end of the frontal depression. From this point, the maxillo-frontal suture curves anterolaterally for about 8.0 to meet the lacrimal. The fronto-lacrimal suture then extends down the medial wall of the orbital fossa for about 51.0 before meeting the palatine bone at the sphenopalatine foramen. The maxillo-lacrimal suture leads forward from this foramen into the large elliptical maxillary foramen. The maxillary foramen is about 17.0 high and 6.3 wide. Although it is difficult to trace, the jugo-lacrimal suture apparently leads upward out of the maxillary foramen to cross the medial lip of the orbit, only about 7.0 lateral to the fronto-lacrimal suture. The maxillo-lacrimal suture leads anteroventrally for about 24.0 to meet the jugal. The maxillo-jugal suture continues down the anterior base of the zygomatic arch along the lateral border of the infraorbital foramen. The infraorbital foramen is 13.2 high and has a somewhat pear-shaped outline. The foramen, about 7.5 wide in its basal portion, is located 29.4 above the alveolar border between M^1 and M^2. Upon leaving the infraorbital foramen, the maxillo-jugal suture extends down around the ventral edge of the zygomatic arch and up the anterior wall of the orbital fossa, lateral to the maxillary foramen. In contrast to the other diprotodontids, the anterior portion of the zygomatic arch of *Palorchestes painei* is composed mainly of the jugal rather than of the maxillary.

In the pterygopalatine fossa, the maxillo-palatine suture curves anterodorsally around the end of the very weakly developed maxillary shelf. The suture then extends anterodorsally for 22.0 before curving upward to contact the frontal. The fronto-palatine suture continues posteriorly toward the optic-anterior lacerate foramen, but its exact configuration cannot be determined, because of the finely crushed bone in this region. Below the optic-anterior lacerate foramen the palato-alisphenoid suture extends posteriorly and ventrally, maintaining a distance of about 10.0 from the maxillo-palatine suture. The outline of the orbitosphenoid and the sutural relations between the frontal, squamosal, alisphenoid, and pterygoid bones cannot be determined in this specimen.

The flat anterior surface of the zygomatic arch slants slightly anteroventrally (Fig. 20). Although the tip of the masseteric tuberosity is broken off, it probably did not extend much below the level of the tooth row.

The zygomatic arch is strongly curved, convex dorsally. The dorsal edge continues smoothly posteriorly into the postzygomatic crest which fades out into the temporal region of the squamosal slightly anterior to the lambdoidal crest. The lateral surface of the arch is generally smooth and slightly curved, dorso-ventrally. The ventral fourth of this lateral surface, however, is excavated for the attachment of *M. masseter*. The dorsal rim of the attachment area is developed into an arcuate crest, which fades out posteriorly before reaching the glenoid fossa.

The squamosal extends along the arch to a point about 77.0 to the anterior edge of the glenoid fossa. The zygomatic sulci occur on the dorsal surface of the squamosal, above the glenoid fossa. The sulci are about 49.5 long and 32.0 wide, and are bounded posteriorly by the postzygomatic crests.

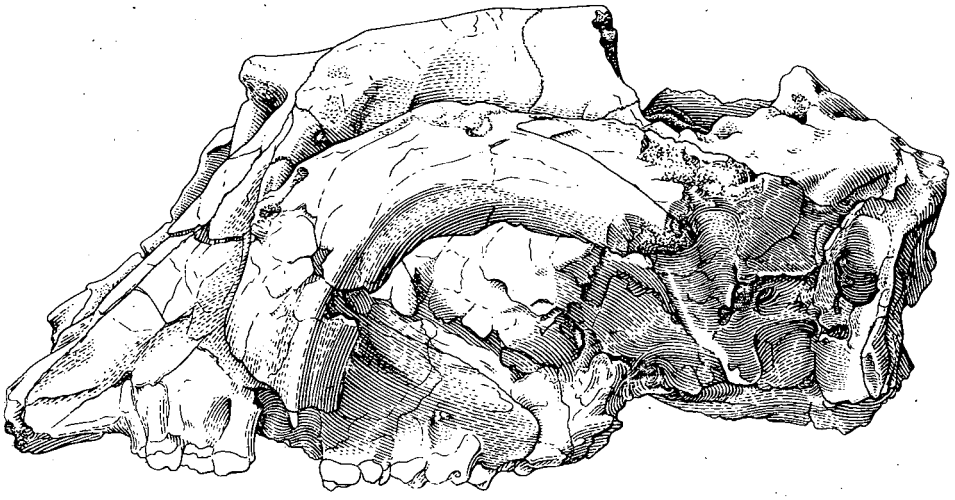

Fig. 20. *Palorchestes painei* **sp. nov. Left lateral view of holotype, CPC 6752. One half natural size.**

Medial to the zygomatic sulci, the lateral expansion of the squamosals is developed anteriorly to include the infratemporal eminences above the optic-anterior lacerate foramen. Anterior to the eminences, the cranium is markedly constricted. The dorsal infratemporal eminence is a low rounded boss which lies about 67.0 posterior to the anterior tip of the orbit and 29.0 dorsal to the ventral eminence. The ventral infratemporal eminence lies slightly dorsal and anterior to the glenoid fossa and is therefore hidden behind the zygomatic arch in Figure 42.

The anterior portion of the squamoso-parietal suture seems to extend postero-dorsally across the dorsal infratemporal eminence. Anteroventrally, the course of the suture is obscured by crushed bone, and posteriorly a large portion of the dorsal surface of the cranium is missing, exposing the matrix-filled cranial cavity. Behind the area of missing bone, the sagittal crest is low and indistinctly developed. Anteriorly, the fronto-parietal suture extends anterolaterally toward the frontal crests. The median fronto-parietal suture lies 57.8 posterior to the median fronto-nasal contact. After crossing the frontal crest, the fronto-parietal suture extends down toward the infratemporal fossa along the medial surface of the dorsal infratemporal eminence. Below this the suture is lost among the fractures in the bone.

In ventral view (Fig. 21) the elongate nearly flat anterior portion of the glenoid fossa extends posteroventrally on to the base of the squamosal tuberosity, which is better developed than the homologous structure in *Ngapakaldia tedfordi*. The postglenoid process is only slightly developed. Anterior to the squamosal tuberosity, the posterior edge of the pterygopalatine fossa extends posterodorsally from the edge of the pterygoid fossa.

The optic and anterior lacerate foramina are evidently confluent. The foramen rotundum lies just behind the optic-anterior lacerate. Both of these orifices are about 10.0 high and 5.0 wide, and are situated below the ventral infratemporal eminence. The transverse canal is located slightly anterior to the entocarotid foramen, in the pterygoid fossa.

The basisphenoid widens posteriorly and contacts the basioccipital opposite the squamosal tuberosity. Just behind the transverse canal a thin ridge of bone leads posterolaterally toward the base of the squamosal tuberosity forming the anterolateral wall of the entocarotid groove. As preserved on the left side of the cranium, the squamosal tuberosity has a subtrapezoidal cross-section. Its posterior base is separated from the petrosal by a narrow cleft. On the right side the matrix-filled remnant of the tuberosity indicates that the structure was hollow in the living animal.

The median lacerate foramen lies just dorsal to the anterior tip of the petrosal. The position of the foramen ovale is not clear; it may be confluent with the median lacerate. The posterior lacerate foramen lies at the posteromedial corner of the petrosal. Just in front of the posterior lacerate, and separated from it by a thin incomplete lamina of bone, is the posterior entocarotid foramen. The opening of the Eustachian canal cannot be determined.

The petrosal is clearly exposed ventrally (Fig. 21). It is broad posteriorly, and tapers anteriorly. Its ventral surface is compressed slightly into the inferior

Fig. 21. *Palorchestes painei* **sp. nov. Ventral view of holotype, CPC 6752. One half natural size.**

periotic crest. Posterodorsally, the promontorium expands slightly into a nodose swelling on the lateral surface of the petrosal. Anterior to the promontorium, the lateral surface is slightly excavated. The length of the petrosal from the promontorium to the anterior tip is 19.5.

Lateral to the petrosal, the tympanic cavity, from which the ossicles are missing, is a shallow, relatively narrow, vertically elongate space. The posteroventral border of the cavity is formed by a thin lip of the squamosal which extends laterally 10.0 from the basiocippital to the anteromedial base of the mastoid process. The posterior border of the tympanic cavity is formed by the mastoid. The anterior surface of the mastoid in this area slants slightly posterolaterally and is interrupted at a point just dorsal to the promontorium by the slender, 19.5 long stylomastoid canal.

The tympanic cavity is roofed dorsally by a thin shelf of bone, partly preserved on the right side in the holotype. The medial surface of this shelf blends ventrally into a longitudinally sulcate portion of the squamosal, which contacts the tegmen tympani of the petrosal. The anterior end of this sulcus lies at the posterodorsal base of the squamosal tuberosity. Its posterior end extends into the laterally ovate mouth of a cavity which may represent the sulcus facialis of the tympanic cavity. This sulcus, about 10.0 high and 5.0 wide, is subtriangular in cross-section, the apex being dorsal. It lies at the posterodorsal corner of the superficies meatus area, about 20.0 posteromedial to the postglenoid process, and extends posterodorsally into the squamosal anterior to the posterior epitympanic fossa. About 4.2 anteroventral to this sulcus and 7.0 posterodorsal to the promontorium is the facial foramen. The fenestra ovalis apparently lies 6.8 anteroventral to the latter. The fenestra rotunda lies just posterior to the dorsal base of the promontorium and 12.7 ventral to the facial foramen. This arrangement differs from that in *Ngapakaldia tedfordi* in having the sulcus facialis dorsal to the three fenestrae. In the Oligocene genus, the sulcus facialis lies posterior to and on a level midway between the fenestra rotunda and ovalis.

As in *Ngapakaldia tedfordi,* the posterior epitympanic fossa extends into the body of the squamosal anterior to the lambdoidal crest. The posterior epitympanic fossa in *Palorchestes painei* is about 17.0 wide, 8.5 high and, as measured from its medial lip, 9.8 deep. The postglenoid, postzygomatic and postsquamosal foramina are not observable in this specimen.

The most conspicuous feature of the auditory region of *Palorchestes painei* is the large subtriangular epitympanic fenestra. It is bounded anteromedially by the medial glenoid process, anteriorly by the postglenoid sulcus, anterolaterally by the small postglenoid process, posterolaterally by the squamosal and medially by the thin lip of bone developed from the squamosal, dorsolateral to the tegmen tympani. The anteroposterior diameter of the fenestra is 23.5; its greatest transverse width is about 26.0, as preserved.

The epitympanic fenestra opens dorsally into the large epitympanic sinus, which accounts for the marked expansion of the squamosal, so conspicuous in dorsal view. Sufficient matrix has been removed to show the irregular internal surface of the sinus. A slender septum extends posteromedially across the roof of the sinus, separating its dorsal extremity into anterior and posterior portions. Except for this minor subdivision, the various parts of the epitympanic sinus are freely confluent. The anterior portion of the sinus extends forward internal to the infratemporal fossa toward the site of the infratemporal eminences. Medially, the sinus does not extend past the level of the medial glenoid process. The posterior portion of the sinus apparently extends back to the occiput, possibly to reach the exoccipital. The sinus may not penetrate the exoccipital, however. Although not all the matrix could be removed, it is evident that the posterior sinus extends farther medially than the anterior portion.

In the occipital region of the cranium, the mastoid forms a transversely elongate winglike projection, the mastoid process. The ventral tip of the paroccipital process is broken off. Its triangular base is visible, however, in ventral view. Lateral to the paroccipital process, the slender mastoid process tapers toward its tip, which is somewhat rounded. On the anterior surface, a 22.5-long ridge extends medially from the tip of the process between the posterior epitympanic pocket and the stylomastoid groove. The lambdoidal crest leads dorsomedially along the dorsal edge of the mastoid process at an angle of about 55°. Posteriorly, the surface of the mastoid process is somewhat rugose. A sharp ridge extends dorsally for about 24.0 from the exposed base of the paroccipital process. A large condyloid sulcus about 12.0 wide and 12.0 deep separates the paroccipital process from the base of the condyle. On the occipital surface, the condyloid sulcus turns medially above the foramen magnum and blends into the rectus capitis dorsalis fossa, which occupies an area 48.0 wide and about 39.5 high. Along the midline of the occiput the fossa is interrupted by a slender crest. Lateral to the rectus capitis dorsalis fossa, dorsal to the condyloid sulcus and dorsomedial to the ridge from the paroccipital process, an 18.5-long eminence is a conspicuous feature of the occiput. These eminences may serve as attachment areas for the complexus musculature. Lateral to the eminence, the surface of the occiput is irregularly excavated. Unfortunately the sutural relations of the bones of the occiput cannot be determined.

Upper dentition: Incisors: only the first and third incisors are preserved in UCMP 70553 (Fig. 22). Their dimensions appear in Table 21 along with those of the three other third incisors in the collection which have been referred to this species. The first incisor is a strongly procumbent tooth with a subtriangular occlusal outline. A slight inflection occurs in the posterior border of the enamel. The enamel extends completely around the tooth. I^1 is smaller than I^3 and presumably smaller than I^2. I^3 is elongate in occlusal view, and tapers posterolaterally. The outer surface is nearly flat and straight, there being no evidence of an anteromedially oriented groove as in many macropodids. The inner surface of the tooth bears an emargination of variable magnitude. The enamel extends farther toward the tip of the root on the outer than on the inner surface. Enamel is absent on the anterior surface, at least in a relatively advanced stage of wear.

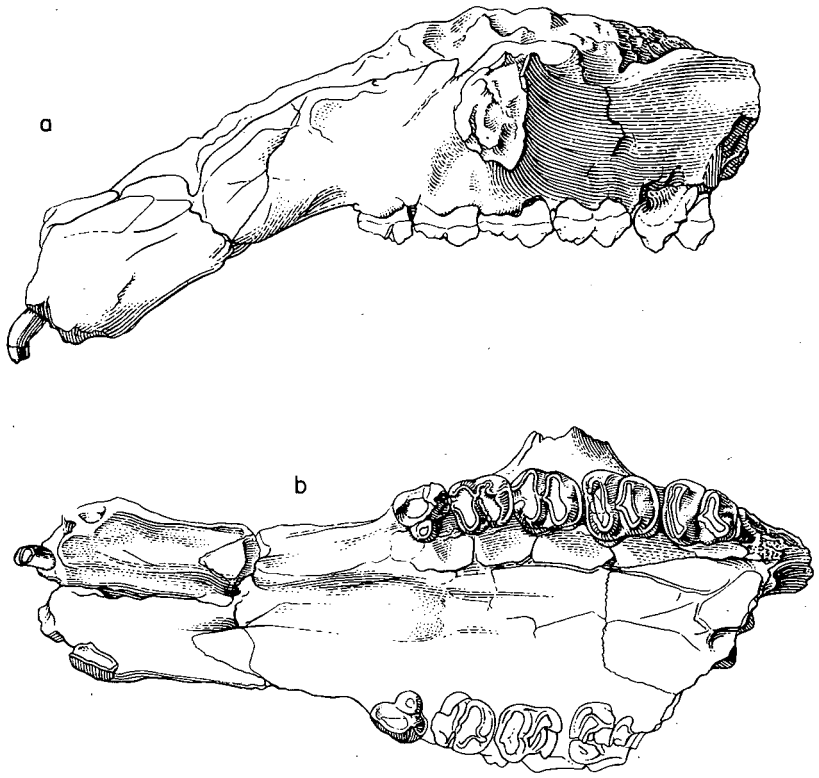

Fig. 22. *Palorchestes painei* **sp. nov.** a, **lateral and** b, **ventral view of palatal fragment, UCMP 70553. One half natural size.**

Premolar: The third upper premolar (Fig. 22, Table 21) is represented by five specimens. None of these is in an early stage of wear. Nevertheless, the simple bicuspid configuration of the tooth is quite evident. The triangular occlusal outline of P^3 is due mainly to the development of the small parastyle anteriorly and the metastyle posteriorly. These cusps are connected by longitudinal crests to the apex of the large external cusp designated here as the parametacone. It is the largest cusp of the premolar both in occlusal diameter and in height. The tip of the parametacone projects 8.2 below the base of the crown in UCMP 66521, and 8.9 in UCMP 70550. The parametacone is directly opposite the protocone, the two cusps being separated by a sharp longitudinal crevice. The protocone is least worn in UCMP 70550. Its apex is 6.2 from the lingual base of the crown. Although the exact distance between the apices of the parametacone and the protocone is difficult to determine because of wear, it is estimated that the two cusps were 6.8 apart in UCMP 70550. A small cingulum is present labial to the metastyle, but not labial to the parastyle or parametacone. A small basal cingulum connects the metastyle to the protocone. In some specimens the cingulum is continuous along the posterolingual base of the tooth. In others (Fig. 22) it blends into the base of the parametacone. There is no

basal cingulum between the protocone and parastyle. Instead the anterolingual border of the tooth is slightly emarginated.

P^3 of *Palorchestes painei* differs from that of *Ngapakaldia tedfordi* and *N. bonythoni* of the Oligocene Ngapakaldi fauna in being larger and higher-crowned,

TABLE 21

Measurements on upper dentition of *Palorchestes painei*

Specimen	Tooth	Side	Length	Width[1]	Width[2]
UCMP 70553	I^1	L	4.6	5.9	
UCMP 70553	I^3	R	12.4	7.0	
UCMP 70559	I^3	R	12.4	6.3	
UCMP 70558	I^3	L	12.6	6.8	
UCMP 70557	I^3	L	12.4	6.0	
UCMP 70553	P^3	R	14.4	13.0	
UCMP 70553	P^3	L	14.0	13.2	
UCMP 70550	P^3	R	13.9	13.7	
UCMP 66521	P^3	L	13.9	13.1	
CPC 6752	P^3	L	13.8	12.6a	
CPC 6752	M^1	L	18.2	14.3a	----
UCMP 70553	M^1	R	16.5a	13.6a	13.8
UCMP 70553	M^1	L	16.8	14.4	13.7
UCMP 70550	M^1	R	16.7	13.9a	13.7
UCMP 66521	M^1	L	17.8	14.0a	13.2a
UCMP 70553	M^2	R	17.8a	14.8	----
UCMP 70553	M^2	L	18.1	15.5a	14.3
UCMP 70550	M^2	R	18.0	15.3	13.1
UCMP 66521	M^2	L	18.1	----	13.3
CPC 6752	M^3	L	18.0a	15.3a	12.6a
UCMP 70553	M^3	L	19.4	16.3	14.1
UCMP 70550	M^3	R	18.5	15.0	12.9
UCMP 66521	M^3	L	18.0	----	13.6a
CPC 6752	M^4	L	18.6a	14.4	----
UCMP 70553	M^4	L	20.1	15.6	12.7
UCMP 70550	M^4	R	20.2	----	12.3
UCMP 66521	M^4	L	19.9	----	12.3

[1] transverse width of incisors and premolars; width of protoloph in molars.

[2] width of metaloph in molars.

a = approximate.

in being more symmetrically triangular, in being nearly as wide as long, and in having the paracone nearly centred along the labial length of the tooth. Comparison of the Alcoota material with statements and figures in Woods (1958) indicates that *P. painei* is closest to *P. parvus*. The premolar of *P. painei* differs chiefly in being smaller and relatively wider and in lacking a cingulum between the protocone and anterior tip of the tooth.

Molars (Fig. 22, Table 21): None of the five first molars which have been collected is unworn. M^1 is best preserved in UCMP 70553. The protoloph is slightly wider than the metaloph. A short forelink connects the protoloph to the anterior cingulum. The anterior cingulum is narrow; it is continuous from the base of the paracone to the anterolingual corner of the protocone. The lingual base of the protoloph separates the anterior cingulum from the lingual cingulum. The lingual cingulum is narrow and slightly convex, and is directed somewhat posterolabially toward the hypocone. The transverse valley between the protoloph and metaloph is tightly V-shaped in labial or lingual view. The valley is interrupted by the low short midlink, which is located about 4.5 from the labial mouth of the transverse valley. This is less than halfway across the tooth from the labial side. There is no labial cingulum. The labial ends of the protoloph and metaloph are outwardly convex. A well developed hindlink is present on M^1. Neither this nor the forelink appears to be double. In UCMP 66521, a double midlink can be seen. The posterior cingulum extends across the base of the metaloph, but does not continue around to the lingual surface.

Although M^1 is subrectangular, the outline of the other molars becomes more and more trapezoidal posteriorly. A short single forelink is present on M^2-M^4; the hindlink is absent save for a remnant on M_4. In UCMP 66521 and 70550, the midlink may be double in M^2, but it is single in M^3-M^4. The configuration of the anterior, lingual, and posterior cingula in M^2-M^4 is similar to that in M^1. The tooth row is only slightly curved from P^3 to M^4. It does, however, diverge from the midline posteriorly. Inspection of Table 21 reveals that the molars generally increase posteriorly in length and in the width of the protoloph, but that the metaloph, always narrower than the protoloph, decreases in width posteriorly. The posterior portion of the midlink becomes stronger posteriorly.

The molars of *Palorchestes painei* differ from those of *Ngapakaldia tedfordi* and *N. bonythoni* in being larger and higher-crowned, in having well developed forelinks, midlinks, and hindlinks, in the transverse valleys being uniformly V-shaped, in lacking parastyles on M^1 and M^2, and in possessing lingual cingula. They resemble those of *P. parvus* in all these characters, but differ in being smaller and lower-crowned, having a double midlink in M^1 and M^2, and a single forelink and hindlink on M^1.

Mandible: The mandible (Figs 23, 24, Table 22) is relatively robust. For purposes of description, the mandible has been oriented with the occlusal plane of the cheekteeth as nearly horizontal as possible. The symphysis is slightly downturned. It extends at least 59.0 anterior to P_3. The diastemal crests are narrow and bladelike near P_3, but tend to broaden and flatten anteriorly. In

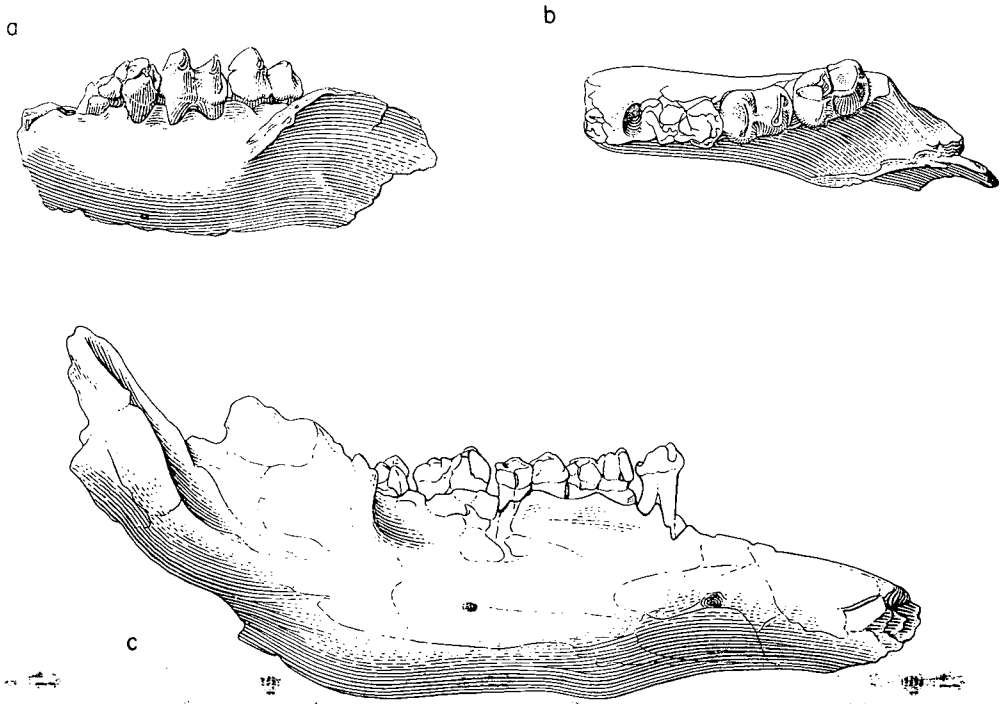

Fig. 23. *Palorchestes painei* **sp. nov.** a, **labial and** b, **occlusal view of left mandible fragment with M_2-M_4, UCMP 66596.** c, **labial view of left half of paired mandibles with P_3-M_4, UCMP 70547. P_3 restored from opposite. One half natural size.**

occlusal view, the diastemal crests are straight, and parallel to each other. In UCMP 70547, the crests are 25.5 apart at a point dorsal to the mental foramen. The symphyseal sulcus is 12.6 deep here, but becomes shallower anteriorly.

The ventral profile of the symphysis is nearly straight; the ventral surface becomes concave posteriorly in lateral view as it continues on back to the horizontal ramus. A pair of small genial pits occur on the posterior surface of the symphysis in UCMP 70546. The pits are 6.0 apart. There is no transverse torus.

The ventral edge of the horizontal ramus is nearly straight in lateral view and approximately parallels the plane of occlusion of the cheekteeth. The ventral edge of the ramus develops a strong convexity below the hypolophid of M_4, at which point the angular portion rises sharply posterodorsally. The horizontal ramus is slightly deeper below M_3 than below M_1. The labial surface of the ramus is rather convex, but becomes flatter anteriorly, below P_3. The medial surface of the ramus is nearly flat, except for a slight antero-ventral convexity above the shallow digastric fossa. The postalveolar shelf and process are variably developed. The medial coronoid furrow, which extends antero-laterally between the medial surface of the ascending ramus and the lateral

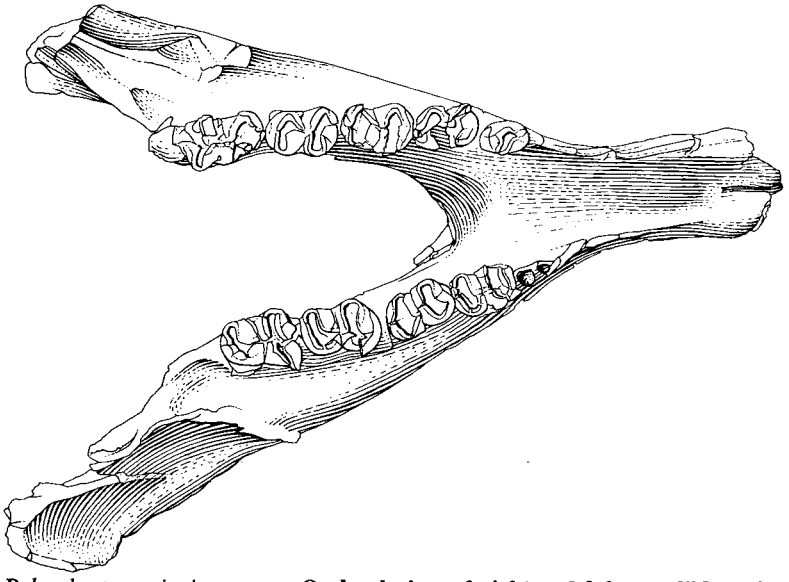

Fig. 24. *Palorchestes painei* **sp. nov. Occlusal view of right and left mandibles with LP_3-M_4 and RM_1-M_4, UCMP 70547. One half natural size.**

alveolar border, is about 11.0 wide. The mandibular foramen is preserved in two specimens. It lies dorsal to the shallow elongate pterygoid fossa at about the same level as the alveolar border of the cheekteeth. In UCMP 70551, the mandibular foramen is 32.4 posterior to M_4. In UCMP 70549 it is 38.0.

The angular process is not preserved in the specimens at hand. Laterally the masseteric fossa extends down to a level about 21.5 below the alveolar border. Posteriorly, the fossa is bounded by a smoothly rounded posterior masseteric eminence.

The articular condyle is preserved in UCMP 70551. Unfortunately, this fragment is not attached to the ascending ramus. In dorsal view the condyle is nearly straight. It extends slightly anteromedially across the long axis of the ascending ramus. The fovea pterygoidea is not prominent, but exists as a shallow excavation on the anteromedial surface. The condyle is about 49.0 wide transversely. Its anteroposterior dimension is 16.2 laterally and 14.1 medially. An elongate lateral excavation occurs below the alveolar border from M_1 to M_4.

In occlusal view the cheektooth rows diverge only slightly posteriorly. The width between right and left M_1 in UCMP 70547 is 32.6, and between right and left M_4, 38.0.

The mandible of *Palorchestes painei* differs from that of *Ngapakaldia* and *Pitikantia* (Stirton, 1967a) in being larger and more robust, having a longer slightly downturned symphysis, having a longer digastric fossa, a stronger posterior masseteric eminence, and a prominent subalveolar excavation on the lateral surface between M_1 and M_4.

TABLE 22

Measurements on mandible of *Palorchestes painei*

	Length, symphysis	Length, dorsal edge of incisor alveolus to rear, M_4	Length, dorsal edge incisor alveolus to postalveolar process	Length, P_3-M_4	Length, anterior root P_3 to rear, mental foramen	Depth, diastemal crest to ventral edge, mental foramen	Depth, horizontal ramus below anterior and M_1
UCMP 70547 . . .	88.0	150.5	166.5	92.6a	9.0	20.0	51.2
UCMP 70546 . . .	----	----	----	----	8.5	15.7	48.0
UCMP 70552 . . .	----	----	----	----	----	----	----
UCMP 70549 . . .	----	----	----	----	----	----	----
UCMP 70551 . . .	----	----	----	----	----	----	----
Range	88.0	150.5	166.5	92.6a	8.5–9.0	15.7–20.0	48.0–51.2

a = approximate

* Criteria for designating stage of maturity are those defined in Woodburne (1966). Measurements in this table were derived from mature individuals.

	Depth, horizontal ramus below rear M_4	Length, postalveolar process to rear M_4	Length, postalveolar process to mandibular canal	Anteroposterior width condyle at main axis, ascending ramus	Transverse width, condyle	Width, mandible at rear of M_4	Length diastema, I_1-P_3	Stage of maturity*
UCMP 70547 . . .	53.1	15.0	----	----	----	24.9	63.0a	4
UCMP 70546 . . .	----	----	----	----	----	25.0	----	4
UCMP 70552 . . .	43.6	----	----	----	----	26.0	----	3
UCMP 70549 . . .	45.5	----	----	----	----	22.2	----	3
UCMP 70551 . . .	45.4	11.5	22.8	13.9	49.0	24.8	----	4
Range	43.6–53.1	11.5–15.0	22.8	13.9	49.0	22.2–26.0	63.0a	

TABLE 23

Measurements on lower cheekteeth of *Palorchestes painei*

	Tooth	Side	Length	Width[1]	Width[2]	Height, protoconid	Height, hypoconid	Height, metaconid	Height, entoconid
UCMP 70547 . . .	P_3	L	12.3	8.3	7.4				
UCMP 70547 . . .	M_1	R	16.8a	11.5a	11.7a				
UCMP 79546 . . .	M_1	R	15.1	10.4	10.3				
UCMP 70546 . . .	M_1	L	16.0	10.7	10.2				
UCMP 70547 . . .	M_2	R	18.3	12.2	12.2				
UCMP 70547 . . .	M_2	L	18.2	----	----				
UCMP 70546 . . .	M_2	R	17.4	11.5	11.5				
UCMP 70546 . . .	M_2	L	17.5	12.5a	11.4				
UCMP 70547 . . .	M_3	R	19.7	----	11.1	----	----	----	----
UCMP 70547 . . .	M_3	L	19.4	12.7	11.5	----	----	----	----
UCMP 70546 . . .	M_3	R	18.0	12.7	11.4	----	----	----	----
UCMP 70546 . . .	M_3	L	18.5	12.5	11.5	----	----	----	----
UCMP 70552 . . .	M_3	R	----	----	11.6	----	8.4	----	7.4
UCMP 67147 . . .	M_3	R	19.0a	12.9	----	----	----	----	----
UCMP 66596 . . .	M_3	L	18.0	12.6	11.9	----	----	----	----
UCMP 70549 . . .	M_3	L	----	----	11.9	----	----	----	----
UCMP 79551 . . .	M_3	L	17.8	12.8	12.3	----	----	----	----
UCMP 70546 . . .	M_4	R	19.6	13.1	11.2	----	----	----	----
UCMP 70546 . . .	M_4	L	19.2	12.8	11.4	----	----	----	----
UCMP 67147 . . .	M_4	R	----	13.0	12.3	----	----	----	----
UCMP 66596 . . .	M_4	L	----	13.6a	12.6	8.0s	7.4s	----	7.8s
UCMP 70549 . . .	M_4	L	----	13.5	----	8.9	----	9.8	----
UCMP 70551 . . .	M_4	L	18.8	13.7	12.2	----	----	----	----

[1] width of trigonid.

[2] width of talonid.

a = approximate; s = slightly worn.

As compared with a cast of the mandible of *Palorchestes parvus* that of *P. painei* differs in being more robust, being deeper below M_3 than below P_3, and having a wider median coronoid furrow, a smaller more poorly developed digastric process and postdigastric sulcus, and a more prominent masseteric fossa. Otherwise the rami of the two species are similar.

As suggested by figures and measurements in Woods (1958) the mandible of *P. painei is* smaller and less robust than that of *P. azael.* Also, in *P. painei,* the cheektooth rows are nearly parallel, not sharply divergent posteriorly, the symphysis is U-shaped posteriorly instead of being V-shaped, and the diastemal crests are straighter in occlusal view, not concave as in *P. azael.*

Lower dentition: Incisors: Only two lower incisors have been recovered which may be referable to *P. painei.* UCMP 70555 is the best preserved. It is a rather slender, slightly upcurved, slightly spatulate tooth. The anteroposterior length of the crown, which is slightly worn, is 30.0. The crown does not taper appreciably either anteriorly or posteriorly. Its vertical height is uniformly about 13.0. The enamel occurs chiefly on the lateral side of the tooth, lapping over on to the medial surface only slightly at the dorsal and ventral edges. The posterior edge of the enamel, at the base of the crown, is nearly straight. The root, 22.8 long as preserved, tapers slightly posteriorly. The greatest thickness of the tooth, measured at the base of the crown, is 7.6.

Premolar (Figs 23, 24, Table 23): Only one lower third premolar is present. It is *in situ* in the mandible, UCMP 70547. This is a small non-molariform tooth. It is composed of a large subcentral cuspid, relatively well worn, from which a short steep longitudinal ridge connects to the anterior end of the tooth. A longer, less steeply inclined longitudinal crest leads posteriorly toward the talonid. The talonid is prominent and is raised into a slight conulid at its junction with the posterior crest. A second crest extends posterolingually from the main cuspid. It joins the lingual base of the tooth just anterior to the transverse valley which separates the talonid from the trigonid. There are no other cingula. The greatest width of the tooth is measured across the main cuspid.

P_3 of *P. painei* is considerably smaller than that in *P. parvus.* Although the basic construction of the premolar is similar in the two species, *P. parvus* is not only higher-crowned, but its detailed morphology is more complex. Thus, in *P. parvus,* the posterior longitudinal crest is more trenchant and more labial in position; a thin transverse bladelike lophid is developed just in front of the slender posterior cingulum; a lingual vertical ridge rises up the anterior surface of the posterolingually directed crest; the crest itself extends farther posteriorly, enclosing a basin in the posterolingual quadrant of the tooth; the tooth is wider across the talonid than across the trigonid.

The simple lower premolar in *Ngapakaldia* and *Pitikantia* shows no particularly close resemblance to P_3 of *Palorchestes.*

Molars (Figs 23, 24): The dimensions of the molars are given in Table 23. These are hypsobrachyodont, bilophodont teeth. In general, length and width increase steadily from M_1 to M_4. In M_1 and M_2, the trigonid is about the same width as the talonid. In M_3 and M_4 the talonid becomes progressively narrower. The lophids are slightly crescentic anteriorly when unworn, and slant slightly anterolabially across the tooth. The forelink extends anteromedially from the protoconid to the slender anterior cingulum. The forelink is more strongly developed in the posterior molars. The midlink extends anteromedially from the hypoconid to meet its post-protolophid component near the midpoint of the transverse valley. In M_1 and M_2 the midlink is slightly labial to the midline; in M_3 and M_4 it falls on the midline of the tooth. The hindlink connects the hypolophid to the posterior cingulum. In unworn teeth, the slight posterolabial orientation of the hindlink may be seen. In occlusal outline, the molars are subrectangular. Cingula are absent at the labial and lingual ends of the transverse valley. The valley is broadly V-shaped in labial view.

The construction of the molars in *P. painei* is essentially like that in *P. parvus*. Molars of *P. painei* differ in being smaller and lower crowned, in having less strongly developed links, and in lacking well developed labial cingula.

Remarks: *Palorchestes painei* is sufficiently close to *P. parvus* from the Chinchilla Sands of south-eastern Queensland to warrant its being included in the genus. It is considerably closer to *P. parvus* than to the Pleistocene *P. azael* or to *Ngapakaldia tedfordi, N. bonythoni,* or *Pitikantia dailyi* from the late Oligocene Ngapakaldi fauna.

Palorchestes painei differs from *P. parvus* chiefly in being smaller, and in having a more simple, lower-crowned upper and lower dentition. The mandible of *P. painei* is more massive than that of *P. parvus,* particularly in relation to the size of the cheekteeth. *P. painei* also differs conspicuously from *P. parvus* in the relatively small size of its lower premolar as compared to the size of its molars.

The dorsally excavated rostrum in *P. painei* differs conspicuously from the long, low tubular shape of that part of the cranium in *Ngapakaldia.* The basicranium of *Palorchestes,* with its small postglenoid process, extensive epitympanic fenestra, laterally expanded squamosals, and large epitympanic sinuses is basically like that seen in *Ngapakaldia.* There can be little doubt that of all known diprotodontids, *Ngapakaldia* is the most suitable ancestor for *Palorchestes,* at least as far as the basicranium and auditory region are concerned. As indicated in Stirton, Woodburne, & Plane (1967), some of the features in the dentition of *Pitikantia,* the other palorchestine genus in the Ngapakaldi fauna, show incipient development toward *Palorchestes.* Unfortunately, the cranium of *Pitikantia* is unknown.

Subfamily NOTOTHERIINAE Stirton, Woodburne, & Plane, 1967

PYRAMIOS Woodburne, 1967

Genotypic species: Pyramios alcootense Woodburne, 1967

Revised generic diagnosis: The generic diagnosis given in Woodburne (1967) is amended by the addition of the following cranial characters. Cranium: rostrum with triangular cross-section; diastemal crests massive, laterally concave, diastemal palate narrow, deep interdiastemal sulcus; well defined fossa on lateral surface of rostrum ventral to facial crest; infraorbital foramen with round cross-section; jugal extends in front of anterior edge of orbit; cranium only slightly constricted at anterior end of infratemporal crests; sagittal crest probably not present; temporal area of cranium broad, relatively low; zygomatic sulcus slopes anteroventrally at steep angle relative to orientation of postorbital region of cranium; condyles at level of ventral edge of orbit when cranium oriented with plane of occlusion of cheek-teeth on a horizontal line; mastoid process very massive, slants posteroventrally, cross-section subrectangular; glenoid notch as ventrally open triangular slot; glenoid fossa oriented nearly transversely in ventral view; foramen magnum transversely elongate; basioccipital strongly excavated for ventral rectus capitis muscles; pterygoid fossa small, open laterally; poorly developed buccinator fossa on antero-ventral base of zygomatic arch; squamoso-frontal suture short (about 7.5).

PYRAMIOS ALCOOTENSE Woodburne, 1967

(Figs 25-27, Table 24)

Holotype: CPC 6749, nearly complete skull lacking only right first and second incisors, left second and third incisor, and a portion of the left zygomatic arch (Woodburne, 1967).

Paratypes: As in Woodburne (*ibid.*).

Specific diagnosis: That of the genus until other species are described (*ibid.*).

Type locality: Paine Quarry, V6345, Waite Formation, 4 miles south-west of Alcoota station, 2.1 miles south-west of junction of Waite and Ongeva Creeks, Northern Territory, Australia.

Age: Alcoota fauna; late Miocene or possibly early Pliocene.

Cranium: In the following description, the cranium of *Pyramios alcootense* has been oriented with the occlusal surface of the cheekteeth parallel to a horizontal surface. The cranium of *Pyramios* is large and massive (see Table 24 for measurements). Although the cranium is almost completely preserved, the bone is broken into a multitude of small pieces by a myriad of cracks, and the

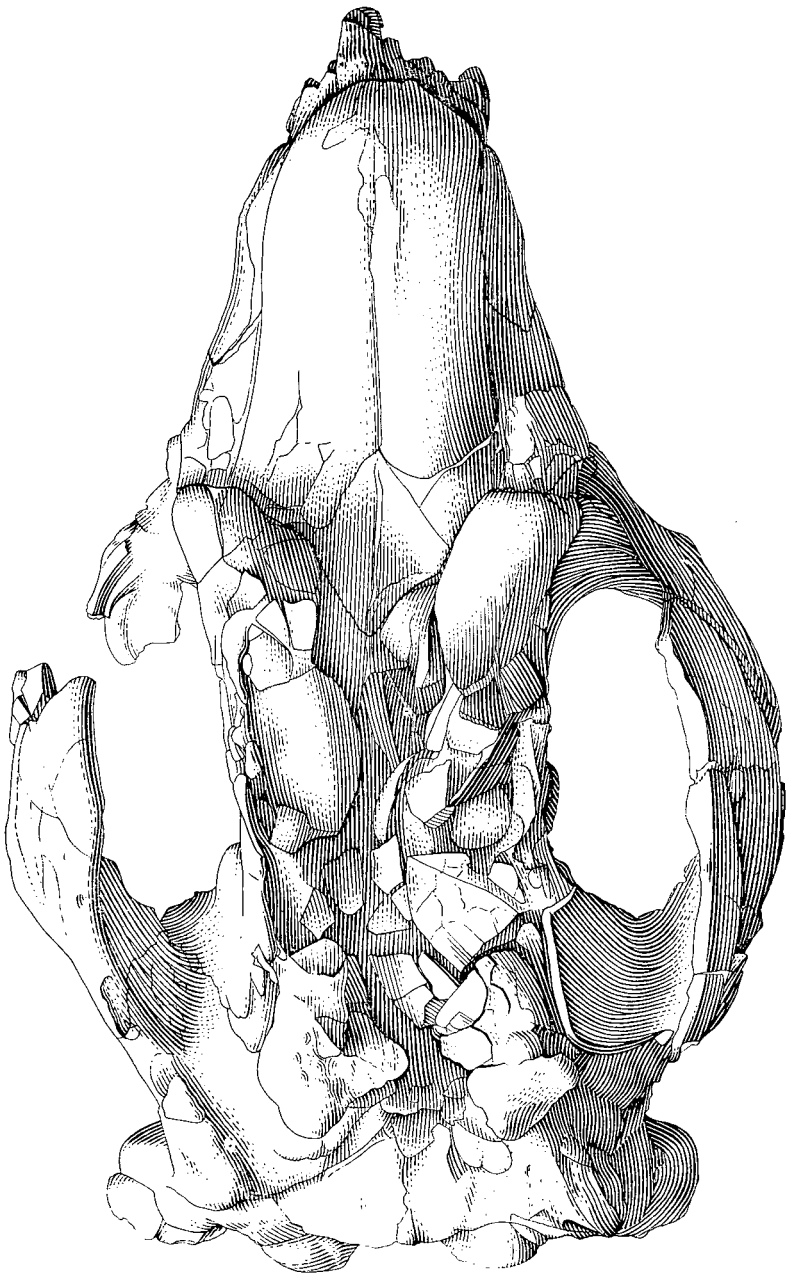

Fig. 25. *Pyramios alcootense* **Woodburne. Dorsal view of holotype cranium, CPC 6749. One third natural size.**

roof is extensively crushed downward in the frontal and parietal region. The dorsal surface of the rostrum is also slightly crushed downward relative to the premaxillaries, but the bones are intact.

The rostrum is short and deep (Figs 25-27). Its length (186.5 from the anterior edge of the orbit to the tip of I_1) is 40 percent greater than its depth (119.8 as measured above the diastemal crests, just anterior to P^3). The anterior tip of the rostrum (Fig. 25) is broadly rounded; its sides diverge slightly posteriorly to the anterior edge of the orbits, at which point the base of the zygomatic arch begins to flare posterolaterally. The premaxillaries are an elongate pair of bones which form the lateral borders of the narial cavity dorsally and support the incisors anteroventrally. The incisors lie on a plane considerably below that of the cheekteeth (Fig. 26) and form the foremost point on the rostrum.

The premaxillo-nasal suture is nearly horizontal and leads back about 73.0 from the anterior edge of the narial aperture. The premaxillo-maxillary suture is then directed posteroventrally for 35.0, and drops down along the lateral surface of the rostrum in a broad, posteriorly concave arc for about 65.0 before turning anteroventrally to cross the diastemal crests. Except for a slight lip, the anterior edge of the premaxillary is straight. In contrast to the condition in *Ngapakaldia tedfordi,* the narial notch is nearly vertical in *Pyramios.* The rear of the narial notch lies about 80.5 anterior to P^3 and the infraorbital foramen. At the ventral edge of the narial aperture, the anterior premaxillary crest forms a moderately small conical projection in the midline (Fig. 26). The small size of this structure in *Pyramios* is in sharp contrast to the deep, narrow flange-like element which is found in *Zygomaturus.*

In ventral view, the premaxillo-maxillary suture crosses the diastemal crest opposite the incisive foramen, then continues posteromedially across the palate to the midline (Fig. 27). The median premaxillary suture is about 98.0 long. The width of the diastemal palate is considerably less than that in the region of the cheekteeth. This contrasts strongly with the condition in members of the Palorchestinae (see Stirton, Woodburne, & Plane, 1967). The diastemal crests are more strongly developed, and the space between them is more deeply excavated than in *Zygomaturus* or an undescribed cranium of *Nototherium* from the Chinchilla Sands, Queensland[1]. The incisive foramina of *Pyramios* are set close together about midway between the incisors and the cheekteeth. Anterior to the foramina, the palatal surface widens out into a deep spoon-shaped concavity. The incisors are arranged in a broadly curved arc at the anterior border of this concavity. Posterior to the incisive foramina, a median palatal depression extends back to the anterior edge of P^3.

The nasals, which form the transversely rounded dorsal roof of the narial cavity, are downturned and broadly pointed anteriorly. This gives the narial

[1] This latter specimen is currently in the collections of the Museum of Paleontology, but because it may become a type, which would require its return to Queensland Museum, a UCMP specimen number has not been assigned. All references to *Nototherium* crania in this Bulletin are based on this specimen.

Fig. 26. *Pyramios alcootense* **Woodburne. Right lateral view of holotype cranium, CPC 6749. One third natural size.**

aperture, which is wider than deep, a bilobed outline in anterior view. The median nasal suture extends posteriorly for 211.0 before reaching the frontals in the anterior portion of the frontal depression. The fronto-nasal suture then extends anterolaterally about 74.0 to contact the maxillary. The maxillo-nasal

TABLE 24

Cranial measurements on CPC 6749, holotype of *Pyramios alcootense*

Length, condyles to anterior edge I^1	468.7
Length, rostrum, from anterior edge of orbit to anterior edge I^1	186.5
Length, rostrum, from anterior edge of orbit to tip of snout above narial aperture	173.6
Length, lacrimal foramen to condyles	305.5
Length, lacrimal foramen to lambdoidal crest at midline	—
Length, fronto-parietal suture to lambdoidal crest	—
Length, tip of rostrum dorsal to narial aperture to fronto-nasal suture at midline	211.4
Length, diastema, I^3-P^3 —	
Right	91.2
Left	86.8
Length, tooth row, P^3-M^4 —	
Right	136.1
Left	139.3
Length, tip of masseteric process to condyles	251.4
Length, tip of masseteric process to rear of paroccipital process	186.0
Length, anterior edge choanal aperture to condyles	207.9
Width, cranium at anterior edge of orbit	173.5
Width, greatest, across zygomatic arch just posterior to transverse palatine ridge	309.0
Width, across rostrum at level of infraorbital foramen	145.9
Width, across tips of masseteric processes	213.0
Width, occiput at lateral edge of mastoid processes	229.6
Width, between medial edges of I^3	50.7
Width, across diastemal crests at level of infraorbital foramen	38.1
Width, between medial edge of alveoli of P^3	48.6
Width, across lateral surface of maxillaries between M^2 and M^3	122.7
Width, between medial alveoli of M^4	79.9
Width, choanal fossa	55.4
Width, condyles	108.8
Width, narial aperture	73.3
Depth, narial aperture from dorsal tip to posterior edge of premaxillary crest	46.5
Height, rostrum above rear alveolus of I^3	142.9
Height, rostrum above palate just anterior to P^3	119.8
Height, frontal depression, above metacone of M^2	182.5
Height, cranium above metacone of M^4	—
Height, occiput, condyle to lambdoidal crest	—

suture continues anteriorly for 78.0 to the premaxillary. The greatest combined transverse width of the nasals (115.0) is measured across the junction of the nasal, frontal, and maxillary bones.

The dorsal portion of the maxillary lies on the lateral surface of the rostrum posterior to the premaxillary and ventral to the nasal. Posterodorsally, the 27.0 contact between the frontal and maxillary separates the nasal from the lacrimal. The maxillo-lacrimal suture is difficult to locate precisely because of the fractured bone, but it seems to descend anteroventrally for about 50.0. Thereafter, the maxillo-jugal suture passes down along the lateral anterior edge of the masseteric process. The maxillary contributes the major share of the masseteric process; the jugal is limited to a relatively thin lamination on its lateral surface.

The masseteric process is relatively narrow transversely (31.5 at its dorsal base) compared to its length (about 55.0 just below the ventral edge of the zygomatic arch). The anterior surface of the masseteric process is rounded, as is its ventral tip. The tip of the process extends downward below the level of the cheekteeth (Fig. 26). The masseteric process of *Pyramios* is not developed into a flange-like structure as in *Nototherium;* the anterior surface of the zygomatic arch is not flattened as in *Zygomaturus*. A shallow buccinator fossa is developed on the anteroventral base of the arch above the anterior three cheekteeth in CPC 6749. An elongate facial crest extends anteriorly out on to the rostrum from the base of the zygomatic arch. The crest curves anteroventrally to fade out on the lateral surface of the premaxillary above I^3. Below the facial crest the rostrum is excavated into a broad but shallow fossa. This fossa, which probably housed the dilator and depressor snout musculature, is better developed in *Pyramios* than in the other Alcoota diprotodontids. The general configuration of the fossa in *Pyramios* approaches that seen in the cranium of *Nototherium,* but is not so deeply excavated.

The circular infraorbital foramen emerges from the rear of the fossa; it is about 11.5 high and 14.0 wide, and lies just below the facial crest and above the anterior end of P^3.

The maxillo-jugal suture continues up the posterior surface of the masseteric process, and extends anterodorsally along the medial surface of the zygomatic arch to contact the lacrimal about 9.0 anterior to the maxillary foramen. The jugal separates the rostral portion of the maxillary from the orbital portion by 24.0. The full extent of the orbital portion of the maxillo-lacrimal suture cannot be determined in the holotype because of crushing. The maxillo-frontal contact within the orbit is rather short, probably about 30.0 in the holotype. The suture seems to bisect the sphenopalatine foramen, which is 59.0 posterior to the lacrimal foramen. In UCMP 69789, a small juvenile cranium, the maxillary foramen is a broadly circular opening in the anterior surface of the maxillary below the maxillo-lacrimal suture. The lacrimal and maxillary foramina are separated by a ridge which extends posteriorly along the upper edge of the orbit.

In the holotype, the maxillary contacts the palatine 54.0 anterior to the optic-anterior lacerate foramen. This foramen is a vertical slit, and lies at the boundary

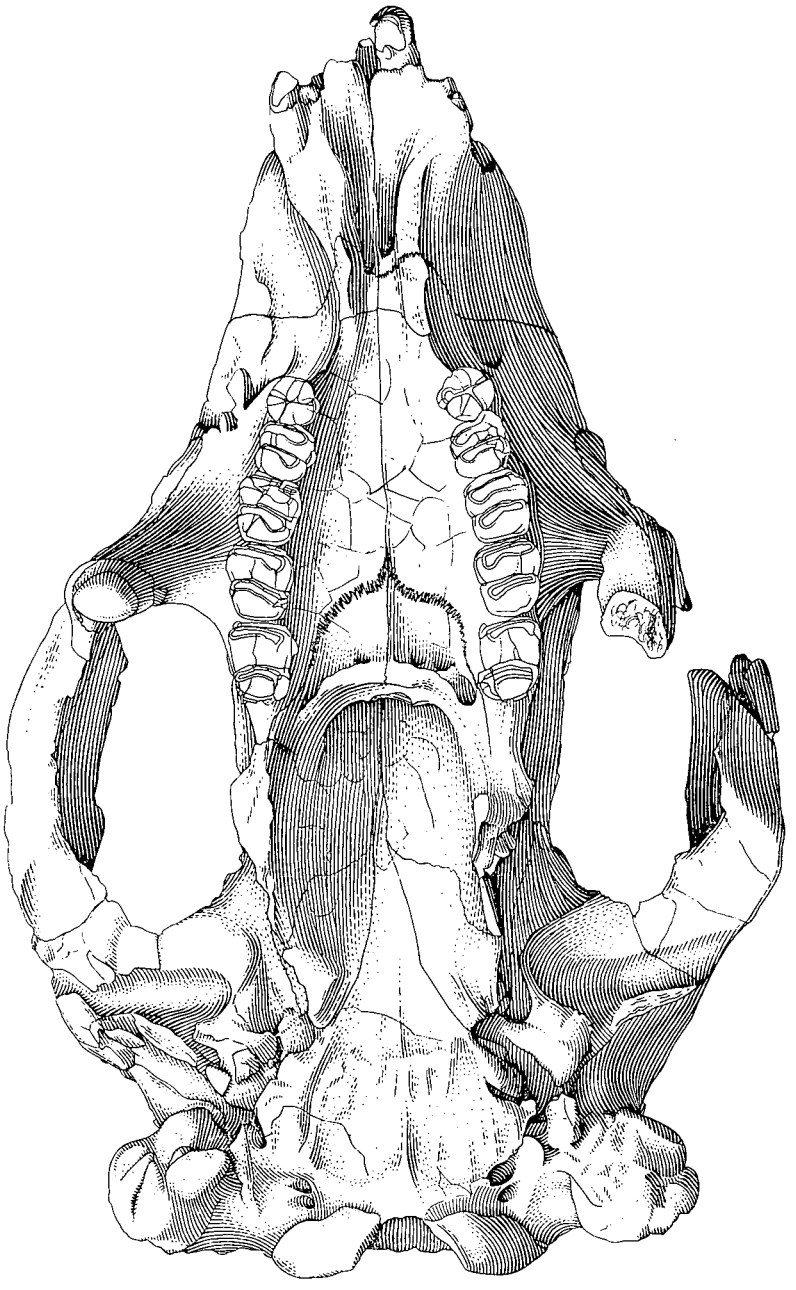

Fig. 27. *Pyramios alcootense* **Woodburne. Ventral view of holotype cranium, CPC 6749. One third natural size.**

between the pterygopalatine fossa and the infratemporal fossa. The maxillo-palatine suture continues posteroventrally for about 65.0 before turning antero-ventrally toward the lateral rim of the interpterygoid fossa. The suture crosses over the ventral edge of the fossa about 23.5 behind M^4, and continues anteriorly, medial to the last molar, to bisect the anterior palatine foramen and turn toward the midline. The median suture between the maxillary bones is 123.0 long.

The cheekteeth are arranged in a pair of slightly curved, posteriorly divergent rows. The anteromedial corner of the last molar is somewhat inset relative to the preceding tooth (Fig. 27). The rear of the last molar is opposite the posterior palatine ridge. The anterior base of the zygomatic arch joins the lateral surface of the maxillary opposite the protoloph of M^3 in the holotype. In other specimens this juncture may occur between the second and third molars.

The palatine bones bound the anterior portion of the interpterygoid fossa and enter into the hard palate. The maxillo-palatine suture has already been described. The median palatine suture is 54.0 long. A strong transversely oriented posterior palatine ridge extends across the rear of the hard palate between the metalophs of the last molars and forms the anteroventral border of the interpterygoid fossa. Within this fossa, the palato-pterygoid suture leaves the basisphenoid about 29.0 behind its apex and is directed laterally for about 40.0 before being lost in the fractured bone. The pterygoids probably bound most of the posterior portion of the interpterygoid fossa and may be exposed laterally along the ventral portion of the pterygopalatine fossa. However, the sutural relationships between the pterygoids and alisphenoids cannot be determined.

The posterior portion of the palato-alisphenoid suture within the pterygo-palatine fossa is difficult to trace. The suture may extend anterodorsally just below the optic-anterior lacerate foramen. The sutures of the orbitosphenoid in this area cannot be determined. Anteriorly, the fronto-palatine suture extends dorsally and posteriorly from the maxillary about 19.0 posterior to the spheno-palatine foramen. The fronto-palatine suture seems to be about 26.0 long, although this is not exactly determinable in the holotype.

The frontal bones are crushed dorsally so that it is difficult to determine their original configuration. The dorsal excavation of the frontals, which marks the separation between the rostrum and the rest of the cranium, is not as pronounced as in *Zygomaturus;* the frontal depression in *Pyramios* would probably have been broadly triangular as in *Nototherium*. The frontal crests which form the lateral boundaries of the depression do not seem to have been sharply developed. These crests are broadly rounded transversely and continue posteriorly nearly to the occiput in the juvenile cranium, UCMP 69789.

In the holotype, only the dorsal portion of the posteroventrally directed fronto-lacrimal suture is preserved near the anterior end of the frontal crests. In UCMP 69789, the suture is directed posteroventrally into the orbit and joins the maxillary slightly anterior to the sphenopalatine foramen. The fronto-maxillary suture then continues posteriorly to contact the palatine just posterior to that

foramen. It appears that the fronto-alisphenoid suture leads dorsally and slightly posteriorly, anterodorsal to the optic-anterior lacerate foramen, to contact the squamosal. The fronto-squamosal suture begins about 79.0 anterior to the glenoid fossa in the holotype and leads posterodorsally into the crushed dorsal portion of the cranium. In UCMP 69789, the squamosal-frontal contact is only about 7.5 long. The alisphenoid is thus separated from the parietal by this short distance. The fronto-parietal suture leads anterodorsally out of the infratemporal fossa on to the dorsal surface of the cranium and continues anteromedially for about 17.5 before turning sharply posteriorly across the frontal crests about 24.5 from the midline.

Because of the crushing of the dorsal temporal area of the holotype it is impossible to determine the configuration of the frontoparietal suture, the squamoso-parietal suture, the nature of the parietal bones, and the configuration of the lambdoidal crest. In UCMP 69789, the squamoso-parietal suture continues posterodorsally from the upper corner of the fronto-squamosal contact and extends posteriorly to reach the lambdoidal crest 36.5 lateral to the midline.

The lacrimal lies between the maxillary, frontal, and jugal bones at the anterior end of the orbit. The lacrimal is broadly triangular and contacts the maxillary on the lateral surface of the rostrum 20.0 anterior to the orbit. The low, rather broad and poorly defined lacrimal tuberosity is located about 10.0 posteroventral to the junction of the lacrimal with the maxillary and frontal. The lacrimal foramen lies medial to the rim of the orbit about 20.5 ventromedial to the lower end of the lacrimal tuberosity. The lacrimal foramen is only 8.5 anterodorsal to the maxillary foramen in the holotype, and 11.3 in UCMP 69789. Behind the lacrimal foramen the bone is broken away in the holotype. I estimate, however, that the anterior edge of the bone would have been about 46.0 long, its dorsal edge about 75.0 and its ventral edge about 77.0.

The jugal covers the anterior base of the zygomatic arch as a relatively thin lamina and most of its sutural relationships with other bones have already been described. The jugosquamosal suture is 135.0 long and slightly arched in lateral view. The suture extends back to the anterior edge of the glenoid fossa.

The zygomatic arch is deepest (96.5) just anterior to the glenoid fossa. The glenoid notch, which is the lateral expression of the glenoid fossa, forms an abrupt inverted V-shaped indentation below the postzygomatic crest. The zygomatic arch in *Pyramios* is more anteroposteriorly arcuate than in either *Nototherium* or *Zygomaturus*. The greatest transverse width of the cranium is measured across the zygomatic arches posterior to the masseteric process in *Pyramios*. The lateral surface of the zygomatic arch slants somewhat dorsomedially as seen in anterior view. The masseteric process slants ventrolaterally. The low ridge on the lateral surface which marks the dorsal limit of the attachment of the masseteric musculature extends upward from the anterior edge of the masseteric process, curves posteriorly and continues, below the jugosquamosal suture, to the anteroventral edge of the glenoid notch.

The squamosal consists of a cranial portion and a zygomatic portion. The latter occupies the zygomatic arch above the jugal. The dorsal edge of the arch curves posterodorsally from the orbit (Fig. 26) to the zygomatic sulcus. The zygomatic sulcus, which lies between the lateral surface of the cranium and the dorsal edge of the squamosal above the glenoid notch, is relatively narrow (54.2 above the anterior edge of the glenoid fossa) and slants anteroventrally at a moderately steep angle (about 60°).

The configuration of the squamosal on the dorsolateral surface of the cranium cannot be determined in the holotype. In UCMP 69789, the squamoso-parietal suture extends anteriorly from the lambdoidal crest as a broad anteroventrally directed arc toward the posterodorsal edge of the infratemporal fossa. In both the holotype and the juvenile cranium, the squamosal is not markedly expanded dorsolaterally and the cranial walls are not conspicuously constricted in the infratemporal fossa. A pair of infratemporal crests are developed near the posterodorsal edge of the alisphenoid. The more ventral of these crests occurs on the alisphenoid bone. The more dorsal, 25.0 above and slightly posterior to the former, occurs on the squamosal. In *Ngapakaldia tedfordi* the squamoso-parietal suture extends anteroventrally to contact the frontal in the infratemporal fossa. The fronto-squamosal suture continues downward to meet the alisphenoid. The alispheno-squamosal suture then extends posteroventrally between the infratemporal crests, while the fronto-alisphenoid suture continues anteroventrally. Also, the alisphenoid and parietal are separated by the short fronto-parietal contact in *Ngapakaldia* (see Stirton, 1967a). Although the sutures in this area are difficult to see in the holotype of *Pyramios,* they are sufficiently preserved in UCMP 69789 to indicate that the interrelationship of the bones in the infratemporal fossa of *Pyramios* resembles the condition seen in *Ngapakaldia.* Furthermore, the alisphenoid does not appear to enter into the auditory region in *Pyramios* and a moderately massive squamosal tuberosity is present just posterior to the medial edge of the glenoid fossa (Fig. 27). Unlike the wombats, where this tuberosity is a thinly walled, posteriorly open structure, the squamosal tuberosity of *Pyramios* is massive and its bony walls are complete.

The configuration of the parietal bones is visible only in the small cranium UCMP 69789. The squamoso-parietal and fronto-parietal sutures have been described. The contact between the parietal and exoccipital bones probably corresponds to the lambdoidal crest. No sutures can be found which would represent the contact between the parietals and the interparietal and the presence or absence of the latter in *Pyramios* cannot be established. There is no sagittal crest in UCMP 69789, although this may reflect the immaturity of the specimen. The lambdoidal crests apparently converged toward the midline at the posteromedial edge of the occiput.

Most of the sutural contacts of the alisphenoid have been described previously. The exact outline of this element is not determinable because of the fractures in the bone. There is no evidence to suggest, however, that the general character of the alisphenoid in *Pyramios* is basically different from that described for *Ngapakaldia* by Stirton (1967a).

A deep, narrow, transversely elongate groove occupies the posterior edge of the glenoid fossa and lies at the foot of the slender postglenoid process. Except for the posteromedial curvature of its medial portion, the fossa is oriented transversely with respect to the long axis of the cranium. Anterior to the groove, the fossa is a broad flat surface. It faces laterally along the base of the squamosal tuberosity, then curves outward on to the zygomatic arch and turns slightly anteriorly as it crosses over on to the jugal. *Pyramios* differs from both *Ngapakaldia* and the wombats in having a well developed postglenoid process and lacking a large open cavity in the superficies meatus area of the auditory region. Instead, the tympanic cavity of *P. alcootense* is nearly completely closed off by the large mastoid process of the squamosal.

A deep, narrow, anterolaterally directed groove separates the squamosal tuberosity from the postglenoid process. Posterior to the tuberosity, the tympanic bone may be represented by a thin wedge-shaped element in the ventral superficies meatus of UCMP 66097. A slender ramus of the tympanic may extend anterolaterally in the roof of the fissure between the squamosal tuberosity and the postglenoid process. A pit occurs in the ventral surface of the tympanic. As seen in *Nototherium* and *Diprotodon,* a ventral extension of the tympanic may have carried laterally, forming the ventral boundary of the external auditory meatus. In *Pyramios* the meatus is developed chiefly lateral to the small tympanic and thus has no extensive ventral boundary.

As exposed on the right side in the holotype, a highly fragmented element of dense bone lies deep to the position of the tympanic in the superficies meatus area. This may represent the petrosal, but it is not sufficiently well preserved for its features to be determined.

The foramen ovale is a circular opening about 7.0 in diameter at the anteromedial base of the squamosal tuberosity. The median lacerate foramen is evidently confluent with the foramen ovale. The anterior entocarotid foramen is situated in the basisphenoid about 9.5 medial to the foramen ovale. The relatively short, poorly defined entocarotid groove leads posterolaterally from the anterior entocarotid foramen into the posterior entocarotid foramen. The latter occurs at the posteromedial base of the squamosal tuberosity. The entocarotid groove separates the tuberosity from the rectus capitis ridge which forms the lateral edge of the basisphenoid.

The posterior lacerate foramen is found posteromedial to the posterior entocarotid foramen and anteromedial to the base of the paroccipital process. The accessory condyloid foramen lies 24.0 posteromedial to the posterior lacerate. The condyloid foramen occurs 9.0 posterior to the accessory condyloid. The stylomastoid groove leads ventrolaterally from the superficies meatus along the anterior surface of the mastoid process. The massive mastoid process has a nearly square cross-section in ventral view. The paroccipital process is flattened longitudinally and projects 27.0 ventrally and slightly medially from the inner edge of the former. The ventral tip of the paroccipital process is blunt. It appears that the squamoso-mastoid suture traverses the lateral corner of the mastoid

process and would have continued on up toward the lambdoidal crest. The mastoid-exoccipital suture probably extended up the occiput from the paroccipital process toward the lambdoidal crest.

Owing to the large mastoid process in *Pyramios,* the epitympanic fenestra is not extensively developed in the superficies meatus area. A small fenestra may occur just dorsal to the tympanic. This fenestra is about one-fourth the size of that in *Ngapakaldia,* even though *Pyramios* is more than twice as big. The cranium of UCMP 69789 is broken just posterior to the postglenoid process, and an epitympanic sinus can be seen. The sinus extends ventrally into the base of the postglenoid process and dorsally into the posterior base of the zygomatic arch. A second cavity is present within the squamosal tuberosity and could have communicated freely with the more lateral portion of the sinus. Thus, although it is not well exposed in the superficies meatus area, the epitympanic sinus of *Pyramios* is nearly as extensive as that in *Ngapakaldia* (see Stirton, 1967a). The epitympanic fenestra and epitympanic sinus are developed to varying degrees in other marsupials, but only in the Diprotodontidae has the epitympanic sinus been formed into such a large internally continuous cavity.

The sutures bounding the mastoid bone in *Pyramios* cannot be determined. This element is probably exposed on the lateral surface of the mastoid process, narrowing posterodorsally to taper out below the lambdoidal crest.

Medial to the auditory region, the basioccipital bears a pair of broad but relatively shallow cavities on either side of a low, short (23.0) midline keel which lies anterior to the foramen magnum. Anterior to these cavities, a low, transversely elongate, rather rugose ridge indicates the position of the basioccipito-basisphenoid suture. The triangular basisphenoid then tapers anteriorly into the roof of the interpterygoid fossa. The fossa in *Pyramios* is U-shaped in cross-section rather than V-shaped as in *Nototherium* and *Zygomaturus.*

The lateral borders of the basisphenoid are in contact (for 68.5) with the alisphenoids, which form the posterior portion of the walls of the interpterygoid fossa. The anterior tip of the basisphenoid expands slightly in front of its contact with the alisphenoid, then tapers anteriorly between the palatine bones.

The condyles lie at the same level as the ventral edge of the orbit, dorsal to that of the tips of the paroccipital process, are oriented ventromedially, and bound a transversely elongate foramen magnum. Above the foramen magnum, the occipital surface, as preserved, is nearly flat and rather smooth. It slopes anterodorsally at an angle of about 30°. The dorsal portion of the occiput is missing in the holotype and other crania of *Pyramios.*

Remarks: *Pyramios alcootense* is the earliest known member of the diprotodontid subfamily Nototheriinae. As indicated in Stirton, Woodburne, & Plane (1967) at least three of the four known subfamilies of the Diprotodontidae had become differentiated by the middle Tertiary. Fortunately, *Ngapakaldia tedfordi,* a primitive member of the Palorchestinae from the late Oligocene

Ngapakaldi fauna of South Australia, is known from cranial material and can be compared with the Alcoota diprotodontids. It has been stated *(ibid.)* that the Palorchestinae, as represented in the Oligocene by *N. tedfordi,* are not necessarily the basic stock from which all other diprotodontids arose. On the other hand, the basal position of *Ngapakaldia tedfordi* with respect to the other members of the Diprotodontidae is shown by the similarity of the arrangement of the cranial sutures in *N. tedfordi* and the later forms, the presence of a large but apparently unsegmented epitympanic sinus, and 'the rather normal profile of the cranium, the absence of a digastric process and digastric sulcus in the mandible, and in alveoli for vestigial upper canines' *(ibid.).*

Pyramios alcootense is considerably advanced over *Ngapakaldia tedfordi*: it is much larger; it has a conspicuously constricted diastemal palate; it lacks a posterior premaxillary spur which extends into the lacrimal region; it has a nearly vertical lateral outline of the narial aperture with the incisors lying almost directly beneath the tip of the nasals; the cranium is not conspicuously constricted at the anterior end of the infratemporal crests; it has a prominent postglenoid process; it lacks a large epitympanic fenestra in the superficies meatus area of the cranium; it lacks any evidence of an upper canine; it has a massive mandible with a small digastric sulcus and process and strong posterior masseteric eminence; and its lower incisor has an enamel cap which covers the medial surface of the crown and a lower third premolar which possesses a posterior cingulum.

Other known members of the Nototheriinae include *Nototherium watutense* from the Awe fauna of New Guinea and *Meniscolophus mawsoni* of the late Pliocene Palankarinna fauna, South Australia. As pointed out by Plane (1967a), similarities between *P. alcootense* and *N. watutense* 'chiefly involve the molars: the broadly V-shaped transverse valleys, and the labial cingula rising as crests up the labial ends of the lophids. The former feature is suggestive of a general stage of advancement similar to that of *Pyramios alcootense,* but the latter character is of no significance in showing close relationships, for it occurs in only one of the specimens of *P. alcootense* and furthermore is found in *Meniscolophus mawsoni* and, to judge from Owen's illustrations, the type mandible *of Nototherium inerme.'*

As indicated in Plane *(ibid.)* and Stirton, Woodburne, & Plane (1967) resemblances between *Pyramios alcootense* and *Meniscolophus mawsoni* only serve to show that the two genera are broadly related within the subfamily. On the other hand, many of the features in which *P. alcootense* and *M. mawsoni* can be compared only emphasize their separation. *P. alcootense,* with its broadly spatulate, twisted, lower incisor with enamel present on the medial surface, lower molars with broadly V-shaped transverse valleys and weakly developed metalophids and narrow, deep mandible, is not closely related to any other known nototheriine.

The general level of advancement represented by *Pyramios alcootense* is intermediate between that of Oligocene palorchestines and late Tertiary nototheriines.

Although the cranium of *Pyramios* differs from that of *Nototherium* in many details, both have a fossa for the snout musculature below the facial crest, a nearly circular infraorbital foramen, a buccinator fossa at the anterior base of the zygomatic arch (incipient in *Pyramios*), and a sharply V-shaped glenoid notch. This combination of features may be common to members of the Nototheriinae as it is not found in *Zygomaturus* or the Alcoota zygomaturines, the palorchestines as currently known, or the diprotodontines.

Subfamily ZYGOMATURINAE Stirton, Woodburne, & Plane, 1967

KOLOPSIS Woodburne, 1967

Genotypic species: Kolopsis torus Woodburne, 1967

Revised generic diagnosis: The generic diagnosis was presented by Woodburne (1966) on dental characters only. Additional diagnostic information is now available, on cranial characters, which are specified here.

Cranium: rostrum tubular; diastemal crests nearly straight; diastemal palate slightly constricted; palatal surface broad and flat posteriorly; no well defined fossa on lateral surface of rostrum nor infraorbital foramen; no facial crest; infraorbital foramen with vertically elongate, slitlike cross-section; anterior portion of jugal extends dorsally above level of ventral edge of lacrimal tuberosity; cranium markedly constricted at anterior end of infratemporal crests; sagittal crest present; temporal surface of cranium expanded, arched laterally; profile of sagittal crest nearly parallel to that of dorsal surface of rostrum in lateral view; zygomatic sulcus slopes at low angle, parallel to general orientation of postorbital region of cranium; condyles at level of ventral edge of orbits; mastoid process oriented vertically, cross-section subtriangular; glenoid notch as inverted 'L'; glenoid fossa oriented anterolaterally in ventral view; foramen magnum transversely elongate; basioccipital strongly excavated for ventral rectus capitis muscles; pterygoideus fossa small, open laterally; well developed buccinator fossa on anteroventral base of zygomatic arch; squamoso-frontal suture short (about 6.5).

Specific diagnosis: Two species of *Kolopsis* have been described: *K. torus* Woodburne, 1967, from the late Miocene or early Pliocene Alcoota fauna in central Australia, and *K. rotundus* Plane, 1967, from the middle Pliocene Awe fauna of New Guinea. *K. torus* can be distinguished from *K. rotundus* by the following characters:

I^1: radius of curvature of outer surface in lateral view considerably less (25.0-32.0 in *torus*; 51.0 in *rotundus*).

P^3: crest from metacone to posterior end of tooth longer, slopes at shallower angle; posterior cingulum with low contact to metaconal crest; parastyle more

angular, pyramidal, less conical, with sharp labial and lingual ridges; labial cingulum often continues anterior to base of paracone; lingual base between paracone and protocone emarginated; paracone and metacone slender; protocone connected to paracone by low rather than high ridge.

M^3-M^4: Postparaconal crest weak to absent.

I_1: root narrows posteriorly; blade oriented at about 45° to root; enamel cap restricted to thin strip which just overlaps on to medial surface and parallels dorsal and ventral borders of tooth.

P_3: smaller, less robust; main anteroposterior crest straight; moderate to strong indentation in labial surface just posterior to base of main cuspid.

M_1: cingulum present on anterior corner; U-shaped transverse valley; axes of lophids vertical.

Mandible: slender; small hypocone developed.

KOLOPSIS TORUS Woodburne, 1967

(Figs 28-30, Table 25)

Holotype: CPC 6747, nearly complete skull, lacking only left zygomatic arch, right and left I^2 and I^3.

Type locality: Paine Quarry, V6345, Waite Formation, 4 miles south-west of Alcoota station, 2.1 miles south-west of junction of Waite and Ongeva Creeks, Northern Territory, Australia.

Age: Alcoota fauna; late Miocene or possibly early Pliocene.

Cranium: The cranium of *Kolopsis torus*, CPC 6747, is long and slender. It is smaller than that of *Pyramios alcootense* (see Table 25 for measurements). The bone is highly fractured. The dorsal surface of the rostrum and that of the cranium just posterior to the frontal depression have been crushed somewhat. In other areas, the masseteric processes, paroccipital processes, part of the mastoid processes, and the left zygomatic arch are missing. In the following description the cranium is oriented as though the plane of occlusion of the cheekteeth is horizontal.

The elongate tubular rostrum is 43 percent longer (as measured from the anterior edge of the orbit to I^3) than deep (measured above the diastemal crests just anterior to P^3). The tips of the incisors (Fig. 29) are considerably lower than the cheekteeth, and although the dorsal surface of the rostrum is nearly horizontal, the ventral surface slopes downward conspicuously anterior to P^3. The anterior edge of the narial aperture is nearly vertical, but below this the tips of the premaxillaries are quite decurved. The midline premaxillary crest

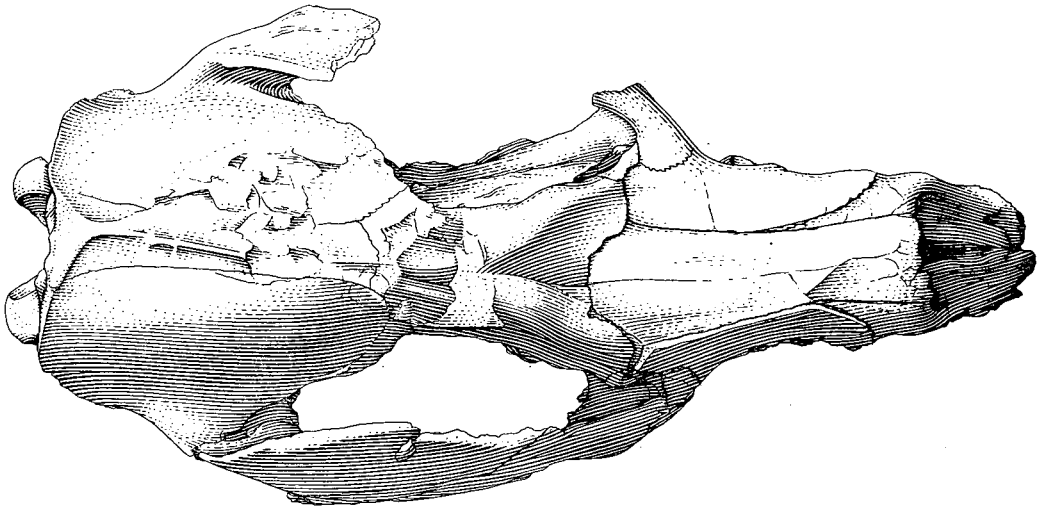

Fig. 28. *Kolopsis torus* **Woodburne. Dorsal view of holotype cranium, CPC 6747. One third natural size.**

extends anteroventrally in a prominent ridge for about 34.5. This, together with the anteroventral orientation of the diastemal crests, causes the rostrum to deepen considerably anterior to P^3. In anterior view, the nearly circular narial aperture is slightly deeper than wide. The tips of the nasals are broken at the dorsal edge of the aperture. On the other hand, the relatively strong premaxillary crest divides the ventral portion of the aperture into two lobes. This is just the opposite of the condition in *Pyramios,* where the aperture is wider than deep and is divided into dorsal lobes by the strongly downturned tips of the nasals.

The premaxillaries bound the anterior portion of the rostrum with the exception of the dorsal surface, which is formed by the nasals. The premaxillo-nasal suture is nearly horizontal and extends back 50.7 behind the anterior edge of the narial aperture. The premaxillo-maxillary suture then descends in a broad, posteriorly concave arc for about 56.5 before turning anteroventrally toward the diastemal crests. After crossing over the diastemal crests, the premaxillo-maxillary suture leads posteromedially into the lateral border of the incisive foramina, then anteromedially out of their medial edges toward the midline. The joint premaxillary suture is about 49.0 long at the midline.

The diastemal crests, in ventral view, are nearly parallel and lie about 26.0 apart (Fig. 30). The crests in *Kolopsis* are much less prominent than in *Pyramios.* The incisive foramina in *Kolopsis* are located just anterior to the premaxillo-maxillary suture. The foramina are about 13.0 apart and 21.7 posterior to I^3. The groove which leads forward from each foramen becomes slightly wider and shallower anteriorly. Behind the foramina, the palate is smooth and nearly flat.

The nasals form the roof of the narial cavity. In the holotype, these bones have been pushed slightly ventrally relative to the dorsal edge of the premaxillaries and maxillaries. The 134.4 suture between the two halves of the nasals would have been somewhat longer had the anterior tips of these bones been preserved. The fronto-nasal suture extends anterolaterally about 28.0 across the anterior edge of the frontal depression, to meet the maxillaries. The maxillo-nasal suture then continues anteriorly for about 60.0 to contact the premaxillaries. The greatest combined width of the nasals (40.5) is measured across the joint maxillo-fronto-nasal suture. The nasals are separated from the lacrimals by the 13.8 maxillo-frontal contact.

The anterior and dorsal contacts of the maxillary have already been described. Posteriorly, the rostral portion of the maxillary is sutured to the frontals for 13.8 and the lacrimal for 15.5. The maxillo-jugal suture, which begins at the ventral end of the lacrimal, leads about 22.0 anteriorly before turning ventrally toward the masseteric process of the zygomatic arch (the process is missing). In contrast to *Pyramios,* the facial crest is not developed along the side of the rostrum of *Kolopsis* and no fossa is formed for the snout musculature. The infraorbital foramen is a vertically elongate slit 17.3 high and 8.0 wide on the lateral surface of the rostrum. The lower edge of the foramen is about 25.0 above the diastemal crest anterior to P^3.

On the medial surface of the anterior base of the zygomatic arch, the maxillo-jugal suture continues anterodorsally to meet the lacrimal at the anterior edge of the orbit and about 20.0 posteroventral to the facial maxillo-lacrimal jugal suture.

The course of the maxillo-lacrimal suture is difficult to determine, but it seems to extend posteromedially above the maxillary foramen, and curves posteriorly to join the fronto-maxillary suture, presumably near the spheno-palatine foramen. Posteriorly, the maxillo-palatine suture seems to extend along the medial edge of the strongly developed maxillary shelf. The maxillary shelf is much more prominent than in *Pyramios.* The maxillo-palatine suture continues ventrally and anteromedially around the edge of the interpterygoid fossa on to the hard palate in CPC 6747.

On the palate, the maxillo-palatine suture seems to extend anteriorly, medial to the last molar, to a point opposite the protoloph of M^3 before turning medially toward the midline. The length of the midline maxillary suture on the palate is about 99.0. There are no palatal fenestrae. Only one anterior palatine foramen is present on each side between M^4 and the posterior palatine ridge. Anteriorly, a small nutrient foramen occurs about 9.3 medial to the hypocone of P^3 on the right side of the palate, while that on the left is about 7.0 medial to the parastylar root of P^3. The tooth rows diverge posteriorly, but M^4 is set inward relative to M^3.

Posteriorly, the palatine bones form the rest of the palate. The midline palatine suture is about 44.5 long. A slender, arcuate, posterior palatine ridge forms

the anteroventral border of the interpterygoid fossa. As in *Pyramios* the cross-section of this fossa is U-shaped. Unfortunately, the sutural relationships of the bones within the interpterygoid, orbital, pterygopalatine, and infratemporal fossae are almost impossible to determine. The lateral edges of the interpterygoid fossa are so broken that the pterygoid bones are probably largely missing. The pterygoid fossa, on the lateral surface of the alisphenoid anteromedial to the glenoid fossa, seems to be small and open laterally. The sphenopalatine foramen is an elongate opening at the medial edge of the maxillary shelf dorsal to the protoloph of M^4 and about 34.5 posterior to the maxillary foramen. The maxillary foramen is a nearly circular orifice 9.1 high and 10.0 wide; it is about 9.0 posteroventral to the lacrimal foramen. The optic-anterior lacerate foramen is about 64.4 posterior to the sphenopalatine.

Behind the frontal depression the frontal bones are somewhat crushed. The frontal depression is only slightly excavated, the cavity being only about 11.0 deeper at the midline than at its lateral edges. A pair of poorly developed lateral frontal ridges bound the depression and converge posterodorsally to meet the sagittal crest at the fronto-parietal suture, about 126.0 anterior to the lambdoidal crest.

The anterior contact of the frontal with the nasal and maxillary bones has already been described. The fronto-lacrimal suture leads posteroventrally, dorsal to the small lacrimal tuberosity, but the route of this suture within the orbital fossa cannot be determined.

The fronto-palatine suture seems to emerge from the sphenopalatine foramen and continue posteriorly about 11.0 above the maxillo-palatine suture. The course of the fronto-alisphenoid suture is difficult to determine, but it may rise posterodorsally, about 38.0 posterior to the sphenopalatine foramen, to meet the squamosal. Because the position of the squamoso-parietal contact is not readily apparent, the length of the fronto-squamosal suture is difficult to determine. It may be about 6.0 long, so that the squamoso-parieto-frontal junction would lie rather high on the cranium, only about 8.0 below the sagittal crest. Anterior to this the fronto-parietal suture evidently leads anteromedially toward the midline for 25.0. The midsagittal frontal suture is 99.0 long.

The anterodorsal corner of the lacrimal occurs 13.8 posteroventral to the maxillo-fronto-nasal contact and 11.5 anterodorsal to the lacrimal tuberosity. This tuberosity is 15.5 long and extends anteroventrally. The ventral end of the tuberosity is 17.0 dorsal and somewhat lateral to the small lacrimal foramen. The lacrimal of *Kolopsis* seems to have the generally triangular shape common to diprotodontids, but because of the difficulty of establishing its sutural contacts, its exact configuration is not determinable.

The jugal composes the anterior portion of the zygomatic arch. Its contacts with the maxillary and lacrimal have been indicated above. Anteriorly, the jugal curves strongly upward to lie slightly dorsal to the ventral edge of the lacrimal tuberosity. Posteriorly, the jugal sweeps back to taper out below the

squamosal at the anterior edge of the glenoid fossa. An elongate, dorsally convex ridge separates the ventral half of the jugal from the dorsal portion, and indicates the upper limit of the masseteric muscle attachment. As far as can be determined, this ridge consists of only a single arc rather than two as in *Pyramios*. Below the ridge the surface of the jugal faces ventrolaterally; above it, dorsolaterally. The slightly arched jugo-squamosal suture is about 10.7 long. There is no post-orbital process.

TABLE 25

Cranial measurements on CPC 6747, holotype of *Kolopsis torus*

Length, condyles to anterior edge I^1	397.4
Length, rostrum, from anterior edge of orbit to anterior edge of I^1	139.6
Length, rostrum, from anterior edge of orbit to tip of snout above narial aperture	115.7+
Length, lacrimal foramen to condyles	241.0
Length, lacrimal foramen to lambdoidal crest	223.5
Length, along midline from fronto-parietal suture to lambdoidal crest	126.3
Length, tip of rostrum dorsal to narial aperture to fronto-nasal suture	136.3+
Length, diastema, I^3-P^3—	
Right	65.8
Left	66.8
Length, tooth row, P^3-M^4—	
Right	109.2
Left	108.1
Length, tip of masseteric processes to occipital condyles	—
Length, tip of masseteric process to rear of paroccipital process	—
Length, anterior edge choanal aperture to condyles	195.0
Width, cranium at anterior edge of orbit	87.3
Width, greatest, across zygomatic arch just anterior to glenoid fossa	200.5
Width, across rostrum at level of infraorbital foramen	69.5
Width, across tips of masseteric processes	—
Width, occiput at lateral edge of mastoid processes	124.6
Width, between medial edges of I^3	35.5
Width, across diastemal crests at level of infraorbital foramen	29.4
Width, between medial edge of alveoli of P^3	34.3
Width, across lateral surface of maxillaries between M^2 and M^3	89.6
Width, between medial alveoli of M^4	40.9
Width, choanal fossa	35.4
Width, condyles	74.6
Width, narial aperture	45.6
Depth, narial aperture, from dorsal tip to posterior edge of premaxillary crest	47.0
Height, rostrum above rear alveolus of I^3	97.0
Height, rostrum above palate just anterior to P^3	80.0
Height, frontal depression above metacone of M^2	102.4
Height, cranium above metacone of M^4	126.9
Height, occiput, condyle to lambdoidal crest	98.8

The masseteric processes of the zygomatic arch are broken off, but they probably would not have descended below the level of the cheekteeth. The greatest depth of the zygomatic arch (62.3) occurs just anterior to the glenoid fossa. This is considerably greater than the vertical depth of 39.0 which was measured just posterior to the base of the masseteric process. The zygomatic arches of *Kolopsis* are nearly as long (191.2 from the rear of the zygomatic sulcus to the anterior edge of the orbit) as in *Pyramios* (217.8), but are much more slender and are less strongly curved in lateral view. The glenoid notch is a broad ventrally concave arch, not a sharp inverted V as in *Pyramios*. The greatest width of the cranium is measured across the arches (200.5) just anterior to the glenoid fossa. Above the fossa, the zygomatic sulci are about 41.2 wide and, in contrast to *Pyramios,* slant anteroventrally at a shallow angle (about 30°). The rear of each sulcus is formed by the postzygomatic crest, which continues posteromedially from the dorsal edge of the arch, but does not reach the lambdoidal crest.

The zygomatic portion of the squamosal, which lies atop the jugal, deepens posteriorly toward the glenoid fossa. The temporal portion of the squamosal is broadly expanded relative to the infratemporal fossa. In the latter the cranium is constricted to a width of only 49.2. The dorsal contact of the squamosal with the parietal is not clearly marked. The elongate, broadly arched suture may leave the lambdoidal crest 16.0 lateral to the midline and reach anteriorly, only 13.0 lateral to and slightly below the sagittal crest, to contact the frontal about 35.0 posterodorsal to the dorsal infratemporal crest (Fig. 29). The dorsal and ventral infratemporal crests are not easily differentiated in this specimen. The fronto-squamosal suture seems to lead anteroventrally across the dorsal crest, but the continuation of this suture is lost in the many fractures of the bone in the infratemporal fossa.

The squamoso-alisphenoid suture is difficult to locate, but it probably leads posteroventrally below the infratemporal crests, medial to the squamosal tuberosity,

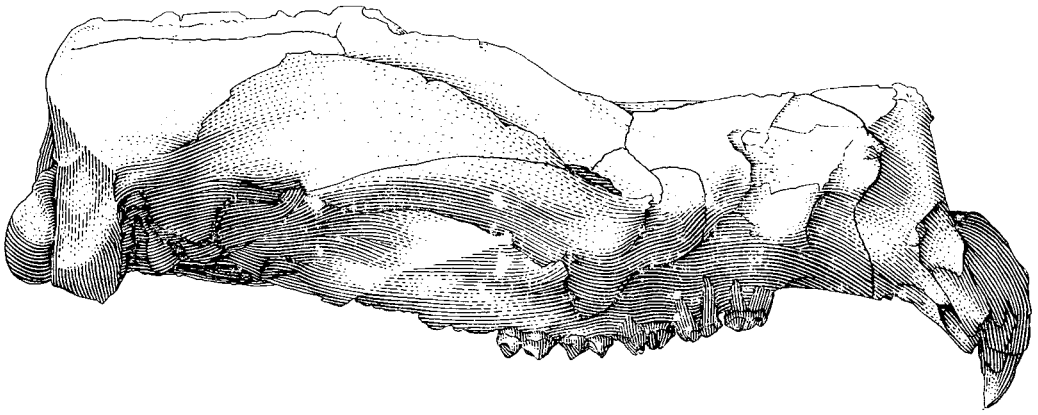

Fig. 29. *Kolopsis torus* **Woodburne. Right lateral view of holotype cranium, CPC 6747. One third natural size.**

to contact the basisphenoid in the entocarotid groove. Similarly, the contact between the squamosal and mastoid cannot be determined. The squamosal probably occupies at least the anterior half of the mastoid process, however. Except as outlined in the preceding description, the sutural relations of the alisphenoid cannot be determined in this specimen.

Most of the sutural contacts of the parietal bones have already been described. At the midline the joint parietal suture is about 120.0 long. The presence or absence of the interparietal cannot be determined. The sagittal crest is only slightly developed. It is slightly arched and is nearly parallel to the dorsal surface of the rostrum in lateral view. The highest point of the cranium occurs about 54.0 anterior to the lambdoidal crest, above the posterior edge of the zygomatic sulcus. The medial surface of the temporal fossa, formed by the squamosal and parietal bones, is smooth and slightly arched, somewhat as in *Pyramios*. *Kolopsis* differs from the known material of *Pyramios,* however, in the presence of a distinct sagittal crest.

At the posterior edge of the cranium, the lambdoidal crest is nearly straight transversely. In *Pyramios,* the lambdoidal crest curves markedly anteriorly toward the midline. In *Kolopsis,* the lambdoidal crest also curves anteroventrally along the dorsal border of the mastoid process and continues down on to its anterolateral corner. The mastoid process is aligned nearly vertically in posterior view so that the greatest width of the occiput (128.4) is measured across the lambdoidal crest at about the level of the external auditory meatus. The tip of the broken paroccipital process lies slightly below the condyles. As preserved, the cross-section of the combined paroccipital and mastoid process is sub-triangular, and its apex is posterior.

The condyles are the hindmost elements of the cranium; the paroccipital process extends as far back as the anterior edge of the condyle. The condyles taper as they extend ventromedially toward the floor of the transversely elongate foramen magnum. The occipital surface is generally smooth except for a pair of vertically elongate shallow depressions on either side of a 36.0-long nuchal ridge which begins about 17.0 above the foramen magnum. These depressions probably represent insertion areas for the dorsal rectus capitis musculature. Unfortunately the sutural relations of the mastoid, squamosal, exoccipital, interparietal, parietal, and supraoccipital bones in the occipital area cannot be determined.

The pair of elongate ovoid depressions on the basioccipital, which probably correspond to the insertion areas for the ventral rectus capitis muscles, are better developed than in *Pyramios*. A 7.5 wide groove occurs about 2.0 lateral to each depression. The lateral edges of the basioccipital converge anteriorly along the medial boundary of the entocarotid groove. The basisphenoid tapers anteriorly from its contact with the basioccipital. The basispheno-basioccipital suture probably occurs about 13.5 anterior to the median keel between the rectus capitis depressions on the basioccipital.

As in *Pyramios,* the squamosal tuberosity of *Kolopsis* is an anterolaterally oriented structure, separated by a deep fissure from the postglenoid process. The

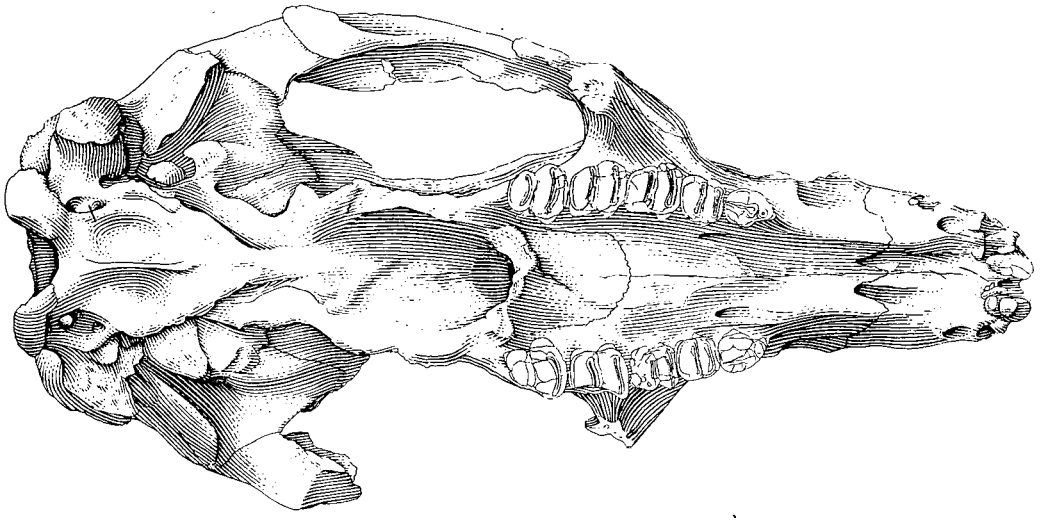

Fig. 30. *Kolopsis torus* **Woodburne. Ventral view of holotype cranium, CPC 6747. One third natural size.**

lateral surface of the tuberosity is smooth and flat, and slants ventrolaterally. The nearly longitudinally oriented crest, which ascends the anterior slope of the process, is continuous with the anterior edge of the smooth glenoid surface. The surface of the glenoid extends transversely, then anteriorly on to the posterior tip of the jugal. The postglenoid process is slender anteroposteriorly but elongate anterolaterally. The process diminishes in height to merge into the lateral edge of the glenoid notch; in posterior view the process is deepest near its medial edge.

The median lacerate-ovale foramen occurs at the medial base of the squamosal tuberosity. About 34.5 anteromedial to the base of the tuberosity, the anterior entocarotid foramen opens into the basisphenoid. The prominent entocarotid groove leads posterolaterally into the posterior entocarotid foramen at the medial base of the squamosal tuberosity. The posterior lacerate foramen is located at the medial base of the paroccipital process. The accessory condyloid foramen lies 13.0 posteromedial to the posterior lacerate foramen. The condyloid foramen leads posterodorsally into the foramen magnum 8.0 posterior to the accessory condyloid foramen. Both these foramina are enclosed in an elongate ovoid depression anterior to the condyles.

Only part of the tympanic bone is preserved. Its inner edge reaches nearly to the petrosal. The tympanic lies in the ventral portion of the superficies meatus area posterior to the postglenoid process and anterior to the mastoid process. The external auditory meatus, a ventrally open, anterolaterally directed U-shaped slot 7.3 wide, occurs at the lateral tip of the tympanic.

The rather wide promontorium of the petrosal is visible on the right side in the holotype. The ovalis and rotunda fenestrae are not visible, however.

The nasals form the roof of the narial cavity. In the holotype, these bones have been pushed slightly ventrally relative to the dorsal edge of the premaxillaries and maxillaries. The 134.4 suture between the two halves of the nasals would have been somewhat longer had the anterior tips of these bones been preserved. The fronto-nasal suture extends anterolaterally about 28.0 across the anterior edge of the frontal depression, to meet the maxillaries. The maxillo-nasal suture then continues anteriorly for about 60.0 to contact the premaxillaries. The greatest combined width of the nasals (40.5) is measured across the joint maxillo-fronto-nasal suture. The nasals are separated from the lacrimals by the 13.8 maxillo-frontal contact.

The anterior and dorsal contacts of the maxillary have already been described. Posteriorly, the rostral portion of the maxillary is sutured to the frontals for 13.8 and the lacrimal for 15.5. The maxillo-jugal suture, which begins at the ventral end of the lacrimal, leads about 22.0 anteriorly before turning ventrally toward the masseteric process of the zygomatic arch (the process is missing). In contrast to *Pyramios*, the facial crest is not developed along the side of the rostrum of *Kolopsis* and no fossa is formed for the snout musculature. The infraorbital foramen is a vertically elongate slit 17.3 high and 8.0 wide on the lateral surface of the rostrum. The lower edge of the foramen is about 25.0 above the diastemal crest anterior to P^3.

On the medial surface of the anterior base of the zygomatic arch, the maxillo-jugal suture continues anterodorsally to meet the lacrimal at the anterior edge of the orbit and about 20.0 posteroventral to the facial maxillo-lacrimal jugal suture.

The course of the maxillo-lacrimal suture is difficult to determine, but it seems to extend posteromedially above the maxillary foramen, and curves posteriorly to join the fronto-maxillary suture, presumably near the spheno-palatine foramen. Posteriorly, the maxillo-palatine suture seems to extend along the medial edge of the strongly developed maxillary shelf. The maxillary shelf is much more prominent than in *Pyramios*. The maxillo-palatine suture continues ventrally and anteromedially around the edge of the interpterygoid fossa on to the hard palate in CPC 6747.

On the palate, the maxillo-palatine suture seems to extend anteriorly, medial to the last molar, to a point opposite the protoloph of M^3 before turning medially toward the midline. The length of the midline maxillary suture on the palate is about 99.0. There are no palatal fenestrae. Only one anterior palatine foramen is present on each side between M^4 and the posterior palatine ridge. Anteriorly, a small nutrient foramen occurs about 9.3 medial to the hypocone of P^3 on the right side of the palate, while that on the left is about 7.0 medial to the parastylar root of P^3. The tooth rows diverge posteriorly, but M^4 is set inward relative to M^3.

Posteriorly, the palatine bones form the rest of the palate. The midline palatine suture is about 44.5 long. A slender, arcuate, posterior palatine ridge forms

the anteroventral border of the interpterygoid fossa. As in *Pyramios* the cross-section of this fossa is U-shaped. Unfortunately, the sutural relationships of the bones within the interpterygoid, orbital, pterygopalatine, and infratemporal fossae are almost impossible to determine. The lateral edges of the interpterygoid fossa are so broken that the pterygoid bones are probably largely missing. The pterygoid fossa, on the lateral surface of the alisphenoid anteromedial to the glenoid fossa, seems to be small and open laterally. The sphenopalatine foramen is an elongate opening at the medial edge of the maxillary shelf dorsal to the protoloph of M^4 and about 34.5 posterior to the maxillary foramen. The maxillary foramen is a nearly circular orifice 9.1 high and 10.0 wide; it is about 9.0 posteroventral to the lacrimal foramen. The optic-anterior lacerate foramen is about 64.4 posterior to the sphenopalatine.

Behind the frontal depression the frontal bones are somewhat crushed. The frontal depression is only slightly excavated, the cavity being only about 11.0 deeper at the midline than at its lateral edges. A pair of poorly developed lateral frontal ridges bound the depression and converge posterodorsally to meet the sagittal crest at the fronto-parietal suture, about 126.0 anterior to the lambdoidal crest.

The anterior contact of the frontal with the nasal and maxillary bones has already been described. The fronto-lacrimal suture leads posteroventrally, dorsal to the small lacrimal tuberosity, but the route of this suture within the orbital fossa cannot be determined.

The fronto-palatine suture seems to emerge from the sphenopalatine foramen and continue posteriorly about 11.0 above the maxillo-palatine suture. The course of the fronto-alisphenoid suture is difficult to determine, but it may rise posterodorsally, about 38.0 posterior to the sphenopalatine foramen, to meet the squamosal. Because the position of the squamoso-parietal contact is not readily apparent, the length of the fronto-squamosal suture is difficult to determine. It may be about 6.0 long, so that the squamoso-parieto-frontal junction would lie rather high on the cranium, only about 8.0 below the sagittal crest. Anterior to this the fronto-parietal suture evidently leads anteromedially toward the midline for 25.0. The midsagittal frontal suture is 99.0 long.

The anterodorsal corner of the lacrimal occurs 13.8 posteroventral to the maxillo-fronto-nasal contact and 11.5 anterodorsal to the lacrimal tuberosity. This tuberosity is 15.5 long and extends anteroventrally. The ventral end of the tuberosity is 17.0 dorsal and somewhat lateral to the small lacrimal foramen. The lacrimal of *Kolopsis* seems to have the generally triangular shape common to diprotodontids, but because of the difficulty of establishing its sutural contacts, its exact configuration is not determinable.

The jugal composes the anterior portion of the zygomatic arch. Its contacts with the maxillary and lacrimal have been indicated above. Anteriorly, the jugal curves strongly upward to lie slightly dorsal to the ventral edge of the lacrimal tuberosity. Posteriorly, the jugal sweeps back to taper out below the

squamosal at the anterior edge of the glenoid fossa. An elongate, dorsally convex ridge separates the ventral half of the jugal from the dorsal portion, and indicates the upper limit of the masseteric muscle attachment. As far as can be determined, this ridge consists of only a single arc rather than two as in *Pyramios*. Below the ridge the surface of the jugal faces ventrolaterally; above it, dorsolaterally. The slightly arched jugo-squamosal suture is about 10.7 long. There is no post-orbital process.

TABLE 25

Cranial measurements on CPC 6747, holotype of *Kolopsis torus*

Length, condyles to anterior edge I^1	397.4
Length, rostrum, from anterior edge of orbit to anterior edge of I^1	139.6
Length, rostrum, from anterior edge of orbit to tip of snout above narial aperture	115.7+
Length, lacrimal foramen to condyles	241.0
Length, lacrimal foramen to lambdoidal crest	223.5
Length, along midline from fronto-parietal suture to lambdoidal crest	126.3
Length, tip of rostrum dorsal to narial aperture to fronto-nasal suture	136.3+
Length, diastema, I^3-P^3—	
Right	65.8
Left	66.8
Length, tooth row, P^3-M^4—	
Right	109.2
Left	108.1
Length, tip of masseteric processes to occipital condyles	—
Length, tip of masseteric process to rear of paroccipital process	—
Length, anterior edge choanal aperture to condyles	195.0
Width, cranium at anterior edge of orbit	87.3
Width, greatest, across zygomatic arch just anterior to glenoid fossa	200.5
Width, across rostrum at level of infraorbital foramen	69.5
Width, across tips of masseteric processes	—
Width, occiput at lateral edge of mastoid processes	124.6
Width, between medial edges of I^3	35.5
Width, across diastemal crests at level of infraorbital foramen	29.4
Width, between medial edge of alveoli of P^3	34.3
Width, across lateral surface of maxillaries between M^2 and M^3	89.6
Width, between medial alveoli of M^4	40.9
Width, choanal fossa	35.4
Width, condyles	74.6
Width, narial aperture	45.6
Depth, narial aperture, from dorsal tip to posterior edge of premaxillary crest	47.0
Height, rostrum above rear alveolus of I^3	97.0
Height, rostrum above palate just anterior to P^3	80.0
Height, frontal depression above metacone of M^2	102.4
Height, cranium above metacone of M^4	126.9
Height, occiput, condyle to lambdoidal crest	98.8

The masseteric processes of the zygomatic arch are broken off, but they probably would not have descended below the level of the cheekteeth. The greatest depth of the zygomatic arch (62.3) occurs just anterior to the glenoid fossa. This is considerably greater than the vertical depth of 39.0 which was measured just posterior to the base of the masseteric process. The zygomatic arches of *Kolopsis* are nearly as long (191.2 from the rear of the zygomatic sulcus to the anterior edge of the orbit) as in *Pyramios* (217.8), but are much more slender and are less strongly curved in lateral view. The glenoid notch is a broad ventrally concave arch, not a sharp inverted V as in *Pyramios*. The greatest width of the cranium is measured across the arches (200.5) just anterior to the glenoid fossa. Above the fossa, the zygomatic sulci are about 41.2 wide and, in contrast to *Pyramios,* slant anteroventrally at a shallow angle (about 30°). The rear of each sulcus is formed by the postzygomatic crest, which continues posteromedially from the dorsal edge of the arch, but does not reach the lambdoidal crest.

The zygomatic portion of the squamosal, which lies atop the jugal, deepens posteriorly toward the glenoid fossa. The temporal portion of the squamosal is broadly expanded relative to the infratemporal fossa. In the latter the cranium is constricted to a width of only 49.2. The dorsal contact of the squamosal with the parietal is not clearly marked. The elongate, broadly arched suture may leave the lambdoidal crest 16.0 lateral to the midline and reach anteriorly, only 13.0 lateral to and slightly below the sagittal crest, to contact the frontal about 35.0 posterodorsal to the dorsal infratemporal crest (Fig. 29). The dorsal and ventral infratemporal crests are not easily differentiated in this specimen. The fronto-squamosal suture seems to lead anteroventrally across the dorsal crest, but the continuation of this suture is lost in the many fractures of the bone in the infratemporal fossa.

The squamoso-alisphenoid suture is difficult to locate, but it probably leads posteroventrally below the infratemporal crests, medial to the squamosal tuberosity,

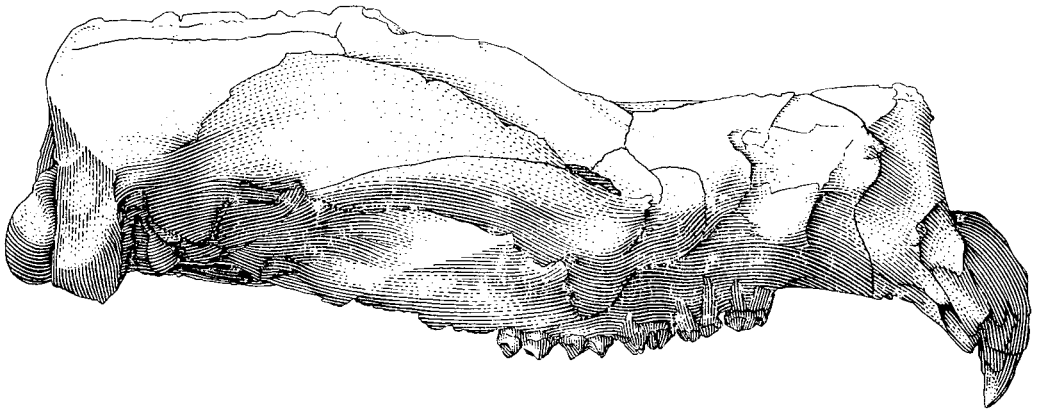

Fig. 29. *Kolopsis torus* **Woodburne. Right lateral view of holotype cranium, CPC 6747. One third natural size.**

to contact the basisphenoid in the entocarotid groove. Similarly, the contact between the squamosal and mastoid cannot be determined. The squamosal probably occupies at least the anterior half of the mastoid process, however. Except as outlined in the preceding description, the sutural relations of the alisphenoid cannot be determined in this specimen.

Most of the sutural contacts of the parietal bones have already been described. At the midline the joint parietal suture is about 120.0 long. The presence or absence of the interparietal cannot be determined. The sagittal crest is only slightly developed. It is slightly arched and is nearly parallel to the dorsal surface of the rostrum in lateral view. The highest point of the cranium occurs about 54.0 anterior to the lambdoidal crest, above the posterior edge of the zygomatic sulcus. The medial surface of the temporal fossa, formed by the squamosal and parietal bones, is smooth and slightly arched, somewhat as in *Pyramios*. *Kolopsis* differs from the known material of *Pyramios,* however, in the presence of a distinct sagittal crest.

At the posterior edge of the cranium, the lambdoidal crest is nearly straight transversely. In *Pyramios,* the lambdoidal crest curves markedly anteriorly toward the midline. In *Kolopsis,* the lambdoidal crest also curves anteroventrally along the dorsal border of the mastoid process and continues down on to its anterolateral corner. The mastoid process is aligned nearly vertically in posterior view so that the greatest width of the occiput (128.4) is measured across the lambdoidal crest at about the level of the external auditory meatus. The tip of the broken paroccipital process lies slightly below the condyles. As preserved, the cross-section of the combined paroccipital and mastoid process is sub-triangular, and its apex is posterior.

The condyles are the hindmost elements of the cranium; the paroccipital process extends as far back as the anterior edge of the condyle. The condyles taper as they extend ventromedially toward the floor of the transversely elongate foramen magnum. The occipital surface is generally smooth except for a pair of vertically elongate shallow depressions on either side of a 36.0-long nuchal ridge which begins about 17.0 above the foramen magnum. These depressions probably represent insertion areas for the dorsal rectus capitis musculature. Unfortunately the sutural relations of the mastoid, squamosal, exoccipital, interparietal, parietal, and supraoccipital bones in the occipital area cannot be determined.

The pair of elongate ovoid depressions on the basioccipital, which probably correspond to the insertion areas for the ventral rectus capitis muscles, are better developed than in *Pyramios*. A 7.5 wide groove occurs about 2.0 lateral to each depression. The lateral edges of the basioccipital converge anteriorly along the medial boundary of the entocarotid groove. The basisphenoid tapers anteriorly from its contact with the basioccipital. The basispheno-basioccipital suture probably occurs about 13.5 anterior to the median keel between the rectus capitis depressions on the basioccipital.

As in *Pyramios,* the squamosal tuberosity of *Kolopsis* is an anterolaterally oriented structure, separated by a deep fissure from the postglenoid process. The

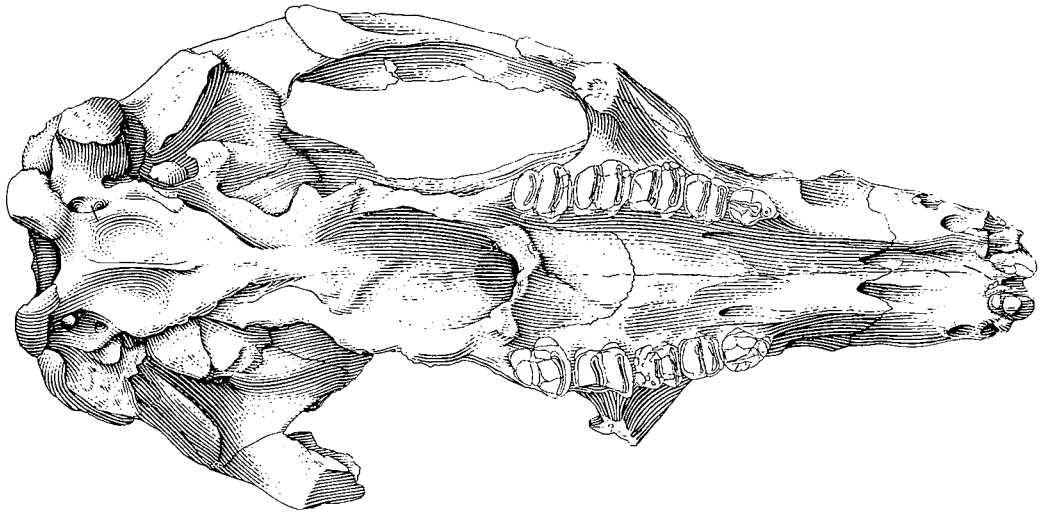

Fig. 30. *Kolopsis torus* **Woodburne. Ventral view of holotype cranium, CPC 6747. One third natural size.**

lateral surface of the tuberosity is smooth and flat, and slants ventrolaterally. The nearly longitudinally oriented crest, which ascends the anterior slope of the process, is continuous with the anterior edge of the smooth glenoid surface. The surface of the glenoid extends transversely, then anteriorly on to the posterior tip of the jugal. The postglenoid process is slender anteroposteriorly but elongate anterolaterally. The process diminishes in height to merge into the lateral edge of the glenoid notch; in posterior view the process is deepest near its medial edge.

The median lacerate-ovale foramen occurs at the medial base of the squamosal tuberosity. About 34.5 anteromedial to the base of the tuberosity, the anterior entocarotid foramen opens into the basisphenoid. The prominent entocarotid groove leads posterolaterally into the posterior entocarotid foramen at the medial base of the squamosal tuberosity. The posterior lacerate foramen is located at the medial base of the paroccipital process. The accessory condyloid foramen lies 13.0 posteromedial to the posterior lacerate foramen. The condyloid foramen leads posterodorsally into the foramen magnum 8.0 posterior to the accessory condyloid foramen. Both these foramina are enclosed in an elongate ovoid depression anterior to the condyles.

Only part of the tympanic bone is preserved. Its inner edge reaches nearly to the petrosal. The tympanic lies in the ventral portion of the superficies meatus area posterior to the postglenoid process and anterior to the mastoid process. The external auditory meatus, a ventrally open, anterolaterally directed U-shaped slot 7.3 wide, occurs at the lateral tip of the tympanic.

The rather wide promontorium of the petrosal is visible on the right side in the holotype. The ovalis and rotunda fenestrae are not visible, however.

The superficies meatus area of the auditory region is closed off dorsally by the large mastoid process. The squamosal tuberosity and postglenoid process are hollow, and were probably penetrated from within by an internally continuous epitympanic sinus. An opening in the dorsal squamosal area of the cranium reveals that the epitympanic sinus not only extended dorsally between the squamosal and lateral edge of the braincase, but continued anteriorly to a point just posterodorsal to the infratemporal crest. The broken mastoid-paroccipital process on the left side of the occiput is filled with matrix, indicating that it, too, was probably penetrated by a branch of the epitympanic sinus. Whether or not this cavity is derived from a posterior epitympanic fossa (Stirton, 1966a) (= hind part of the epitympanic sinus of Van der Klaauw, 1931, p. 82), which has become closed off in *Kolopsis,* is not determined without knowing the historical development of the mastoid process as shown in older, more primitive zygomaturine diprotodontids.

The upper and lower dentition and mandible of *Kolopsis torus* have been described previously (Woodburne, 1967). Pertinent data from these elements are included in the following sections.

Remarks: As pointed out in Stirton, Woodburne, & Plane (1967) *Kolopsis torus* is intermediate, in many features of its dentition, between *K. rotundus* and *Neohelos tirarensis* (of the Miocene Kutjamarpu fauna, South Australia) on the one hand, and *Zygomaturus gilli* (late Miocene to early Pliocene Beaumaris fauna of Victoria), on the other.

In some respects — the dorsolaterally expanded squamosals, the broadly curved outline of the lambdoidal crest in posterior view, the relatively strong separation of the triangular basioccipital and basisphenoid from surrounding parts of the basicranium, the anteriorly sloping lateral borders of the narial aperture, and the relatively flat, straight, posterolaterally oriented zygomatic arch — the cranium of *Kolopsis torus* retains more heritage characters from a *Ngapakaldia*-like ancestor than does that of *Pyramios alcootense.*

Although the features of the dentition of *Kolopsis torus* largely represent advances over those of *Ngapakaldia,* the simple lower molars of the Alcoota species with the vertical axes of the lophs and immaculate transverse valleys point toward an ancestry involving not only *Neohelos tirarensis,* but also an earlier form such as *Ngapakaldia tedfordi.*

On the other hand, the general advancement of the cranium of *Kolopsis torus* over that of *Ngapakaldia tedfordi* is shown in several features: increased size, greater development of the frontal depression, tubular nature of the rostrum, moderate constriction of the palate in the diastemal region, stronger development of the postglenoid process, more massive development of the mastoid process with corresponding restriction of the epitympanic fenestra in the superficies meatus area, the development of a strong buccinator fossa on the anteroventral base of the zygomatic arch, and the loss of the distinct fossa on the lateral surface of the rostrum below the masseteric crest.

The quinquetubercular premolar of *Kolopsis torus* is completely different from the bicuspid tooth present in both *Pitikantia* and *Ngapakaldia.* On the other hand, the general similarity between the upper premolar of *Neohelos tirarensis,* in which a hypocone has already been developed, and that of *K. torus* is striking. Assuming the presence of a parastyle (see Stirton, 1967b), the differentiation of the parametacone into two different cusps is the only other basic requirement to be met before P^3 of *N. tirarensis* would become that of *K. torus.* The general agreement in the morphology of M_4 of *N. tirarensis* and that of *Kolopsis torus* has been pointed out above. Although I^3 of the Kutjamarpu genus is quite different from that of *K. torus,* M^1 of *N. tirarensis* differs primarily from that of the Alcoota form in lacking a metastyle.

As shown by the presence of *K. rotundus* in the Awe fauna, the genus *Kolopsis* continues on into the middle Pliocene. The differences between the two species have been pointed out in the specific diagnosis, in Plane (1967), and in Stirton, Woodburne, & Plane (1967).

The changes which occurred between *K. torus* and *K. rotundus,* as far as the morphology of the premolar is concerned, are largely those which would lead to the level of advancement found in *Zygomaturus gilli* of the early Pliocene Beaumaris fauna of Victoria. It is evident that the genus *Kolopsis* was evolving toward *Zygomaturus; K. rotundus* is so nearly an ideal structural intermediate between *K. torus* and *Z. gilli* that it is virtually certain that this line of descent passed through a *K. rotundus* stage before the time of the Beaumaris fauna and after that of the Alcoota fauna, probably near the end of the Miocene. The middle Pliocene occurrence of *K. rotundus* in New Guinea suggests that the genus lingered on in the equatorial latitudes after having become extinct in the middle latitudes of the Australian continent.

PLAISIODON Woodburne, 1967

Genotypic species: Plaisiodon centralis Woodburne, 1967

Generic diagnosis: To the generic diagnosis given in Woodburne (1967) can be added the following characters — Cranium: rostrum tubular, diastemal crests nearly straight, diastemal palate slightly constricted; palatal surface broad and flat posteriorly; no well defined fossa on lateral surface of rostrum; no facial crest; infraorbital foramen probably with round cross-section; anterior portion of jugal nearly horizontal; cranium markedly constricted at anterior end of infraorbital crests; sagittal crest prominent, temporal surface of cranium slants steeply into infratemporal fossa; profile of sagittal crest extends markedly posterodorsally relative to dorsal surface of rostrum in lateral view; zygomatic sulcus slopes anteroventrally at steep angle by actual measurement, but is parallel to general orientation of postorbital region of cranium; condyles at level of dorsal surface of rostrum when cranium oriented with plane of occlusion of cheekteeth on a horizontal

The superficies meatus area of the auditory region is closed off dorsally by the large mastoid process. The squamosal tuberosity and postglenoid process are hollow, and were probably penetrated from within by an internally continuous epitympanic sinus. An opening in the dorsal squamosal area of the cranium reveals that the epitympanic sinus not only extended dorsally between the squamosal and lateral edge of the braincase, but continued anteriorly to a point just posterodorsal to the infratemporal crest. The broken mastoid-paroccipital process on the left side of the occiput is filled with matrix, indicating that it, too, was probably penetrated by a branch of the epitympanic sinus. Whether or not this cavity is derived from a posterior epitympanic fossa (Stirton, 1966a) (= hind part of the epitympanic sinus of Van der Klaauw, 1931, p. 82), which has become closed off in *Kolopsis,* is not determined without knowing the historical development of the mastoid process as shown in older, more primitive zygomaturine diprotodontids.

The upper and lower dentition and mandible of *Kolopsis torus* have been described previously (Woodburne, 1967). Pertinent data from these elements are included in the following sections.

Remarks: As pointed out in Stirton, Woodburne, & Plane (1967) *Kolopsis torus* is intermediate, in many features of its dentition, between *K. rotundus* and *Neohelos tirarensis* (of the Miocene Kutjamarpu fauna, South Australia) on the one hand, and *Zygomaturus gilli* (late Miocene to early Pliocene Beaumaris fauna of Victoria), on the other.

In some respects — the dorsolaterally expanded squamosals, the broadly curved outline of the lambdoidal crest in posterior view, the relatively strong separation of the triangular basioccipital and basisphenoid from surrounding parts of the basicranium, the anteriorly sloping lateral borders of the narial aperture, and the relatively flat, straight, posterolaterally oriented zygomatic arch — the cranium of *Kolopsis torus* retains more heritage characters from a *Ngapakaldia*-like ancestor than does that of *Pyramios alcootense.*

Although the features of the dentition of *Kolopsis torus* largely represent advances over those of *Ngapakaldia,* the simple lower molars of the Alcoota species with the vertical axes of the lophs and immaculate transverse valleys point toward an ancestry involving not only *Neohelos tirarensis,* but also an earlier form such as *Ngapakaldia tedfordi.*

On the other hand, the general advancement of the cranium of *Kolopsis torus* over that of *Ngapakaldia tedfordi* is shown in several features: increased size, greater development of the frontal depression, tubular nature of the rostrum, moderate constriction of the palate in the diastemal region, stronger development of the postglenoid process, more massive development of the mastoid process with corresponding restriction of the epitympanic fenestra in the superficies meatus area, the development of a strong buccinator fossa on the anteroventral base of the zygomatic arch, and the loss of the distinct fossa on the lateral surface of the rostrum below the masseteric crest.

The quinquetubercular premolar of *Kolopsis torus* is completely different from the bicuspid tooth present in both *Pitikantia* and *Ngapakaldia*. On the other hand, the general similarity between the upper premolar of *Neohelos tirarensis,* in which a hypocone has already been developed, and that of *K. torus* is striking. Assuming the presence of a parastyle (see Stirton, 1967b), the differentiation of the parametacone into two different cusps is the only other basic requirement to be met before P^3 of *N. tirarensis* would become that of *K. torus*. The general agreement in the morphology of M_4 of *N. tirarensis* and that of *Kolopsis torus* has been pointed out above. Although I^3 of the Kutjamarpu genus is quite different from that of *K. torus,* M^1 of *N. tirarensis* differs primarily from that of the Alcoota form in lacking a metastyle.

As shown by the presence of *K. rotundus* in the Awe fauna, the genus *Kolopsis* continues on into the middle Pliocene. The differences between the two species have been pointed out in the specific diagnosis, in Plane (1967), and in Stirton, Woodburne, & Plane (1967).

The changes which occurred between *K. torus* and *K. rotundus,* as far as the morphology of the premolar is concerned, are largely those which would lead to the level of advancement found in *Zygomaturus gilli* of the early Pliocene Beaumaris fauna of Victoria. It is evident that the genus *Kolopsis* was evolving toward *Zygomaturus; K. rotundus* is so nearly an ideal structural intermediate between *K. torus* and *Z. gilli* that it is virtually certain that this line of descent passed through a *K. rotundus* stage before the time of the Beaumaris fauna and after that of the Alcoota fauna, probably near the end of the Miocene. The middle Pliocene occurrence of *K. rotundus* in New Guinea suggests that the genus lingered on in the equatorial latitudes after having become extinct in the middle latitudes of the Australian continent.

PLAISIODON Woodburne, 1967

Genotypic species: Plaisiodon centralis Woodburne, 1967

Generic diagnosis: To the generic diagnosis given in Woodburne (1967) can be added the following characters — Cranium: rostrum tubular, diastemal crests nearly straight, diastemal palate slightly constricted; palatal surface broad and flat posteriorly; no well defined fossa on lateral surface of rostrum; no facial crest; infraorbital foramen probably with round cross-section; anterior portion of jugal nearly horizontal; cranium markedly constricted at anterior end of infraorbital crests; sagittal crest prominent, temporal surface of cranium slants steeply into infratemporal fossa; profile of sagittal crest extends markedly posterodorsally relative to dorsal surface of rostrum in lateral view; zygomatic sulcus slopes anteroventrally at steep angle by actual measurement, but is parallel to general orientation of postorbital region of cranium; condyles at level of dorsal surface of rostrum when cranium oriented with plane of occlusion of cheekteeth on a horizontal

line; mastoid process oriented posteroventrally, cross-section subtriangular; glenoid notch broadly arcuate; glenoid fossa oriented anterolaterally in ventral view; foramen magnum nearly equidimensional; basioccipital weakly excavated for ventral rectus capitis muscles; pterygoid fossa large, open posteromedially; well developed buccinator fossa on anteroventral base of zygomatic arch; squamosofrontal suture long (about 42.5).

PLAISIODON CENTRALIS Woodburne, 1967

(Figs 31-33, Table 26)

Holotype: CPC 6748, skull lacking incisor and most left molar dentition, left zygomatic arch and occiput.

Paratypes: As given in Woodburne (1967).

Specific diagnosis: That of the genus until other species are described (*ibid.*).

Type locality: Paine Quarry, V6345, Waite Formation, 4 miles south-west of Alcoota station, 2.1 miles south-west of junction of Waite and Ongeva Creeks, Northern Territory, Australia.

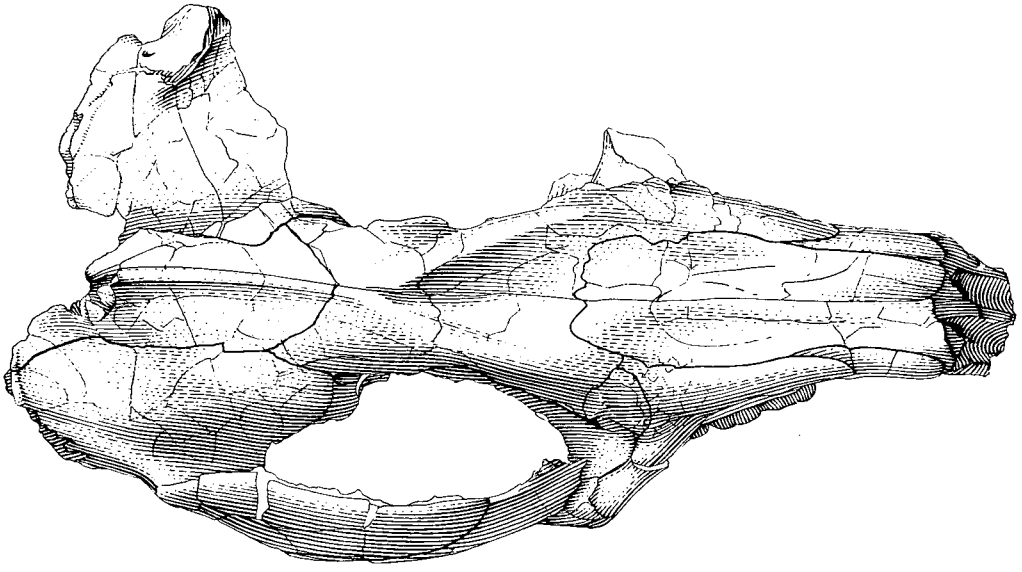

Fig. 31. *Plaisiodon centralis* **Woodburne. Dorsal view of holotype cranium, CPC 6748. One third natural size.**

Age: Alcoota fauna, late Miocene or possibly early Pliocene.

Cranium: The holotype of *Plaisiodon centralis,* CPC 6748, is not as complete as that of *Pyramios* or *Kolopsis*. The tip of the premaxillaries, the left zygomatic arch, the basicranium, the occiput, and part of the palate are missing. Fortunately most of these features are preserved in a second cranium which lacks the rostrum, UCMP 70021, and a partial occiput, UCMP 70983. As indicated in Table 26, UCMP 70021 is from a larger individual than the holotype, and the measurements from the two crania have been kept separate. Both crania are well preserved; both are highly fractured. The position of the condyles, the mastoid processes, the posterodorsal edge of the occiput, the glenoid fossa, and all cranial elements posterior to the palate is much higher relative to the cheek-teeth in *Plaisiodon* than in the other Alcoota diprotodontids. In this respect, the cranium of *Plaisiodon* most closely resembles that of the Pleistocene genus *Zygomaturus*.

In the holotype, the rostrum is elongate and tubular as in *Kolopsis,* but the dorsal surface has been too greatly crushed to allow an adequate determination of its true height. Because of this crushing, the shape of the narial aperture is slightly distorted; it was probably nearly equidimensional, as in *Kolopsis*.

The premaxilliaries bound the narial aperture laterally and ventrally and support the incisor dentition. The dorsal premaxillo-nasal contact is relatively straight in the holotype and extends 67.7 behind the narial aperture. The premaxillo-maxillary suture forms a strong posteriorly concave arc as it drops down along

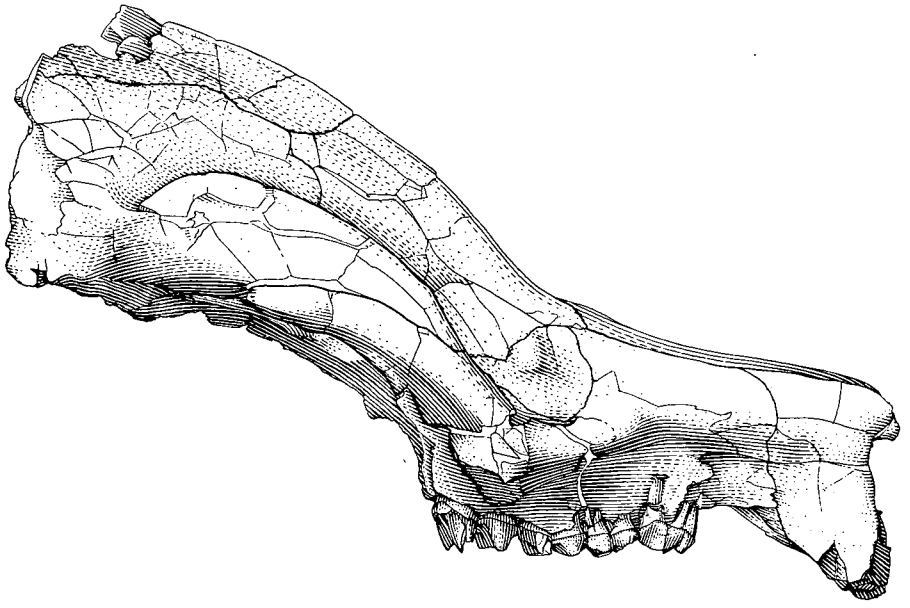

Fig. 32. *Plaisiodon centralis* **Woodburne. Right lateral view of holotype cranium, CPC 6748. One third natural size.**

the lateral surface of the rostrum for about 32.0 before turning anteroventrally toward the diastemal crests. As in *Kolopsis,* the lower end of the arc is at the level of the infraorbital foramen. Ventrally, the premaxillo-maxillary suture crosses the diastemal crests as an anteriorly open chevron, and meets the median premaxillary suture, which is 51.0 long, near the posterior edge of the incisive foramen.

In ventral view (Fig. 33) the rostrum of the holotype is generally like that of *Kolopsis torus,* except that the incisive foramina in CPC 6748 are closer together (7.6) and the median ridge that separates them is less well developed. The diastemal crests in *Plaisiodon* are nearly parallel, but less strongly developed than in *Kolopsis.* The diastemal palate in both genera is only slightly constricted. Comparison of Tables 25 and 26 shows that although the holotype of *K. torus* is smaller than that of *P. centralis,* the length of the rostrum, as indicated by the diastema from P^3-I^3, is actually and relatively shorter in *P. centralis.*

The full extent of the narial notch cannot be determined because the tips of the nasals are missing. The rear edge of the notch lies about 9.4 behind the front of the premaxillary, and the anterior edge of the narial aperture slants anteroventrally. The premaxillary crest is broken away, as is that portion of the bone anterior and dorsal to the alveolus of I^1. As in the other Alcoota diprotodontids, the diastemal crest extends anteroventrally toward I^3. Thus, although the incisors are not preserved in the holotype, they would lie considerably below the occlusal plane of the cheekteeth (Fig. 32).

The nasals, which roof the narial cavity, extend 136.8 posteriorly to meet the frontals at the midline in CPC 6748. The median nasal suture would be somewhat longer than this as the tips of the nasals are missing in the holotype. The fronto-nasal contact extends anterolaterally across the anterior end of the frontal depression for about 31.0 to contact the maxillary. The maxillo-nasal suture then continues anteriorly for 64.1 to meet the premaxillary. Posteriorly, the nasal is separated from the lacrimal by the fronto-maxillary contact, which is about 25.0 long. In contrast to the condition in *Kolopsis* and *Pyramios,* the greatest combined width of the nasals (54.6) is measured about midway along the maxillo-nasal suture in *Plaisiodon.*

The sutural relations of the maxillary with the premaxillary and nasal bones has already been described. The maxillo-frontal suture extends 25.0 posterolaterally from the maxillo-fronto-nasal contact to join the lacrimal above the lacrimal tuberosity. Owing to crushing and fracturing of this portion of the holotype, it is not possible to identify the anterior edge of the lacrimal with certainty. As shown in Figure 31, the maxillo-lacrimal suture probably extends anteriorly for 8.5, then curves anteroventrally for 32.8 to meet the jugal. The maxillo-jugal suture then continues anteriorly to a point dorsal to M^1 before turning posteroventrally along the ventral surface of the facial crest toward the now missing masseteric process.

Although the tips of the masseteric processes are broken off, it does not seem likely that they would have extended as far below the cheekteeth as in *Pyramios.*

TABLE 26

Cranial measurements on CPC 6748, holotype, and UCMP 70021, paratype, of *Plaisiodon centralis*

	CPC 6748	UCMP 70021
Length, condyles to anterior edge, I^1	----	----
Length, rostrum, from anterior edge of orbit to anterior edge I^1	----	----
Length, rostrum, from anterior edge of orbit to tip of snout above narial aperture	136.7+	----
Length, lacrimal foramen to condyles	----	327.3
Length, lacrimal foramen to lambdoidal crest	----	289.0
Length, fronto-parietal suture to lambdoidal crest along midline	----	141.9
Length, tip of rostrum dorsal to narial aperture to fronto-nasal suture	145.4+	----
Length, diastema, I^3-P^3 —		
Right	53.7	----
Left	----	----
Length, tooth row, P^3-M^4 —		
Right	----	----
Left	----	----
Length, tip of masseteric process to condyles	----	----
Length, tip of masseteric process to rear of paroccipital process	----	----
Length, anterior edge choanal aperture to condyles	----	234.0
Width, cranium at anterior edge of orbit	102.2	126.5
Width, greatest, across zygomatic arch just posterior to transverse palatine ridge	----	248.8
Width, across rostrum at level of infraorbital foramen	68.5	----
Width, across tips of masseteric processes	----	----
Width, occiput at lateral edge of mastoid processes	----	191.0
Width, between medial edges of I^3	25.4	----
Width, across diastemal crests at level of infraorbital foramen	33.6	----
Width, between medial edge of alveoli of P^3	22.5	28.5
Width, across lateral surface of maxillaries between M^2 and M^3	93.8	117.4
Width, between medial alveoli of M^4	----	61.2
Width, choanal fossa	----	----
Width, condyles	----	87.6
Width, narial aperture	50.1	----
Depth, narial aperture from dorsal tip to posterior edge of premaxillary crest	30.5+	----
Height, rostrum, above rear alveolus of I^3	74.5+	----
Height, rostrum, above palate just anterior to P^3	64.4+	----
Height, frontal depression above metacone of M^2	106.9	----
Height, cranium, above metacone of M^4	----	202.7
Height, occiput, condyle to lambdoidal crest	----	134.9+

+ = measurement small, would have been larger in uncrushed specimen.

The sides of the rostrum in front of the infraorbital foramen are slightly crushed inward in the holotype, but the facial crest does not seem to have been developed in *Plaisiodon*. The shape of the infraorbital foramen is also obscured by crushing. The foramen lies above the anterior end of P^3. The buccinator fossa at the anteroventral base of the zygomatic arch is very pronounced in UCMP 70021.

The maxillo-jugal suture continues up the posterior internal surface of the zygomatic arch to curve medially, at the anteroventral edge of the orbit, and join the lacrimal once again. The lacrimo-jugal suture extends anterodorsally about 18.0 to meet the rostral portion of the maxillary. In the holotype, the maxillo-lacrimal suture leads posteriorly above the maxillary foramen, to bisect the sphenopalatine foramen 18.3 farther on. In UCMP 70021, the rear of the maxillary foramen is anterior to the front of the sphenopalatine.

Since the anterior edge of the palatine bone reaches the posterior edge of the sphenopalatine foramen, the maxillo-frontal contact is rather short (23.7 in UCMP 70021 and probably about 18.5 in the holotype). Posterior to the sphenopalatine foramen, the maxillo-palatine suture leads posteroventrally along the medial edge of the maxillary shelf, curving ventrally and anteriorly around the posterior end of the shelf. The maxillary shelf in *Plaisiodon* is well developed, as in *Kolopsis* and in contrast to the condition in *Pyramios*.

Most of the bony wall which separates the interpterygoid and pterygopalatine fossae has been broken away in both the holotype and UCMP 70021. The next point at which the maxillo-palatine suture is visible, therefore, is on the palatal surface between M^4 and the posterior palatine ridge. In UCMP 70021, the sutures from each side converge anteriorly to join the midline opposite the metaloph of M^3. The suture bisects the anterior palatine foramen. About 20.0 anterior to this a pair of small foramina are set close together. Farther anteriorly other such foramina can be seen opposite the transverse valley of M^1 and the anterior root of P^3 in UCMP 70021. As in the other Alcoota diprotodontids there are no palatal fenestrae. The cheekteeth diverge posteriorly, but M^4 is set inward relative to M^3. The median maxillary suture is about 102.0 long in the holotype.

The palatine bones occupy the posterior portion of the palate and, as shown in UCMP 70021, bear an arcuate posterior palatine ridge at the anteroventral border of the interpterygoid fossa. Most of the walls of this fossa is missing, but enough bone remains at its anterior end to suggest that its cross-section may have been more V-shaped than in either *Pyramios* or *Kolopsis*.

Remnants of pterygoid fossae are found as a pair of ovoid depressions about 39.5 long and 30.8 wide on either side of the midline near the anterior tip of the basisphenoid in UCMP 70021. Only the dorsal portions of the fossae are preserved. The remaining evidence suggests, however, that the structures were enclosed laterally and medially, but opened posteromedially toward the surface of the basisphenoid. The fossae were probably bounded medially by the pterygoid and laterally by the alisphenoid bones, but it is not possible to determine this with certainty.

The frontal bones are preserved in both CPC 6748 and UCMP 70021. The frontal depression is well marked and is similar to that of *Kolopsis*. The cavity is 10.0 (CPC 6748) and 16.4 (UCMP 70021) deeper at the midline than at its lateral edge. The lateral frontal crests which bound the depression converge posteromedially to join the sagittal crest at the fronto-parietal suture. This lies 136.2 posterior to the fronto-nasal contact in CPC 6748.

The contacts of the frontal with the nasal and maxillary have been described above. The fronto-lacrimal suture is not clearly expressed in the holotype. In UCMP 70021, it seems to extend posteroventrally into the orbital fossa to join the maxillary just anterior to the sphenopalatine foramen. The fronto-palatine suture, best seen in UCMP 70021, extends posteriorly about 17.5 above the maxillo-palatine suture toward the orbitosphenoid. The fronto-orbitosphenoid suture may describe a semicircle which contacts the palatine about 60.8 postero-dorsal to the sphenopalatine foramen and which intersects the alisphenoid near the anterior end of the infratemporal crest. At this point the fronto-alisphenoid suture leads posterodorsally for about 26.5 before joining the squamosal. The fronto-squamosal suture continues posterodorsally for about 68.5 to contact the parietal. The fronto-parietal suture leads steeply anterodorsally 42.5 to the sagittal crest. *Plaisiodon* has by far the longest fronto-squamosal contact of all the Alcoota diprotodontids.

The lacrimal, although poorly outlined, is best seen in the holotype. If the sutural contacts of the lacrimal have been traced even approximately correctly, the bone appears to be shorter in *Plaisiodon* than in the other genera. The lacrimal foramen is not clearly shown in this specimen owing to fracturing and crushing. The lacrimal tuberosity, and 18.3-long anteroventrally elongate process, is better developed in this genus than in any of the other Alcoota diprotodontids.

The contact between the jugal and the maxillary has been described previously. Whereas the anterior portion of the jugal which extends along the ventral edge of the orbit has a conspicuous dorsal curvature in *Kolopsis* and *Pyramios,* it is nearly horizontal in *Plaisiodon.* In conformity with the elevated posterior part of the cranium in *P. centralis,* the jugal rises more steeply posterodorsally than in those other genera. Otherwise, the jugal of *Plaisiodon* is much like that of *Kolopsis.*

The greatest depth of the zygomatic arches in the holotype (53.7) is measured just anterior to the glenoid notch. The notch, visible in UCMP 70021 is a broad, ventrally concave arc, somewhat like that of *Kolopsis.* As in *Kolopsis,* an arcuate elongate ridge which defines the dorsal limit of the masseteric muscle attachment, is developed along the lateral surface of the arch below the squamoso-jugal suture, and fades out before reaching the glenoid fossa. The zygomatic arch is distorted in both crania of *Plaisiodon,* but it appears that, in contrast to *Kolopsis* and *Pyramios,* the greatest width of the cranium is measured about midway along the lateral surface of the arches.

The slender squamosal extends anteriorly from the glenoid fossa to complete the arch. The jugo-squamosal suture is about 96.5 long in the holotype. Above

the glenoid fossa, the zygomatic sulcus is 27.0 wide in the holotype. This measurement may be too small owing to medial compression of the arch. The dimensions of the sulcus cannot be taken in UCMP 70021 because of a moderately large ventral displacement of its squamosal portion. The sulcus is 50.0 long in the holotype and slants anteroventrally at an angle of about 60°. Although this angle of declivity is similar to that in *Pyramios* by actual measurement, the orientation of the door of the sulcus in *Plaisiodon* is parallel to the general attitude of the temporal region of the cranium, as in *Kolopsis*.

Above the zygomatic sulcus, the squamosal extends steeply dorsomedially toward the parietals so that the surface of the temporal portion of the squamosal is not expanded dorsolaterally as in *Kolopsis*. In the holotype, the squamoso-parietal suture leaves the lambdoidal crest about 33.5 lateral to the midline and extends forward as a broad arc for about 102 to meet the frontal. The fronto-squamosal suture continues anteroventrally toward the dorsal infratemporal crest, as shown most clearly in UCMP 70021. The contact between the alisphenoid and squamosal extends posteroventrally along the dorsal infratemporal crest into the infratemporal fossa. The further continuation of the suture is not clearly demonstrated by the available material, but it seems to extend posteromedially toward the foramen ovale between the pterygoid fossa and the squamosal tuberosity. Anterior to the infratemporal crests, the cranium is constricted to a width of 61.4 in the holotype and 52.8 in UCMP 70021.

The sutural contacts of the parietals have been described above. The parietal rises dorsomedially from the squamosal to form the sagittal crest. The crest is about 142.5 long from the median fronto-parietal suture to the lambdoidal crest in UCMP 70021. In lateral view (Fig. 32), the sagittal crest is directed steeply posterodorsally relative to dorsal surface of the rostrum. This is in marked contrast to the condition in *Pyramios* and *Kolopsis,* in which the lateral profile of the sagittal crest is nearly parallel to that of the rostrum. The suture between the parietal and exoccipital bones is not determinable in *Plaisiodon,* but it probably coincides with the lambdoidal crest. The presence or absence of the interparietal cannot be definitely ascertained.

Anteroventral to the squamosal, the alisphenoid is a relatively slender strip of bone dorsal to the orbitosphenoid and palatine bones. The sutural relationships of the alisphenoid have been largely described above.

In UCMP 70021, the lateral base of the pterygoid fossa, formed by the alisphenoid, is separated from the squamosal tuberosity by a shallow groove which leads anterolaterally out of the foramen ovale and follows the squamoso-alisphenoid suture. This is best seen in the cranial fragment, UCMP 70983.

The transverse canal opens anteromedially into the basisphenoid just posterior to the pterygoid fossa. On the left side of UCMP 70021 the bone is broken away along the anterior dorsal roof of the pterygoid fossa, exposing a canal which leads anterolaterally to emerge, presumably from the orbitosphenoid, as the optic-anterior lacerate foramen.

The squamosal tuberosity is broken on both sides in UCMP 70021, revealing that the structure is hollow and opens dorsally into the major portion of the epitympanic sinus. The longitudinal ridge which remains at the base of the external surface of the process curves anterolaterally as the anterior edge of the glenoid fossa. The fossa extends laterally and anteriorly on to the postero-ventral tip of the jugal.

As in *Kolopsis,* and in contrast to the condition in *Pyramios,* the postglenoid process in *Plaisiodon* is oriented anterolaterally at an angle of about 45° relative to the midline. The postglenoid process is separated from the squamosal tuberosity by a deep, narrow groove. This groove is bridged ventrally by the tympanic. The tympanic is poorly preserved, but it seems to be a dense, rather slender, elongate element which tapers laterally and forms the ventral boundary of the external auditory meatus. The petrosal, best seen in the occipital fragment, UCMP 70983, lies dorsomedial to the tympanic and deep to the rectus capitis ridge of the basioccipital. Only a ventral, triangular knob-like process of the petrosal can be seen in this specimen. The structure lies just posterior to the posterior entocarotid foramen and may represent the promontorium. The facial foramen, fenestra ovalis, and fenestra rotunda are not visible.

In UCMP 70983 the posterior lacerate foramen lies posterior to the petrosal and descends along the anteromedial base of the paroccipital process. Lateral to this the stylomastoid groove traverses the anterior base of the mastoid process, posterior to the tympanic, and opens out on to the lateral surface of the cranium 18.0 ventral to the roof of the external auditory meatus.

The moderately short 5.2-wide entocarotid groove leads anteromedially from the ventral lip of the posterior entocarotid foramen in UCMP 70983. The anterior entocarotid foramen leads anteromedially into the basisphenoid 11.4 posterior to the transverse canal. This is most clearly shown in UCMP 70021. As indicated in UCMP 70983, the foramen ovale leads anterolaterally between the squamosal tuberosity and posterolateral wall of the pterygoid fossa. The condyloid and accessory condyloid foramina lie in the ventral portion of the condyloid sulcus medial to the paroccipital process.

The paroccipital and mastoid processes are broken open in UCMP 70021, revealing their hollow interior. A small epitympanic fenestra may be represented by a circular orifice dorsal to the petrosal in UCMP 70021. The fenestra opens dorsally into a large posterior epitympanic sinus. This cavity extends transversely to the lateral wall of the braincase and anteriorly to a bony partition which closes off the sinus at a level dorsal to the external auditory meatus. As preserved in UCMP 70021 the internal surface of the posterior epitympanic sinus is irregular. A conspicuous pocket in the sinus extends medially just internal to the base of the left rectus capitis depression on the occiput. A second pocket extends ventromedially toward the base of the left condyle.

An anterior epitympanic sinus apparently lies in front of the posterior sinus and extends forward to the level of the infratemporal crests. This sinus is

confluent ventrally with the squamosal tuberosity, but whether or not it was continuous with the posterior epitympanic sinus is difficult to judge. The various cavities into which the epitympanic sinus seems to be divided in *Plaisiodon* may correspond to the pockets of the epitympanic sinus of *Ngapakaldia* described by Stirton (1967a). The presence of an anterior and a posterior dorsal epitympanic sinus is suggested in the case of *Pyramios;* the evidence regarding this feature in *Kolopsis* is equivocal.

The occipital surface of *Plaisiodon* is best preserved in UCMP 70021. The condyles lie at the hindmost point on the cranium. Above them, the occipital profile, as seen in lateral view, slants anterodorsally at an angle of about 60°. As seen from behind, the condyles of *Plaisiodon* are about 47.4 high, are more vertically oriented than in *Kolopsis* or *Pyramios,* and the foramen magnum is more equidimensional than in those two genera. Above the foramen magnum, a pair of dorsal rectus capitis fossae about 71.0 long lie ventral to the lambdoidal crest, which is displaced somewhat posteriorly in this specimen. A prominent ventrally concave chevron-shaped depression is situated about 29.5 dorsal to each condyle and lateral to the rectus capitis fossae. At the dorsal edge of the occiput, the lambdoidal crests slant ventrolaterally for about 100.0 and curve anteriorly to fade out over the dorsal base of the mastoid processes. The sutures of the exoccipital and supraoccipital cannot be determined in the material at hand.

The mastoid process forms the posterolateral corner of the cranium, and most of the lateral surface of the process is probably formed by the mastoid bone, although its sutures with adjacent elements cannot be found. The tip of the mastoid process occurs as a low eminence posterior to the external auditory meatus and on a level below the tip of the postglenoid process. The paroccipital process, probably formed mainly of the exoccipital, arises from the medial border of the mastoid process and curves somewhat ventromedially in posterior view. The cross-section of the combined paroccipital and mastoid processes is triangular, with its apex directed anteromedially.

Anterior to the condyles, the basioccipital forms a flat surface 67.4 wide in UCMP 70021 and about 64.0 wide in UCMP 70983. The median keel is poorly developed. On either side of this are ovoid depressions associated with the ventral rectus capitis musculature. At the ventrolateral edge of the basioccipital the relatively prominent rectus capitis ridge extends anteromedially on to the basisphenoid. The basioccipito-basisphenoid suture probably occurs about midway between the anterior and posterior entocarotid foramina.

Descriptions of the upper area lower dentition and mandible of *Plaisiodon centralis* have been presented previously (Woodburne, 1967). Pertinent information drawn from these elements is included in the following section.

Remarks: *Plaisiodon centralis* is clearly a member of the Zygomaturinae (Stirton, Woodburne, & Plane, 1967). In the anterodorsal flexion of the postorbital portion of the cranium and nearly equidimensional foramen magnum,

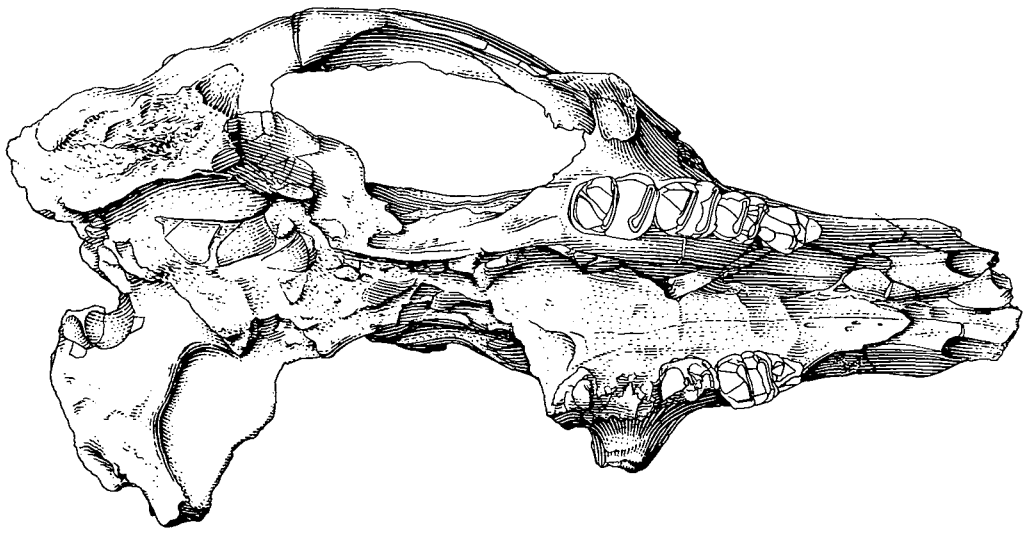

Fig. 33. *Plaisiodon centralis* **Woodburne. Ventral view of holotype cranium, CPC 6748. One third natural size.**

P. centralis foreshadows trends which apparently recurred in later zygomaturines, such as the Pleistocene *Zygomaturus trilobus*. On the other hand, the sharp sagittal crest and corresponding steep flat surface of the temporal region, the very elongate fronto-squamosal suture, and the very prominent pterygoid fossae in the basicranium seem to be unique to *P. centralis*.

In other features, i.e., the configuration of the rostrum, the excavation of the anteroventral base of the zygomatic arch, the anterolateral orientation of the glenoid fossa, the degree of development of the frontal depression, the amount of palatal constriction in the diastemal area, and the expansion of the mastoid process, *Plaisiodon centralis* is just as advanced over *Ngapakaldia tedfordi* as is *Kolopsis torus*. Furthermore, except for the degree of palatal constriction and expansion of the mastoid process, the cranial morphology of the Alcoota zygomaturines is more advanced relative to the primitive palorchestines of the Ngapakaldi fauna than is *Pyramios alcootense*.

As indicated in Stirton, Woodburne, & Plane (1967), *Neohelos tirarensis* Stirton, 1967, is, in some features, more closely ancestral to *P. centralis* than to *K. torus*. The salient features which demonstrate this relationship are the presence of a hypocone on P^3, a single parametacone on P^3, a broadly triangular I^3 lacking a strong cleft in its labial surface, and the absence of a distinct cusp in the position of the metastyle on M^1. On the other hand, its large size, the well developed anterior and posterior cingula on the upper molars, the absence of a longitudinal postparaconal crest on M^1, and the presence of a distinct metalophid on the lower molars of *Plaisiodon centralis,* point to the separation of the two forms. 'From the available evidence it appears that the two genera

[*Plaisiodon* and *Neohelos*] are only broadly related within the subfamily and probably had a common ancestry prior to Kutjamarpu time. *Plaisiodon centralis* may represent an early branch of the Zygomaturinae which became extinct in the late Miocene or early Pliocene. It has not been found in the later faunas' *(ibid.)*.

The presence of *Palorchestes painei, Pyramios alcootense, Kolopsis torus,* and *Plaisiodon centralis* in the Alcoota fauna indicates that at least three of the major lineages within the Diprotodontidae were well separated in the middle Tertiary. The Palorchestinae are known to occur in faunas of probable late Oligocene age, and the Zygomaturinae extend back into the Miocene. The sharp separation of *Pyramios alcootense* from the Alcoota zygomaturines indicate that the Nototheriinae was also a distinct phyletic group in the Miocene. The relatively simple premolar of *Neohelos tirarensis,* the earliest zygomaturine, was presumably derived from an ancestor with a yet simpler dentition prior to Kutjamarpu time. Such an ancestor may have been common to the Nototheriinae as well, but was probably still distinct, in basicranial characters, from primitive palorchestines such as those of the Ngapakaldi fauna. The palorchestine lineage probably leads back into the early Tertiary in concert with the archetypal zygomaturo-nototherе. The morphology of the form from which these two branches ultimately arose is difficult to interpret. Its cranial morphology may not have been too different from that of *Ngapakaldia.* Various characters in the interrelationships of the bony elements of the cranium of the later Tertiary diprotodontids, as well as the epitympanic fenestration, postepitympanic pocket, and medial glenoid process of *Ngapakaldia* (see Stirton, 1967a) suggest that the stem diprotodontid may have resembled the stem vombatid to a large degree.

DIPROTODONTIDAE, indeterminate

A relatively large number of diprotodontid postcranial elements of various sorts are represented in the collection. These are largely phalangeal and carpal and tarsal elements, but vertebrae, ribs, and scapulae are present along with elements of the fore and hind limb. Because of the nature of the fossil deposit, there is no way in which these elements can be confidently assigned to any one of the four genera of diprotodontid present in the fauna. In general, the size of these elements is slightly closer to those of *Diprotodon optatum* than those of *Ngapakaldia tedfordi.* On the other hand, the extreme specializations seen in the manus and pes of *D. optatum* are not encountered in comparable elements in the Alcoota material. In gross stage of evolution the Alcoota diprotodontids seem to be closer to *Ngapakaldia* in postcranial morphology. However, in view of the problems in evaluating the taxonomic position of the elements and because the postcranial bones of *Ngapakaldia* are totally undescribed while those of *Diprotodon* are only partly described, further discussion of the morphology of the diprotodontid postcranial material in the Alcoota fauna is beyond the scope of the present study.

BIOSTRATONOMY AND PALAEOECOLOGY

Palaeoecology is a broad topic, whose general content deals with the conditions under which the animals of a fossil fauna lived. Students of palaeoecology have grouped the fossils of a given locality into assemblages representative of communities which were either close to or far from the site of deposition (Shotwell, 1955, etc.). In some cases this procedure increases the probability with which members of a biocoenose may be segregated from an assemblage which is surely a thanatocoenose. Other workers have drawn insights as to the conditions under which a former assemblage lived based on the living requirements of its modern representatives, as well as upon the morphologies of the fossils. In most of these studies, however, the conditions under which the animals died and the means by which they came to the site of deposition have not been studied with a comparable degree of thoroughness. Data drawn from a study of such considerations as these (which fall to a certain extent into the realm of geology as well as that of biology) can form an important basis for the more classical palaeoecological conclusions, and they should receive as much attention as is consistent with their importance. The term, biostratonomy, was coined by J. Weigelt (1927) for considerations such as these.

Biostratonomy: Originally, Weigelt intended that the term be used to indicate the study of the arrangement and orientation of fossils in the rock. Subsequently, A. H. Müller (1957, p. 16) expanded the limits of the term to include all the events and processes to which the animal is subjected from the time of its death until its final burial. Classical palaeoecology is primarily concerned with how animals live; biostratonomy is primarily concerned with how animals die, what happens to their soft and hard parts before deposition, and what happens to their hard parts during and after deposition. In this way, the fossilized remains of an organism are treated as integral parts of the surrounding rock and, like other constituents of the rock, can be made to yield data bearing on the depositional setting and history of the deposit. The appearance of fossilized remains reflects to a large extent the events and processes which the animal sustained after death. Since, to be preserved, a specimen must usually be buried relatively rapidly, a study of the biostratonomy of a fossil assemblage may yield information which will sensitively portray the conditions which existed immediately before burial and preservation. When coupled with information gained from more classical studies on palaeoecology and sedimentation, the data from biostratonomy can make an important contribution to the total concept of the biological and geological setting in which the fossils were assembled.

Vertebrate fossils are found in four localities in the Waite Formation. Three of the quarries have yielded fossils from the basal part of the formation, mainly from the green lacustrine siltstone. In two of these three quarries a certain amount of the fossil material came from the immediately overlying red siltstone. A meagre concentration of bone much higher in the fluviatile beds has come from locality V6347. The origin of the fossils from this locality was probably quite different from that of the other quarries, and it is possible that a different depositional environment is indicated.

V6345: *Paine Quarry*. Fossil remains come from the green lacustrine siltstone and red fluviatile siltstone of the lower part of the Waite Formation east of the low north-east-trending rise (see Fig. 2). At the western edge of the locality the beds are horizontal. Five feet to the east, their attitude changes to a strike of 046°, dip 12°SE.

The fossil deposit is typically a tabular mat of randomly oriented, completely disarticulated and unassociated bones which show no effect of stream transport and only slight effects of postdepositional compaction. About 90 percent of the bones occur in units 3 and 4 of section 9.

Taxa represented: Crocodile, birds, *Thylacinus potens,* ?peramelid, ?vombatid, *Dorcopsoides fossilis, Hadronomas puckridgi,* cf. *Hadronomas puckridgi,* ?protemnodont, ?sthenurine, *Palorchestes painei, Pyramios alcootense, Kolopsis torus,* and *Plaisiodon centralis.*

V6346: *Newsome Quarry*. Fossils have been recovered from the basal green and the overlying red siltstones of the lower part of the Waite Formation, 416 feet at 022° from Paine Quarry on the west slope of the north-east-trending rise. The lithological characteristics of the red and green units are similar to those at Paine Quarry, but the bedding has been obscured by the numerous rabbit burrows which penetrate the deposit in all directions.

The fossils at Newsome Quarry occur primarily in the red siltstone. They are more fragmented and less well preserved than those in Paine Quarry and characteristically are coated with secondarily precipitated calcium carbonate. In contrast to the smooth surface of the bone and enamel found at Paine Quarry, the surfaces at Newsome Quarry are pitted and leached. The bones are more fragmented, probably because the fossils occur closer to the surface in Newsome than in Paine Quarry, and have thus been disturbed by movements in the soil and subsoil caused by seasonal moistening and drying. The persistently red colour of the siltstone and the existence of relatively large amounts of secondary calcium carbonate around the bones suggests that the bone deposit at Newsome Quarry has been above the local ground water table ever since the fossils were deposited. The fossils at Newsome Quarry show no other conspicuous differences from those at Paine Quarry, and probably resulted from a similar mode of accumulation, transport, and deposition.

Taxa represented: birds, *Hadronomas puckridgi, Pyramios alcootense, Kolopsis torus,* and *Plaisiodon centralis.*

V6349: *Rochow Localities 1 and 2*. These are surface accumulations on the raised spaces between gilgais immediately west and north-west of Paine Quarry. The fossils found here are blue-black hard bones which have been highly fragmented by seasonal expansion and contraction of the ground. The rare complete teeth show numerous fine cracks in the enamel. Toe bones, which are small and compact and thus more resistant to disruptive forces than other limb elements, are most common. A maxillary fragment of *Dorcopsoides fossilis* with M^1-M^4

was found, however. Almost all other specimens over 1 to 2 inches in length are broken. The hardness and dark colour of the bone itself are probably due to secondary chemical activities occurring above the water table and not to significant original differences from the deposits and depositional environment of the adjacent quarry. This is supported by the fact that the excavation for Paine Quarry began as an exploratory pit to determine if the bones of the rich deposit indicated by the countless surface fragments would be more intact at depth.

Taxa represented: crocodile, *Dorcopsoides fossilis, Hadronomas puckridgi, Kolopsis torus,* and *Plaisiodon centralis.*

V6347: *Red Hill Locality,* high in the fluviatile part of the formation on the west side of Hill 1. The mottled light green and buff to red brown medium to fine sandstone occurs 35 feet below the top of the hill. Sparse, much abraded and waterworn limb bones and vertebrae of emu-like ground birds found here clearly show that they were transported by streams of stronger flow or longer duration than were the bones in the other quarries. This is consistent with the strongly fluviatile nature of the enclosing sediments as compared with the lower-energy mode of deposition of the deposits in the other quarries.

In conclusion, Paine Quarry, Rochow localities 1 and 2, and Newsome Quarry show that the fossiliferous portion of the Waite Formation extends for at least 400 feet along the west flank of the low north-east-trending rise which lies west of Hill 1, and is equally fossiliferous over its whole length. As the beds dip toward the south-east, the three-dimensional extent of the fossiliferous siltstone cannot be determined, but a test pit dug 400 feet at 082° of Newsome Quarry revealed the presence of bone in green siltstone at a depth of 6.5 feet (see Fig. 6).

At its completion, the excavation at Paine Quarry was 20 feet long and 15 feet wide. From this area (300 square feet) the total minimum number of individuals (see Shotwell, 1955, p. 330 for definition) recovered was 92. Assuming that the fossiliferous unit extended at least 15 feet to the south-east (as at Paine Quarry) a rough estimate indicates that at least 1400 individuals are represented by the fossil deposit between Paine and Newsome Quarries. This number would, of course, be much greater if the probable extension of the fossiliferous deposits lying under the rise were taken into account.

When the bones are examined, they show no evidence of attrition due to transport. Except for the denser elements, such as toe bones and metatarsals of the smaller macrapodid, the bones are all fractured. This fracturing usually occurs in a reticular pattern and probably resulted from postdepositional expansion and contraction of the beds in response to seasonal alternation between wet and dry periods.

Where the long bones are broken, the breaks are sharp and generally transverse to the long axis. There is no evidence of splintering, nor is there any evidence that the bones were bent while still in a relatively elastic state. The bones were apparently broken when they were no longer 'green'. In other words, they have

been broken while they were settling out of the suspended load of the stream during transport from the site of accumulation, or during postdepositional compaction of the sediments; but not by trampling of the relatively fresh carcases or skeletons by other animals.

Most of the marsupial species are best represented by their dentition. *Kolopsis torus* is nearly as well represented by mandibles as it is by dental material. Although the assignment of the small macropodid foot elements to *Dorcopsoides* was relatively certain, the larger foot elements could not be assigned to *Hadronomas* with a comparable degree of probability. Because there are two large species and two small species of diprotodontid, segregation of their postcranial elements was not attempted.

The elements are completely disassociated, and were probably completely separated before being brought to their final resting place. There is no evidence that they were subaerially leached, so the animals presumably died in a moist place, or actually in water: water would also hasten the disintegration of the soft parts and disassociation of the bones.

But the remains are not only disassociated: they are also disoriented; and elements of dentition are preponderant. Therefore it seems that the remains were transported, and sorted during transportation. So they did not die at the place where they are now found. Just where they died, and why they died at that place, can only be surmised. The climate probably varied seasonally. During the dry seasons, animals have been forced to move to permanent waterholes. The Waite Basin, either as a low marshy river valley, or as a lake, may have been such a place. During the yearly visitations, some animals would inevitably die, and their carcases might easily come to lie in the water near the edge of the basin, particularly if they had become trapped in the sticky mud around the margin. Disarticulation of the skeletons may have been aided to some extent by the actions of crocodiles, the remains of which are plentiful in the fossil deposit, but under relatively moist conditions maceration proceeds rapidly.

As indicated by the presence of lacustrine gastropods (McMichael, 1967), by the presence of well defined even bedding in the deposits, by the relatively fine and homogeneous size of the clastic particles, by the presence of primary limestones in which leaf remains are embedded, and by the fact that the water table was high enough to reduce the red colour of the sediments being supplied to the Waite Basin, the basin seems to have been the site of a lake or at least a body of permanent water with a low energy regimen.

It is thought that the fossils were brought to the site of deposition by streams which, being revitalized during the onset of the wet season, picked up the scattered bones near the periphery of the basin and carried them farther out until they were dropped from suspension. Although the bones themselves are of various sizes, they are almost all larger than the largest clastic particles of the enclosing sediments and would probably tend to drop out together. The fact

that the bones are most highly concentrated at the base of the fossiliferous units while the particle size of the siltstones remains constant throughout suggests that the bones were dropped out first and that the enclosing sediments settled down later.

The large diprotodontid crania which have been recovered are rather crushed, but unabraded, and it is somewhat more difficult to imagine large elements such as these being carried in the suspended load of a river or strong lake current. It is possible, however, that the oil content of these large elements had not completely leached away before deposition or that some other factor such as trapped air pockets within the cranial cavity increased their buoyancy so that they were more easily transportable. The possibility that the 12° dip of the deposits, as observed at Paine Quarry, represents the initial slope of the lake floor would increase the probability that such elements would eventually reach the quarry site under the combined influences of gravity, wave action, and lake and stream currents.

It is unlikely that each fossiliferous unit at Paine Quarry represents the product of a single season, because of the rather large number of individuals represented along the outcrop area, not to mention those possibly still buried under the rise to the east.

One species of thylacinid, one ?peramelid, one ?vombatid, two species of macropodid and four species of diprotodontid are represented at Paine Quarry (Table 27). These are all terrestrial animals: none are arboreal and none are aquatic. Aquatic mammals are very rare in the modern Australian fauna and, although arboreal forms are common, they are rare in the fossil state. Their absence here is not surprising. Of the forms preserved, only one is definitely a carnivore, and this is in keeping with the carnivore-herbivore ratio of the modern fauna. In comparison with the modern fauna, the Alcoota assemblage is peculiar in that the herbivores are so predominantly large. This may be due to the vagaries of accumulation and deposition. On the other hand, the large herbivores at Alcoota are diprotodontids, which are now extinct. Their presence here may prove to be typical of Tertiary faunas in general. Of all the taxa in the fauna, *Dorcopsoides* is the most completely represented by cranial and postcranial material. Essentially all ontogenetic ages of the genus are present; the sample does not seem to be biased in favour of any particular age group. The matrix is the same both within and around the bones, so that none of the fossils seems to be remanié.

A final peculiarity of the fossil deposit is the presence of large, smoothly rounded clasts, most commonly of quartz. These clasts are not known to occur in such a well-worn condition in the surrounding source area. The only local source of quartz is the Archaean quartzites; fragments derived from these would be quite angular. The only reasonable conclusion to be made concerning these clasts is that they represent gastroliths. Both large crocodiles and terrestrial birds inhabited the area in Alcoota time. According to Wermuth (1953, p. 406) stones and other foreign objects taken in with the crocodiles' food become

gastroliths, and play an important part in digestion. In general, crocodiles living in waters where fish are plentiful (mainly coastal areas) tend to have fewer gastroliths than species living in continental waters, which tend to eat more mammals and birds than fish.

Palaeoecology: As indicated by Wermuth (*ibid.*, p. 405) crocodilians live in all the tropical and subtropical areas of the world except Europe. Forms such as *Crocodylus niloticus* and *C. johnsoni* inhabit rivers and lakes in the interiors of continents. *C. porosus* is a decidely brackish-water form, and because of this enjoys a particularly wide distribution.

The nesting habits of crocodiles are sufficiently like those of alligators to warrant the inference that their habitats would also be similar (see Woodburne, 1959). Thus the presence of crocodiles in the Alcoota fauna seems to indicate the presence of a permanent body of water in a subtropical or tropical area.

The other element in the Alcoota fauna with strong palaeoecological implications is *Dorcopsoides fossilis*. Its closest relatives are now restricted to the forests of New Guinea and adjacent islands. *Dorcopsis hageni* and *D. venterum* 'are both primarily rainforest animals' (Van Deusen, 1957, p. 17), while *D. atrata* was taken from the 'mid-montane forest of oaks and *Castanopsis* . . .' (*ibid.*, p. 22). The species probably ranged upward into the beech-tree fern forest with its more open canopy and downward into the mixed rainforest as well.

The chief contrast between the habitat of *Dorcopsis* and *Dorcopsulus* and that probably occupied by *Dorcopsoides* is physiographical. The areas in which the modern representatives live, although tropical, are mountainous; *Dorcopsis* does, however, occur in the lowland rainforests of Papua at an elevation of about 200 feet (Brass, 1956, p. 139). The area around Alcoota is now and probably was in the past one of relatively low relief and elevation. It is also probable that, as it is near the centre of Australia, the climate was more continental in the middle Tertiary than that around the coastal areas. The major difference of the past climate at Alcoota to be inferred from the presence of the crocodiles and *Dorcopsoides* is a higher level of effective precipitation, which would encourage the growth of a more luxuriant type of vegetation than that now in the area. This inference is also supported by the presence of the large herbivores *Hadronomas, Palorchestes, Pyramios, Kolopsis,* and *Plaisiodon*. Thus, the Waite Basin seems to have been a depressed area containing a relatively large permanent source of water. The water was inhabited by crocodiles and freshwater, lacustrine gastropods. Around the margin of the basin a fairly luxuriant vegetation probably extended for some distance up the slopes. The major stream valleys leading into the basin were probably well forested. Farther upslope, the forest would give way to brushy woodlands and grasslands.

TABLE 27

Total number of specimens represented by the more easily recognizable elements and the minimum number of individuals present for each marsupial taxon in the collection from Paine Quarry

Element	*Thylacinus potens*		?peramelid		?vombatid		*Dorcopsoides fossilis*		*Hadronomas puckridgi*		cf. *Hadronomas puckridgi*	
	n^t	n^m	n^t	n^m	n^t	n^m	n^t	n^m	n^t	n^m	n^t	n^m
Cranium	1	1					1	1				
I^1					1	1						
I^2												
I^3												
P^2							3	2				
dP^3							4	3				
P^3	2	1					8	5	5	3		
M^1	2	1					9	6	1	1		
M^2	2	1					5	3	3	2		
M^3	3	2					6	4	5	4		
M^4	3	2					6	3	3	3		
Mandible	1	1	1	1			10	6	4	2		
I_1							5	3	4	2		
P_2							2	2				
dP_3							2	2				
P_3							4	3	6	3		
M_1							7	4	6	4		
M_2	1	1					9	5	4	2		
M_3	1	1	1	1			10	6	5	2		
M_4	1	1	1	1			7	4	4	2		
Astragalus	1	1					15	9			5	3
Calcaneum	1	1					21	12			2	1
Cuboid							7	4			6	4
Mtt. III	1	1										
Mtt. IV	2	2					21	14			6	4
Mtt. V							11	8			4	3
Prox. Ph. IV							17	12			10	8
Prox. Ph. V							9	6				
Min. No.	2		1		1		14		4		8	

TOTAL NUMBER OF INDIVIDUALS FROM PAINE QUARRY = 95

n^t = total number of specimens.

n^m = minimum number of individuals per element.

TABLE 27 (Continued)

Element	?protemnodont		?sthenurine		*Palorchestes painei*		cf. *Palorchestes painei*		*Pyramios alcootense*		*Kolopsis torus*		*Plaisiodon centralis*	
	n^t	n^m	n^t	n^m	n^t	n^m	n^t	n^m	n^t	n^m	n^t	n^m	n^t	n^m
Cranium . .					1	1			3	3	1	1	3	3
I^1	4	3	3	2	1	1	1	1	20	11	20	10	8	5
I^2							2	1	6	4	6	4	9	5
I^3			2	1	4	2			7	5	8	5	16	10
P^2														
dP^3													1	1
P^3					5	3			14	9	28	13	15	8
M^1					5	3			13	8	23	12	13	7
M^2					4	2			9	5	25	15	14	8
M^3					5	3			12	7	26	14	9	5
M^4					4	3			14	7	17	10	3	3
Mandible . .					9	5			14	8	45	27	31	16
I_1					2	1			8	6	24	13	18	10
P_2														
dP_3														
P_3					1	1			4	2	30	16	20	11
M_1					4	2			8	5	40	24	19	11
M_2					6	4			10	6	44	24	20	11
M_3					9	5			10	5	48	27	27	15
M_4					9	5			10	5	42	26	27	15
Astragalus .														
Calcaneum .														
Cuboid														
Mtt. III . . .														
Mtt. IV . . .														
Mtt. V . . .														
Prox. Ph. IV														
Prox. Ph. V														
Min. No.	3		2		5		1		11		27		16	

THE AGE OF THE ALCOOTA FAUNA

The Alcoota fauna is somewhat limited taxonomically, but a rather firm estimation of its position relative to the other known Australian mammalian faunas can be derived from a study of the forms which have been preserved. In this regard, the representatives of the Diprotodontidae, of which the fauna is largely composed, are particularly useful. The temporal significance of the genera will be considered individually and, as far as is possible, the age of the Alcoota fauna with respect to the standard European Tertiary epochs will be evaluated.

Crocodylus sp.: Except that its apparent affinity with various living species of the genus might suggest a later rather than an earlier Tertiary age, this form is of little temporal significance.

Aves: The birds of the Alcoota fauna will be studied elsewhere. Inferences about their temporal significance must await completion of this study.

Thylacinus potens: As mentioned in the description, the Alcoota thylacine is quite removed, morphologically, from the Pleistocene and Recent species of the genus. Except for *T. rostralis* of Queensland, all Pleistocene thylacines seem to represent the modern species, *T. cynocephalus* (see Ride, 1964). Furthermore, it is evident from casts of the type dentition of *T. rostralis* that, except for a few proportions, the Queensland species is quite close to *T. cynocephalus*. Since it appears that the Alcoota thylacine is not directly ancestral to either *T. cynocephalus* or *T. rostralis,* it is difficult, in the absence of any other phyletic data, to estimate the temporal position of *T. potens* accurately. On the other hand, the small palatal fenestrae, the presence of a stylar cusp anterior to the metastyle of M^3, the more symmetrical arrangement of the components of the upper molars, and the strong labial cleft in the outline of the upper molars in *T. potens* may indicate that the Alcoota species represents a phyletically primitive form. This, together with the high level of morphological advancement shown by Pleistocene and Recent members of the genus, indicates that the most reasonable temporal assignment to be given to *Thylacinus potens* is pre-Pleistocene.

Dorcopsoides fossilis: Though *D. fossilis* clearly belongs to the lineage leading to *Dorcopsis* and *Dorcopsulus,* its primitive position is demonstrated by its shorter juvenile and adult premolar dentition, relatively lower-crowned teeth, weaker postparaconal and premetaconal crests, and the more widely open transverse valleys of its upper molars. Unfortunately, the Alcoota genus seems to be the oldest member of this branch of the Potoroinae; potoroines of the Kutjamarpu (middle Miocene) and Ngapakaldi (late Oligocene) faunas of South Australia belong to other lineages. The temporal significance of *Dorcopsoides fossilis* can only be evaluated as probably late rather than early Tertiary.

Hadronomas puckridgi: The other macropodid of the Alcoota fauna seems to be a relatively large, massive animal which may be close to the lineage leading toward *Sthenurus*. In general, its dentition is considerably more generalized than that of the late Pliocene sthenurines of the Chinchilla fauna (Bartholomai,

1963). However, owing to the largely unresolved complexity of what appears to be a highly diversified group of animals, a reliable determination of the descendant species of *H. puckridgi* cannot be made at this time. The form can only be stated to be earlier than late Pliocene.

Palorchestes painei: This diprotodontid is more primitive than *P. parvus* from the late Pliocene Chinchilla Sands of south-eastern Queensland. This is readily apparent from its smaller tooth size, lower-crown height, and poorer development of molar midlinks. On the other hand, the elongate, deeply excavated rostrum, the deep frontal region of the cranium, and the robust, deep mandible of *P. painei* represent, in addition to the features of its dentition, a marked advancement over the palorchestines of the Ngapakaldi fauna. In dental characters, the Alcoota palorchestine represents a stage of advancement nearer to *Palorchestes parvus* than to *Pitikantia dailyi* or *Ngapakaldia tedfordi*. It is also by no means certain that these late Oligocene forms are directly ancestral to *Palorchestes*. The relative age of *Palorchestes painei* is post-Ngapakaldi and pre-Chinchilla, or at a point between the late Oligocene and late Pliocene.

Pyramios alcootense is the oldest known member of the diprotodontid subfamily Nototheriinae. As indicated previously it represents a more primitive stage of evolution than either *Nototherium watutense* of the Awe fauna of New Guinea or *Meniscolophus mawsoni* of the Palankarinna fauna of South Australia. The Alcoota fauna is thus earlier than either. This determination can be further refined to Middle Tertiary on the basis of inferences drawn on the probable time of separation of the nototheriine and zygomaturine lineages (see Stirton, Woodburne, & Plane, 1967). These lineages are already quite distinct by Alcoota time.

TEMPORAL RELATIONSHIPS OF VARIOUS AUSTRALASIAN TERTIARY FAUNAS

<table>
<tr><th>VICTORIA</th><th>SOUTH AUSTRALIA</th><th>NORTHERN TERRIT.</th><th>QUEENSLAND</th><th>NEW GUINEA</th><th>Lyellian Epoch</th></tr>
<tr><td rowspan="2">BEAUMARIS</td><td>PALANKARINNA</td><td></td><td>CHINCHILLA</td><td>AWE</td><td>PLIOCENE</td></tr>
<tr><td rowspan="2">KUTJAMARPU

NGAPAKALDI</td><td>ALCOOTA</td><td></td><td></td><td>MIOCENE</td></tr>
<tr><td></td><td></td><td></td><td>OLIGOCENE</td></tr>
</table>

Fig. 34. Chart showing temporal relationships of various Australian Tertiary faunas.

Plaisiodon centralis: This zygomaturine diprotodontid is a relatively primitive hold-over from an earlier level of organization such as that seen in *Neohelos tirarensis* from the Kutjamarpu fauna, though it is undoubtedly more advanced. No later relatives of *P. centralis* are presently known.

Kolopsis torus: Of all the forms in the Alcoota fauna this species is the most closely aligned in an ancestor-descendant relationship with other genera and species. It is readily apparent that *K. torus* is more primitive than either *K. rotundus* of the Awe fauna or *Zygomaturus gilli,* the most primitive species of its genus, which occurs in the Beaumaris fauna of Victoria. Furthermore, *K. torus* is clearly more advanced than *Neohelos tirarensis* of the Kutjamarpu fauna.

As pointed out by Plane (1967b; p. 20) the Awe fauna is between 5.7 and 7.6 million years old as determined by the potassium-argon method. According to the evidence presented by Evernden, Savage, Curtis, & James (1964, p. 167), this falls within the time span represented by mammalian faunas in North America and Europe which, typological problems notwithstanding (see Savage, 1955, p. 3), have been dated as middle Pliocene by vertebrate palaeontologists.

Although the meagre land mammal remains found at Beaumaris, Victoria, have been found in marine rocks, the position of the deposit relative to the standard Tertiary epochs is not clear cut. The remains of *Zygomaturus gilli* (Stirton, 1967) were found lying on the beach at Beaumaris. Comparison of their fluorine content with materials *in situ* in the adjacent cliff (Gill, 1957, p. 186-187) indicates a strong probability that the diprotodontid material was derived from the Black Rock member of the Sandringham Sands Formation. In addition to the marsupial bones, the Black Rock member, which consists of ferruginous calcareous stratified sandstone of apparent nearshore origin, also contains remains of foraminifera, bryozoans, corals, crustaceans, brachiopods, molluscs, cephalopods, fish, rays, sharks, dolphins, and whales. As determined by Gill (*ibid.*) the Black Rock member belongs to the Cheltenhamian megafossil stage of Singleton (1941, p. 32).

The interrelationships of the Cheltenhamian and contiguous stages have recently been reviewed (Wilkins, 1963). The use of the Cheltenhamian stage for the time-rock unit below the Kalimnan stage and above the Balcombian stage has been generally accepted. The only major exception to this was introduced by Crespin (1943, 1950), in which the Cheltenhamian was considered as being equivalent to the lower part of the Kalimnan. The gap which resulted from this interpretation was filled by a newly-coined stage, the Mitchellian. Until recently, most other workers considered the Cheltenhamian and Mitchellian as synchronous, pending further evidence.

In Wilkins' revision (1963) the Mitchellian is retained as the stage below the classical Kalimnan, but the Kalimnan is in turn divided into an upper and lower part, the upper retaining the name 'Kalimnan' and the lower being called 'Cheltenhamian'. This is essentially the arrangement proposed by Crespin (1943).

The Miocene-Pliocene boundary apparently falls somewhere in the Mitchellian-Cheltenhamian-Kalimnan sequence. The classical approach was that the old Kalimnan represented the early Pliocene in south-eastern Australia and the old Cheltenhamian (= Mitchellian) pertained to the late Miocene. Appraisal of the faunal lists given in Wilkins (1963, p. 58-59) for the type Mitchellian, type Cheltenhamian, and revised Kalimnan shows that of the 31 species listed for the Mitchellian, 14 have their last occurrence in this stage and 17 extend on into the Kalimnan. On the other hand, of 45 species listed for the Cheltenhamian, 18 are restricted to it, 12 are common to the Cheltenhamian and Kalimnan, and, of course, 17 carry on from the Mitchellian into the Kalimnan. None of the species listed for the Cheltenhamian are exclusively allied to those of the Mitchellian. It seems, then, that the most conspicuous faunal break occurs between the Mitchellian and Cheltenhamian stages and that the Cheltenhamian has considerable affinity with the Kalimnan. It is deemed most reasonable, therefore, to follow the preference of Crespin (1943, 1950) in assigning the Mitchellian to the late Miocene, and the classical Kalimnan (= Kalimnan and Cheltenhamian, *sensu* Wilkins) to the early Pliocene.

Although *Kolopsis torus* is morphologically derivable from *Neohelos tirarensis* (Kutjamarpu fauna) the Alcoota species is closer to *Kolopsis rotundus* (Awe fauna) and *Zygomaturus gilli* (Beaumaris fauna). The somewhat anomalous temporal position of *K. rotundus* has been discussed elsewhere (Plane, 1967a; Stirton, Woodburne, & Plane, 1967). The interrelationships of the various Australian Tertiary faunas are shown in Fig. 34. This is essentially the arrangement presented in Stirton, Woodburne, & Plane (*ibid.*). It should be emphasized that while a large part of the information from which the chart was constructed was drawn from an evaluation of the diprotodontids in the various faunas, information yielded from physical stratigraphy, invertebrate biostratigraphy, mammalian biostratigraphy, and isotopic geochronometry was also utilized.

An evaluation of the interval of time involved in the progression from *N. tirarensis* to *K. torus* and *Z. gilli* suggests that the Alcoota and Beaumaris faunas are temporarily closer to each other than are the Alcoota and Kutjamarpu faunas. It is estimated that the time span between the Alcoota and Beaumaris faunas is of less than Stage-Age magnitude. The age of the Alcoota fauna, in terms of the standard European Tertiary epochs is, therefore, considered to be late Miocene, or possibly early Pliocene.

REFERENCES

ABBIE, A. A., 1939—A masticatory adaptation peculiar to some diprotodont marsupials. *Proc. zool. Soc. Lond.*, 109, 261-279.

BARTHOLOMAI, A., 1963—Revision of the extinct macropodid genus *Sthenurus* Owen in Queensland. *Mem. Qld Mus.*, 14, 51-76.

BRASS, L. J., 1956—Results of the Archbold Expeditions. No. 75. Summary of the fourth Archbold Expedition to New Guinea. *Bull. Amer. Mus. nat. Hist.*, 111, 77-152.

BRETZ, J. H., and HORBERG, L., 1940—Caliche in south-western New Mexico. *J. Geol.*, 57, 493-511.

BROWN, C. N., 1956—The origin of caliche on the north-eastern Llano Estacado, Texas. *J. Geol.*, 64, 1-15.

CRESPIN, I., 1943—The stratigraphy of the Tertiary marine rocks in Gippsland, Victoria. *Bur. Min. Resour. Aust., Bull.* 9, *Pal. ser.* 4 (mimeographed).

————. 1950—Australian Tertiary microfaunas and their relationships to assemblages elsewhere in the Pacific Region. *J. Paleont.*, 24, 421-429.

DE VIS, C. W., 1893—A thylacine of the earlier Nototherian Period in Queensland. *Proc. Linn. Soc. N.S.W.*, 2, 443-447.

EVERNDEN, J. F., SAVAGE, D. E., CURTIS, G. H., and JAMES, G. T., 1964—Potassium-argon dates and the Cenozoic mammalian geochronology of North America. *Amer. J. Sci.*, 262, 145-198.

FRANKEL, J. J., and KENT, L. E., 1938—Grahamstown surface quartzites (silcretes). *Trans. geol. Soc. S. Afr.*, 40, 1-43.

GILL, E. D., 1957—The stratigraphical occurrence and palaeoecology of some Australian Tertiary marsupials. *Mem. nat. Mus. Vic.*, 21, 135-203.

GRIM, R. E., 1953—CLAY MINERALOGY. *N.Y. McGraw Hill.*

————. 1958—Concept of diagenesis in argillaceous sediments. *Bull. Amer. Ass. Pet. Geo.*, 42, 246-253.

HALLSWORTH, E. G., ROBERTSON, and GIBBONS, F. R., 1955—Studies in pedogenesis in New South Wales. VII. The 'Gilgai' soils. *J. Soil. Sci.*, 6, 1-31.

HARRIS, G. P., 1807—Description of two new species of *Didelphis* from Van Diemen's Land. *Trans. Linn. Soc. Lond.*, 9, 174-178.

HIBBARD, C. W., and TAYLOR, D. W., 1960—Two late Pleistocene faunas from south-western Kansas. *Contrib. Univ. Mich. Mus. Paleont.*, XVI, 1-223.

HOSSFELD, P. S., 1954—Stratigraphy and structure of the Northern Territory of Australia. *Trans. Roy. Soc. S. Aust.*, 77, 103-161.

JOKLIK, G. F., 1955—The geology and mica-fields of the Harts Range, Central Australia. *Bur. Min. Resour. Aust., Bull.* 26, 1-226.

JONES, F. W., 1924—The mammals of South Australia, pt. II. *Adelaide, Govt. Printer.*

KAELIN, J. A., 1933—Beiträge zur vergleichenden Osteologie des Crocodilidenschädels. *Zool. Jb. (Anat. Ontog.)*, 57, 535-712.

KREFFT, G., 1868—Description of a new species of thylacine (*Thylacinus breviceps*). *Ann. Mag. nat. Hist.*, 4, 296-297.

LLOYD, A. R., 1967—An outline of the Tertiary geology of Northern Australia. *Bur. Min. Resour. Aust. Bull.* 80.

MADIGAN, C. T., 1932—The geology of the eastern MacDonnell Ranges, Central Australia. *Trans. Roy. Soc. S. Aust.*, 56, 71-118.

McMICHAEL, D. F., 1967—Non-marine mollusca from Tertiary rocks in Northern Australia. *Bur. Min. Resour. Aust. Bull.* 80.

MULACHY, M. H., 1960—Laterites and lateritic soils in south-western Australia. *J. Soil. Sci.*, 11, 206-225.

MUELLER, A. H., 1957—Lehrbuch der Paläozoologie. 1. Allgemeine Grundlagen. *Jena, Gustav Fischer.*

NEWSOME, A. E., and ROCHOW, K. A., 1964—Vertebrate fossils from Tertiary sediments in Central Australia. *Aust. J. Sci.*, 26, 352.

OWEN, H. B., 1954—Bauxite in Australia. *Bur. Min. Resour. Aust. Bull.* 24.

OWEN, R., 1845—Descriptive and illustrated catalogue of the fossil organic remains of Mammalia and Aves contained in the Museum of the Royal College of Surgeons of England. *London, Taylor.*

OWEN, R., 1877—Researches on the fossil remains of the extinct mammals of Australia, with a notice of the extinct marsupials of England. *London, Erxleben.*

PEARSON, J., 1950—The relationships of the Potoroidae to the Marcopodidae (Marsupialia). *Pap. Roy. Soc. Tas.*, 1949, 211-229.

PERRY, R. A., *et al.*, 1962—General report on lands of the Alice Springs Area, Northern Territory, 1956-57. *Sci. ind. Res. Org., Melb., Land Res. Ser.* 6, 1-280.

PLANE, M. D., 1967a—Two new diprotodontids from the Pliocene Otibanda Formation, New Guinea. *Bur. Min. Resour. Aust. Bull.* 85.

PLANE, M. D., 1967b—Stratigraphy and vertebrate fauna of the Otibanda Formation, Morobe District, New Guinea. *Bur. Min. Resour. Aust. Bull.* 86.

RIDE, W. D. L., 1964—A review of Australian fossil marsupials. *J. Roy. Soc. W. Aust.*, 47, 97-131.

ROSS, C. S., 1945—Minerals of the montmorillonite group; their origin and relation to soils and clays. *U.S. geol. Surv. prof. Pap.* 205-B, 23-79.

SAVAGE, D. E., 1955—Non-marine lower Pliocene sediments in California, a geochronologic-stratigraphic classification. *Univ. Calif. Publ. geol. Sci.*, 31, 1-26.

SCHMIDT, K. P., 1928—A new crocodile from New Guinea. *Field Mus. nat. Hist., zool. Ser.*, 12, 177-182.

SHOTWELL, J. A., 1955— An approach to the paleoecology of mammals. *Ecology*, 36, 327-337.

SINGLETON, F. A., 1941—The Tertiary geology of Australia. *Proc. Roy. Soc. Vic.*, 35,1-125.

SISSON, S., and GROSSMAN, S. D., 1953—THE ANATOMY OF THE DOMESTIC ANIMALS, *Philadelphia and London, Saunders.*

STIRTON, R. A., 1955—Late Tertiary marsupials from South Australia. *Rec. S. Aust. Mus.*, 11, 247-268.

STIRTON, R. A., 1963—A review of the macropodid genus *Protemnodon. Univ. Calif. Publ. geol. Sci.*, 44, 97-162.

STIRTON, R. A., 1967a—Diprotodontidae from the Ngapakaldi fauna, South Australia. *Bur. Min. Resour. Aust. Bull.* 85.

STIRTON, R. A., 1967b—A diprotodontid from the Miocene Kutjamarpu fauna, South Australia. *Ibid.*

STIRTON, R. A., 1967c—Two new species of *Zygomaturus* and additional observations on *Meniscolophus*, Pliocene Palankarinna fauna of South Australia. *Ibid.*

STIRTON, R. A., TEDFORD, R. H., and MILLER, A. H., 1961—Cenozoic stratigraphy and vertebrate paleontology of the Tirari Desert, South Australia. *Rec. S. Aust. Mus.*, 14, 19-61.

STIRTON, R. A., WOODBURNE, M. O., and PLANE, M. D., 1967—A phylogeny of the Tertiary Diprotodontidae and its significance in correlation. *Bur. Min. Resour. Aust. Bull.* 85.

TATE, G. H. H., 1948—Results of the Archbold Expeditions. No. 59. Studies on the anatomy and phylogeny of the Macropodidae (Marsupialia). *Amer. Mus. nat. Hist., Bull.* 91, 233-352.

TINDALE, N. B., 1931—Geological notes on the Iliaura country, north-east of the MacDonnell Range, Central Australia. *Trans. Roy. Soc. S. Aust.*, 50, 32-38.

VAN DEUSEN, H. M., 1957—Results of the Archbold Expeditions. No. 76. A new species of Wallaby (genus *Dorcopsis*) from Goodenough Island, Papua. *Amer. Mus. Novit.*, 1826, 1-25.

VAN KLAAUW, C. J., 1931—The auditory bulla in some fossil mammals. *Amer. Mus. nat. Hist., Bull.* 91, 1-352.

WEIGELT, J., 1927—Rezente Wirbeltierleichen und ihre paläobiologische Bedeutung. *Leipzig, Max Weg.*

WERMUTH, H., 1953—Systematik der Rezenten Krokodile. *Mitt. zool. Mus. Univ. Berlin*, 29, 375-514.

WHITEHOUSE, F. W., 1940—Studies on the late geological history of Queensland. *Pap. Univ. Qld Dep. Geol.*, 2, 2-22.

WILKINS, R. W. T., 1963—Relationships between the Mitchellian, Cheltenhamian and Kalimnan Stages in the Australian Tertiary. *Proc. Roy. Soc. Vic.*, 76, 39-59.

WOODARD, G. D., 1955—The stratigraphic succession in the vicinity of Mt. Babbage station, South Australia. *Trans. Roy. Soc. S. Aust.* 78, 8-17.

WOODBURNE, M. O., 1959—A fossil alligator from the lower Pliocene of Oklahoma and its climatic significance. *Pap. Mich. Acad. Sci.*, 44, 47-50.

WOODBURNE, M. O., 1967—Three new diprotodontids from the Tertiary of the Northern Territory. *Bur. Min. Resour. Aust. Bull.* 85.

WOODS, J. T., 1958—The extinct marsupial genus *Palorchestes* Owen. *Mem. Qld Mus.*, 13, 177-193.

WOODS, J. T., 1960—The genera *Propleopus* and *Hypsiprymnodon* and their position in the Macropodidae. *Ibid.*, 5, 199-212.

WOOLNOUGH, W. G., and DAVID, T. W. E., 1926—Cretaceous glaciations in Central Australia. *Quart. J. geol. Soc. Lond.*, 82, 332-356.

APPENDIX 1

Measured sections 1 - 13

Measured section 1

Beginning at pit at base of south-west side of Hill 1 and transversing up that face to the top.

Unit	Description	Thickness in feet
	Waite Formation	
8.	Rubble of let-down caprock blocks, not in place.	2.0
	Unconformity, angular; slump	
7.	*Sandstone,* earthy red brown. Conglomeratic at base. A 5-ft. unit 5.5 feet from base with high content of angular to rounded bedrock clasts up to 6 inches in diameter. Random orientation, or at least none preferred to indicate direction of channel. Above this, upward decrease in conglomeratic content, with coarse fraction of medium sand size rather than coarse to very coarse at bottom. Weathering in steep-sided columnar terraces. Coarse clasts concentrated on south-west face of hill.	28.0
6.	*Sandstone,* conglomeratic, massive grey-buff colour. Larger particles chiefly subangular to rounded quartz; basement rock types present. Also rounded to tabular dark red-brown ironstone pellets, possibly reworked from laterite profile.	2.0
5.	*Sandstone,* medium to fine, mottled light green to red-brown. Subrounded quartz particles. Calcareous content increases upward. Lime cement. Occasional ironstone pellets, increase in upper third. Sparse fossils, as weathered fragments in more reduced pockets. V6347 in this unit on north-west face of hill.	5.4
4.	*Pebble conglomerate,* light buff, calcareous cement. Matrix chiefly quartz sandstone. Pebbles apparently of ferruginous siltstone with coarser quartz particles medium sand size with ochre-yellow weathering rind 1-2 mm thick. Pellets probably derived from laterite profile. Occasional rounded white quartz pebbles. Gradational upper and lower contact.	6.9
3.	*Sandstone,* alternating light tan and dark red, calcareous cement, coarse fraction of angular to subrounded quartz and some basement rock types up to 0.2 inches in diameter. Upward increase in $CaCO_3$ making progressively thinner laminae.	9.3
2.	*Sandstone,* red-brown, well to moderately sorted. Clastic content of angular quartz particles. Black ferruginous particles scattered throughout.	1.5
1.	*Siltstone,* earthy red-brown, occasional mica flakes. Scattered subangular to coarse sand size quartz particles. Black ferruginous partings. Differential $CaCO_3$ cementation in upper third results in production of angular to rounded dark masses up to 0.5 inches in diameter. Base not reached. Bottom of section.	4.0
	TOTAL	57.1+

Measured section 2

On the south face of the north-east end of Hill 2.
Type section of the Waite Formation.

Unit	Description	Thickness in feet
Waite Formation		
5.	*Caprock;* silicified arenaceous limestone. Silicification decreases toward base. Dull pearly grey colour, surface pitted. Fractured into large blocks.	8.1
4.	*Sandstone,* light brown, calcareous cement; $CaCO_3$ fills veinlets and cracks. Matrix of fine sand to silt size with angular quartz particles up to 0.2 inch in diameter. Lateral variation in cementation results in dark red siltstone with black stainings. Total upward decrease in size of large clastic portion; essentially uniform grain size at top.	10.8
3.	*Sandstone,* similar to unit 2, but lesser amount of $CaCO_3$. Colour is earthy red-brown with black partings; rock types as above, but with basement rock clasts up to 6 inches in diameter, rounded to angular. Fine fraction finer than in unit 2. Local lenses 5 feet long, 2 to 6 inches thick of coarser rocks with more $CaCO_3$ 11 feet from base. Concentration of large metamorphic clasts 21.6 feet from base about 4 feet thick. Increase in $CACO_3$ cement, decrease in grain size and absence of metamorphic clasts begins 8.1 feet from top.	35.1
2.	*Conglomeratic sandstone,* ledge-former; subrounded to angular quartz fragments of medium to coarse sand size; scattered clasts of basement rock types more concentrated at north-east tip of hill and on north-north-east face; clasts are subrounded to angular cobbles 2 to 4 inches in diameter. Surface weathers dull buff; light grey to light yellow on fresh surface.	3.0
1.	*Siltstone;* green with mottling of red with scattered subangular quartz grains of fine to coarse sand size; local centres of $CaCO_3$ enrichment. Dense, well indurated rock with greasy lustre on freshly broken surface. Interior of red blotches often black. Bottom of section.	6.4+
	TOTAL	63.4+

Measured section 3

North-east end of Hill 3.

Unit	Description	Thickness in feet
Waite Formation		
5.	*Caprock,* chalcedonic replacement of limestone, irregular pitted surface. Slump block.	5.0
Unconformity, angular; slump.		
4.	*Conglomeratic sandstone,* dark red-brown to blackish brown, black partings; ground mass of fine sand-size particles with medium to coarse sand-size fraction of sub-angular to subrounded quartz.	15.6
3.	*Conglomeratic sandstone,* dark dull brownish red on weathered surface, buff to yellowish white on fresh. No black partings. Subangular to subrounded coarse sand-size fraction chiefly quartz, but other minerals represented.	2.0
2.	*Siltstone,* dark red-brown, massive with blocky weathering surface. Blue-black partings present. Punky vesicular structure caused by weathering. Coarse fraction of angular medium to coarse sand-sized particles.	10.5
1.	*Limestone,* arenaceous, light tan on fresh surface, mottled buff on weathered. Fine-grained with silica filling small horizontal fractures. Weathered to massive rectangular blocks up to 2 feet long. Bottom of section.	23.6
	TOTAL	56.1+

Measured section 4.

At middle of southern face of Hill 4.

Unit	Description	Thickness in feet
Waite Formation		
3.	*Caprock,* chalcedonic replacement of limestone. Less silicified limestone at base is white and chalky, not with pearly lustre.	13.5
2.	*Siltstone,* partly covered, red. Scattered subangular to subrounded sand-sized particles; blocky, vuggy weathering; scattered black partings.	21.6
1.	*Covered interval.* Rubble of caprock. Bottom of section.	54.0
	TOTAL	89.1

Measured section 5

South tip of Hill 5

Unit	Description	Thickness in feet
Waite Formation		
10.	*Caprock,* chalcedonic replacement of limestone; increased clastic and limy content at base.	10.8
9.	*Sandstone,* drab grey-reddish brown on weathered surface, grey-maroon on fresh. Upward decrease in particle size, increase in $CaCO_3$ content. Sandstone mainly fine sand size, subangular quartz ranging in colour from clear to red.	5.4
8.	*Siltstone,* red-brown with secondary $CaCO_3$ deposited along fractures. Scattered subangular to subrounded sand-sized particles, chiefly quartz.	8.1
7.	*Sandstone,* similar to unit 9; upper one-third with 1 to 2 inch interbeds of lighter material; $CaCO_3$ in horizontal veinlets at top.	10.8
6.	*Covered interval.*	2.7
5.	*Siltstone,* light reddish buff, weathers dark brown; massive, arenaceous; coarse fraction chiefly quartz; subrounded medium-coarse sand-size particles evenly distributed; $CaCO_3$ veinlets throughout.	3.0
Unconformity, angular.		
4.	*Massive laterite.* Mainly claystone with scattered coarse sand-size particles, subangular to subrounded. Black partings. Dark red-brown, mottled with black. Small-scale blocky weathering.	5.4
3.	*Covered interval;* suggestion of gradational contact between units above and below.	10.8
2.	*Mottled laterite.* Punky soft siltstone, pastel reds, pinks, greens, and yellows. Extremely weathered. Parent rock structures almost completely destroyed, visible only as coloured outlines of probably feldspar and other laths, etc.	37.8
1.	*Covered interval.* Sand and vegetation, to base of stream. Bottom of section.	10.8
	TOTAL	105.6

Measured section 6a.

At west side of Hill 6.

Unit	Description	Thickness in feet
Waite Formation		
12.	*Caprock,* chalcedonic replacement of limestone.	10.8
11.	*Sandstone,* ochre-red, micaceous, fine-grained. Becomes coarse toward top, with angular quartz fragments of coarse sand size; well sorted at base, no mottling as in unit 8, section 6b.	3.0
10.	*Siltstone,* arenaceous, mottled dark brown, red-brown to light buff, coarser at base. Mainly subangular to subrounded quartz. Better sorted at top than unit 7, section 6b. Mica confined mainly to upper layers.	4.9
9.	*Siltstone,* dark maroon; mottled light tan in patches of increased $CaCO_3$. Coarse sand-sized quartz at top.	1.5
8.	*Siltstone,* calcareous, with upward increase in grain size. Patchy secondary siliceous enrichment.	5.4
7.	*Siltstone,* arenaceous, friable, green, with angular quartz fragments. Calcareous cement.	0.5
6.	*Sandstone,* ochre-yellow, moderately well sorted; chiefly subangular to subrounded quartz and bedrock particles.	2.0
Unconformity, angular.		
5.	*Mottled laterite.* Siltstone, mottled maroon and light grey, friable. Quartz present in remnant structure, feldspars altered.	5.4
4.	*Mottled laterite.* As above, but denser; micas present.	5.4
3.	*Mottled laterite.* As above, but rock soft, punky, friable. Colour various pastels.	5.4
2.	*Pallid laterite.* Weathered metasediment, light grey-green. Quartz in remnant structures, fractured into angular lathlike fragments of coarse sand-size; feldspars soft but still visible — opaque white. Remnant foliation 197°; dips 82° SE.	10.8
1.	*Covered interval* down to unaltered bedrock; gneiss. Bottom of section.	5.4
	TOTAL	60.5

Measured section 6b.

at east side of Hill 6.

Unit	Description	Thickness in feet
Waite Formation		
9.	*Caprock,* chalcedonic replacement of limestone.	10.8
8.	*Sandstone,* mottled light maroon and tan at base to ochre yellow at top. Micaceous, fine-grained with angular quartz fragments of coarse sand-size.	3.0
7.	*Siltstone,* arenaceous, mottled dark brown, to light buff; bottom 18 inches coarser. Clastics mainly subangular to subrounded quartz, occasional ironstone pebbles up to 0.5 in. in diameter. Micaceous.	5.4
6.	*Sandstone,* mottled light buff to brown. Fine-grained with sparse rounded to subangular coarser quartz particles.	5.4
5.	*Conglomeratic* sandstone, light tan, calcareous cement. Coarse fraction of quartz and basement rock types; moderately rounded and sorted.	1.5
4.	*Limestone,* arenaceous, massive, light buff with angular quartz fragments of medium sand-size scattered throughout.	2.5
Unconformity, angular.		
3.	*Massive laterite.* Strongly ferruginised, vuggy, fine-grained structureless rock with coarse angular quartz particles. No blocky weathering effect.	5.4
2.	*Mottled laterite.* Weathered bedrock with angular coarse quartz fragments. aligned in remnant foliation.	5.4
1.	*Mottled laterite.* Weathered bedrock; fine grained with angular coarse quartz fragments; light pink, mottled with light grey. Bottom of section.	16.2
	TOTAL	55.6

Measured section 7.

At north-east side of Hill 7.

Unit	Description	Thickness in feet
Waite Formation		
9.	*Caprock;* chalcedonic replacement of limestone. Basal 10 inches not silicified.	10.8
8.	Sandstone, light brown orange, lime-enriched. Colour darkens as lime decreases toward top. Angular to subrounded quartz particles up to 0.2 inches in diameter.	8.8
7.	*Limestone,* silicified, ledge-former.	5.4
6.	*Sandstone,* light grey, friable; probably less indurated continuation of unit. 5. Bottom three-fourths covered.	5.4
5.	*Sandstone,* light buff. Moderately well sorted quartz sandstone with coarse bedrock clasts up to 1 inch in diameter. Cemented into ledge-forming unit in upper 4 inches. Unit is lenticular.	1.0
Unconformity, angular.		
4.	*Massive laterite.* Poorly textured punky, vuggy, fine-grained rock; mottled light tan and dark red. Fine fraction of fine to medium rounded quartz particles; coarse fraction of rounded ironstone pellets and subangular quartz particles up to 0.3 inch in diameter. Coarse fraction diminished in upper one-third.	16.2
3.	*Massive laterite.* Fine-grained friable rock with rounded to angular quartz particles of medium sand size. Dull red ochre.	3.9
2.	*Covered interval.* Probably continuation of unit 1.	16.2
1.	*Mottled laterite.* Mottled, vuggy, fine-grained rock. Dull red-brown. Angular quartz fragments of coarse sand-size and larger. Rounded dark red to blue-black ironstone pellets weather out. Bottom of section.	3.5
	TOTAL	71.2

Measured section 8

400 feet at 194° from Paine Quarry. Limestone Pit.

Unit	Description	Thickness in feet
Waite Formation		
3.	*Limestone,* moderately low arenaceous content. Grey. Wood and reed-like plant remains preserved, some replaced by silica. Flaggy, weathers to individual pieces up to 6 inches thick.	1.0
2.	*Siltstone,* mottled light green to light tan; alternating with $CaCO_3$ lenses. Lithology similar to that at Paine Quarry but with less quartz and black partings. $CaCO_3$ lenses more indurated and thicker (2 to 3 inches) at top, becoming finer and more punky with depth.	3.0
1.	*Siltstone,* earthy brown; same composition as that above but with addition of quartz and black partings. Mottled patches of lighter brown, probably due to occurrence of $CaCO_3$. Base not reached. Bottom of section.	2.0
	TOTAL	6.0+

Measured section 9

Paine Quarry (V6345)
1,475 feet from Hill 1 at 279°.

Unit	Description	Thickness in feet
Waite Formation		
7.	*Siltstone,* red-brown, with coarse to fine sand-sized quartz particles, angular to subrounded. Black partings. Massive, thickness to over 4 feet within 10 feet to the east. Basal 6 inches transitional to unit 6. Bone fragments very rare.	1.0
6.	*Siltstone,* light olive-green; essentially same as unit 7 except for colour. Weathers into small angular to subrounded blocks with black-stained surfaces. Blocks average 0.5 inch diameter. Occasional bone. Attitude changes.*	1.5
5.	*Siltstone,* light orange brown. Thin unit with fine to medium sand-sized quartz particles in coarse fraction. Attitude changes.*	0.04
4.	*Siltstone,* dark olive-green, higher $CaCO_3$ content than but otherwise similar to unit 6. Blocky weathering, but blocks average smaller than in unit 6. Gradational contact with unit below. Bone present, but not as concentrated as in unit 3. Black stain on surface of blocks. Attitude changes.*	0.8
3.	*Sandstone,* fine, pale green. $CaCO_3$ as punky lenses following bedding planes and as hard dense nodules and concretions around bone. Some punky blocks up to 4 inches thick. Unit coarser than unit 4. Large smooth rounded white quartz clasts up to 3 inches in diameter. Other clasts include rose quartz, angular metamorphic clasts and rare unreduced ferruginous siltstone masses. Rare rounded clasts of silicified mudstone ("billy"). This is the main bone concentration. Attitude changes.*	1.0
2.	*Siltstone,* similar to unit 5.	0.004
1.	*Siltstone,* light green. No $CaCO_3$ lenses, no large clasts, no fossils. Black partings present. Base not exposed. Attitude changes.* Bottom of section.	0.5+
	TOTAL	4.88+

* At the eastern edge of the quarry pit the beds are horizontal. Within a distance of 5 feet to the east the beds change attitude to strike 226°, dip 12° SE.

Measured secion 10

East Pit, 275 feet at 112° from Paine Quarry.

Unit	Description	Thickness in feet
Waite Formation		
6.	*Soil.* Red sandy alluvium. Gradational upward transition of unit 5 into soil. More friable than unit 5.	2.5
5.	*Siltstone,* pale green, with subangular to subrounded quartz particles of medium sand-size. Reticulum of $CaCO_3$ enclosing subangular to subrounded blocks siltstone. Occasional gastropods.	1.4
4.	*Siltstone,* olive-green; large quartz particles rare. $CaCO_3$ content decreased, number of blue-black partings increased. Occasional gastropods.	1.0
3.	*Siltstone,* pale-green, with subangular to subrounded quartz particles of medium sand size. Reticulum of $CaCO_3$ enclosing subangular to subrounded blocks of siltstone. Occasional gastropods.	0.7
2.	*Siltstone,* white to light green-grey, friable with subrounded to subangular quartz particles of fine sand size. Scattered black partings.	0.17
1.	*Siltstone,* pale green with subangular to subrounded quartz particles of medium sand size. $CaCO_3$ as irregular laminae, not reticulum. Base not reached. Bottom of section.	0.17+
	TOTAL	5.94+

Measured section 11

Newsome Quarry (V6346), 416 feet at 022° from Paine Quarry.

Unit	Description	Thickness in feet
Waite Formation		
3.	*Soil,* red sandy siltstone.	0.25
2.	*Siltstone,* red, arenaceous; poorly sorted. Quartz is prevailing rock type, but wide variety of minerals in sand-size fraction. Moderately indurated, scattered fine black partings. One-inch concentration of $CaCO_3$ at base. Main fossil horizon. Within 30 feet to south-east this unit thickens to over 2 inches.	1.1
1.	*Siltstone,* greenish buff, arenaceous. Quartz and $CaCO_3$ chief coarse fraction. Scattered bone. Less diverse mineralogy than in unit 2. Base not reached. Bottom of section.	2.0+
	TOTAL	2.35+

Measured section 12

North Pit, 410 feet at 082° from Newsome Quarry

Unit	Description	Thickness in feet
Waite Formation		
4.	*Soil,* red, arenaceous, with let-down rubble of caprock fragments.	1.4
3.	*Siltstone,* dark red-brown, with quartz particles and black partings. Same as that of unit 7 at Paine Quarry. Gradational contact with unit 2.	0.83
2.	*Siltstone,* dark olive-green. Weathers into small rectangular blocks with black surface stain as in section 9, unit 6.	2.17
1.	*Siltstone,* pale green. Three lime-enriched layers 0.5 to 3.0 inches thick variably separated by 5 to 6 inches of lith similar to that of unit 2 but with higher $CaCO_3$ content. Bottom 1 inch with increased black staining and filling above basal lime layer. Single fossil bone fragment recovered from basal calcareous layer. Base not reached. Bottom of section.	2.17+
	TOTAL	6.57+

Measured section 13

Undippa site.

On east face of mesa, 4 miles south of Mt. Swan road, 16 miles east of Alcoota.

Unit	Description	Thickness in feet
Waite Formation		
8.	*Caprock.* Chalcedonic replacement of arenaceous limestone.	5.4
7.	*Covered interval.* Apparently containing dark red poorly sorted quartz sand.	21.6
6.	*Chalcedony.* Replacement of arenaceous limestone.	8.1
5.	*Sandstone,* conglomeratic, light greyish buff; white on fresh surface with upward increase in $CaCO_3$ cement. Poorly sorted angular fragments with quartz predominant; metamorphic bedrock clasts present up to 3 inches in diameter.	9.9
4.	*Siltstone,* red, earthy, fine-grained. $CaCO_3$ as veinlets in fractures. Mottled on fresh surface.	13.5
Unconformity, angular.		
3.	*Massive laterite.* Ironstone pebbles 0.25 inch to 1.0 inch in diameter weather out of red earthy fine-grained structureless rock. Grades into unit 2.	10.0
2.	*Massive laterite.* Red, ochreous, earthy, structureless fine-grained rock. No evidence of remnant quartz. Forms surface which dips 1 to 2° north-east. Gradational contact with unit 1.	21.6
1.	*Mottled or pallid laterite.* Coherent weathered metasediment with remnant foliation averaging N. 72° E., vertical dip. Feldspars have been weathered. Base not reached. Bottom of section.	27.0+
	TOTAL	117.1+

Measured section 14*

New Well Site

On east side of mesa 1.2 miles at 200° from New Well,
15 miles south-west of Alcoota along Waite Creek.

Unit	Description	Approximate Thickness in feet
Waite Formation		
5.	*Caprock.* Chalcedony replacement of limestone.	11.0
4.	*Covered interval;* caprock rubble and soil on east side of mesa sloping down to valley floor.	39.0
3.	*Chalcedonic limestone.* 1000 yards south of fossil site, about 9.0 feet vertically above fossils; possibly stratigraphically above them as well.	2.0
2.	*Covered interval.* Soil and grass on surface between chalcedonic limestone and fossil site.	9.0
1.	*Siltstone,* dark grey, friable. Contains thoroughly rounded and silicified bone fragments.	1.0
	TOTAL	62.0

* This is a composite section. Mesas capped by chalcedonic limestone occur south and west of New Well. The fossil site is a surface accumulation of rounded silicified bone fragments in a dark grey to black fine sandstone to siltstone matrix. The site is a sub-circular area some 10 feet across, surrounded by red alluvial soil which forms the floor of the alley and extends laterally to the base of the mesas, which rise some 50 feet above the valley floor. The only exposure on the sides of these mesas is the caprock, which is similar to that covering the Waite Formation in the type area.

About 1/4 mile south of the fossil site are some outcrops of silicified limestone which are topographically lower than the mesa caprock and topographically above the fossils.

The significance of these observations is (1) that other fossils of possible Tertiary age can be found in the Waite basin, and (2) the chalcedony-capped sediments found in mesas south of New Well may represent southern exposures of the Waite Formation.